Dublin City University
Ollscoil Chathair Bhaile Átha Cliath

Analysis of 8-oxo-7,8-dihydroGuanine Formation and Oxidation Mediated by Fenton Reaction induced DNA Oxidative Stress

by

Blánaid White B.Sc.

Thesis submitted for the Degree of Doctor of Philosophy

Supervisor:
Prof. Malcolm R. Smyth

Dublin City University **June 2005**

Declaration

I hereby certify that this material, which I now submit for assessment on the programme of study leading to the award PhD is entirely my own work and has not been taken from the work of others save and to the extent that such work has been cited and acknowledged within the text of my work.

Signed: Blánaid White

ID No.: 97007528

Date: 19 June 2005

for my Grandparents

Acknowledgements

Firstly, I would like to sincerely thank my supervisor, Prof. Malcolm Smyth, for all his support, encouragement, advice and enthusiasm and for all the opportunities that he afforded me during the past four years. Thank you too for all the great trips away and the embarrassing charades!

I would also like to thank Gill, Aoife, Máire, Tony, Eimear and Kathleen for all their support and their friendship, which meant so much to me every time the going got a little tough. Chocolate and magazine Fridays were always worth looking for to. Thanks too to all the members of the Sensors and Separations Research group, John, Clodagh, Adriano, Padraic, Dave and Xiliang. Thanks to all my fellow postgraduate students, and especially to the technicians in the School of Chemical Sciences, who always helped me in every way they could.

I was lucky enough to spend some time in the University of Connecticut, and I would like to thank Prof. Jim Rusling for all his support and advice both during and after my visit. Thanks to Dr. Stuart for his invaluable HPLC knowledge. Sincere thanks too to Pene for looking after me when I was there, and to Maricar, Jing, Liping, Abhay and Treese for all their help and lifts everywhere I needed to go.

I would also like to thank those with whom I collaborated, Maricar Tarun, Lynn Dennany, Michelle Boyle and Michele Kelly. Special thanks to Lynn for her friendship and support throughout my time in DCU.

I would to thank in a special way my parents. Thanks Mam and Dad for everything - the endless phone credit and regular donations, and for your unwavering support for me in every decision I've made. Thanks too to Aoife and Maeve, Mary, and especially to Philip, for patiently helping me through every mini crisis that occurred, and for always being there for me.

To everyone I've mentioned, a sincere thank you for helping me through the highs and the lows of the last four years. I couldn't have done it without you, and I'm very grateful to each and every one of you. I'll be repaying favours until I'm 90.

Table of Contents

Abbreviations

$[Cu(phen)_2]^2$	copper 1,10-phenanthroline complex
$^1O_2$	singlet oxygen
5'-dGMP	2-deoxyguanosine-5'-monophoshate
8-OHdG	8-oxo-7,8-dihydro-2'-deoxyguanosine
8-OHG	8-hydroxyguanine
8-oxoA	8-oxo-7,8-dihydroadenine
8-oxoG	8-oxo-7,8-dihydroguanine
A	Adenine
ACN	acetonitrile
Ag/AgCl	silver/silver chloride (reference electrode)
APCI	atmospheric pressure chemical ionisation
ATP	adenosine tri-phosphate
bp	base pairs
bpy	2,2-bipyridine
BR	Briggs-Rauscher
Br^-	Bromide
Br_2	Bromine
BrMA	Bromomalonic acid
BZ	Belousov-Zhabotinskii
C	Cytosine
CE	capillary electrophoresis
Ce(III)	Cerium(III)
CP	ceruloplasmin
CpI	Compound I, HRP radical form containing iron(IV)
CpII	Compound II, HRP form containing iron(IV)
CpIII	Compound II, HRP form containing iron(III)
ct DNA	calf thymus DNA
Cu	copper
Cy	Cyanuric acid
DABCO	1,4-diazabicyclo[2.2.2]octane
DCYTB	Duodenal cytochrome B
DEB	Diepoxybutane

dG	2-deoxyGuanosine
DMP1	divalent metal transporter 1
DMPO	5,5-dimethyl-1-pyrroline N-oxide
DMSO	dimethyl sulfoxide
DNA	DeoxyriboNucleic Acid
DOPA	3,4-dihydroxyphenylalanine
dppz	dipyridophenazine
ds DNA	double-stranded DNA
e^-	electron
EC	electrochemical detection
EDTA	ethylenediaminetetraacetic acid
EIC	extracted ion chromatogram
ELISA	competitive enzyme-linked immunosorbent assay
ESI	electrospray ionisation
ESR	Electron Spin Resonance
FapyA	4,6-diamino-5-formamidopyrimidine
FapyG	2,6-diamino-4-hydroxy-5-formamidopyrimidine
Fe^{2+}	Ferrous iron
Fe^{3+}	Ferric iron
FPG	Formamidopyrimidine DNA glycosylase
FT	ferritin
FTR	ferritin receptor
G	Guanine
GC	gas chromatography
Gh	Guanidinohydantoin
H	Hydrogen
H^+	proton
H_2O_2	hydrogen peroxide
HAA	heterocyclic aromatic amine
HMDE	hanging mercury drop electrode
HO	heme oxygenase
HPLC	high performance liquid chromatography
HRP	Horseradish Peroxidase

I^-	Iodide
I_2	Iodine
Ia	Iminoallantoin
IMA	Iodomalonic acid
Iz	2,5-diaminoimidazolone
LIP	labile iron pool
LOD	limit of detection
m/z	mass to charge ratio
MA	Malonic acid
MB	Methylene Blue
MeOH	methanol
MS	mass spectrometry
NADH	Nicotinamide Adenine Dinucleotide
NaOH	sodium hydroxide
NBTI	non transferrin bound iron
oc DNA	open circular (nicked) DNA
•OH	hydroxyl radical
Oxa	Oxaluric acid
oxGh	oxidised Guanidinohydantoin
oxIa	oxidised Iminoallantoin
Oz	2,2,4-triaminooxazalone
Pa	Parabanic acid
PCET	proton-coupled electron transfer
phen	1,10-phenanthroline
phi	phenanthrene diimine quinone
PO	Peroxidase-Oxidase
PolyG	Polyguanylic acid
Rh	Rhodium
RH	Organic substrate
ROO•	peroxyl radical
ROS	Reactive Oxygen Species
RSD	Relative Standard Deviation
Ru	Ruthenium

SSB	Single strand break
S/N	signal to noise ratio
sc DNA	supercoiled (closed circular) DNA
Sp	spiroiminodihydantoin
SPE	solid phase extraction
ss DNA	single-stranded DNA
st DNA	salmon testes DNA
SWV	square wave voltammetry
T	Thymine
Tn	transferrin
TAN	2,2,6,6,-tetramethyl-4-piperidone-N-oxyl
TBI	transferrin bound iron
TIC	total ion chromatogram
TLC	thin layer chromatography
TMPD	2,2,6,6-tetramethyl-4-piperidone
TMS	trimethylsilane
TR	transferrin receptor
U	Uracil
UV	Ultra violet
X	Xanthine

Analysis of 8-oxo-7,8-dihydroGuanine Formation and Oxidation Mediated by Fenton Reaction Induced DNA Oxidative Stress

DNA undergoes an estimated 10,000 oxidative hits per day. Oxidative DNA damage caused by reactive oxygen species (ROS) can result in multiple base modifications, which have been implicated in mutagenesis, disease and aging. The primary product of G oxidation is 8-oxo-7,8-dihydroguanine (8-oxoG), which is considered by many as a biomarker for oxidative DNA damage. 8-oxoG has an oxidation potential about 0.5 V lower than G, and so can be accurately quantified using electrochemical (EC) detection. EC detection coupled to HPLC resulted in a sensitive and accurate mode of detection for 8-oxoG without requiring any preconcentration or removal of undamaged G, which was simultaneously detected by UV detection.

The aim of this investigation was to measure the rate of 8-oxoG formation in DNA subjected to continuous oxidative attack. The hydroxyl radical, the most aggressive ROS, was generated via the iron-mediated Fenton reaction, and used to generate 8-oxoG in both free G and double stranded DNA. HPLC-UV-EC was utilised for the quantitative analysis of both G and 8-oxoG concentrations with respect to incubation time with the hydroxyl radical. The concentration of 8-oxoG was observed to oscillate with respect to time. After approximately 18 min incubation with Fenton reagents, a maximum 8-oxoG concentration of 0.68 μM was detected in DNA. Thereafter, however, there was an overall decrease in 8-oxoG concentration over time. 8-oxoG concentration was not found to be proportional to the level of oxidative damage which occurred. The concentration of G was also observed to decrease with increasing DNA oxidation, so that as oxidation continued, both G and 8-oxoG were oxidised.

Copper, another important biological metal ion, binds tightly to DNA, inducing significant oxidative DNA damage. It was also investigated as a metal catalyst for the Fenton reaction-mediated DNA oxidation. Again, 8-oxoG concentration was found to oscillate with increasing oxidation of DNA. There were significant differences between the iron- and copper-mediated oxidation of DNA. Oscillation periods for copper-mediated oxidation were shorter, with greater concentration amplitudes. A maximum 8-oxoG concentration of 4.2 μM was detected after 35 min oxidation. Overall, however, the trend was again towards oxidation of both G and 8-oxoG with increasing oxidation of DNA.

8-oxoG is a hotspot for further oxidation. It was observed in both studies outlined above to be further oxidised during DNA oxidation by the Fenton reaction. The final products of 8-oxoG oxidation were determined using HPLC-MS/MS. Oxidised guanidinohydantoin (oxGh) was identified as the primary product of 8-oxoG oxidation, when both iron and copper catalysts were used. A mechanism for the formation of oxGh by hydroxyl radical attack of 8-oxoG was also proposed.

Chapter One

Oxidative DNA Damage: A Literature Survey

1.1 Introduction

The Human Genome Project, completed in 2003, was a 13-year project whose primary aim was to identify all the approximately 20,000-25,000 genes in human DNA and to determine the sequences of the 3 billion chemical base pairs that constitute human DNA.[1] A gene is a segment of DNA, located in a specific position, whose base sequence contains the information necessary for protein synthesis. Damage to DNA, which could affect the base sequence, can potentially lead to disease or an increased susceptibility to disease. Four significant endogenous processes that lead to DNA damage are oxidation, methylation, deamination and depurination.[2] One of the more investigated processes that leads to DNA damage is oxidation, one of the reasons being that DNA has been reported to be subjected to approximately 10,000 oxidative hits per day, based on urine analysis.[3]

This literature review begins with a broad outline of the structure of DNA, and the types of damage to base pairs in the DNA sequences (which may lead to mutations during DNA replication) that may occur. Long-range charge transfer, as a potential mechanism for the altering of both the nature of the damage to the DNA, and the position in the DNA sequence where the mutation occurs, is presented. A primary product of DNA damage, 8-oxo-7,8-dihydroGuanine, is discussed in terms of its formation and its mutagenic effects within DNA. Problems associated with the use of 8-oxo-7,8-dihydroGuanine as a primary indicator of DNA damage are discussed. The second part of this literature survey presents the primary mechanisms that generate oxidative DNA damage, with particular emphasis on reactive oxygen species (ROS) produced *in vivo* which lead to such damage. In the final section, the predominant methods used for detection of oxidative DNA damage are discussed. Two main approaches, direct and indirect, are examined. The direct approach involves the identification of the amount and identity of the oxidised DNA bases generated. The indirect approach measures the number of strand breaks that are caused to the DNA strand either by damaging agents themselves, or by DNA repair enzymes which, depending on the specificity of the substrate and the enzyme, should nick the DNA at a specific oxidised DNA base.

1.2 Introduction to DNA

1.2.1 DNA within the cell

Cells are the fundamental working units of every living system. All the instructions needed to direct their activities (their genetic material) are contained within their DNA (deoxyribonucleic acid). A eukaryote is an organism whose cells each have a distinct membrane-bound nucleus, within which DNA is contained. In such cells, the DNA double helix is packaged by special proteins called histones (a set of simple basic proteins - Hl, H2A, HZB, H3, H4), to form a protein/DNA complex called chromatin. The DNA coils around a histone octamer,[4] so that the structure resembles a bead on a string, as shown in Fig. 1.1. The DNA octamer complex is called a nucleosome, which is the structural unit of chromatin. Each nucleosome contains about 146 base pairs of DNA and 60 base pairs of spacers between core particles. The individual nucleosomes then coil around another histone, H1, to form a "coiled-coil structure", the chromatin fibre. This is 30 nm wide, and each turn contains 6-8 nucleosomes. The higher order structure of the chromatin fibre in the cell is not known in detail.[5]

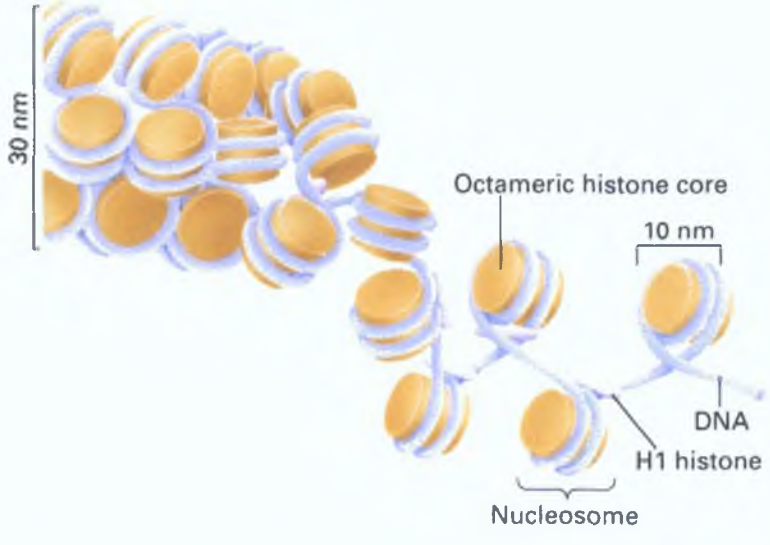

Fig. 1.1: Chromatin fibre showing DNA coiled around histone octamer beads. (reproduced from McGill University website[6])

1.2.2 Structure of DNA

The biological role of DNA is to store and code genetic information. It determines the nature of the cell, controls cell growth and division, and directs biosynthesis of the enzymes and other proteins required for all cellular functions. The structure of DNA, first described by James Watson and Francis Crick in 1953,[7] is illustrated in Fig. 1.2.

Fig. 1.2: DNA double helical structure. (reproduced from Lertola, J.[8])

There are four DNA bases, two purines guanine (G) and adenine (A) and two pyrimidines cytosine (C) and thymine (T), as shown in Scheme 1.1. Also illustrated is the sugar-phosphate backbone, with 2-deoxyribose sugar joined at both the 3'-hydroxyl and 5'-hydroxyl groups to phosphate groups in ester links, also known as "phosphodiester" bonds. DNA nucleoside (base plus deoxyribose sugar) and nucleotide (base plus sugar phosphate) structures are also shown. DNA consists of 2 polymer backbones running in opposite directions, 5'- to 3'- from top to bottom. These chains wind around each other to form a right-handed double helical structure, with about 10 nucleotide pairs per helical turn. Each spiral strand, composed of a

sugar phosphate backbone and attached bases, is connected to a complementary strand by hydrogen (H) bonding between paired bases; A with T (two H bonds) and G with C (three H bonds). Each helical turn contains about ten bases and is 34 Å in length and 20 Å in diameter.

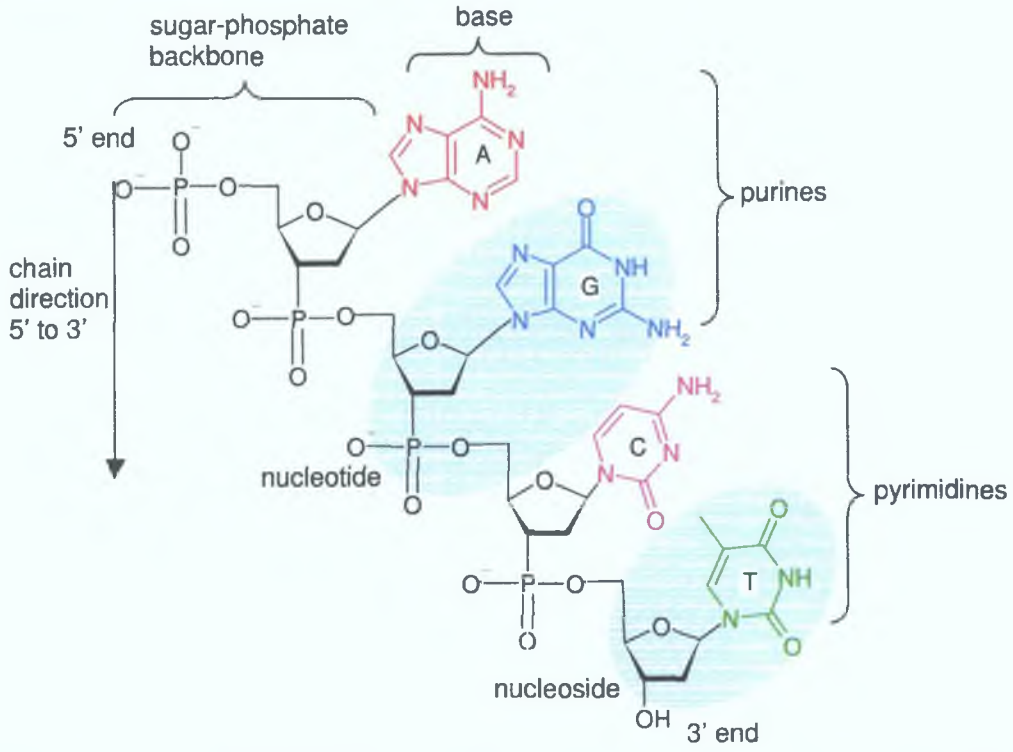

Scheme 1.1: DNA bases adenine (A) depicted in red, guanine (G) depicted in blue, cytosine (C) depicted in pink and thymine (T) depicted in green, and the DNA nucleoside (base plus deoxyribose sugar) and DNA nucleotide (base plus sugar phosphate) structure.

DNA carries information by means of the linear sequence of its nucleotides. Genetic information, contained in the nucleotide sequence, is copied by a process called replication. During this process, the DNA strands in the double helix are separated and each strand serves as a template for production of a new complementary strand. DNA replication is extremely accurate, with fewer than one mistake in 10^9 nucleotides added.[9] When a DNA base has been damaged such that the incorrect base is incorporated opposite it, a mistake, called a mutation, does occur, however. The consequences of this error can be significant, depending on the

function of the DNA in which they occur. A number of mutations can occur, including insertion of a nucleotide into the DNA sequence, deletion of a nucleotide from the sequence, or a point mutation of a single DNA nucleotide within the sequence. A substitution point mutation, when a base pair is exchanged for a different base pair, can be either a transition mutation (where the purine/pyrimidine orientation on a given strand remains the same) or a transversion mutation (where the purine/pyrimidine orientation on a given strand is changed).[10]

1.2.3 Charge transport through DNA

Long range charge transport (LRCT) through DNA has the potential to alter both the nature and the position of the damaged DNA base, and therefore the nature and position of the substitution mutations which occur during replication in DNA, which can in turn alter the consequence of the mutation. Therefore, the extent to which LRCT occurs has been examined in detail in recent years. LRCT is a very controversial subject among scientists. Several recent publications have shifted the debate from *whether* charged species can be transported over long distances, to *how* it takes place.[11] This debate has yielded some very interesting and contentious theories.[12] Underlying the majority of hypothesis proposed for charge transfer are two fundamental mechanisms: superexchange (tunnelling) and thermally induced hopping (TIH). Superexchange charge transfer involves the transfer of charge through DNA bases with a high degree of electronic contact, where the bridge orbitals of intervening DNA bases couple electron donor and electron acceptor. This charge transfer occurs on a nanosecond timescale and its rate, β, decays exponentially with increasing distance. TIH on the other hand displays a very weak dependence on this distance over which the charge transfer occurs, and characterisation of this dependence by β is misleading. In this instance, the electron coupling of the DNA bases between the initial charge donor and acceptor is significantly less than for superexchange, and charge transfer occurs primarily by hopping of the charges along DNA bases, towards the acceptor. Charge transport can involve either electron transport, which involves excess electron propagation through unoccupied DNA orbitals (LUMOs), or hole transport, which involves

propagation of electrons through DNA HOMOs (highest occupied molecular orbitals).[13] Hole migration involves electron transfer from neutral G to neighbouring $G^{+\bullet}$ (G cation radical), as G has the lowest ionisation potential of the four DNA bases (having the lowest HOMO)[14], as shown in Table 1.1.[15]

Table 1.1: Redox potential of the four DNA bases. [15]

DNA base	Redox potential vs. NHE
Guanine	+1.29 V
Adenine	+1.42 V
Cytosine	+1.60 V
Thymine	+1.70 V

Most of the theories that have evolved to explain LRCT involve the participation of these two mechanisms to varying degrees, with a level of agreement emerging that superexchange occurs over less than 4 base pairs, while TIH is the predominant mechanism over longer base sequences. One such theory of LRCT, which incorporates both superexchange and TIH, called "the hopping mechanism" was put forward by Giese *et al.*[16] In this mechanism a cation radical (*e.g.* $G^{+\bullet}$) is generated and injected into the DNA double helix. It then "hops" from G base to G base until it reaches a site of lowest ionisation energy. This was found to be the 5'-G in a GG cluster.[17] As the HOMO resides primarily on the 5'-G of the GG cluster, its ionisation potential (IP) drops from 1.07 V (IP of isolated G) to 0.95 V and its oxidation is enhanced by a factor of 12.[18] The low IP of the 5'-G of the GG cluster makes migration out of it slow, and so the hole is fixed at the cluster for further oxidation. Therefore, at 5'-G, $G^{+\bullet}$ is trapped and oxidative damage occurs here, as shown in Scheme 1.2.

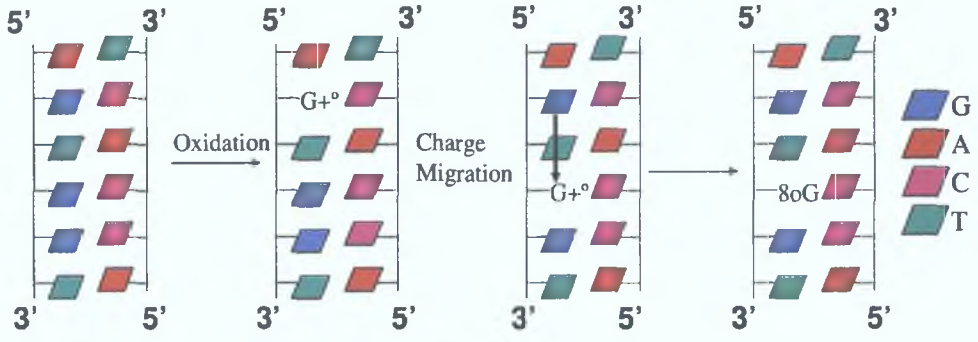

Scheme 1.2: Long range charge transport via the hopping mechanism. (reproduced from Giese et al.[17]*)*

Damage occurs primarily at G, as $G^{+\bullet}$ oxidises primarily G bases. The cation radical is transported by hopping between G bases only. A:T base pairs impede charge transfer, with sequences containing five or more sequential A:T base pairs completely inhibiting the charge transport. LRCT in the hopping mechanism is therefore a series of short-range tunnelling processes (superexchange), and is consequently dependant on the sequence of interspersed base pairs, with the overall rate determining steps of this transport being the largest hop between neighbouring G bases.[19] The overall distance dependence, therefore, is not described by the superexchange mechanism;[20] instead the overall efficiency of the multistep reaction has an algebraic dependence on the number of hopping steps. LRCT was since shown, however, to occur over DNA base sequences of more than five sequential A:T base pairs, and so it was proposed that a change in reaction mechanism, namely from superexchange to TIH, occured.[21] It was proposed that where G was separated by long A:T sequences, endothermic transfer of the positive charge from $G^{+\bullet}$ to adjacent A bases becomes faster than direct transfer to the nearest (but distant) G. A thermally induced hole is injected from $G^{+\bullet}$ to A, followed by hopping between A bases.[22] In this way, hole hopping between G bases connected by an $(AT)_n$ bridge was proposed to occur by superexchange for $n>3$, but by TIH for $n<3$.[23]

In contrast to the hopping mechanism proposed above by Giese *et al.*, where superexchange only occurs over a short number of bases, Barton *et al.*[24] proposed a "superexchange π-way", where superexchange charge transfer is proposed as the predominant LCRT mechanism over the entire DNA duplex. Central to this theory are the electron clouds of the bases in the DNA double helix. The arrangement of these bases allows for electrons shared by multiple atoms to inhabit donut-shaped electron clouds (π-orbitals) above and below each ring of bases within the helix.[25] In this way, the DNA helix can be seen as a stack of π-orbitals, which are in electrical contact with each other, as in Fig. 1.3.

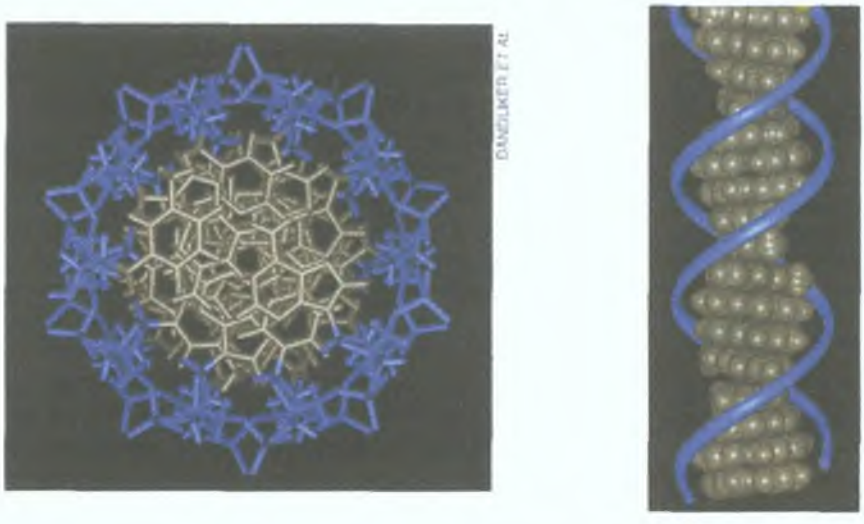

Fig. 1.3: DNA base pairs form a π-stack, shown left looking through the centre of the double helix, and shown right looking along the double helix. (reproduced from Barton et al.[25]*)*

Barton *et al.*[26] proposed that this π-stack acts as a "wire" for electron transfer, having a continuous, delocalised molecular orbital. The Ruthenium (Ru) and Rhodium (Rh) complexes $Ru(phen')(bpy)(dppz)^{2+}$ and $Rh(phi)_2bpy^{3+}$ * were intercalated with the double helix and both complexes oxidised G bases far removed from the site of intercalation, with very little dependence on the distance between the

* phen, phenanthrene; bpy, 4-butyric acid-4'-methylbipryidine; dppz, dipyridophenazine; phi, phenanthrene diimine quinone

metal intercalator and the G site,[24] in extremely fast timescales. The charge could travel over 40 Å in less than 1 ns. G oxidation was, however, profoundly sensitive to the extent of intercalation of the electron donor and the stacking of the DNA bases, with significant reduction of oxidative damage detected when base mismatches were incorporated into the DNA duplex.[27] It was therefore proposed that LRCT had the potential to sensitively detect perturbations in base stacking. The rate of charge transport through the DNA double helix was subsequently found to depend on the energy of the charge donor, with the π-stack, being extremely sensitive to base stack structure and dynamics, able to act as both an insulator and a molecular wire.[28] Low temperature analysis revealed that tunnelling (superexchange) was not solely responsible for the charge transport observed; conformational motion of the DNA duplex was also required. Due to the sensitivity of charge transport to the dynamic structure of DNA, LRCT was proposed to proceed via a process of "domain hopping" – hopping along DNA domains defined dynamically as stacked regions within the duplex through which charge is delocalised along the extended π-orbital.[29]

Charge delocalisation is also central to a hypothesis outlined by Schuster *et al.*, where charge transport was proposed to occur by "phonon-assisted polaron hopping".[30] (A polaron is a radical ion self-trapped by structural distortion of its containing medium.) A cation radical is formed by irradiation of an anthraquinone derivative, which can result in either electron transfer to the DNA double helix, or in hydrogen atom abstraction. However, the dominant pathway was shown to be that of electron transfer to the double helix.[31] The cation radical is injected into the double helix, where it forms a base cation radical, *e.g.* $G^{+\bullet}$ (as in the hopping mechanism). $G^{+\bullet}$ is electron deficient and so the positive charge is stabilised by its delocalisation onto adjacent bases, *i.e.,* by bringing neighbouring bases closer by changing their angle of inclination, and/or unwinding the double helix. This structural distortion of the bases surrounding the radical ion is called a polaron. Thermal (phonon) activation causes base pairs in and near the distortion to join or leave the polaron, and so movement of the charge through the helix is analogous to that of compression in a coiled spring, causing the phonon-assisted polaron hopping, as illustrated in

Scheme 1.3. The hop size of the polaron will be determined by the number of bases required to stabilise the cation charge. The three or four bases involved in the polaron do have π-electron overlap, and so superexchange can occur between these bases, but, Schuster asserts, this is the extent to which the double helix behaves like a molecular wire for electron transport. In contrast to Giese, charge transport was determined to be independent of sequence, and it was concluded that structural averaging of DNA occurs.[32] The DNA double helix was found to be a dynamic structure with an almost liquid-like internal structure, resulting in a mixing of both tunnelling and hopping mechanisms. It was concluded that polaron hopping between GG clusters connected by an $(A)_n$ bridge was proposed to occur by superexchange for $n<3$, where the charge was delocalised on the entire bridge; but TIH predominated for $n>4$, where the bridge was now an intermediate complex and A bases participated as chemical intermediates.[33]

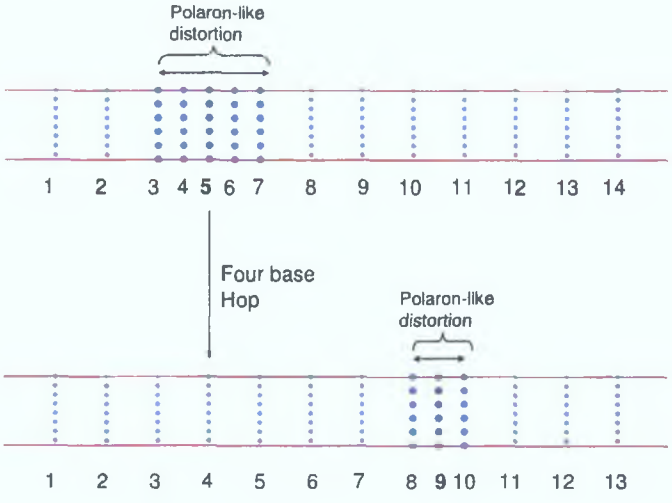

Scheme 1.3: Schematic representation of DNA showing a four base hop of a polaron (reproduced from Schuster et al.[30]) Vertical (blue) lines represent the base pairs, and the horizontal (red) lines represent the sugar-phosphate backbone.

While agreeing that superexchange was the predominant mechanism for charge transfer for short bridges (less than three base pairs), Renger and Marcus proposed that for longer bridges, TIH was not sufficient to explain the LRCT

observed.[34] They proposed that TIH occurred via two channels, partly delocalised (reorganisation energy of the local hole state, $\lambda <$ electronic coupling) and localised ($\lambda >$ electronic coupling) states. The two channels are an approximation for the actual situation in DNA, where one channel exists that contains partly delocalised states, but takes into account a dynamic localisation of states by so-called self-trapping.

A consensus is beginning to emerge between the different mechanisms proposed to explain LRCT. It is now accepted that both superexchange and TIH occur, although the extent of the participation of these two mechanisms is disputed. LRCT is sensitive to the base stack structure, and can be severely impeded by oxidised bases or mismatched base pairs.

1.2.4 DNA damage product 8-oxo-7,8-dihydroGuanine

DNA is of limited stability, and undergoes hydrolysis, oxidation and non-enzymatic methylation at significant rates *in vivo*.[35] It has been estimated that human cellular DNA undergoes over 10,000 oxidative hits per day (~ $9*10^4$ hits/cell/day), based on urine analysis of oxidised G products (the validity of which remains to be verified).[36] Ubiquitous DNA repair processes counteract this damage, but in spite of these, significant steady state levels of damage have been recorded. Steady state levels of oxidative damage are one or more orders of magnitude higher than those of non-oxidative adducts.[3] As discussed in Section 1.1.3, G has the lowest IP of the four DNA bases,[15] and LRCT delivers the charged species, which is capable of inflicting oxidative damage, to G sites in DNA. Its ease of oxidation, coupled with its accessibility via LRCT, make G bases in the DNA double helix the most probable sites for oxidative damage. One of the most potent and well documented (over 1500 publications to date) oxidised G species is 8-oxo-7,8-dihydroGuanine (8-oxoG), which has been linked to mutagenesis, disease and aging.[37]

8-oxoG* was first reported in 1984 by Kasai and Nishimura.[38] Hydroxyl free radicals (•OH) mediate the formation of 8-oxoG via the Udenfriend system (ascorbic acid, Fe^{II}, EDTA, O_2). By using •OH, 8-oxoG was very straightforward to synthesise, its two main differences from its parent base G being that it was slightly less soluble in water due to its additional OH group,[39] and had an ionisation potential about 0.5 V lower than G.[40]

The tautomeric forms of 8-oxoG are shown in Scheme 1.4. The 6,8-diketo form is in the lowest energy state, *i.e.*, is the most stable form of the molecule. [41] The 6-enol, 8-keto form is only slightly less stable, while the 6-keto, 8-enol form is the least stable of the tautomeric forms.

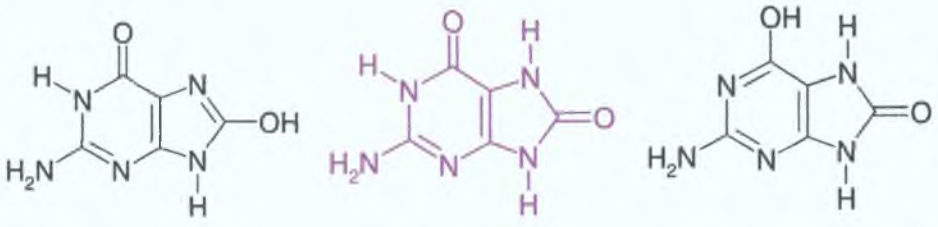

Scheme 1.4: Chemical structures of 8-oxoG, with the most stable form depicted in purple. [41]

The oxidation of G to form 8-oxoG has been well studied, and based on electrochemical studies, it has been concluded that it involves a two proton (2 H^+), two electron (2 e^-) oxidation.[42] It was also observed that oxidation to 8-oxoG occurs over a wide pH range, from pH 2.5 to pH 10.0. The initial reaction involves 1 H^+, 1 e^- oxidation of G to give the free radical, G•, which undergoes further oxidation to give 8-oxoG. The initial step was studied by Weatherly *et al.*,[43] who concluded that both the proton and the electron were removed in a single step, *i.e.*, that it was a proton-coupled electron transfer (PCET) reaction. G could transfer its proton to the

* also known as 8-hydroxyguanine [8-OHG] or 6,8-dihydroxy-6-aminopurine, or in nucleoside form it is normally referred to as 8-oxo-7,8-dihydro-2'-deoxyguanosine [8-OH-dG]

solvent from within the double helix on a time scale that allowed for the coupling of the electron and proton transfers. When G oxidation occurred in a medium that did not accept protons the reaction was slowed dramatically, as it was forced to form a protonated cation radical. A proposed scheme for the two step, 2 H^+, 2 e^- oxidation of G is outlined in Scheme 1.5. Once G has been converted to 8-oxoG, the 8-oxoG is incorporated into the double helix with very few structural perturbations.[44] There is no steric interaction of the 8-oxygen with the phospho-deoxyribose backbone, and 8-oxoG readily forms Watson-Crick base pairs, where the C is opposite it.

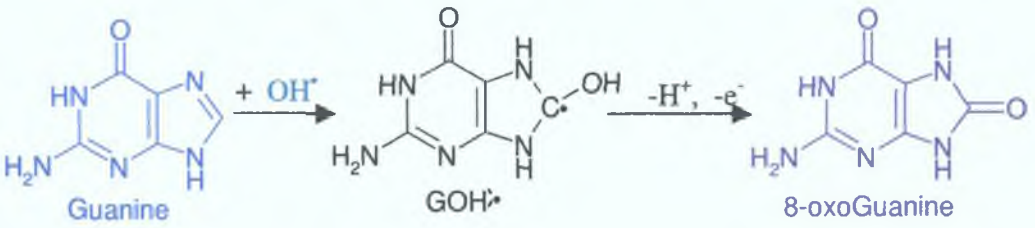

Scheme 1.5: Proposed scheme for guanine (depicted in blue) oxidation to 8-oxo-7,8-dihydroGuanine (depicted in purple).[42]

1.2.5 Mutation effects of 8-oxo-7,8-dihydroGuanine

Three years after they first reported 8-oxoG, in 1978, Kasai and Nishimura were involved in a study to determine if 8-oxoG incorporation led to misreading of the DNA template.[45] They found that 8-oxoG directed the insertion of A, T, G or C (point mutations, both transversion and transition substitution mutations) with almost equal frequencies. Therefore, 8-oxoG completely lacked base pairing specificity. A 1991 publication by Shibutani *et al.*[46] contradicted the earlier findings, suggesting that only C (the correct base pair for G) and A (which would result in a transversion mutation during replication) were incorporated opposite 8-oxoG. It concluded that the Klenow fragment (a DNA polymerase, used to synthesise complimentary strands of DNA *in vitro*), which was used by the earlier researchers was not suitable for synthesis of double stranded DNA from single stranded templates that incorporated 8-oxoG. A year later a research group including Kasai and Nishimura also found that 8-oxoG directed the incorporation of A and C only.[47]

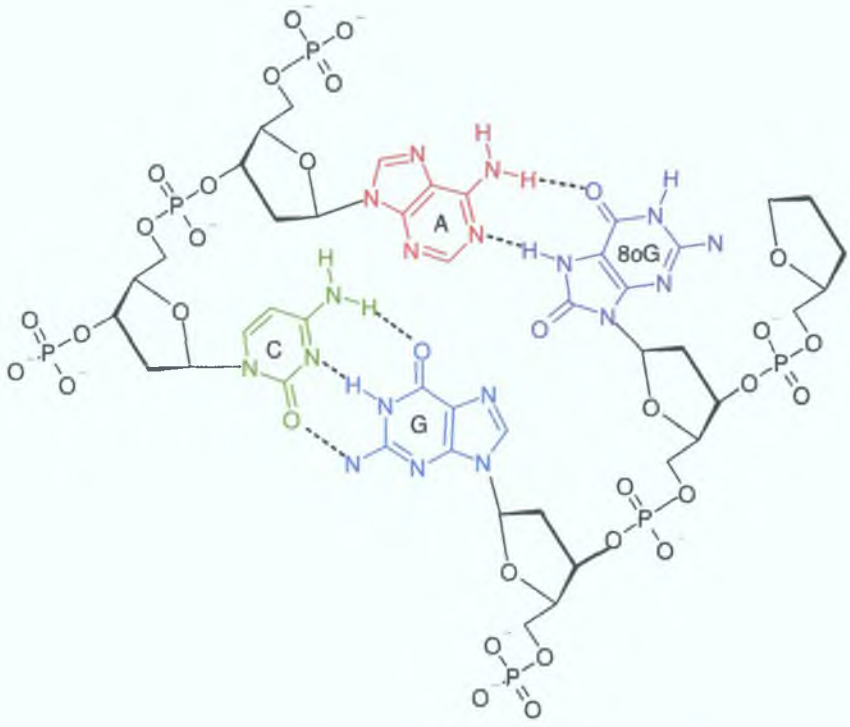

Scheme 1.6: Watson-Crick base pair C:G and base pair A:8-oxoG in helical DNA.[44]

It was found that in 99% of cases, C was incorporated opposite 8-oxoG, and so in these cases there were no long-term effects of G oxidation. In approximately 1% of cases, however, A was incorporated opposite 8-oxoG, which leads to a G:C → T:A transversion mutation[47] (also written as a G → T substitution mutation), which has been implicated in carcinogenesis.[48] The reason for the misincorporation of A opposite 8-oxoG is that the oxidation of G alters the hydrogen bonding functionality of the base, so that it now has the same pattern of hydrogen bond acceptors/donors as T, as shown in Scheme 1.6.[44]

8-oxoG, one of the primary oxidation products of G, can be formed and has mutagenic effects, albeit at a low frequency. This, along with the fact that it is straightforward to measure and is present in sufficient quantities to allow for sensitive measurement, have helped it to become a biomarker for oxidative DNA damage.[2]

1.2.6 8-oxo-7,8-dihydroGuanine reliability as an oxidative DNA damage biomarker

Even before the isolation of 8-oxoG in 1984, it was observed that oxidative damage to DNA might play a major role in cancer, heart disease and aging.[49] By 1989, 8-oxoG had become a biological marker (biomarker) for oxidative DNA damage.[50] Electrochemical detection of the compound in urine using liquid chromatography represented a non-invasive, selective and sensitive means of measurement. It was felt by the authors to be a highly accurate measurement of overall levels of 8-oxoG in the body, as oxidised DNA was being continually repaired, and then the oxidised bases excreted in urine. The validity of urine analysis has yet to be determined, however. During normal cellular function, 8-oxoG is excised instead of being incorporated during DNA replication, and this significant source of 8-oxoG could not reflect DNA oxidation. During the above analysis, however, this source of 8-oxoG was not considered. Enzymatic and chemical oxidation of 2'-deoxyguanosine (dG, G nucleoside) was felt to be unlikely as cytosolic enzymes and cytochrome P-450 did not catalyse its oxidation. Urinary levels of the base 8-oxoG and the nucleoside 8OHdG (8-oxo-7,8-dihydro-2'-deoxyguanosine, 8-oxoG nucleoside) were found to be independent of diet.[51] Control experiments were performed, where radio-labelled deoxyguanosine (dG) was injected intravenously and urine analysed consequently.[50] This did not result in any radio-labelled 8-OHdG; however, no experiments were recorded to test for the presence of the radiolabel in other excreted compounds. When radio-labelled 8-OHdG was injected intravenously, 66% was recovered in urine within 24 hours. The location of the remaining 34%, or the possibility that it could have been degraded was not considered. Based on this analysis it was concluded that humans excreted an average 178 8-OHdG residues per cell per day. A 1990 commentary by Floyd[41] acknowledged that there was very little experimental evidence directly linking 8-oxoG to cancer. He did, however, show a striking correlation between formation of 8-oxoG and carcinogenesis. A range of known cancer-causing agents, from asbestos to radiation to exposure to tumour promoters all resulted in a several-fold increase in

levels of 8-oxoG, often dose dependant. In 1991 it was shown that humans excrete approximately 200 pmol 8-OHdG/kg/day using a more sensitive method of detection than in 1989.[52] As discussed in the next section, however, the levels of human urinary 8-oxoG as detected by HPLC-EC have varied by up to four orders of magnitude.

There are problems, however, with the idea of 8-oxoG as a biomarker for DNA damage. One such problem is that it may be subject to artifactual oxidation, *i.e.,* during sample preparation and pre-concentration G may be oxidised to 8-oxoG to give an artificially high concentration.[53] This has been of huge significance in GC-MS analysis where derivatisation has created considerable amounts of artifactually oxidised 8-oxoG.[54] Hydrolysis of G nucleotides in the DNA precursor pool has been proposed as a possible source of urinary 8-oxoG, which would not reflect DNA oxidation.[55] Measuring solely 8-oxoG as a marker for oxidative DNA damage can be misleading. It is only one of about 60 products of DNA oxidation formed, and is not always one of the main oxidative products produced, in which case an increase in oxidative damage would not be highlighted as the levels of 8-oxoG may not increase.[56] It must also be considered that a decrease in 8-oxoG levels excreted may not necessarily be due to a decrease in oxidative damage; it could also indicate an increased rate of oxidative damage repair, *e.g.* ascorbate intake may stimulate DNA repair, and so lower steady state levels of 8-oxoG. Also worth noting is that while 8-oxoG can mediate G $\rightarrow$ T substitutions during DNA replication, this is not the only pathway by which these mutations can occur. In addition, a question of critical importance which has yet to be answered is that of cause and effect: does oxidative DNA damage initiates the disease process or is just a by-product of the disease?[57] Another major problem utilising 8-oxoG as a biomarker for DNA damage is also coming to light. As a base adduct with a lower IP than all four unmodified bases, it is most easily oxidised. When incorporated into the DNA double helix, it has been identified as a 'hot spot' for further DNA oxidation.[58] The products of 8-oxoG oxidation will be discussed further in Chapter 4.

1.3 DNA damage resulting from initial oxidation

Oxidative damage to DNA can occur from a variety of sources, including γ-irradiation, photoionisation, reactive oxygen species (ROS) and a variety of chemicals, some of which are only toxic when metabolised in the human body. A number of oxidative lesions are produced as a result of these oxidative stresses. It is necessary, therefore, to examine each of the oxidative stresses individually, and ascertain what lesions are formed and what damaging effects they exert on DNA. It must be remembered, however, that there is as yet no direct and compelling evidence that oxidative DNA damage is a biomarker for cancer development.

1.3.1 Photoionisation

It is well established that solar radiation is a genotoxic agent.[59] Ultraviolet (UV) radiation is the most harmful and mutagenic component of the solar radiation spectrum, and can be divided into three sections: UVA (315-400 nm), UVB (280-315 nm) and UVC (100-280 nm). UVB is particularly damaging, as DNA bases directly absorb incident UVB photons.[60] UVA light has also been shown to cause cytotoxic (weakly poisonous to living cells) and mutagenic (induce genetic mutations) effects. UVA radiation causes significant oxidative DNA damage, which can generate 8-oxoG by two mechanisms, Type I and Type II.[61] In Type I reactions a base cation radical (particularly $G^{+\bullet}$) is formed by electron transfer from the base to an excited photosensitiser. Type II mechanisms can be divided into two subsections, major pathways and minor pathways. The major pathway involves the formation of singlet oxygen ($^1O_2$) by energy transfer from an excited photosensitiser to molecular oxygen. The electron transfer to molecular oxygen generates $O_2^{\cdot-}$ and hydroxyl radicals (•OH) via the minor pathways. Direct production of •OH is rarely observed, but may be generated by electron transfer, which can generate $O_2^{\cdot-}$, followed by formation of H_2O_2 and its subsequent decomposition to form •OH.[62]

In Type I mechanisms the large range of excited photosensitisers that act as electron acceptors can include riboflavin (Vitamin B_2)[63] and pterins.[64] When calf thymus (ct) DNA was exposed to visible light in the presence of riboflavin, 8-oxoG was generated. Subsequent experiments which utilised $^1O_2$ and •OH scavengers did not decrease the levels of 8-oxoG produced, suggesting that neither of the ROS were involved in its formation.[63] The presence of FapyG (along with 8-oxoG and Oxazolone, Oz) also excluded $^1O_2$ as a potential ROS.[65] A later investigation of photoirradiated DNA in the presence of riboflavin also showed the generation of 8-oxoG.[66] In this study, however, 8-oxoG was established as only a minor product of the oxidation, with Imidazolone, Iz, which was subsequently shown to be a precursor to Oz,[67] identified as the major product formed. When DNA was exposed to 365 nm light in the presence of pterin, 6-carboxypterin, biopterin, neopterin and folic acid; 8-oxoG was again generated.[64] 8-oxoG formation was specific to G located 5' to G, which is often considered a signature for LRCT within DNA,[68] and so a Type I mechanism was proposed as the probable mechanism for the 8-oxoG lesions formed. Indeed photoirradiation of DNA was used by Giese,[16] Schuster[30] and Barton[24] to probe for long-range electron transport. Barton was also involved in a study of photoirradiation of DNA in the presence of ethidium bromide, which binds to the major groove of DNA.[69] This also resulted in a Type I mechanism for 8-oxoG formation.

Type II mechanisms involve ROS, primarily $^1O_2$. UV irradiation of ct DNA at 254 nm produced a dose dependant generation of 8-oxoG, up to a concentration of approximately 2.5% of G present. [70] When •OH scavengers were used, an increase in the level of 8-oxoG detected was observed, and the use of deuterium oxide (D_2O), which prolongs the half-life of $^1O_2$, also substantially increased the 8-oxoG yield. It was therefore concluded that $^1O_2$ was the major oxidation pathway, with oxidation by •OH possibly a minor pathway.[37] Type II photooxidation was shown to result in 4R* and 4S* diastereoisomers of spiroiminodihydantoin (Sp), cyanuric acid (Cy) and Oz during 8OHdG oxidation, but oxaluric acid (Oxa) and its precursor parabanic acid (Para) were generated when DNA itself was oxidised. [60]

UVB radiation results in a range of dimeric pyrimidine lesions produced by direct absorption of incident photons.[60] The major lesions were cyclodibutadipyrimidines, caused by the cycloaddition of C5-C6 double bonds of adjacent pyrimidine bases.[71] These were found to be mutagenic 'hot-spots' for C:C→T:T transversions.[59] 8-oxoG was also formed, but was at least two orders of magnitude lower than by major type II pathways.

1.3.2 γ-irradiation

In 1985, a year after it was first reported in DNA, 8-oxoG was isolated and characterised from γ-irradiated G, 2-deoxyguanosine-5'-monophoshate (5'-dGMP, G nucleotide) and DNA.[72] Samples were irradiated in a ^{60}Co γ source. The same source was used to irradiate female mice, after which HeLa cells from their liver were isolated and analysed for 8-oxoG lesions.[73] A yield of 0.032 8-oxoG/10^5 G/krad was recorded for *in vivo* γ-irradiated samples. This was three orders of magnitude lower than *in vitro* γ-irradiated samples, however, suggesting that there must be mechanisms for the prevention of 8-oxoG and/or its repair in intact cells. Further evidence for *in vivo* repair was the fact that 8-oxoG produced in liver DNA by the γ-irradiation of mice decreased with time, *i.e.*, as the time between irradiation and liver isolation increased, the level of 8-oxoG decreased.

Unlike photoionisation, the major mechanistic pathway of γ-irradiation is not the oxidation of the G base. 5-hydroxy-5-methylhydantoin, thymine glycol, 5-hydroxyhydantoin, 5-(hydroxymethyl)uracil, 5,6-dihydroxycytosine, cytosine glycol, 4,6-diamino-5-formamidopyrimidine (FapyA), 8-oxo-7,8-diydroadenine (8-oxoA), and 2,6-diamino-4-hydroxy-5-formamidopyrimidine (FapyG) in addition to 8-oxoG have been isolated from chromatin of γ-irradiated cultured human cells.[74] Yields of G derived bases (FapyG and 8-oxoG) constituted about 45% of the net modified bases, the rest of which consisted of A, C and T derived bases in approximately equal quantities. The modified bases were typical of those normally produced by •OH attack on DNA bases, indicating its possible involvement. The G derivative FapyG is produced by G8OH• reduction, whereas 8-oxoG is generated on

oxidation of G8OH•. A study comparing the yields of both in γ-irradiation[75] concluded that the presence of oxygen favoured the formation of 8-oxoG at the expense of FapyG. Purging with nitrogen to remove oxygen increased the levels of FapyG at the expense of 8-oxoG. 8-oxoG incorporation into oligodeoxynucleotides was shown to result in damage 'hot-spots' for γ-irradiation,[58] *i.e.*, when irradiated with ^{60}Co, most of the ensuing damage occurred at 8-oxoG. During these experiments, the DNA was in the form of a dry film, and not in solution.

1.3.3 Chemical oxidation

Chemical oxidation can occur via chemicals that exist in the human body, or via chemicals that can enter the human body that are themselves toxic or can be metabolised to a toxic form *in vivo*. The naturally occurring amino acid 3,4-dihydroxyphenylalanine (DOPA) was shown to mediate DNA damage.[76] Exposure of ct DNA to free DOPA, insulin-bound DOPA and BSA-bound DOPA caused no significant damage, but when Cu(II) was added to the reaction mixture a significant formation of 8-oxoG and 5-hydroxycytosine was recorded. Investigations indicated that DOPA triggered the reduction of Cu(II) to Cu(I), catalysing the generation of •OH. Estrogens with a catechol structure, shown in Scheme 1.7, were also shown to induce DNA damage in a number of ways.[77] These estrogens were shown to enhance endogenous DNA adducts, generate free radicals by redox cycling between their quinone and hydroquinone forms, and induce free radical damage to DNA such as single strand breaks, and the formation of 8-oxoG.

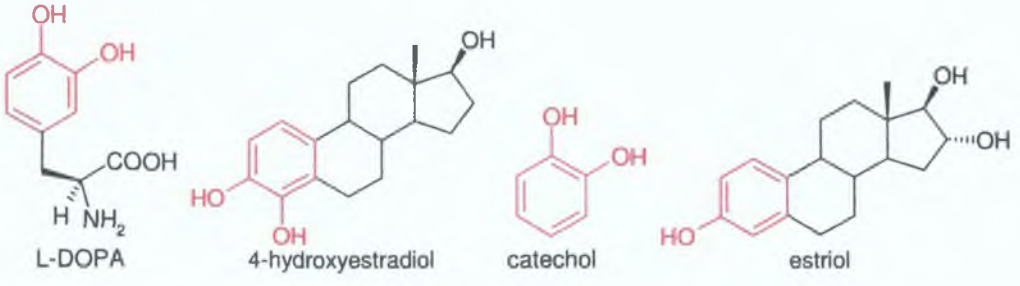

Scheme 1.7: Structure of L-DOPA, 4-hydroxyestrogen, catechol, estriol. [76]

Estrogens retaining the catechol structure were also shown to induce strand breaks in plasmid DNA and ct DNA, and to generate 8-oxoG when in the presence of EDTA-Fe(II).[78] No significant damage was caused, however, in the presence of ADP-Fe(II), possibly due to the stronger chelation agent. Estrogens which did not contain the catechol structure caused no significant damage. Catecholamines were also found, in the presence of chromium, to generate oxidative DNA damage.[79] Transition elements, particularly copper, were also responsible for enhancing the oxidative DNA damage generated by a number of carcinogenic chemicals, including 4-aminobiphenyl (rubber antioxidant),[80] ethylbenzene (air pollutant)[81] and acetamide (solubiliser and plasticiser).[82] A number of chemicals may also be metabolised to toxic forms *in vivo*, including DEB (diepoxybutane, used in rubber production),[83] HAAs (heterocyclic aromatic amine, mutagen caused by cooking proteinaceous food)[84] and styrene.[85,86]

1.3.4 Reactive Oxygen Species

Oxygen is essential for normal respiratory function; however, it has many toxic effects.[87] Many of the damaging effects of oxygen can be attributed to the formation of O_2 radicals *in vivo*.[88] In its natural state, the two outermost electrons of O_2 are unpaired and are located singly in two π^* 2p orbitals, and so have parallel spins. An input of energy can cause the two electrons to reside in a single π^* orbital, resulting in the generation of singlet oxygen ($^1O_2$). Two forms of $^1O_2$ are possible, however, the higher energy triplet state ($^3\Sigma_g^-$) is only observed in gaseous molecules, and so the lower energy state ($^1\Delta_g$) is normally only considered for aqueous solutions.[89] This highly oxidising molecule is very unstable and rapidly decays back to O_2. If O_2 accepts a single electron, that electron enters one of the π^* orbitals to fill it. The other π^* orbital still has a lone electron. This compound is known as superoxide and is a weak oxidising agent. If another electron is added the second π^* orbital is filled and no unpaired electrons remain. The resulting peroxide ion, O_2^{2-} is immediately protonated at physiological pH to form hydrogen peroxide, *e.g.* by the action of superoxide dismutase. Scheme 1.8 outlines the electron configuration for the various states.

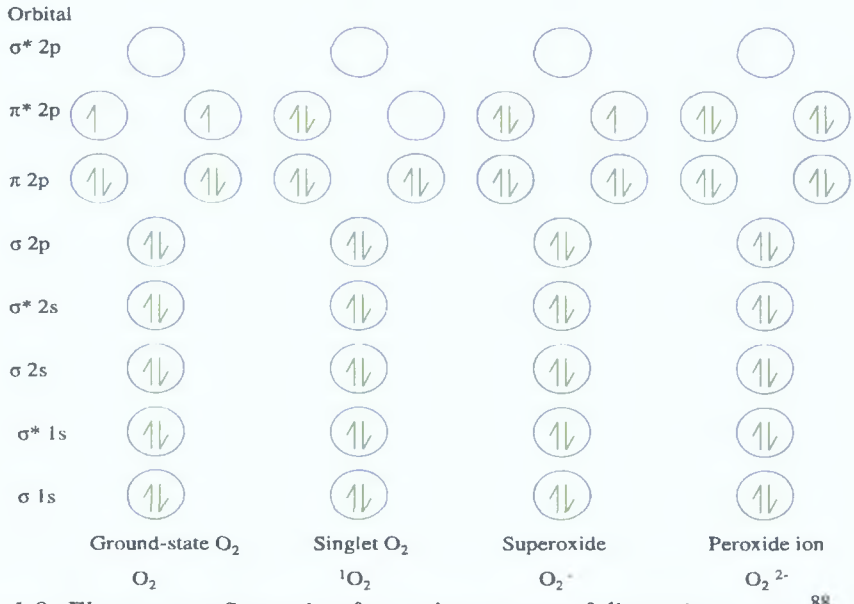

Scheme 1.8: Electron configuration for various states of diatomic oxygen. [88]

H_2O_2 decomposes upon heat or ionising radiation to produce two hydroxyl radicals (•OH), according to Reaction 1.1;

$$H_2O_2 \xrightarrow{\Delta} 2HO\cdot \qquad \text{(Reaction 1.1)}$$

With the availability of ROS via normal cellular metabolism *in vivo*, antioxidant defences have evolved to protect against ROS. Oxidative stress therefore only occurs when these defence mechanisms do not fully protect against ROS. Of critical importance is the level of oxidative stress produced.[90] Very low levels may be efficiently repaired, while very high levels may lead to cell death, so that initiated cells (the first step of carcinogenesis) do not remain in the organism. Intermediate levels of oxidative base lesions are therefore more likely to have a mutagenic effect. Another important feature of ROS is that, by reaction with non-radical species they generate new radicals, and so start chain reactions.[91] In a recent study, ROS were found to attack the ROS-generating cell in order to increase 8-oxoG formation in a study with leukaemia cells. Therefore 8-oxoG formation could be induced in cellular DNA without the need to add considerable amounts of ROS.[92] ROS have also been implicated in 60-70% of DNA strand breaks in radiation-induced carcinogenesis.[93]

DNA isolated from cells and tissues has provided information about the nature of ROS involved in the damage to DNA *in vivo*, *e.g.*, DNA isolated from people suffering from Alzheimer type senile dementia were shown to have a pattern of purine and pyrimidine damage that suggested attack by •OH, while cells isolated from Parkinson's disease patients showed selective oxidation of G,[55] which indicated that $^1O_2$ damage may have occurred.

1.3.4.1 Hydroxyl Radical

•OH is probably the most noxious of the ROS generated from O_2, reacting directly with all known biomolecules at diffusion limited rates (~ 10^7-10^{10} $M^{-1}s^{-1}$).[94] It is the most electrophilic radical to which DNA is normally exposed.[95] It is also the only oxygen radical that has a strong tendency for both addition across a double bond and hydrogen abstraction. •OH also has high thermokinetic reactivity, *i.e.*, when it reaches a reaction site such as a DNA base, it has the thermokinetic energy to add to it. All components of the highly electron dense DNA are subject to •OH attack: the deoxyribose backbone, the purine bases and the pyrimidine bases.[91] At least four types of damage may be generated by this radical, including oxidised bases, abasic sites, strand breaks and DNA-protein cross links.[96]

About 20% of •OH radicals attack the deoxyribose sugars of the DNA backbone, extracting hydrogen from the carbon atoms, with extraction at the C4 position probably the most important process.[97] This causes single strand breaks, which are usually not lethal to the cell, but may cause a mutagenic effect.

The numerous lesions to all four DNA bases have become a signature for its attack. In Thymine there are two sites for •OH addition, the C5-C6 double bond.[98] The •OH binds preferentially at C5, (approximately 60% of addition takes place here) as this is the site of highest electron density. However, the methyl group sterically hinders addition at C5, and so a relatively high level (~ 31%) of addition takes place at C6. The remaining 9% of •OH abstracts H^+ from the methyl group.

Different oxidative lesions are formed under both anaerobic and aerobic conditions,[97] as seen in Schemes 1.9 and 1.10 respectively.

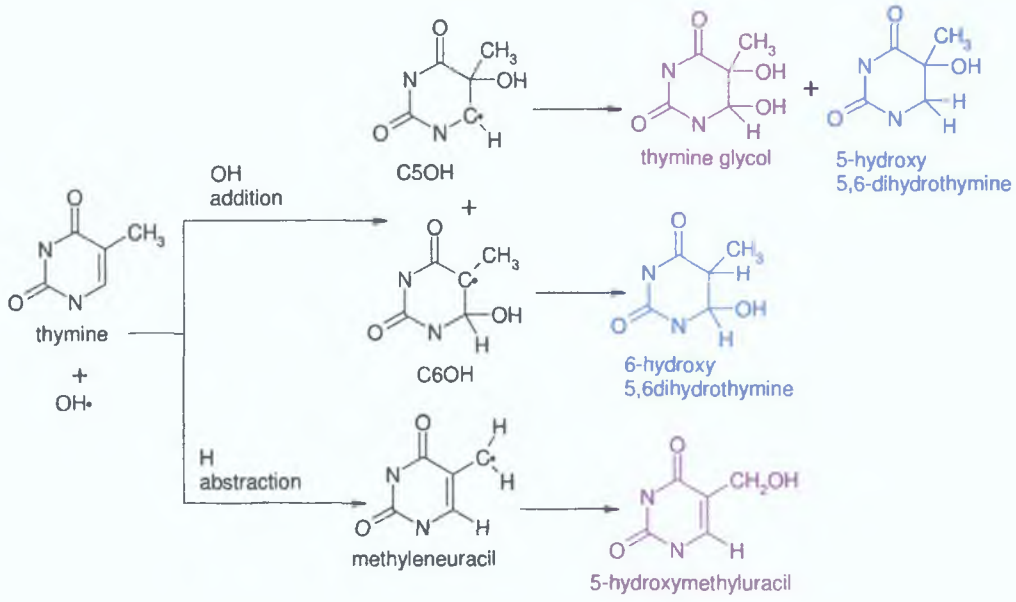

Scheme 1.9: Thymine lesions generated under anaerobic conditions by attack of •OH.[97] *Bases depicted in purple are also generated in aerobic systems; bases depicted in blue are only generated under anaerobic conditions.*

Under anaerobic conditions the major C5OH adduct is further oxidised at C6 and the resulting cation quenched with water to generate 5,6-dihydroxy-5,6-dihydrothymine (thymine glycol), or a proton is abstracted from DNA to give 5-hydroxy-5,6-dihydrothymine. The minor C6OH lesion is reduced to form 6-hydroxy-5,6-dihydrothymine. The radical formed by proton abstraction from the methyl group (methyleneuracil radical) is oxidised to generate 5-hydroxymethyluracil.

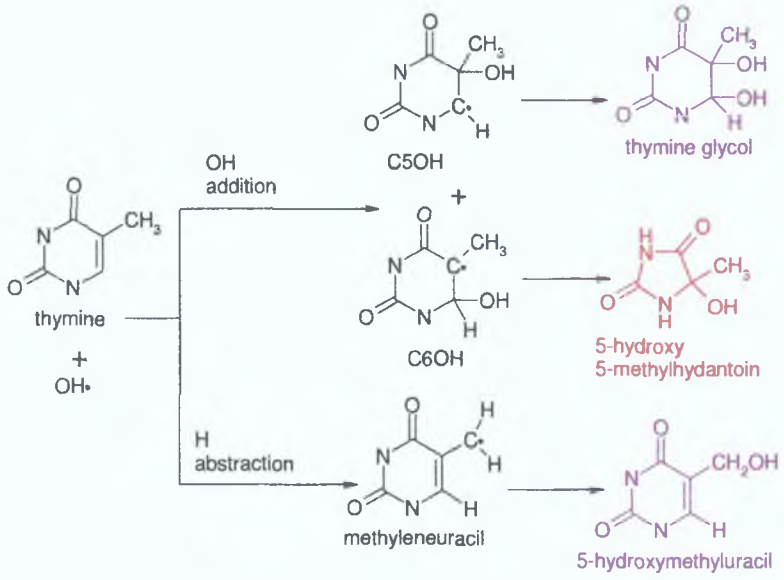

Scheme 1.10: Thymine lesions generated under aerobic conditions by attack of •OH.[97] *Bases depicted in purple are also generated in anaerobic systems; bases depicted in red are only generated under aerobic conditions.*

Under aerobic conditions, thymine glycol and 5-hydroxymethyluracil are again observed. The C5OH, C6OH and methyleneuracil intermediates can also be decomposed to give 5-hydroxy-5-methylhydantoin and 5-hydroxymethyluracil.

Cytosine chemistry is quite similar to that of Thymine. C5-C6 is again the predominant site for proton or •OH addition, but the double bond between N3 and C4 is also a potential additional reaction site.[99] As with Thymine, different lesions were formed under anaerobic and aerobic conditions, as shown in Scheme 1.11. No evidence for addition at C4-N3 was found. Again the C5 position of the C5-C6 was found to be the preferential reaction site, with approximately 87% of additions taking place here. The C5 radical was found to have reducing properties while the C6 radical is a weak oxidant.

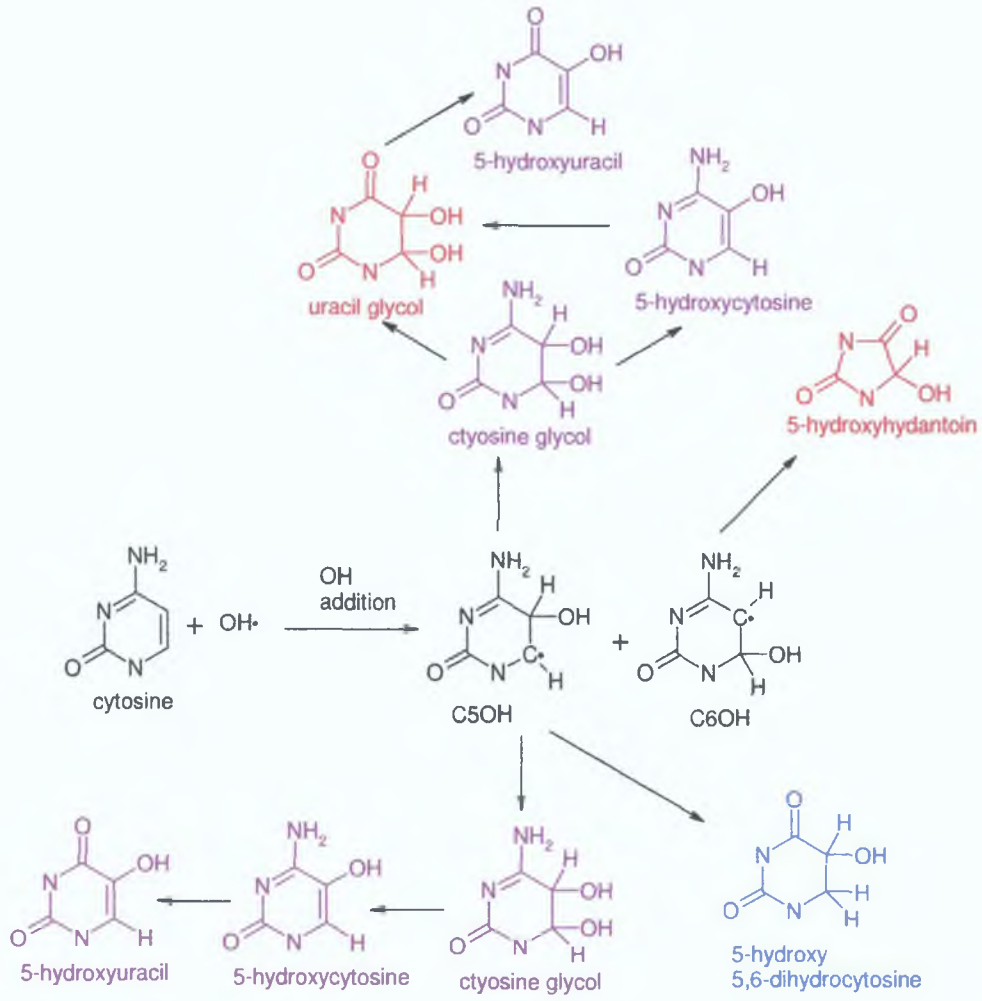

Scheme 1.11: Cytosine lesions generated under anaerobic and aerobic conditions by attack of •OH.[97] *Bases depicted in purple are generated in both systems, bases depicted in red are generated in aerobic systems only, bases depicted in blue are formed in anaerobic systems only.*

In both systems the major product formed is 5,6-dihydroxy-5,6-dihydrocytosine (cytosine glycol), which is formed in an analogous manner to thymine glycol. This dehydrates to 5-hydroxycytosine. Under anaerobic conditions 5-hydroxy-5,6-dihydrocytosine is formed, again by analogy to Thymine. This rapidly deaminates to 5-hydroxy-5,6-dihydrouracil (not shown in Scheme 1.11). In oxygenated systems cytosine glycol can deaminate to give uracil glycol, which in

acidic conditions can lose water to form 5-hydroxyuracil. As with Thymine, hydroperoxides may be formed that decompose to 5,6-dihydroxyuracil and 5-hydroxyhydantoin.

A large number of lesions have also been reported for the purine bases Adenine and Guanine. Purine OH adducts, however, demonstrate a phenomenon called "redox ambivalence", *i.e.,* they are mesomeric structures that are easily oxidised and reduced.[100] Therefore the relative yields of each lesion formed cannot be obtained using a mass balance. •OH adds to C4, C5 and C8 of guanine. C8OH is probably the most studied adduct, and exhibits redox ambivalence. Reduction of C8OH gives a formamidopyrimidine (FapyG), while oxidation results in 8-oxoG. Interestingly, the adducts formed at C4 and C5 may decay back to form the original base, in a type of "auto-repair" mechanism, as a minor reaction.[97] In addition, oxidation products such as Imidazolone and Oxazolone are generated as a major reaction of the neutral radical G(-H)•.[101] Due to the minor repair reaction therefore, although addition at C8 can account for just 25% of the •OH addition,[100] it can generate a significantly higher amount of base lesions. H extraction from a Guanine sugar at C5 can cause a cyclic adduct with the Guanine base itself, 8,5'-cyclo-2'-deoxyguanosine. In the presence of O_2, however, this reaction is suppressed, as it reacts with the sugar radical before it can cyclise.[97] Intermediates and adducts of Adenine are analogous to that of Guanine, though their redox properties differ slightly.[100] •OH radicals have been found to add to C4 (82%) and C8 (18%). As with G, the C4OH adduct regenerates the base itself. C8OH, also redox ambivalent, reduces to form FapyA and 8-oxoA. A cyclic adduct analogous to Guanine, 8,5'-cyclo-2'-deoxyadenosine, is also generated, but again this is a minor product under aerobic conditions.[97] The lesions generated by •OH addition to Guanine are shown in Scheme 1.12.

•OH on average travels of maximum of 3 nm *in vivo* (about 5-10 molecular diameters) before it reaches a molecule with which to react, and cannot cross biological membranes.[94] Therefore it can only inflict damage on DNA if it is

generated in very close proximity to the double helix. H_2O_2, a precursor for •OH, can, however, cross biological membranes, and so if a metal catalyst is localised very close to DNA, •OH can be generated close enough to inflict oxidative damage.[90] The major endogenous source of •OH within cells is the transition metal-mediated Fenton reaction. H_2O_2 is ubituous in the human body as it is a biproduct of enzymatic reactions.

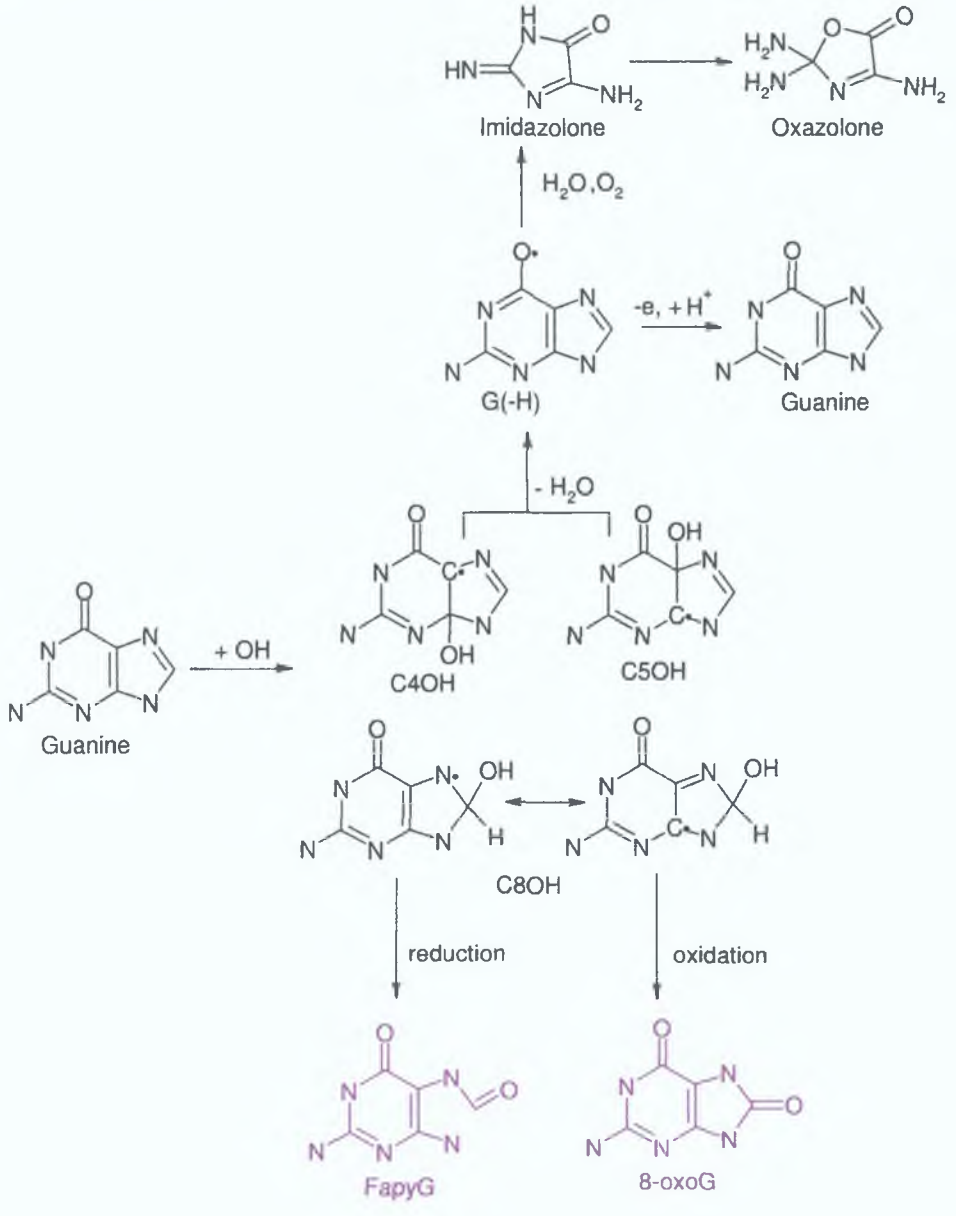

Scheme 1.12: Guanine lesions generated by attack of •OH. [97]

1.3.4.1.1 Fenton reaction

The Fenton reagent is so called after H. J. H. Fenton reported in 1894 that ferrous iron and H_2O_2 reacted with various organic compounds, presumably via the formation of •OH. In 1975 Walling re-examined this reaction as a primary source of •OH-mediated damage to organic substrates.[102] The following model of a Fenton oxidation reaction was proposed, where R is an organic species:

$$H_2O_2 + Fe(II) \xrightarrow{k_1} Fe(III) + HO^- + HO\cdot \quad \text{(Reaction 1.2) } k_1 = 76\ lmol^{-1}s^{-1}$$

$$HO\cdot + Fe(II) \xrightarrow{k_2} Fe(III) + HO^- \quad \text{(Reaction 1.3) } k_2 = 3 \times 10^8\ lmol^{-1}s^{-1}$$

$$HO\cdot + RH \xrightarrow{k_3} H_2O + R\cdot \quad \text{(Reaction 1.4) } k_3 = 10^7\text{-}10^{10}\ lmol^{-1}s^{-1}$$

$$R\cdot + Fe(III) \xrightarrow{k_4} Fe(II) + product \quad \text{(Reaction 1.5)}$$

$$2R\cdot \xrightarrow{k_5} product(\text{dim}er) \quad \text{(Reaction 1.6)}$$

$$R\cdot + Fe(II) \xrightarrow[H^+]{k_6} Fe(III) + RH \quad \text{(Reaction 1.7)}$$

The overall rate limiting step in this reaction is the generation of •OH. Once formed, it reacts at diffusion limited rates, both with further iron(II), and with the organic species, R. R• then can react with ferric and iron(II), and with other R•. It can also react with O_2 as follows:

$$R\cdot + O_2 \rightarrow RO_2\cdot \xrightarrow{Fe(II)} RO_2^- + Fe(III) \quad \text{(Reaction 1.8)}$$

•OH is also capable of reacting with the two starting compounds, as shown:[88]

$$HO\cdot + Fe(II) \rightarrow Fe(III) + HO^- \quad \text{(Reaction 1.9)}$$

$$HO\cdot + H_2O_2 \rightarrow H_2O + H^+ + O_2^- \quad \text{(Reaction 1.10)}$$

$$O_2^- + Fe(III) \rightarrow Fe(II) + O_2 \quad \text{(Reaction 1.11)}$$

If the organic species is guanine, Reaction 1.4 would result in the loss of an electron and a proton, to generate $G^{+\bullet}$, which has been reported as the initial compound generated by one-electron oxidation of G.[43] $G^{+\bullet}$ oxidation in Reaction 1.5 could lead to 8-oxoG, while reduction in Reaction 1.7 could lead to FapyG.[97] Reaction 1.6 involves two radicals reacting with each other to form a dimeric complex. Goyal *et al.*[42] reported a dimer generated by the reaction of $G^{+\bullet}$ and 8-oxo$G^{+\bullet}$, as shown in Scheme 1.13.

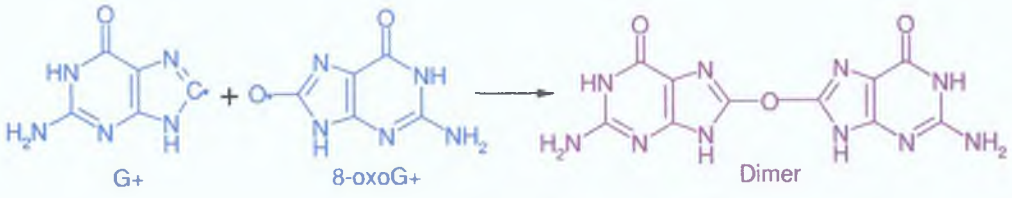

Scheme 1.13: Proposed dimer formation from $G^{+\bullet}$ and 8-oxo $G^{+\bullet}$.[42]

According to Reaction 1.8, a peroxyl radical may also be formed. While none have been isolated to date, Cadet *et al.*[96] suggest that they may be generated from reactions involving the C4OH intermediate. When reactions were carried out in solution saturated with $^{18}O_2$, the ^{18}O atom was incorporated in some of the final oxidation products. This reaction could not be measured by pulse radiolysis, however, suggesting that it occurred at a rate very much slower than 10^7 $lmol^{-1}s^{-1}$.

For the Fenton reaction to mediate DNA damage *in vivo*, both H_2O_2 and iron(II) must be available to react, and must be located adjacent to the DNA base, as the •OH will react with the first biomolecule it encounters.[90] Zastawny *et al.* [103] examined mammalian cells exposed to exogenous iron(II). The •OH scavenger DMSO was ineffective in inhibiting its formation, leading to the conclusion that •OH-mediated damage was caused by a site specific mechanism which involved metal ions bound to the DNA double helix itself. Henle *et al.*[104] showed that Fenton reaction-mediated damage to DNA caused strand breaks selectively at G triplets at

H_2O_2 concentrations of 5-50 mM, and at TGA or TGG sequences at concentrations of 0.05-2.5 mM H_2O_2. It was proposed that the sequence selectivity was due to preferential iron binding at these sequences. This would result in •OH generation also occurring preferentially at these sequences, and therefore any •OH damage would be only be caused in this vicinity. N7 of G is the strongest possible chelation site for transition metals due to its high electronegativity. This binding would be supported by adjacent G bases, and would place the iron in close proximity to the deoxyribose sugar, allowing for strand cleavage to occur. Similarly if the iron bound to the N7 of G in a major groove next to T, it would be close enough to the 2'-deoxyribose sugar to cause strand cleavage without having to distort the double helix. This theory was also supported by an in depth NMR study by Rai *et al.*[105]

The formation of •OH via the Fenton reaction (Reaction 1.2) has not been universally accepted, however. A 1994 kinetic study of the Fenton oxidation mechanism concluded the reaction of iron(II) and H_2O_2 lead to two intermediates; neither exhibiting the reactivity of •OH.[106] Scheme 1.14 outlines the mechanism proposed. Initial reaction of the iron(II) and H_2O_2 generated a metal containing oxidant (k_1), termed X, which was found to be more selective than •OH. This intermediate was then depleted by the competitive reactions of second order processes (k_2) and unimolecular decay (k_3). The decay of X (which is rate limiting) proceeds via a second metal containing oxidising intermediate, Y, which subsequently decays to form Fe(III). Both X and Y were found to be capable of 1 electron oxidation and therefore could be mistaken for •OH. Based on the reactivity of both species, it was proposed that X was probably a peroxo complex, *e.g.* Fe(II)(OOH), and Y an iron(IV)oxo complex, *e.g.* FeO^{2+}.

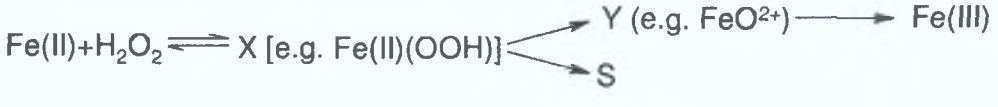

Scheme 1.14: Proposed mechanism for reaction of iron(II) and H_2O_2.[106]

A subsequent publication in 1995 examined the feasibility of the Fenton reaction on thermodynamic grounds.[107] It found that the familiar outer sphere mechanism used to represent the Fenton reaction (Reaction 1.2) was thermodynamically unfavourable and therefore it was felt that it was unlikely to occur. The kinetic likelihood of the reaction occurring was not considered. Instead, an inner sphere mechanism involving the formation of a transient ferrous peroxide complex was proposed, as in Reaction 1.12. This could still result in the formation of •OH, however, as shown in Reaction 1.13 – Reaction 1.15. The effect of the ligand, L, on the nature of the final oxidation product was not investigated in detail.

$$L-Fe(II)+H_2O_2 \rightarrow L-Fe(H_2O_2)^{2+} \qquad \text{(Reaction 1.12)}$$

$$L-Fe(H_2O_2)^{2+} \rightarrow L-Fe(III)+\cdot OH+OH \qquad \text{(Reaction 1.13)}$$

or $$\rightarrow L-Fe(IV)+2OH^- \qquad \text{(Reaction 1.14)}$$

or $$+R \rightarrow L-Fe(III)+OH^- +\cdot ROH \qquad \text{(Reaction 1.15)}$$

Where the compound R is one that can be directly oxidised by $Fe(H_2O_2)^{2+}$, the mechanism may be altered so that very little •OH is produced. Whether •OH is formed depends, however, on the solution composition. •OH generation is usually preceded by reactive intermediates, and it is extremely difficult to discern whether free •OH or a reactive intermediate is generated.[108] Reaction 1.2, the Fenton reaction, is nonetheless generally accepted as a probable mechanism for the production of •OH *in vivo*.[83] Differences between the reaction products of •OH generated by the Fenton reaction and by γ-irradiation of water have been attributed to the presence of a reducing species, *i.e.,* iron(II) in the Fenton reaction.[109]

1.3.4.2 Singlet oxygen

Singlet oxygen, $^1O_2$, has also been implicated in ROS-mediated damage to DNA. Unlike •OH, lesions have not been reported for all four bases; instead G is the main target for $^1O_2$ attack, where it preferentially undergoes cycloaddition. 8-oxoG

is the main adduct reported, a mechanism proposed for its generation is outlined in Scheme 1.15.[62]

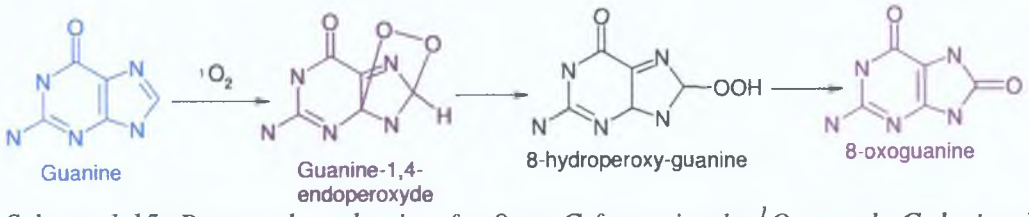

Scheme 1.15: Proposed mechanism for 8-oxoG formation by $^1O_2$ attack, G depicted in blue and 8-oxoG depicted in purple. [62]

It was subsequently proposed that 8-oxoG was not the final product of $^1O_2$ oxidation, but underwent further reaction with $^1O_2$ to generate oxaluric acid via a guanidinohydantoin intermediate, as shown in Scheme 1.16.[110]

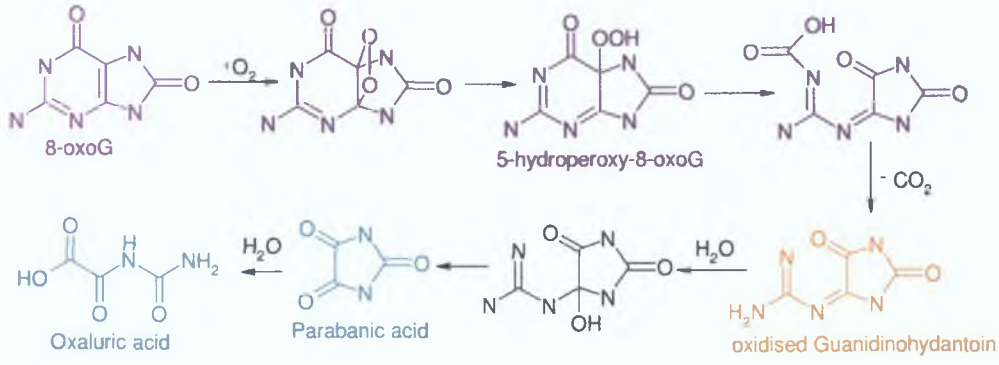

Scheme 1.16: Proposed mechanism for Oxa formation from 8-oxoG by $^1O_2$ attack, 8-oxoG depicted in purple, intermediate oxidised Guanidinohydantoin depicted in orange and final oxidation products depicted in green.[110]

In 1990 Floyd *et al.* noted that they had recently discovered that methylene blue plus light generated 8-oxoG.[37] Because of the absolute dependence on oxygen and the strong D_2O effect it was proposed that $^1O_2$ was involved in the 8-oxoG formation. They subsequently showed that single strand breaks were also generated, but their frequency was approximately 17-fold less than the frequency of 8-oxoG. •OH radicals were ruled out as possible reactants during the oxidation.[111] $^1O_2$ was

demonstrated to selectively target G bases for oxidation in a study of $^1O_2$ induced mutations in mammalian cells.[112] 98.4% of the mutations induced involved G:C base pairs. G:C→T:A transverions were the most frequent mutation (50.8%), followed by G:C→C:G transversions (32.8%).[112]

DNA was irradiated by 254 nm light in a study by Wei *et al.*,[70] which found that 8-oxoG was formed in a dose-dependant fashion. Again •OH was ruled out as the major pathway for the base lesion formation; instead it was proposed that $^1O_2$ was the main mechanism by which damage occurred. (•OH may have been a minor oxidation pathway.) This is in agreement with Type II photoirradiation, which proposes that ROS are involved in oxidative DNA damage by UV light, with $^1O_2$ the major pathway and •OH the minor pathway (see Section 1.3.1). Hickerson *et al.*[113] demonstrated that when 8-oxoG was incorporated into a DNA strand, reactions with $^1O_2$ resulted in oxidation primarily with the 8-oxoG with little sequence selectivity. The reaction was thought to occur via cycloaddition, though no oxidised species were proposed. Oxaluric acid was suggested as a final oxidation species in 2000 by Duarte *et al.*[110] It was proposed that $^1O_2$ oxidation of 8-oxoG occurred via cycloaddition to form 5-hydroperoxy-8-oxoG, which decomposed to give guanidinohydantoin. This was oxidised to parabanic acid, and on further oxidation yielded oxaluric acid, the final product of the $^1O_2$ oxidation.

1.3.4.3 Peroxyl Radical

Very little study has been carried out on peroxyl radicals (ROO•) to date, even though they are present in normal cells at high steady state concentrations, and have a long biological half-life in comparison to the other ROS.[114] ROO• generates adducts with all four DNA bases, though it does not generate as many adducts as •OH, as it is a weaker, more specific oxidant. It oxidises pyrimidines with slightly greater ease than purines. ROO• reacts with the major groove of DNA, avoiding any steric hindrance from Watson-Crick base pairing in the double helix. Reaction with pyrimidines forms the monohydroxy and dihydroxy derivatives. Reaction with the purine bases generates primarily 8-oxoG and 8-oxoA. Adenine-6-hydroxylamine,

production which had not been detected during •OH attack, was also formed via ROO•-mediated oxidation, shown in Scheme 1.17. It was therefore proposed as a biomarker for ROO• oxidation.

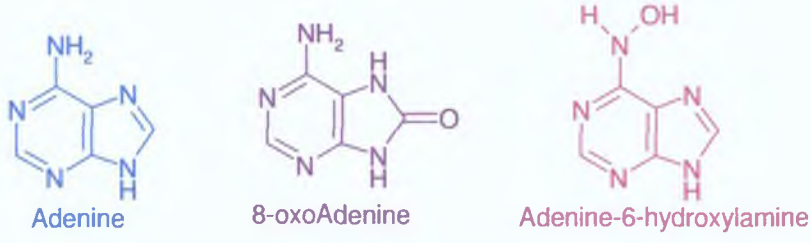

Scheme 1.17: Adenine adducts generated by peroxyl radical attack.[114]

1.3.4.4 Superoxide and Hydrogen Peroxide

Superoxide and hydrogen peroxide have been reported not to undergo any chemical reactions with DNA and therefore cannot be involved in direct attack.[90] They can, however, catalyse the formation of other radicals, such as •OH, that can react directly with DNA, and so they should be considered to be of potential danger to the integrity of the double helix. Superoxide, for example, is reported to be formed from 1-2% of total O_2 consumption, during respiration. This can dismutate (via superoxide dismutases) to yield H_2O_2. The reactivity of H_2O_2, a ubiquitous oxidative species, is primarily due to its reactions with metal ions to produce •OH, which directly react with DNA.[91] It can cross biological membranes, unlike •OH, allowing for •OH formation in close proximity to the double helix. A study of H_2O_2 interactions with DNA disagreed that it did not directly inflict any damage, concluding that it was a very weak oxidant.[115] It concluded that the adduct adenine N-1-oxide was formed by ionic oxidation by H_2O_2 and not by •OH, as it was not formed during hydroxyl radical attack on DNA.

1.4 Methods of detection of DNA damage generated by oxidation

Two main approaches, indirect and direct, have been developed to detect DNA damage.[116] The indirect approach keeps DNA intact, and the oxidative damage is measured using one of two techniques. The first uses biological methods such as Comet or ELISA assays to detect damaged DNA bases by inducing strand breaks where the damaged DNA bases occurred. The second subjects the DNA to repair enzymes, which nick the DNA where adducts have been formed. Gel sequencing techniques are then used to quantify the number of strand breaks. A significant advantage of indirect techniques is the reduced amount of cells required for analysis.[117] The direct approach uses either acidic hydrolysis to release the bases or enzymatic hydrolysis to release nucleosides or nucleotides. The lesions are then separated from unmodified bases and subjected to analysis. A range of techniques can be used for direct analysis, including mass spectrometry, amperometry, and radio-activity (^{32}P-postlabelling). For direct analysis, a sensitivity of at least 1 lesion/10^6 DNA bases is required.[75]

1.4.1 Voltammetric techniques

The electrochemical oxidation and reduction of nucleic acids has become an invaluable tool in the detection of DNA damage.[118-120] Detection of DNA damage involves the immersion of an electrode, which has double stranded DNA immobilised onto its surface, in a solution known to induce DNA damage. The electrode is then immersed in a solution containing complexes that enhance the voltammetric signal generated by the damage. Although electrochemical methods are also capable of measuring base reduction, in the literature two strands of DNA damage detection have emerged, with single strand breaks (SSBs) detected using supercoiled (sc) DNA with mercury electrodes, while base adducts are detected using calf thymus or salmon testes DNA. [121]

sc DNA, immobilised onto a hanging mercury drop electrode (HMDE)* to test for strand cleaving agents, can detect a single strand break in the DNA sugar-phosphate backbone.[118] For example, a sc DNA-modified electrode was immersed into a solution containing the iron Fenton reagents.[122] •OH-mediated single strand breaks were generated in the sc DNA, which caused it to unwind from its tightly bound closed circular form to a much looser open circular (oc) or nicked form. This oc DNA had a much higher a.c. voltammetric response than sc DNA when measured by linear sweep or square wave voltammetry (SWV). The sensitivity of this method was not determined either qualitatively or quantitatively, however, by using any other analytical method. γ-irradiated DNA samples were also nicked to form oc DNA on HMDE electrodes.[123] Adsorptive transfer stripping a.c. voltammograms revealed the presence of a third peak at approximately -1.4 V vs. SCE when the single-strand nicks had been introduced into sc DNA on the electrode surface. When iron was replaced by copper the third peak of the transfer stripping voltammogram was also observed.[124]

Two approaches have emerged for the detection of base adduct formation. In the first approach, linear DNA, either calf thymus or salmon testes, is immobilised onto the surface of a carbon electrode. The electrode is then immersed into suspected toxic chemicals, and subsequently dipped into a solution of DNA intercalators. These intercalators function in one of two ways. Firstly, the intercalators can catalyse the oxidation of damage caused to DNA, so that an increase in voltammetric signal is generated when damage occurs to the double helix which causes single strand breaks or unwinding of the double helix.[125] Secondly, they can bind preferentially with double stranded DNA so that a decrease in signal is recorded for damaged DNA.[126] For the second approach, DNA and a metal catalyst are immobilised on the electrode surface, and immersed in the suspected toxic chemical. Damage to DNA causes an increase in the electrochemical signal of the metal catalyst, detected by SWV.[127] Rusling *et al.* have worked extensively on such

* as mercury is a highly toxic material in modern analysis a suitable alternative to HMDE electrodes should be explored.

sensors, using the toxic compound styrene oxide as a model for their systems.[125,128,129]

The information gained by these voltammetric techniques is limited, however, in that the type of oxidative DNA damage caused can only be quantified. The position of the SSBs in sc DNA or the identity of the base adducts cannot be ascertained. Dennany *et al.*,[130] however, have recently incorporated Osmium, which specifically oxidises 8-oxoG,[131] into polymer films, which are layered with DNA films on modified electrodes, and so have successfully identified both the nature and extent of 8-oxoG generated by the Fenton reaction.

1.4.2 Electrochemical detection with chromatography & electrophoresis

For the separation of 8-oxoG in damaged DNA, two main chromatographic techniques have emerged: high performance liquid chromatography (HPLC) and capillary electrophoresis (CE). Both HPLC and CE techniques have been coupled to electrochemical detectors (EC), with varying degrees of success. EC detection is based on the fact that 8-oxoG has an ionisation potential about 0.5 V lower than G,[40] which itself has the lowest ionisation potential of the four DNA bases.[15] Coupling of EC to HPLC is straightforward, and does not require any interface, as the EC can be connected in series to the UV detector and the eluent flows from the column through both detectors. Coupling to CE, however, is significantly more problematic. Separation by CE is based on a voltage in the order of up to 40 KV being applied to the capillary, while EC detection typically occurs at a potential of less than 1 V (vs. Ag/AgCl). This has resulted in commercial CE systems being completely unsuitable for EC detection. So called "in-house", *i.e.,* homebuilt, systems must be constructed, and the EC detection cell fitted to the capillary in such a way that it remains unaffected by the separation voltage. CE does, however, have a higher separation efficiency than HPLC, and only one extraction step is needed for urine analysis in comparison to the multiple steps needed for HPLC.[132] In addition, CE-EC has the potential to be developed as a microfluidic device, as it does not require any pumps

or elaborate set ups, and both the separation and detection units have successfully been miniaturised separately. This is one of the reasons driving the inherently more difficult CE-EC system.[133,134]

1.4.2.1 HPLC-EC

Two years after it was reported by Kasai and Nishimura,[38] 8-OHdG, in the presence of dG, was sensitively detected in the presence of unmodified bases for the first time by Floyd *et al.*,[135] using HPLC-EC at approximately 0.5 V vs. Ag/AgCl. Also in 1986, 8-OHdG was detected at a background level of 0.6 – 1.4 8-OHdG/10^5 dG (= 1.3 – 3.1 8-OHdG/10^5 nucleosides) in DNA of HeLa and mouse liver cells.[73] Three years later in 1989, 8-OHdG in urine was detected by Shigenaga *et al.* using HPLC-EC for the first time.[50] A series of solid phase extraction (SPE) steps were carried out prior to analysis to separate the 8-oxoG from other urinary constituents. Using this assay it was estimated that humans excrete 168 8-OHdG lesions per cell per day (~ 5.1*10^{15} 8-OHdG/day ~ 130-300 pmol/kg/day).

Ravanat *et al.* [136] determined that the background level of 8-oxoG in rats to be 2 – 5 8-oxoG/10^6 DNA bases, with limit of detection (LOD) of approximately 1 8-oxoG/10^6 DNA bases. The background level of 8-oxoG in human cells is probably between 0.3 – 4.2 8-oxoG/10^6 DNA bases, although the levels measured by HPLC-EC have fluctuated from 0.35 – 2000 8-OHdG/10^6 nucleosides.[137] HPLC-EC is also used for the determination of urinary levels of 8-OHdG. The LOD of 8-OHdG, at 0.4 nM, is over ten fold lower than the reported range in human urine (6.2 – 37.9 nM).[138] Due to the strong interference of uric acid in urine, however, the sensitivity of 8-oxoG detection by HPLC-EC is still too high, with a LOD of 80 nM. Tagesson *et al.*[139] successfully utilised HPLC-EC to examine the levels of 8-OHdG in urine in cancer patients, considering it to be the most sensitive technique to date for quantifying low levels of the lesion. 8-OHdG levels in cancer patients, approximately 40% higher than in healthy individuals, were found to increase by approximately 20% after therapy oncological onset.

1.4.2.2 CE-EC

CE-EC is a recent development, with very few research groups developing in-house systems. Two that have are those of Lunte *et al.* [132] and Inagaki *et al.* [140] In 2000, Weiss and Lunte[132] reported the detection of 8-oxoG in urine using only a single SPE step. This was the first time that nanomolar quantities (approximately 1 8-oxoG/10^6 DNA bases) had been detected using CE-EC. A LOD of 50 nM (S/N=3) 8-OHdG was reported, and the level of 8-OHdG in human urine using the system was measured to be 42 ± 26.9 nM (despite a LOD of 50 nM), using a potential across the electrochemical cell of 0.50 V *vs.* Ag/AgCl. A year later Inagaki *et al.* reported the detection of dG, 8-OHdG and N^2-ethyl-dG using CE-EC.[140] The amperometric detector was set to 1.0 V vs. Ag/AgCl. LODs of $1.0x10^{-6}$ mol/l for dG, $5.9x10^{-7}$ mol/l for 8-OHdG, and $7.9x10^{-6}$ mol/l for N^2-ethyl-dG were reported. This represented a sensitivity about 10-fold lower than that of Weiss and Lunte. This was attributed to the fact that a higher detection potential was used to detect for dG as well as 8-OHdG, hence lowering the S/N. With an LOD of 4.3 nM, (ten fold higher than HPLC-EC) the CE-EC detection of urinary 8-OHdG was successfully demonstrated, concluding that 8-OHdG levels are twice as high in smokers (31.4 ± 18.9 nM) than in non smokers (14.4 ± 7.6 nM).[141]

1.4.3 Mass spectrometry

Mass spectrometry (MS) is normally coupled to either HPLC or gas chromatography (GC) for the detection of DNA damage adducts generated from oxidation. It has the potential to detect all DNA lesions formed, and can provide information about the mass of the lesion and its structure, and so is a much more powerful technique than chromatography alone. In 1985 Dizdaroglu[142] detected not only the four unmodified DNA bases, but also the adducts 5-hydroxy-5,6-dihydrothymine, thymine glycol, 5-hydroxyuracil, 5-hyroxy-5,6-dihydrouracil, 5,6-dihydroxyuracil, 8-oxoG, FapyG, 8-oxoA and FapyA from a single GC-MS run of γ-irradiated ct DNA. In all cases trimethylsilyl (TMS) derivatives were used for MS detection. Subsequently this technique was used to probe for •OH-mediated damage

to DNA in mammalian chromatin.[143] GC-MS allowed this analysis without the need to isolate the DNA from the chromatin. In addition to detecting the base lesions of •OH attack outlined in Section 1.3.4.1, this method also identified damage caused to the sugar backbone of DNA. An LOD of 1 adduct/10^6 nucleotides was achieved, with a sensitivity of approximately 5 fmol/adduct. This method was enhanced with the use of isotope-dilution mass spectrometry to quantitatively assess oxidative DNA damage, where stable isotope-labelled analogues were used as internal standards.[144] The labelled isotope of 8-oxoG, for example, was 8-oxoG-1,3-$^{15}N_2$-(5-amino-^{15}N)-2-^{13}C. By using the isotope 8-[4,5,6,8-$^{13}C_4$]oxoG, the level of 8-oxoG in commercial G was measured as 7.7 ± 1.76 8-oxoG/10^6 DNA bases.[145] This experiment also highlighted one of the biggest problems with GC-MS: artifactual 8-oxoG formation during derivatisation with TMS (also applicable to other base adducts). When the derivatisation temperature increased from 23 °C to 140 °C, the level of 8-oxoG recorded in G soared to 431.4 ± 41.36 8-oxoG/10^6 DNA bases. In a comparison between HPLC-EC and GC-MS, a 50-fold higher level of background 8-oxoG was recorded for GC-MS,[54] even though both systems have comparable LODs (approx 1 8-oxoG/10^6 nucleotides). The unreliability of GC-MS was further illustrated by its failure to detect dose response induced 8-oxoG.[137]

Recently HPLC-MS has emerged as an excellent technique for detecting DNA adducts, being the first technique that allowed for the accurate detection and quantification of dimeric cyclobutadipyrimidines, the primary products of UVB radiation.[71] It avoids the derivatisation process and the artifactual oxidation that accompanies it. An interface is required, however, to ionise the liquid adducts prior to MS analyses. Two techniques, electrospray ionisation (ESI) and atmospheric pressure chemical ionisation (APCI) are commonly used for this ionisation process.[146,147] Comparing HPLC-MS and GC-MS in 2001, Dizdaroglu *et al.* [148] found that the sensitivity of the latter was much greater, even when HPLC-MS/MS (tandem MS) was used. In a separate publication the same year, however, the author reported that the sensitivity of both methods were comparable, with both techniques capable of quantifying base adducts at a level of 1 adduct/10^6 bases, even though

GCMS suffers from significant artifactual oxidation, as previously discussed.[149] Gangl *et al.*[150] increased the LOD significantly of standard MS detection, also in 2001. Using capillary liquid chromatography/microelectrospray mass spectrometry, a LOD approaching 1 adduct/10^9 bases was observed, 1000 times lower than that of previous HPLC-MS or GC-MS (or HPLC-EC), comparable to that of ^{32}P-postlabelling. DNA adducts caused by chemical oxidation by heterocyclic aromatic amines (HAAs) (chemicals found in cigarette smoke and cooked proteinaceous food that may cause genetic damage) were detected using this system. DNA from monkey liver was isolated and enzymatically digested for this analysis, with SPE prior to injection. HPLC-MS/MS, however, is emerging as the method of choice for measurement with enhanced sensitivity, as shown in a 2002 publication by Paehler *et al.* [84] The dual MS detectors result in a massive reduction in background noise, with a concurrant increase in sensitivity. HAA-mediated adducts were again being measured, and a LOD of 1 adduct/10^8 bases was reached. Weimann *et al.*[151] reported the level of 8-oxoG in urine as 212 nmol/day using HPLC-MS, a value comparable to that reported using HPLC-EC. As with CE-EC, however, the LOD for the detection of urinary 8-OHdG, at 3.5 nM, was ten fold higher than HPLC-EC, but still adequate for background 8-OHdG detection.[152]

1.4.4 ^{32}P-postlabelling

^{32}P-postlabelling is one of the most sensitive and widely accepted methods of oxidative DNA damage detection.[153] In ^{32}P-postlabelling, DNA is enzymatically digested to 3'-monophosphates of unmodified nucleosides and adducts, which are then 5'-labeled with ^{32}P by a polynucleotide kinase and [γ-^{32}P]ATP. The adducts are separated using thin layer chromatography (TLC) followed by autoradioactivity,[154] which is capable of detecting 1 adduct/10^7 nucleotides.[155] Analysis of γ-irradiated DNA resulted in a similar sensitivity.[156] These LODs are several orders of magnitudes higher than the theoretical LOD of ^{32}P-postlabelling of 1 adduct/$10^{9\text{-}10}$ nucleotides. The main reasons for this discrepancy are the poor separation of TLC, and the high ^{32}P background.[157] To reduce the practical LOD, HPLC was used for separation in preference to TLC. This resulted in an increase in sensitivity to 26 8-

oxoG/10^8 bases. With enrichment of adducts prior to ^{32}P-postlabeling, an LOD of 1 adduct/10^{9-10} nucleotides is achievable.[158] ^{32}P-postlabelling also suffers, however, from artifactual oxidation due to radioactive decay of the radioactive labels, which has been shown to oxidise neighbouring DNA bases. [159]

1.4.5 Biological assays

Biological techniques used for the determination of DNA adducts include the enzyme linked immunosorbent assay (ELISA) immunoassay and the single-cell gel electrophoresis assay (Comet assay).[137] In 1992 a monoclonal antibody was raised against 8-oxoG, 8-OHG and 8-OHdG.[160] The resulting immunoaffinity column was unsuitable for detecting these adducts in enzymatic digests of DNA, however, as it had a high cross-reactivity to dG. This limited its use to quantifying the biomarkers in biological fluids. A competitive enzyme-linked immunosorbent assay (ELISA) was developed in 1995 for the determination of 8-OHdG.[161] Two monoclonal antibodies were raised against the lesion, but both were found again to cross-react with dG, and several structurally related derivatives. Levels of the 8-OHdG measured by this ELISA were approximately 6 times higher than when measured with HPLC-EC. If, however, urine samples were subjected to preparative HPLC prior to analysis by ELISA, a good correlation was observed between the HPLC-EC and ELISA for levels of 8-oxoG present.[162] The preparative HPLC removes any substances which might cross-react with the 8-oxoG lesion.

The single-cell gel electrophoresis assay is used to measure single strand breaks and alkali labile sites in individual cells.[163] It is commonly known as the comet assay because DNA with increased damage exhibits increased migration from the nucleus of the cell, appearing like a comet tail. In the comet assay, cells are mixed with agarose and then placed on a microscope slide coated with agarose. The cells are lysed and then the DNA migrates out of the cell during electrophoresis which can subsequently be visualised after staining with a fluorochrome dye. This assay can measure as low as 200 strand breaks per cell. This assay was used to demonstrate that nickel chloride at a concentration of 250-1000 μM induced

significant damage to DNA in human lymphocytes.[164] The comet assay was compared to HPLC-EC in 2002 by Gedik *et al.* [165] When measuring 8-oxoG induced by radiation both methods were shown to be equally efficient at detecting the lesions generated, with a good correlation between the mean values recorded for the different samples. There was no correlation, however, between individual values. Formamidopyrimidine DNA gylcosylase (FPG) was used to induce strand breaks at 8-oxoG sites. FPG is not specific to 8-oxoG, however, and also induces SSBs at sites of ring opened pyrimidines (FapyG and FapyA). Therefore, if there is a significant amount of FapyG or FapyA in the DNA, this will lead to an overestimation of the level of 8-oxoG present.[165]

1.5 Conclusions and Thesis Outline

Oxidative DNA damage has been the subject of intensive research, from a range of viewpoints. The endogenous methods by which it may be created have been investigated, with a number of ROS, including •OH and $^1O_2$ subjected to an in depth analysis. The Fenton reaction was shown to be one of the primary methods by which •OH could be generated *in vivo*. A primary product of oxidative DNA damage by such ROS was found to be 8-oxo-7,8-dihydroGuanine, which was formed from the oxidation of the DNA base Guanine. 8-oxo-7,8-dihydroGuanine has been investigated in detail, and it was found to have a lower ionisation potential than any of the unmodified DNA bases, and serves as a 'hotspot' for further DNA oxidation. Studies are being carried out to investigate the oxidation products of 8-oxo-7,8-dihydroGuanine in DNA under continuing oxidative stress. To date, however, no studies have been undertaken to determine the rate of 8-oxo-7,8-dihydroGuanine oxidation under these conditions.

A number of techniques to detect the products of oxidative DNA damage including 8-oxo-7,8-dihydroGuanine, both directly and indirectly, have also been developed. While the indirect approach has the advantage of requiring significantly less DNA for analysis, the direct approach offers unrivalled information of the quantity, nature and structure of any oxidative DNA adducts generated. Of the direct approaches, HPLC, with its ease of coupling to a number of modes of detection, has emerged as the primary method for separating the unmodified DNA bases and any oxidised products generated. The modes of detection used in conjunction with HPLC include EC, MS and ^{32}P-postlabelling. EC can detect 8-oxo-7,8-dihydroGuanine in the presence of significantly higher quantities of other DNA bases, while MS can be used to detect all potential DNA adducts, and can also be used to obtain structural information about the compound being analysed.

The aim of this thesis was to investigate the rate at which 8-oxo-7,8-dihydroGuanine is both generated and further oxidised when DNA was subjected to

continuing oxidative stress, and to identify what, if any products were formed from 8-oxo-7,8-dihydroGuanine oxidation. The Fenton reaction was used to subject DNA to oxidative attack, as this was one of the primary methods suspected of generating ROS *in vivo*. HPLC-EC, as a recognised sensitive and selective technique for the measurement of 8-oxo-7,8-dihydroGuanine, was used to monitor the concentration of 8-oxo-7,8-dihydroGuanine with increasing oxidation. HPLC-MS was used to identify any products of 8-oxo-7,8-dihydroGuanine oxidation.

In *Chapter 2*, DNA was subjected to oxidative stress, via the iron(II)-mediated Fenton reaction, which generated •OH. The concentration of 8-oxo-7,8-dihydroGuanine was monitored with continuing incubation of the DNA with the Fenton reagents. Although overall, its concentration was found to decrease with increasing incubation time, this decrease was not linear, but occurred via a series of oscillations in 8-oxo-7,8-dihydroGuanine concentration. Guanidinohydantoin was identified as a potential product of 8-oxo-7,8-dihydroGuanine oxidation. In *Chapter 3*, DNA was again subjected to oxidative stress, with the copper(II)-mediated Fenton reaction. Again, the concentration of 8-oxo-7,8-dihydroGuanine was found to oscillate with increasing incubation time, but these oscillations differed both in magnitude and period to those observed for the iron(II)-mediated Fenton reaction. It was proposed that the copper(II) Fenton reaction did not generate •OH, but rather $^1O_2$. In *Chapter 4*, the products of both iron(II) and copper(II) Fenton reaction mediated oxidation of 8-oxo-7,8-dihydroGuanine were investigated using HPLC-MS. It was found that it both cases, oxidised Guanidinohydantoin was the primary product formed, and that it was formed in similar magnitudes for both reactions. It was therefore proposed that a similar reactive species was responsible for the oxidation of 8-oxo-7,8-dihydroGuanine in both reactions, and therefore that iron(II) and copper(II) Fenton reactions generated the same reactive species. In *Chapter 5*, oscillatory reactions, which have been investigated in detail in the literature, are discussed. A possible mechanism for the oscillatory behaviour of 8-oxo-7,8-dihydroGuanine with continuing oxidation is proposed, which consists of two competing processes controlled by the concentration of [•OH].

1.6 References

1. http://www.ornl.gov/sci/techresources/Human_Genome/home.shtml; The Human Genome Program of the U.S. Department of Energy Office of Science.

2. Ames, B. N.; Endogenous oxidative DNA damage, aging and cancer, *Free Radical Research Communications* **1989**, *7*, 121-128.

3. Beckman, K. B.; Ames, B. N.; Oxidative decay of DNA, *Journal of Biological Chemistry* **1997**, *272*, 19633-19636.

4. Zubay, G. *Biochemistry*, 3rd ed.; Wm. V. Browne: Dubuque, Iowa, 1993.

5. http://www.nobel.se/medicine/educational/dna/a/transcription/chromatin.html. The Nobel Foundation; 2004, F., Ed., 15 May 2001.

6. http://ww2.mcgill.ca/biology/undergra/c200a/sec2-3.htm. McGill University, Montreal, Quebec, Canada.

7. Watson, J. D.; Crick, F. H. C.; Genetical implications of the structure of deoxyribonucleic acid, *Nature* **1953**, *171*, 964-967.

8. Lertola, J. In *Time*, 2003; Vol. 161.

9. Alberts, B.; Bray, D.; Lewis, J.; Raff, M.; Roberts, K.; Watson, J. D. *Molecular Biology of the Cell*; Garland Publishing, Inc.: New York and London, 1989.

10. http://wiki.cotch.net/index.php/Gene_mutation. Evolution Education Wiki.

11. Jackson, N. M.; Hill, M. G.; Electrochemistry at DNA-modified surfaces: new probes for charge transport through the double helix, *Current Opinion in Chemical Biology* **2001**, *5*, 209-215.

12. Grinstaff, M. W.; How do charges travel through DNA?- an update on a current debate, *Angewandte Chemie International Edition* **1999**, *38*, 3629-3635.

13. Volobuyev, M.; Adamowicz, L.; Computational model of hole transport in DNA, *Journal of Physical Chemistry B* **2005**, *109*, 1048-1054.

14. Yamamoto, K.; Kawanishi, S.; Hydroxyl free radical is not the main active species in site-specific DNA damage induced by copper (II) ion and hydrogen peroxide, *Journal of Biological Chemistry* **1989**, *264*, 15435-15440.

15. Steenken, S.; Jovanovic, S. V.; How easily oxidisable is DNA? One-electron transfer reduction potentials of adenosine and guanosine radicals in aqueous solution Steen Steenken, Slobadan V. Jovanovic, *Journal of the American Chemical Society* **1997**, *119*, 617-618.

16. Giese, B.; Long-distance charge transport in DNA: the hopping mechanism, *Accounts of Chemical Research* **2000**, *33*, 631-636.

17. Saito, I.; Nakamura, T.; Nakatani, K.; Yoshioka, Y.; Yamaguchi, K.; Sugiyama, H.; Mapping of the hot spots for DNA damage by one-electron oxidation: efficiency of GG doublets and GGG triplets as a trap in long-range hole migration, *Journal of the American Chemical Society* **1998**, *120*, 12686-12687.

18. Sistare, M. F.; Codden, S. J.; Thorp, H. H.; Effects of base stacking on guanine electron transfer: rate constants for G and GG sequences of oligonucleotides from catalytic electrochemistry, *Journal of the American Chemical Society* **2000**, *122*, 4742-4749.

19. Giese, B.; Wessely, S.; Spormann, M.; Lindemann, U.; Meggers, E.; Michel-Beyerle, M. E.; On the mechanism of long-range electron transfer through DNA, *Angewandte Chemie International Edition* **1999**, *38*, 996-998.

20. Meggers, E.; Michel-Beyerle, M. E.; Giese, B.; Sequence dependent long range hole transport in DNA, *Journal of the American Chemical Society* **1998**, *120*, 12950-12955.

21. Giese, B.; Amaudrut, J.; Koehler, A.-K.; Spormann, M.; Wessely, S.; Direct observation of hole transfer through DNA by hopping between adenine bases and by tunneling, *Nature* **2001**, *412*, 318.

22. Bixon, M.; Jortner, J.; Long-range and very long-range charge transport in DNA, *Chemcial Physics* **2002**, *281*, 393-408.

23. Berlin, Y. A.; Burin, A. L.; Ratner, M. A.; Elementary steps for charge transport in DNA: thermal activation vs. tunneling, *Chemical Physics* **2002**, *275*, 61-74.

24. Nunez, M. E.; Hall, D. B.; Barton, J. K.; Long-range oxidative damage to DNA: effects of distance and sequence, *Chemistry and Biology* **1999**, *6*, 85-97.

25. Taubes, G.; Double helix does chemistry at a distance - but how?, *Science* **1997**, *275*, 1420-1421.

26. Kelley, S. O.; Jackson, N. M.; Hill, M. G.; Barton, J. K.; Longe-range electron transfer through DNA films, *Angewandte Chemie International Edition* **1999**, *38*, 941-945.

27. Bhattacharya, P. K.; Barton, J. K.; Influence of intervening mismatches on long-range guanine oxidation in DNA duplexes, *Journal of the American Chemical Society* **2001**, *123*, 8649-8656.

28. O'Kelley, S.; Barton, J. K.; Electron transfer between bases in double helical DNA, *Science* **1999**, *283*, 375-381.

29. Williams, T. T.; Dohno, C.; Stemp, E. D. A.; Barton, J. K.; Effects of the photooxidant on DNA-mediated charge transport, *Journal of the American Chemical Society* **2004**, *126*, 8148-8158.

30. Schuster, G. B.; Long-range charge transfer in DNA: transient structural distortions control the distance dependence, *Accounts of Chemical Research* **2000**, *33*, 253-260.

31. Breslin, D. T.; Schuster, G. B.; Anthraquinone photonucleases: mechanisms for GG-selective and nonselective cleavage of double stranded DNA, *Journal of the American Chemical Society* **1996**, *118*, 2311-2319.

32. Henderson, P. T.; Jones, D.; Hampikian, G.; Kan, Y.; Schuster, G. B.; Long-distance charge transport in duplex DNA: the phonon-assisted polaron-like hopping mechanism, *Proceedings of the Natural Academy of Sciences* **1999**, *96*, 8353-8358.

33. Liu, C. S.; Hernandez, R.; Schuster, G. B.; Mechanism for radical cation transport in duplex DNA oligonucleotides, *Journal of the American Chemical Society* **2004**, *126*, 2877-2884.

34. Renger, T.; Marcus, R. A.; Variable-range hopping electron transfer through disordered bridge states: application to DNA, *Journal of Physical Chemistry A* **2003**, *107*, 8404-8419.

35. Lindahl, T.; Instability and decay of the primary structure of DNA, *Nature* **1993**, *362*, 709-715.

36. Ames, B. N.; Shigenaga, M. K.; Hagen, T. M.; Oxidants, antioxidants and the degenerative diseases of aging, *Proceedings of the Natural Academy of Sciences USA* **1993**, *90*, 7915-7922.

37. Floyd, R. A.; West, M. S.; Eneff, K. L.; Schneider, J. E.; Wong, P. K.; Tingey, D. T.; Hogsett, W. E.; Conditions influencing yield and analysis of 8-hydroxy-2'-deoxyguanosine in oxidatively damaged DNA, *Analytical Biochemistry* **1990**, *188*, 155-158.

38. Kasai, H.; Nishimura, S.; Hydroxylation of deoxyguanosine at the C-8 position by ascorbic acid and other reducing agents, *Nucleic Acids Research* **1984**, *12*, 2137-2145.

39. Albert, A.; Brown, D. J.; Purine Studies. Part 1. Stability to acid and alkali solubility. Ionization. Comparison with Pteridines, *Journal of the Chemistry Society* **1954**, 2060-2071.

40. Prat, F.; Houk, K. N.; Foote, C. S.; Effect of guanine stacking on the oxidation of 8-oxoguanine in B-DNA, *Journal of the American Chemical Society* **1998**, *120*, 845-846.

41. Floyd, R. A.; The role of 8-hydroxyguanine in carcinogenesis, *Carcinogenesis* **1990**, *11*, 1447-1450.

42. Goyal, R. N.; Jain, N.; Garg, D. K.; Electrochemical and enzymic oxidation of guanosine and 8-hydroxyguanosine and the effects of oxidation products in mice, *Bioelectrochemistry and Bioenergetics* **1997**, *43*, 105-114.

43. Weatherly, S. C.; Yang, I. V.; Armistead, P. A.; Thorp, H. H.; Proton-coupled electron transfer in guanine oxidation effects of isotope, solvent and chemical modification, *Journal of Physical Chemistry B* **2003**, *107*, 372-378.

44. Lipscomb, L. A.; Peek, M. E.; Morningstar, M. L.; Verghis, S. M.; Miller, E. M.; Rich, A.; Essigmann, J. M.; Williams, L. D.; X-ray structure of a DNA decamer containing 7,8-dihydro-8-oxoguanine, *Proceedings of the Natural Academy of Sciences USA* **1995**, *92*, 719-723.

45. Kuchino, Y.; Mori, F.; Kasai, H.; Inoue, H.; Iwai, S.; Miura, K.; Ohtsuka, E.; Nishimura, S.; Misreading of DNA templates containing 8-hydroxydeoxyguanosine at the modified base and at adjacent residues, *Nature* **1987**, *327*, 77-79.

46. Shibutani, S.; Takeshita, M.; Grollman, A. P.; Insertion of specific bases during DNA synthesis past the oxidation-damaged base 8-oxodG, *Nature* **1991**, *349*, 431-434.

47. Cheng, K. C.; Cahill, D. S.; Kasai, H.; Nishimura, S.; Loeb, L. A.; 8-hydroxyguanine, an abundant form of oxidative DNA damage, causes G T and A C Substitutions, *Journal of Biological Chemistry* **1992**, *267*, 166-172.

48. Strauss, B. S.; The origin of point mutations in human tumor cells, *Cancer Research* **1992**, *52*, 249-253.

49. Ames, B. N.; Dietary carcinogens and anticarcinogens. Oxygen radicals and degenerative diseases, *Science* **1983**, *221*, 1256-1264.

50. Shigenaga, M. K.; Gimeno, C. J.; Ames, B. N.; Urinary 8-hydroxy-2'-deoxyguanosine as a biological marker of in vitro oxidative DNA damage, *Proceedings of the Natural Academy of Sciences USA* **1989**, *86*, 9697-9701.

51. Olinski, R.; Gackowski, D.; Rozalski, R.; Foksinski, M.; Bialkowski, K.; Review: oxidative DNA damage in cancer patients: a cause or a consequence of the disease development?, *Mutation Research/Fundamentals and Molecular Mechanisms of Mutagenesis* **2003**, *531*, 177-190.

52. Shigenaga, M. K.; Ames, B. N.; Assays for 8-hydroxy-2'-deoxyguanosine: a biomarker of in vivo oxidative DNA damage, *Free Radical Biology and Medicine* **1991**, *10*, 211-216.

53. Kasai, H.; Analysis of a form of oxidative DNA damage, 8-hydroxy-2'-deoxyguanosine, as a marker of cellular oxidative stress during carcinogenesis, *Mutation Research/Reviews in Mutation Research* **1997**, *387*, 147-163.

54. Ravanat, J.-L.; Turesky, R. J.; Gremaud, E.; Trudel, L. J.; Stadler, R. H.; Determination of 8-oxoguanine in DNA by gas chromatography-mass spectrometry and HPLC-electrochemical detection: overestimation of the background level of the oxidized base by the gas-chromatography-mass spectrometry assay, *Chemical Research in Toxicology* **1995**, *8*, 1039-1045.

55. Halliwell, B.; Oxygen and nitrogen are pro-carcinogens. Damage to DNA by reactive oxygen, chlorine and nitrogen species: measurement, mechanism and the effects of nutrition., *Mutation Research/Genetic Toxicology and Environmental Mutagenesis* **1999**, *424*, 37-52.

56. Halliwell, B.; Effect of diet on cancer development: is oxidative DNA damage a biomarker?, *Free Radical Biology and Medicine* **2002**, *32*, 968-974.

57. Olinski, R.; Gackowski, D.; Foksinski, M.; Rozalski, R.; Roszkowski, K.; Jaruga, P.; Oxidative DNA damage: Assessment of the role in carcinogenesis, atherosclerosis, and acquired immunodeficiency sydrome (Serial Review), *Free Radical Biology and Medicine* **2002**, *33*, 192-200.

58. Doddridge, Z. A.; Cullis, P. M.; Jones, G. D. D.; Malone, M. E.; 7,8-dihydro-8-oxo-2'-deosyguanosine residues in DNA are radiation damage "hot" spots in the direct radiation damage pathway, *Journal of the American Chemical Society* **1998**, *120*, 10998-10999.

59. Besaratinia, A.; Bates, S. E.; Synold, T. W.; Pfeifer, G. P.; Similar mutagenicity of photoactivated porphyrins and ultraviolet A radiation in mouse embryonic fibroblasts: involvement of oxidative DNA lesions in mutagenesis, *Biochemistry* **2005**, *43*, 15557-25566.

60. Ravanat, J.-L.; Douki, T.; Cadet, J.; Direct and indirect effects of UV irradiation on DNA and components, *Journal of Photochemistry and Photobiology B: Biology* **2001**, *63*, 88-102.

61. Kawanishi, S.; Hiraku, Y.; Oikawa, S.; Mechanism of guanine-specific DNA damage by oxidative stress and its role in carcinogenesis and aging, *Mutation Research/Reviews in Mutation Research* **2001**, *488*, 65-76.

62. Paillous, N.; Vicendo, P.; Mechanisms of photosensitized DNA cleavage, *Journal of Photochemistry and Photobiology B: Biology* **1993**, *20*, 203-209.

63. Kasai, H.; Yamaizumi, Z.; Berger, M.; Cadet, J.; Photosensitized formation of 7,8-dihydro-8-oxo-2'-deoxyguanosine (8-hydroxy-2'-deoxyguanosine) in DNA by riboflavin: a non singlet oxygen mediated reaction, *Journal of the American Chemical Society* **1992**, *114*, 9692-9694.

64. Ito, K.; Kawanishi, S.; Photoinduced hydroxylation of deoxyguanosine in DNA by pterins: sequence specificity and mechanism, *Biochemistry* **1997**, *36*, 1774-1781.

65. Douki, T.; Cadet, J.; Modification of DNA bases by photosensitized one-electron oxidation, *International Journal of Radiation Biology* **1999**, *75*, 571-581.

66. Kino, K.; Saito, I.; Product analysis of GG-specific photooxidation of DNA via electron transfer: 2-amioimidazole as a major guanine oxidation product, *Journal of the American Chemical Society* **1998**, *1202*, 7373-7374.

67. Ravanat, J.-L.; Remaud, G.; Cadet, J.; Measurement of the main photooxidation products of 2'-deoxyguanosine using chromatographic methods coupled to mass spectroscopy, *Archives of Biochemistry and Biophysics* **2000**, *374*, 118-127.

68. Saito, I.; Takayama, M.; Sugiyama, H.; Nakatani, K.; Photoinduced DNA cleavage via electron transfer: demonstration that guanine residues located 5' to guanine are the most electron-donating sites, *Journal of the American Chemical Society* **1995**, *117*, 6406-6407.

69. Hall, D. B.; Kelley, S. O.; Barton, J. K.; Long-range and short-range oxidative damage to DNA: photoinduced damage to guanines in ethidium-DNA assemblies, *Biochemistry* **1998**, *37*, 15933-15940.

70. Wei, H.; Cai, Q.; Rahn, R.; Zhang, X.; Singlet oxygen involvement in ultraviolet (254 nm) radiation-induced formation of 8-hydroxy-deoxyguanosine in DNA, *Free Radical Biology and Medicine* **1997**, *23*, 148-154.

71. Cadet, J.; Sage, E.; Douki, T.; Ultraviolet radiation-mediated damage to cellular DNA, *Mutation Research/Fundamentals and Molecular Mechanisms of Mutagenesis* **2005**, *571*, 3-17.

72. Dizdaroglu, M.; Formation of an 8-hydroxyguanine moiety in deoxyribonucleic acid on γ-irradiation in aqueous solution, *Biochemistry* **1985**, *24*, 4476-4481.

73. Kasai, H.; Crain, P. F.; Kuchino, Y.; Nishimura, S.; Ootsuyama, A.; Tanooka, H.; Formation of 8-hydroxyguanine moiety in cellular DNA by agents producing oxygen radicals and evidence for its repair, *Carcinogenesis* **1986**, *7*, 1849-1851.

74. Nackerdien, Z.; Olinski, R.; Dizdaroglu, M.; DNA base damage in chromatin of ?-irratiated cultured human cells, *Free Radical Research Communications* **1992**, *16*, 259-273.

75. Douki, T.; Martini, R.; Ravanat, J.-L.; Turesky, R. J.; Cadet, J.; Measurement of 2,6-diamino-4-hydroxy-5-formamidopyrimidine and 8-oxo-7,8-dihydroguanine in isolated DNA exposed to gamma radiation in aqueous solution, *Carcinogenesis* **1997**, *1997*, 12.

76. Morin, D.; Davies, M. J.; Dean, R. T.; The protein oxidation product 3,4-dihydrophenylalanine (DOPA) mediates osidative DNA damage, *Biochemical Journal* **1998**, *330*, 1059-1067.

77. Roy, D.; Liehr, J. G.; Estrogen, DNA damage and mutations, *Mutation Research/Fundamentals and Molecular Mechanisms of Mutagenesis* **1999**, *424*, 107-115.

78. Miura, T.; Muraoka, S.; Fujimoto, Y.; Zhao, K.; DNA strand break and 8-hydroxyguanine formation induced by 2-hydroxyestradiol dispersed in liposomes, *Journal of Steroid Biochemistry and Molecular Biology* **2000**, *74*, 93-98.

79. Pattison, D. I.; Davies, M. J.; Levina, A.; Dixon, N. E.; Lay, P. A.; Chromium (VI) reduction by catechol(amine)s results in DNA cleavage in vitro: relevance to chromium genotoxicity, *Chemical Research in Toxicology* **2001**, *14*, 500-510.

80. Murata, M.; Tamura, A.; Tada, M.; Kawanishi, S.; Mechanism of oxidative DNA damage induced by carcinogenic 4-aminobiphenyl, *Free Radical Biology and Medicine* **2001**, *30*, 765-773.

81. Midorikawa, K.; Uchida, T.; Okamoto, Y.; Toda, C.; Sakai, Y.; Ueda, K.; Hiraku, Y.; Murata, M.; Kawanishi, S.; Kojima, H.; Metabolic activation of carcinogenic ethylbenzene leads to oxidative DNA damage, *Chemico-Biological Interactions* **2004**, *150*, 271-181.

82. Sakano, K.; Oikawa, S.; Hiraku, Y.; Kawanishi, S.; Mechanism of metal-mediated DNA damage induced by a metabolite of carcinogenic acetamide, *Chemico-Biological Interactions* **2004**, *149*, 51-59.

83. Packer, L.; Oxygen Radicals in Biological Systems, *Methods in Enzymology* **1984**, *Vol. 105*, 7.

84. Paehler, A.; Richoz, J.; Soglia, J.; Vouros, P.; Turesky, R. J.; Analysis and quantification of DNA adducts of 2.Amino-3,8-dimethylimidazo[4,5-f]quinoxaline in liver of rats by liquid chromatography/electrospray tandem mass spectrometry, *Chemical Research in Toxicology* **2002**, *15*, 551-561.

85. Koshinen, M.; Vodickova, L.; Vodicka, P.; Warner, S. C.; Hemminki, K.; Kinetics of formation of specific styrene oxide adducts in double stranded DNA, *Chemico-Biological Interactions* **2001**, *138*, 111-124.

86. Tarun, M. C.; Rusling, J. F.; Quantitative measurement of DNA adducts using neutral hydrolysis and LC-MS. Validation of genotoxicity sensors, *Analytical Chemistry* **2005**, *77*, 2056-2062.

87. Halliwell, B.; Gutteridge, J. M. C.; Oxygen toxicity, oxygen radicals, transition metals and disease, *Biochemical Journal* **1984**, *219*, 1-14.

88. Halliwell, B.; Gutteridge, J. M. C. *Free Radicals in Biology and Medicine*, 2nd ed.; Clarendon Press, 1989.

89. Martinez, G. R.; Ravanat, J.-L.; Cadet, J.; Miyamoto, S.; Medeiros, M. H. G.; Di Mascio, P.; Energy transfer between singlet ($^1\Delta_g$) and triplet ($^3\Sigma_g^-$) molecular oxygen in aqueous solution, *Journal of the American Chemical Society* **2004**, *126*, 3056-3057.

90. Halliwell, B.; Arouma, O. I.; Review: DNA damage by oxygen-derived species. Its mechanism and measurement in mammalin systems, *FEBS Letters* **1991**, *281*, 9-19.

91. Dreher, D.; Junod, A. F.; Review: Role of oxygen free radicals in cancer development, *European Journal of Cancer* **1996**, *32A*, 30-38.

92. Takeuchi, T.; Nakajima, M.; Morimoto, K.; Establishment of a human system that generates O2- and induces 8-hydroxydeoxyguanosine, typical of oxidative DNA damage, by a tumor promoter, *Cancer Research* **1994**, *54*, 5837-5840.

93. Lunec, J.; Free radicals: their involvement in disease processes, *Annals of Clinical Biochemistry* **1990**, *27*, 173-182.

94. Aust, A. E.; Everleigh, J. F.; Mechanisms of DNA oxidation, *Experimental Biology and Medicine* **1999**, *222*, 246-252.

95. Pryor, W. A.; Why is the hydroxyl radical the only radical that commonly adds to DNA? Hypothesis: it has a rare combination of high electrophilicity, high thermochemical reactivity, and a mode of production that can occur near DNA., *Free Radical Biology and Medicine* **1988**, *4*, 219-223.

96. Cadet, J.; Delatour, T.; Douki, T.; Gasparutto, D.; Pouget, J.-P.; Ravanat, J.-L.; Sauvaigo, S.; Hydroxyl Radicals and DNA base damage, *Mutation Research/Fundamentals and Molecular Mechanisms of Mutagenesis* **1999**, *424*, 9-21.

97. Breen, A. P.; Murphy, J. A.; Reactions of oxyl radicals with DNA, *Free Radical Biology and Medicine* **1995**, *18*, 1033-1077.

98. Fujita, S.; Steenken, S.; Pattern of OH radical addition to uracil and methyl- and carboxyl-substituted uracils. Electron transfer of OH adducts with *N,N,N',N'*,-tetramethyl-p-phenylenediamine and tetranitromethane, *Journal of the American Chemical Society* **1981**, *103*, 2540-2545.

99. Hazra, D. K.; Steenken, S.; Pattern of OH radical addition to cytosine and 1-, 3-, 5-, and 6-substituted cytosines. Electron transfer and dehydration reactions of the OH adducts, *Journal of the American Chemical Society* **1983**, *105*, 4380-4386.

100. Steenken, S.; Purine bases, nucleosides, and nucleotides: aqueous solution chemistry and transformation reactions of their radical cations and e- and OH adducts, *Chemistry Reviews* **1989**, *89*, 503-520.

101. Cadet, J.; Douki, T.; Gasparutto, D.; Ravanat, J.-L.; Review: Oxidative damage to DNA: formation, measurement and biochemical features, *Mutation Research/Fundamentals and Molecular Mechanisms of Mutagenesis* **2003**, *531*, 5-23.

102. Walling, C.; Fenton's reagent revisited, *Accounts of Chemical Research* **1975**, *8*, 135-131.

103. Zastawny, T. H.; Altman, S. A.; Randers-Eichhorn, L.; Madurawe, R.; Lumpkin, J. A.; Dizdaroglu, M.; Rao, G.; DNA base modifications and membrane damage in cultured mammalin cells treated with iron ions, *Free Radical Biology and Medicine* **1995**, *18*, 1013-1022.

104. Henle, E. S.; Han, Z.; Tang, N.; Rai, P.; Lou, Y.; Linn, S.; Sequence-specific DNA cleavage of Fe2+-mediated Fenton reactions has possible biological implications, *Journal of Biological Chemistry* **1999**, *274*, 962-971.

105. Rai, P.; Cole, T. D.; Wemmer, D. E.; Localization of Fe2+ at an RTGR sequence within a DNA duplex explains preferential cleavage by Fe2+ and H2O2, *Journal of Molecular Biology* **2001**, *312*, 1089-1101.

106. Wink, D. A.; Nims, R. W.; Saavedra, J. E.; William E. Utermahlen, J.; Ford, P. C.; The Fenton oxidation mechanism: reactivities of biologically relevant substrates with two oxidizing intermediates differ from those predicted for the hydroxyl radical, *Proceedings of the Natural Academy of Sciences USA* **1994**, *91*, 6604-6608.

107. Winterbourne, C. C.; Toxicity of iron and hydrogen peroxide: the Fenton reaction, *Toxicology Letters* **1995**, *82/83*, 969-974.

108. Goldstein, S.; Meyerstein, D.; Czapski, G.; The Fenton reagents, *Free Radical Biology and Medicine* **1993**, *15*, 435-445.

109. Frelon, S.; Douki, T.; Favier, A.; Cadet, J.; Comparative study of base damage induced by gamma radiation and Fenton reaction in isolated DNA, *Journal of the Chemistry Society, Perkin Transactions 1* **2002**, 2866-2870.

110. Duarte, V.; Gasparutto, D.; Yamaguchi, L. F.; Ravanat, J.-L.; Martinez, G. R.; Medeiros, M. H. G.; Mascio, P. D.; Cadet, J.; Oxaluric acid as the major product of singlet oxygen-mediated oxidation of 8-oxo-7,8-dihydroguanine in DNA, *Journal of the American Chemical Society* **2000**, *122*, 12622-12628.

111. Schneider, J. E.; Price, S.; Maidt, L.; Gutteridge, J. M. C.; Floyd, R. A.; Methylene blue plus light mediates 8-hydroxy-2'-deoxyguanosine formation in DNA preferentially over strand breakage, *Nucleic Acids Research* **1990**, *18*, 631-635.

112. Oliveira, R. C. d.; Ribiero, D. T.; Nigro, R. G.; Marco, P. D.; Menck, C. F. M.; Singlet oxygen induced mutation spectrum in mammalian cells, *Nucleic Acids Research* **1992**, *20*, 4319-4323.

113. Hickerson, R. P.; Prat, F.; Muller, J. G.; Foote, C. S.; Burrows, C. J.; Sequence and stacking dependence of 8-oxoguanine oxidation: comparison of one-electron versus singlet oxygen mechanism, *Journal of the American Chemical Society* **1999**, *121*, 9423-9428.

114. Simandan, T.; Sun, J.; Dix, T. A.; Oxidation of DNA bases, deoxyribonucleosides and homopolymers by peroxyl radicals, *Biochemical Journal* **1998**, *335*, 233-240.

115. Mouret, J.-F.; Polverelli, M.; Sarrazini, F.; Cadet, J.; Ionic and radical oxidations of DNA by hydrogen peroxide, *Chemico-Biological Interactions* **1991**, *77*, 187-201.

116. Cadet, J.; Weinfeld, M.; Detecting DNA damage, *Analytical Chemistry* **1993**, *65*, 675A-682A.

117. Cadet, J.; Douki, T.; Frelon, S.; Sauviago, S.; Pouget, J.-P.; Ravanat, J.-L.; Assessment of oxidative base damage to isolated and cellular DNA by HPLC-MS/MS measurement (Serial review), *Free Radical Biology and Medicine* **2002**, *33*, 441-449.

118. Palecek, E.; Fojta, M.; Tomschik, M.; Wang, J.; Electrochemical biosensors for DNA hybridization and DNA damage, *Biosensors and Bioelectronics* **1998**, *13*, 621-628.

119. Fojta, M.; Electrochemical sensors for DNA interactions and damage: Review, *Electroanalysis* **2002**, *14*, 1449-1463.

120. Palecek, E.; Past, present and future of nucleic acids electrochemistry, *Talanta* **2002**, *56*, 809-819.

121. Palecek, E.; Fojta, M.; Detecting DNA hybridization and damage, *Analytical Chemistry* **2001**, *73*, 75A-83A.

122. Fojta, M.; Stanková, V.; Palecek, E.; Koscielniak, P.; Mitáš, J.; A supercoiled DNA-modified mercury electrode-based biosensor for the detection of DNA strand cleaving agents, *Talanta* **1998**, *46*, 155-161.

123. Fojta, M.; Palecek, Emil; Supercoiled DNA-modified mercury electrode: a highly sensitive tool for the detection of DNA damage, *Analytica Chimica Acta* **1997**, *342*, 1-12.

124. Fojta, M.; Havran, L.; Kubicárová, T.; Palecek, E.; Electrode potential-controlled DNA damage in the presence of copper ions and their complexes, *Bioelectrochemistry* **2002**, *55*, 25-27.

125. Yang, J.; Zhang, Z.; Rusling, J. F.; Detection of chemically-induced damage in layered DNA films with Co(bpy)33+ by square wave voltammetry, *Electroanalysis* **2002**, *14*, 1494-1500.

126. Zhou, L.; Rusling, J. F.; Detection of chemically induced DNA damage in layered films by catalytic square wave voltammetry using Ru(bpy)32+, *Analytical Chemistry* **2001**, *73*, 4780-4786.

127. Dennany, L.; Forster, R. J.; White, B.; Smyth, M. R.; Rusling, J. F.; Direct Electrochemiluminescence detection of oxidized DNA in ultrathin films containing [Os(bpy)2(PVP)10]2+, *Journal of the American Chemical Society* **2004**, *126*, 8835-8841.

128. Zhou, L.; Yang, J.; Estavillo, C.; Stuart, J. D.; Schenkman, J. B.; Rusling, J. F.; Toxicity screening by electrochemical detection of DNA damage by metabolites generated in situ in ultrathin DNA-enzyme films, *Journal of the American Chemical Society* **2003**, *125*.

129. Rusling, J. F.; Sensors for toxicity of chemicals and oxidative stress based on electrochemical catalytic DNA oxidation, *Biosensors and Bioelectronics* **2004**, *20*, 1022-1028.

130. Dennany, L.; Forster, R. J.; White, B.; Smyth, M. R.; Rusling, J. F.; Direct Electrochemiluminescence Detection of Oxidized DNA in Ultrathin Films Containing [Os(bpy)2(PVP)10]2+, *Journal of the American Chemical Society* **2004**, *126*, 8835-8841.

131. Ropp, P.; Thorp, H. H.; Site-selective electron transfer from purines to electrocatalysts: voltammetric detection of a biologically relevant deletion in hybridized DNA duplexes, *Chemistry and Biology* **1999**, *6*, 599-605.

132. Weiss, D. J.; Lunte, C. E.; Detection of a urinary biomarker for oxidative DNA damage, 8-Hydroxyguanine, by capillary electrophoresis with electrochemical detection, *Electrophoresis* **2000**, *21*, 2080-2085.

133. Gawron, A. J.; Martin, R. S.; Lunte, S. M.; Microchip electrophoretic separation systems for biomedical and pharmaceutical analysis, *European Journal of Pharmaceutical Sciences* **2001**, *14*, 1-12.

134. Righetti, P. G.; Gelfi, C.; Capillary Electrohoresis of DNA in the 20-500bp range: recent developments, *Journal of Biochemical and Biophysical Methods* **1999**, *41*, 75-90.

135. Floyd, R. A.; Watson, J. A.; Wang, P. K.; Altmiller, D. H.; Rickard, R. C.; Hydroxyl free radical adduct of deoxyguanosine: sensitive detection and mechanisms of formation, *Free Radical Research Communications* **1986**, *1*, 163-172.

136. Ravanat, J.-L.; Gremaud, E.; Markovic, J.; Turesky, R. J.; Detection of 8-oxoguanine in cellular DNA using 2,6-Diamino-8-oxopurine as an internal standard for high-performance liquid chromotography with electrochemical detection, *Analytical Biochemistry* **1998**, *260*, 30-37.

137. Collins, A. R.; Cadet, J.; Moeller, L.; Poulsen, H. E.; Vina, J.; Are we sure we know how to measure 8-oxo-7,8-dihydroguanine in DNA from human cells?, *Archives of Biochemistry and Biophysics* **2004**, *423*, 57-65.

138. Lengger, C.; Schoech, G.; Topp, H.; A high-performance liquid chromatographic method for the determination of 8-oxo-7,8-dihydro-2'-deoxyguanosine in urine from man and rat, *Analytical Biochemistry* **2000**, *287*, 65-72.

139. Tagesson, C.; Källberg, M.; Klintenberg, C.; Starkhammar, H.; Determination of urinary 8-hydroxyguanosine by automated coupled-column high performance liquid chromatography: a powerful technique for assaying in vivo oxidative DNA damage in cancer patients, *European Journal of Cancer* **1995**, *31A*, 934-940.

140. Inagaki, S.; Esaka, Y.; Sako, M.; Goto, M.; Analysis of DNA adducts bases by capillary electrophoresis with amperometric detection, *Electrophoresis* **2001**, *22*, 3408-3412.

141. Yao, Q.-H.; Mei, S.-R.; Weng, Q.-F.; Zhang, P.-d.; Yang, Q.; Wu, C.-y.; Xu, G.-Q.; Determination of urinary oxidative DNA damage marker 8-hydrosy-2'-deoxyguanosine and the association with cigarette smoking, *Talanta* **2004**, *63*, 617-623.

142. Dizdaroglu, M.; Applications of capillary gas chromatography-mass spectrometry to chemical characterization of radiation-induced base damage to DNA: implications for assessing DNA repair processes, *Analytical Biochemistry* **1985**, *144*, 593-603.

143. Dizdaroglu, M.; Chemical determination of free radical-induced damage to DNA, *Free Radical Biology and Medicine* **1991**, *10*, 225-242.

144. Dizdaroglu, M.; Quantitative determination of oxidative base damage in DNA by stable isotope-dilution mass spectrometry, *FEBS Letters* **1993**, *315*, 1-6.

145. Hamberg, M.; Zhang, L.-J.; Quantitative determination of 8-hydroxyguanosine and guanine by isotope dilution mass spectrometry, *Analytical Biochemistry* **1995**, *229*, 336-344.

146. Esmans, E. L.; Broes, D.; Hoes, I.; Lemière, F.; Vanhoutte, K.; Liquid chromatography-mass spectrometry in nucleoside, nucleotide and modified nucleotide characterization (Review), *Journal of Chromatography A* **1998**, *794*, 109-127.

147. Hua, Y.; Wainhaus, S. B.; Yang, Y.; Shen, L.; Xiong, Y.; Xu, X.; Zhang, F.; Bolton, J. L.; Breemen, R. B. v.; Comparison of negative and positive ion electrospray tandem mass spectrometry for the liquid chromatography tandem mass spectrometry analysis of oxidised deoxynucleosides, *Journal of the American Society for Mass Spectrometry* **2000**, *12*, 80-87.

148. Dizdaroglu, M.; Jaruga, P.; Rodriguez, H.; Measurement of 8-hydroxy-2'-deoxyguanosine in DNA by high-performance liquid chromatography-mass spectrometry: comparison with measurement by gas chromatography-mass spectrometry, *Nucleic Acids Research* **2001**, *29*, No. 3, e12.

149. Jaruga, P.; Rodriguez, H.; Dizdaroglu, M.; Measurement of 8-hydroxy-2'-deoxyadenosine in DNA by liquid chromatography/mass spectrometry, *Free Radical Biology and Medicine* **2001**, *31*, 336-344.

150. Gangl, E. T.; Turesky, R. J.; Vouros, P.; Detection of in vivo formed DNA adducts at the part-per-billion level by capillary liquid chromatography/microelectrospray mass spectrometry, *Analytical Chemistry* **2001**, *73*, 2397-2404.

151. Weimann, A.; Belling, D.; Poulsen, H. E.; Quantification of 8-oxo-guanine and guanine as the nucleobase, nucleoside and deoxynucleoside forms in human urine by high-performance liquid chromatography-electrospray tandem mass spectrometry, *Nucleic Acids Research* **2002**, *30*, No. 2, e7.

152. Xu, G. W.; Yao, Q. H.; Weng, Q. F.; Su, B. L.; Zhang, X.; Xiong, J. H.; Study of urinary 8-hydroxydeoxyguanosine as a biomarker of oxidative DNA damage in diabetic nephropathy patients, *Journal of Pharmaceutical and Biomedical Analysis* **2002**.

153. Esaka, Y.; Inagaki, S.; Goto, M.; Review: Separation procedures capable of revealing DNA adducts, *Journal of Chromatography B* **2003**, *797*, 321-329.

154. Gupta, R. C.; Earley, K.; ^{32}P-adduct assay: comparative recoveries of structurally diverse DNA adducts in the various enhancement procedures, *Carcinogenesis* **1988**, *9*, 1687-1693.

155. Koc, H.; Swenberg, J. A.; Applications of mass spectrometry for quantitation of DNA adducts (Review), *Journal of Chromatography B* **2002**, *778*, 323-343.

156. Lutgerink, J. T.; Graaf, E. d.; Hoebee, B.; Stavenuitez, H. F. C.; Westra, J. G.; Kriek, E.; Detection of 8-hydroxyguanine in small amounts of DNA by ^{32}P postlabelling, *Analytical Biochemistry* **1992**, *201*, 127-133.

157. Zeisig, M.; Hofer, T.; Cadet, J.; Möller, L.; ^{32}P-postlabelling high-performance liquid chromatography (^{32}P-HPLC) adapted for analysis of 8-hydroxy-2'-deoxyguanosine, *Carcinogenesis* **2000**, *20*, 1241-1245.

158. Gupta, R. C.; Arif, J. M.; An improved ^{32}P-postlabelling assay for the sensitive detection of 8-oxodeoxyguanosine in tissue DNA, *Chemical Research in Toxicology* **2001**, *14*.

159. Cadet, J.; Douki, T.; Ravanat, J.-L.; Artifacts associated with the measurement of oxidized DNA bases, *Environmental Health Perspectives* **1997**, *105*, 1034-1040.

160. Park, E.-M.; Shigenaga, M. K.; Degan, P.; Korn, T. S.; Kitzler, J. W.; Wehr, C. M.; Kolachana, P.; Ames, B. N.; Assay of excised oxidative DNA lesions: isolation of 8-oxoguanine and its nucleoside derivatives from biological fluids with a monoclonal antibody column, *Proceedings of the Natural Academy of Sciences USA* **1992**, *89*, 3375-3379.

161. Yin, B.; Whyatt, R. M.; Perera, F. P.; Randall, M. C.; Cooper, T. B.; Santella, R. M.; Determination of 8-hydroxydeoxyguanosine by an immunoaffinity chromatography-monoclonal antibody-based ELISA, *Free Radical Biology and Medicine* **1995**, *18*, 1023-1032.

162. Shimoi, K.; Kasai, H.; Yokota, N.; Toyokuni, S.; Kinae, N.; Comparison between high-performance liquid chromatography and enzyme-linked immunosorbent assay for the determination of 8-hydroxy-2'-deoxyguanosine in human urine, *Cancer Epidemiology, Biomarkers and Prevention* **2002**, *11*, 767-770.

163. Rojas, E.; Lopez, M. C.; Valverde, M.; Review: Single cell electrophoresis assay: methodology and applications, *Journal of Chromatography B* **1999**, *722*, 225-254.

164. Wozniak, K.; Blasiak, J.; Free radicals-mediated induction of oxidized DNA bases and DNA-protein cross-links by nickel chloride, *Mutation Research/Genetic Toxicology and Environmental Mutagenesis* **2002**, *514*, 233-243.

165. Gedik, C. M.; Boyle, S. P.; Wood, S. G.; Vaughan, N. J.; Collins, A. R.; Oxidative stress in humans: validation of biomarkers of DNA damage, *Carcinogenesis* **2002**, *23*, 1441-1446.

Chapter Two

8-oxo-7,8-dihydroGuanine Formation and Oxidation During Iron-Mediated Hydroxyl Radical Attack

2.1 Introduction

Four significant endogenous processes that lead to DNA damage are oxidation, methylation, deamination and depurination.[1] One of the more investigated processes that leads to DNA damage is oxidation. It has been reported, based on urinary analysis, that DNA is subjected to approx. 10,000 oxidative hits per day, and steady state levels of oxidative damage are one or more orders of magnitude higher than non-oxidative adducts.[2] Oxidative damage can occur from a variety of sources, including γ-irradiation,[3,4] photoionisation,[5,6] chemical oxidation[7-9] and attack by reactive oxygen species (ROS).[10-12]

The hydroxyl radical (•OH) is the most noxious of the ROS, reacting directly with all known biomolecules at diffusion limited rates (~10^{10} $M^{-1}s^{-1}$).[7] Hydroxyl radicals are efficiently generated from hydrogen peroxide (H_2O_2) by reaction with Fe(II) according to Reaction 2.1, also known as the Fenton reaction:[13]

$$H_2O_2 + Fe(II) \xrightarrow{k_1} Fe(III) + HO^- + HO\cdot \quad k_1 = 76\ lmol^{-1}s^{-1} \quad \text{(Reaction 2.1)}$$

The Fenton reaction is often used as a model for *in vivo* oxidative damage.[14] H_2O_2 is ubiquitous in cells; therefore to minimise the risk of Fenton reaction occurring, intracellular levels of Fe(II) are very tightly regulated.[15] There is, however, a physiological demand for easily accessible iron that can be incorporated into a very wide range of iron-containing proteins.[16] This is accommodated by a low molecular weight pool of weakly chelated iron that passes rapidly through the cell, called a labile iron pool (LIP). The iron for the LIP is delivered from a variety of sources, both extracellular and intracellular, as shown in Fig. 2.1 and Fig. 2.2 respectively.

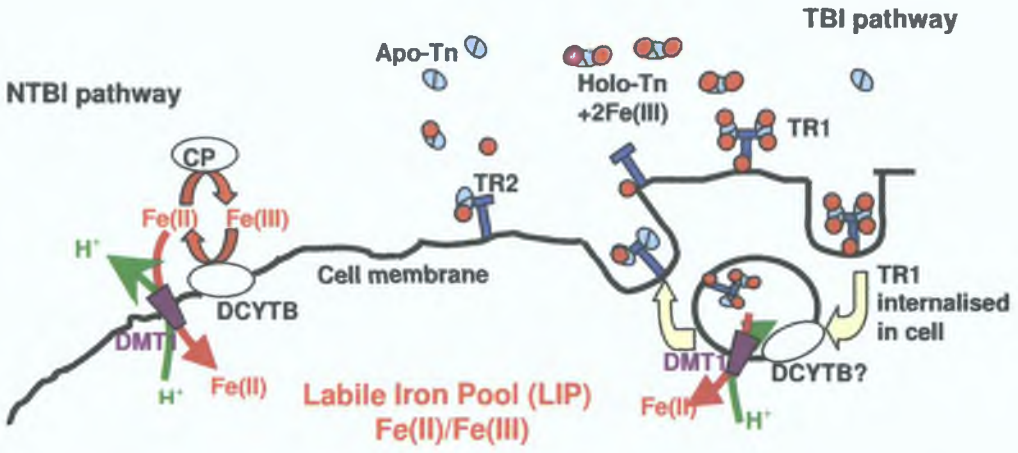

Fig. 2.1: Extracellular origins of cellular Labile Iron Pool include the non transferrin bound pathway (NBTI pathway) and the transferrin bound pathway (TBI pathway).[16] *(reproduced from Kruszewski, M.*[16]*) Non transferrin bound iron (NBTI), transferrin bound iron (TBI), duodenal cytochrome B (DCYTB), divalent metal transporter 1 (DMP1), ceruloplasmin (CP), transferrin (Tn), transferrin receptor 1 (TR1), transferrin receptor 2 (TF2).*

Extracellular sources of labile iron, shown in Fig. 2.1, include both transferrin bound iron (TBI) and non transferrin bound iron (NTBI). Transferrin (Tn) bound iron is taken up via receptor-dependent endocytosis. Apo-Tn binds Fe(III) in blood serum to give diferric holo-Tn, which is bound by the protein Transferrin Receptor (TR), present on the cell surface. The complex is internalised and at reduced pH, Fe(II) ions are released from the holo-Tn and reduced by endosomal ferric reductase-like activity. The actual nature of the reductase is as yet unknown; however, a probable candidate is a duodenal cytochrome B (DCYTB). DCYTB is the protein that facilitates the divalent metal transporter, DMP1. The reduced iron ions are transported to the cytoplasm by DMP1, where it is released into the LIP.[17] Non transferrin bound iron (NTBI) also enters cells via DMT1, facilitated by DCYTB (which reduces the Fe(III) generated by the copper binding glycoprotein ceruloplasmin (CP)), and so can also be released into the LIP.

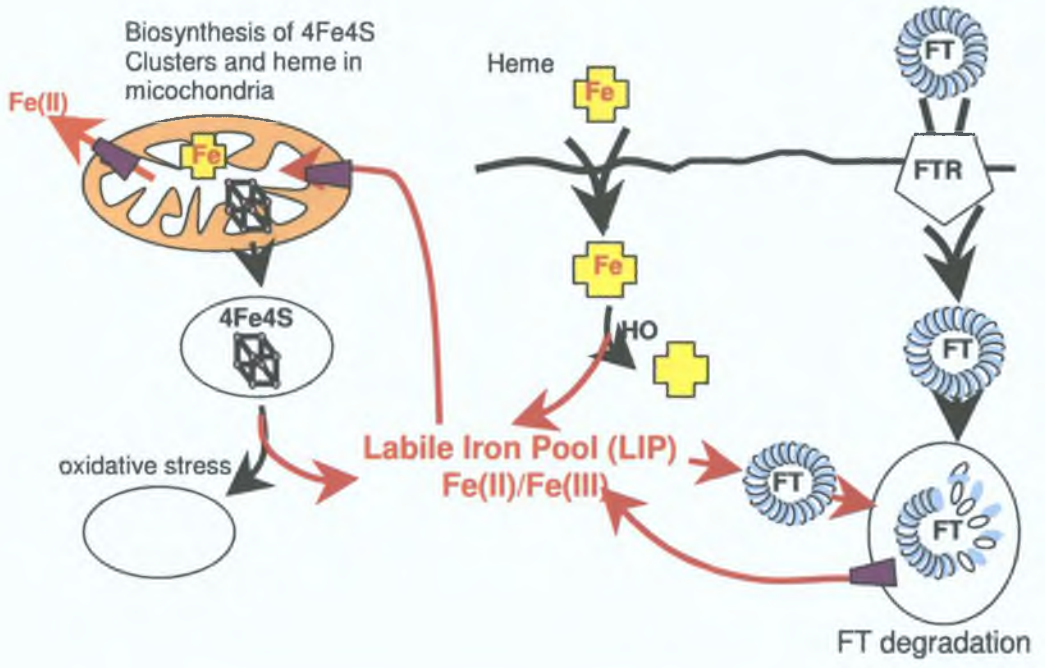

Fig. 2.2: Intracellular origins of cellular Labile Iron Pool from iron-containing proteins.[16] (reproduced from Kruszewski, M.[16]). Iron sulphur cluster (4Fe4S), ferritin (FT), ferritin receptor (FTR), heme oxygenase (HO).

In addition to the extracellular iron uptake, there are a number of potential intracellular sources of LIP, shown in Fig. 2.2. The best known is ferritin (FT), an iron sequestering protein, which is capable of storing 3,500 iron ions per molecule. Although it normally acts an iron sequestering protein protecting cells from iron toxicity, it appears that protein degradation in lysosomes is the prevalent mechanism of iron release from FT. Another potential source of iron for the LIP is heme, which can enter cells as a heme-hemopexin complex. To prevent any toxic action of heme under oxidative stress, heme oxygenase (HO) is introduced. This oxidises heme to release Fe(III), which enters the LIP. Non heme iron proteins, such as iron-sulphur proteins, *e.g.* 4Fe4S, are sensitive to oxidative stress, and upon reaction with H_2O_2 release iron into the LIP. The availability of both iron and H_2O_2 in human cells means that the Fenton reaction, which generates •OH, is possible *in vivo*.

•OH is the most noxious radical to which DNA is normally exposed.[18] •OH reacts with both the DNA backbone and with all four DNA bases, so that a variety of damaged DNA products may be generated, including oxidised bases, abasic sites, strand breaks and DNA-protein cross links.[19] Over 60 different nucleoside adducts have been identified, and these numerous lesions to all four DNA bases have become a signature for its attack. Guanine (G) has the lowest ionisation potential of the four DNA bases,[20] although it should be remembered that •OH is capable of oxidising all four DNA bases. One of the primary oxidised G species is 8-oxo-7,8-dihydroGuanine (8-oxoG), which has been linked to mutagenesis, disease and aging.[21] 8-oxoG is one of the primary lesions formed during •OH attack. It is considered a biomarker for oxidative DNA damage.[22,23] 8-oxoG is not, however, the final product of G oxidation. Instead it is itself readily further oxidised, at a lower potential than even its parent base G.[24] (The oxidation products of 8-oxoG oxidation will be discussed in more detail in Chapter 5.) The ease of 8-oxoG oxidation may complicate the interpretation of steady state concentrations of 8-oxoG, if the oxidation of G, and therefore of 8-oxoG, is site specific, so that there is an increased likelihood of further 8-oxoG oxidation. If the oxidation of 8-oxoG is effective, a low steady state concentration could indicate a number of possible scenarios. It could simply show a low formation of 8-oxoG, or a high rate of both 8-oxoG generation and further oxidation; indeed it could even indicate some intermediate level of both generation and oxidation. Within living systems it could also mean that 8-oxoG repair mechanisms are very effective. In short, without information regarding the rates both of 8-oxoG formation and oxidation, no meaningful conclusions can be drawn from steady state concentrations of 8-oxoG.

The aim of this research was therefore, using the Fenton reaction as a model for *in vivo* oxidative damage, to investigate the generation of 8-oxoG by •OH attack, and to analyse the extent to which it is further oxidised. This was then used to compare the levels of 8-oxoG formation and further oxidation in the free base G and in double stranded DNA, to investigate whether charge transport along the DNA double helix in any way affected either of these rates.

Free G and 8-oxoG were incubated with the Fenton reagents for a range of incubation times. The concentrations of both free G and 8-oxoG were measured simultaneously, using HPLC separation with ultraviolet (UV) and electrochemical (EC) detection, respectively. Polyguanylic acid (PolyG) and double stranded DNA were hydrolysed in 88% formic acid to release the unmodified DNA bases and 8-oxoG. The individual DNA bases were then separated using HPLC-UV-EC. 8-oxoG was immediately generated from free G, PolyG and DNA on incubation with the Fenton reagents Fe(II) and H_2O_2. The concentration of 8-oxoG was found to oscillate with increasing oxidation. In the case of free G, a maximum concentration of 0.68 μM 8-oxoG was observed after 15 min incubation; thereafter the overall trend was towards a decrease in 8-oxoG concentration. A similar pattern was observed for both PolyG and DNA. The rate of oxidation of 8-oxoG itself was observed to be far higher than the rate of G oxidation. Guanidinohydantoin (Gh) was identified by HPLC-MS as a probable product of 8-oxoG oxidation.

2.2 Materials and Methods

2.2.1 Materials

2.2.1.1 Chemicals

8-oxo-7,8-dihydroGuanine (2-amino-6,8-dihydroxypurine) (8-oxoG) (R288608), guanine (G) (G0381), uracil (U) (U0570), cytosine (C) (C3506), thymine (T) (T0376), adenine (A) (A8626), polyguanylic acid potassium salt (PolyG) (P4404), calf thymus DNA sodium salt (D1501) and salmon testes DNA sodium salt (D1626) [2,000 av. base pairs, 41.2% G/C] and 88% formic acid (399388), were purchased from Sigma Aldrich (Dublin, Ireland). 30% (v/v) hydrogen peroxide (H_2O_2) solution was purchased from Merck (Dublin, Ireland). Deionised water was treated with a Hydro Nanopure system to specific resistance > 18 mΩ-cm. LC-MS Chromasolv water (39253) and LC-MS Chromasolv methanol (34966) were purchased from Riedel-de-Haën (Dublin, Ireland). HPLC grade methanol was purchased from Labscan Ltd. (Dublin, Ireland). All other chemicals were of analytical grade and were used without further purification.

Silver/silver chloride (Ag/AgCl) electrodes (RE-6) were purchased from Bioanalytical Systems (BAS) Ltd. (Cheshire, UK). Restek reversed phase Ultra C18 5 µm 4.9 x 250 mm column (9174575-700), Ultra C18 4 x 10 mm guard cartridge (917450210), Trident XG-XF 10 mm guard cartridge fitting (25026) and 4 mm x 2 µm cap frits (25022) were purchased from Restek Ireland (Belfast, Northern Ireland). Supelcosil reversed phase LC-18 5 µm 2.1 x 250 mm column (57935) was purchased from Supelco, Sigma Aldrich. 1 ml Pierce hydrolysis tubes were purchased from Medical Supply Co. (Dublin, Ireland). 47 mm Nylaflo nylon membranes with 0.45 µm pore size and 25 mm Acrodisc GF syringe filters with 0.45 µm pore size were purchased from Pall (MI, USA). UN-SCAN-IT digitising software was purchased from Silk Scientific (UT, USA).

2.2.1.2 Buffers

The mobile phase for gradient HPLC-EC consisted of 50 mM ammonium acetate with 50 mM acetic acid in 5% methanol. For HPLC-MS, the mobile phase consisted of 17 mM ammonium acetate with 20 mM acetic acid in 5% methanol. For this analysis, LC-MS Chromasolv water and methanol were used. All mobile phases were vacuum filtered using 47 mm Pall Nylaflo nylon membranes with 0.45 μm pore size and stirred overnight prior to use.

2.2.2 Apparatus

2.2.2.1 HPLC Instrumentation

The HPLC system consisted of a Waters (Waters Millipore, Milford, MA) Model 600E pump, and a Waters Lambda-Max model 481 LC-spectrophotometer. UV and EC chromatograms were generated using Hewlett Packard 3395 integrators. UN-SCAN-IT digitising software was used to digitise integrator chromatograms, which were then imported into KaleidaGraph or MS Office Excel. A Restek Ultra C-18 reversed phase column (4.6 x 250 mm, particle size 5 μm) with Trident XG-XF 10 mm filter and guard column was used. The running buffer comprised of 50 mM ammonium acetate with 50 mM acetic acid in 5% methanol, pH 5.5, run under isocratic conditions at a flow rate of 1 ml/min. For UV detection of unmodified bases, a wavelength of 254 nm was used.

The electrochemical detector was coupled in series with the UV detector. It consisted of a CC-4 electrochemical cell (BAS) and a LC-4C amperometric detector (BAS). An Ag/AgCl reference electrode and a glassy carbon working electrode were used. The potential across the cell was set at +550 mV vs. Ag/AgCl. Sensitivity was set to 5 nA.

2.2.2.2 Mass Spectrometry

For Mass Spectrometry, a Micromass Quadropole II was used with a Restek Ultra C-18 reversed phase (2.1 mm id x 150 mm) with 1 cm guard column. A flow rate of 0.3 ml/min was used with a mobile phase of 17 mM ammonium acetate with 20 mM acetic acid in 5% methanol (reduced salt concentration to prevent ionisation suppression). Full scan spectra were taken at a cone voltage of 15 V using positive electrospray ionisation (ESI).

2.2.3 Methods

2.2.3.1 Oxidation of Guanine

A stock solution of 10mM Guanine was prepared daily in 0.1 M NaOH, pH 11. 800 µl 10 mM 8-oxoG was incubated with 200 µl 1.5 mM iron(II) sulphate ($FeSO_4 \cdot 6H_2O$) and 200 µl 0.5 M H_2O_2 at 37 °C with constant stirring. Duplicate 100 µl aliquots were taken after various incubation times. 50 µl 10 mM Uracil (prepared daily in 0.1 M NaOH) was added as an internal standard and the reaction was quenched with 1 ml 200 proof cold ethanol. The solution was dried immediately under a stream of nitrogen gas. The dried hydrolysates were refridgerated at 4 °C until further use. Immediately prior to analysis by HPLC, they were redissolved in 100 µl 10 mM NaOH and 900 µl 50 mM ammonium acetate buffer, pH 5.5, and filtered through a 25 mm Pall Acrodisc GF syringe filter with 0.45 µm pore size prior to injection. The final concentration of G was 0.8 mM.

2.2.3.2 Oxidation of 8-oxo-7,8-dihydroGuanine

A stock solution of 2.4 mM 8-oxo-7,8-dihydroGuanine (8-oxoG) was prepared in 0.1 M NaOH, pH 11. It was divided into 1 ml aliquots and frozen until required. Aliquots were defrosted immediately prior to use, to prevent decomposition of 8-oxoG. 800 µl 2.4 mM 8-oxoG was incubated with 200 µl 1.5 mM iron(II) sulphate and 200 µl 0.5 M H_2O_2 at 37 °C with constant stirring. Final concentrations in the reaction flask were 2 mM 8-oxoG, 150 µM iron(II)sulphate and

50 mM H_2O_2. Duplicate 100 µl aliquots were taken after various incubation times. 50 µl 10 mM Uracil was added as an internal standard and the reaction was quenched with 1 ml 200 proof cold ethanol. The solvent was evaporated to dryness under a stream of nitrogen gas. The dried hydrolysates were refridgerated at 4 °C until further use. Immediately prior to analysis by HPLC, they were redissolved in 1 ml 10 mM NaOH and filtered through a 25 mm Pall Acrodisc GF syringe filter with 0.45 µm pore size prior to injection. The final concentration of 8-oxoG was 200 µM.

2.2.3.3 Oxidation of PolyGuanylic Acid

A stock solution of 0.20 mg/ml PolyGuanylic acid (PolyG) was prepared in 50 mM ammonium acetate buffer, pH 5.5. 800 µl 0.20 mg/ml PolyG was incubated with 200 µl 1.5 mM iron(II) sulphate and 200 µl 0.5 M H_2O_2 at 37 °C with constant stirring. Duplicate 100 µl aliquots were taken after various incubation times. 50 µl 10 mM Uracil was added as an internal standard and the reaction was quenched with 1 ml 200 proof cold ethanol. The solvent was evaporated to dryness under a stream of nitrogen gas.

2.2.3.4 Oxidation of DNA

A stock solution of 2.0 mg/ml DNA was prepared in 50 mM ammonium acetate buffer, pH 5.5. It was stored at 4 °C overnight prior to use to allow the DNA dissolve completely. 800 µl 0.20 mg/ml DNA was incubated with 200 µl 1.5 mM iron(II)sulphate and 200 µl 0.5 M H_2O_2 at 37 °C with constant stirring. Duplicate 100 µl aliquots were taken after various incubation times. 50 µl 10 mM Uracil (prepared daily in 0.1 M NaOH) was added as an internal standard and the reaction was quenched with 1 ml 200 proof cold ethanol. The solvent was evaporated to dryness under a stream of nitrogen gas.

2.2.3.5 PolyG and DNA Hydrolysis

Both PolyG and DNA were hydrolysed prior to HPLC analysis. The oxidised PolyG or DNA sample was hydrolysed by adding 600 µl 88% (v/v) formic acid in

evacuated and sealed Pierce hydrolysis tubes and heating at 140 °C for 30 min in a vacuum. The solvent was evaporated to dryness under a stream of nitrogen gas. The dried hydrosylates were refrigerated at 4 °C until further use. Prior to analysis they were redissolved in 1 ml 50 mM ammonium acetate buffer, pH 5.5, and filtered through a 25 mm Pall Acrodisc GF syringe filters with 0.45 μm pore size prior to injection. The final concentration of DNA was 160 μg/ml.

2.3 HPLC Method Development

2.3.1 Acid hydrolysis

Prior to analysis by HPLC-UV-EC, DNA must be hydrolysed to remove the bases from the DNA backbone. This can affect the quantitative results of the analysis. In one extreme it can result in less than 100% release of 8-oxoG. It can also result, however, in the artifactual oxidation of G to 8-oxoG. Two main methods of DNA hydrolysis were examined in the literature: enzymatic hydrolysis, which yields nucleosides and acidic hydrolysis which releases bases. Enzymatic digestion was not favoured initially as the retention time of the nucleosides was about one hour,[25] whereas DNA bases eluted in under 15 min.[26] Tris buffer, used during enzymatic hydrolysis, was found to compete with DNA for •OH, so that the radical had an extra reaction pathway, resulting in a lower yield of 8-oxoG, which would possibly obscure any pattern of 8-oxoG formation that might emerge.[27] Moreover, Helbock *et al.*[26] found that the nuclease P1 or alkaline phosphatase used in enzymatic hydrolysis (which takes at least 24 hours) may not release all the 8-hydroxydeoxyguanosine (8-OHdG) in DNA, and that the true levels may be underestimated by up to 30%. Acid hydrolysis was examined in detail by Ravanat *et al.*[28] DNA was incubated with 60% formic acid at 130 °C for 30 min. After 45 min, however, artifactual oxidation was deemed to occur after this time. At hydrolysis times of less than 45 min, however, it was concluded that 100% release of 8-oxoG occurred in the complete absence of artifactual oxidation. Based on this knowledge, it was decided that acid hydrolysis would be the method of choice for this work. It yields 100% 8-oxoG in 30 min and the resulting HPLC separation was complete in less than 15 min. It should be noted, however, that although 30 min of acid hydrolysis yields 100% of the purine bases G, A and 8-oxoG, 3 hours hydrolysis is required to yield 100% of the pyrimidine bases T and C.

2.3.2 HPLC Mobile Phase Optimisation

Carmicheal *et al.*[29] have examined the levels of 8-oxoG and DNA crosslinks caused by a variety of transition metals acting as Fenton reagents. Ravanat *et al.*[30] detailed an extensive method development for the detection and measurement of 8-oxoG. Both groups used a HPLC mobile phase consisting of 50 mM ammonium acetate with 50 mM acetic acid in 5% methanol and a flow rate of 1 l/min. Carmicheal *et al.*[29] achieved good baseline separation of the nucleosides with a low limit of detection using a 70 min runtime, while Ravanat *et al.*[30] obtained baseline separation of the DNA bases within a 25 min runtime. As an isocratic buffer, it serves to eliminate baseline drift in EC detection that is caused by the use of gradient buffers.[31] Unlike phosphate or citrate, it is suitable for mass spectrometric analysis. At a pH of approx. 5.5, this slightly acidic mobile phase would be expected to give reproducible separation of DNA bases. This mobile phase was chosen for this research.

2.3.3 HPLC Column Selection

As a reference for column selection, the four DNA bases A, C, G and T were initially separated using the mobile phase of 50 mM ammonium acetate with 50 mM acetic acid in 5% methanol and a flowrate of 1 ml/min and using a Supelco reversed phase Supelcosil LC-18 column, which accompanied the HPLC instrumentation. The 4 DNA bases were separated with baseline resolution, but the separation resulted in huge tailing of A, which significantly lengthened the analysis time as illustrated in Fig. 2.3. Moreover, G, a peak of particular interest, showed some peak splitting. Peak tailing grew successively worse with repeat injections, although the retention times were reproducible. The tailing of A would be detrimental to the lifetime of the HPLC column, as such dramatic tailing could lead to a build up of A in the column over time, thereby deteriorating the quality of the column and the data obtained using it.

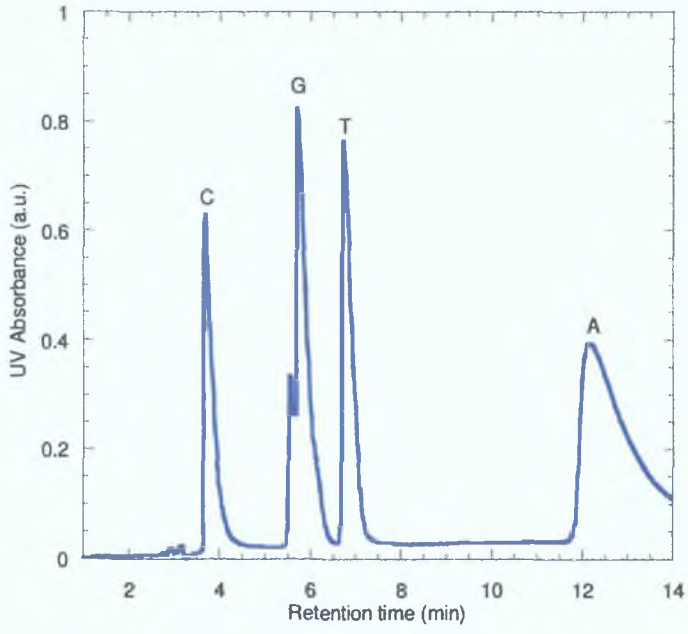

Fig. 2.3: HPLC separation of the 4 base standards C, G, T and A (as eluted) with UV detection at 254 nm using a Supelcosil C18 reversed phase column with mobile phase of 50 mM ammonium acetate with 50 mM acetic acid in 5% methanol and a flowrate of 1 ml/min. (Shoulder on G not identified.)

Zhou[32] extensively investigated a number reversed phase HPLC columns for DNA analysis, including Aquasil C18, Metachem ODS2 (C18), Supelcosil LC-18, Supelco Discovery HS F5-5 and Restek Ultra C-18 columns. The two columns with the highest carbon load (20%), Metachem ODS2 and Restek Ultra C-18, resulted in maximum separation, with the fully endcapped Restek column further reducing tailing. A 25 cm completely endcapped Restek column, Ultra C-18, with Trident™ Direct 10 mm filter and guard column, resulted in excellent baseline resolution of the 4 bases, with virtually no tailing of A. Fig. 2.4 shows the HPLC separation with UV detection obtained using this column.

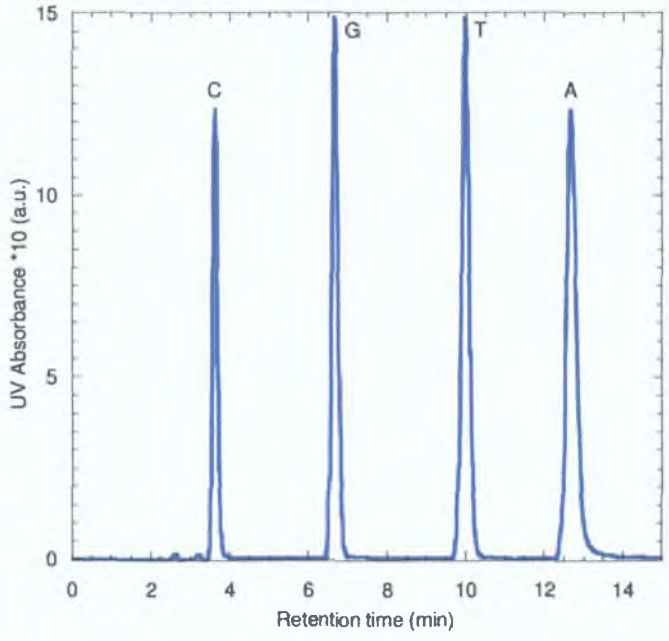

Fig. 2.4: HPLC separation of C, G, T and A with UV detection at 254 nm using a Restek Ultra C-28 fully endcapped column with mobile phase of 50 mM ammonium acetate with 50 mM acetic acid in 5% methanol and a flowrate of 1 ml/min.

The overall analysis time (14 min) was the same for all columns. However, with the Restek column, the A peak returned to the baseline by the end of the analysis. There was no significant tailing for any of the bases as they eluted using this column. All four peaks were symmetric, with very little peak broadening and with good resolution between the four peaks. This column was therefore chosen for all studies. The Trident™ Direct 10 mm filter and guard column were also fitted to the column. This guard column had the same bonded phase as the main column. Both the guard column and the filter contributed slightly to an increase in the overall run time, but served to protect the main column from highly retentive particles and compounds, and so extended its lifetime considerably.

2.3.4 Internal Standard

As illustrated in Fig. 2.4, there are gaps of up to 2 min between the elution of consecutive bases. This allowed for the easy addition of an internal standard to the analysis. The use of an internal standard was desirable to increase the accuracy of the analysis, as there was considerable pre-treatment of samples prior to separation by HPLC. It should also compensate for possible drift between samples. The internal standard should not be present in the sample, by its addition it should not contaminate the sample, it should be chemically and physically compatible with the sample and should not introduce interfere with the modes of detection.[33] In this analysis, G and A are purines, while T and C are pyrimidines. Two close structural species, xanthine (X), a purine, and uracil (U) a pyrimidine, are readily available and have similar chemical properties. Both were considered for use as an internal standard. Scheme 2.1 illustrates the structure of the four DNA bases, and X and U.

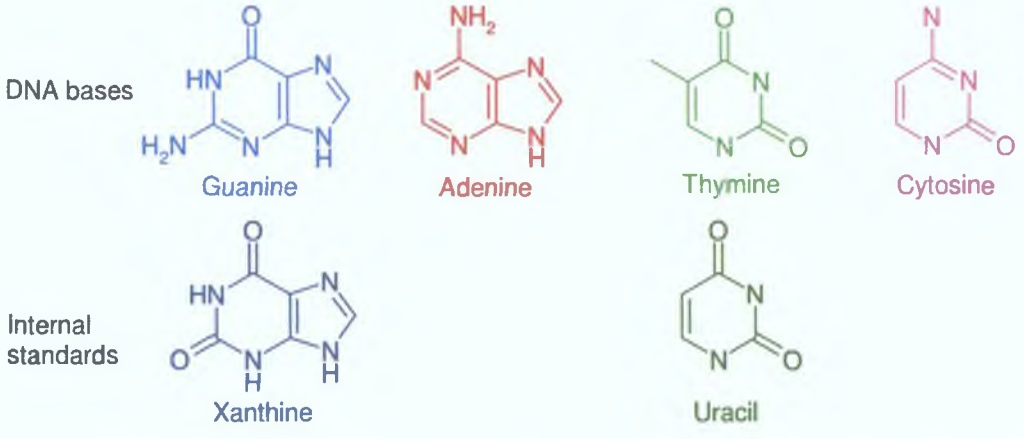

Scheme 2.1: Structure of DNA bases guanine, adenine, thymine and cytosine, and potential internal standards xanthine and uracil.

X was initially investigated as a possible internal standard. However, it coeluted with G, and was therefore unsuitable. As shown in Fig. 2.5, however, U eluted approx 0.5 min after C and was clearly separated from both C and G. Thus U was used as an internal standard in all work.

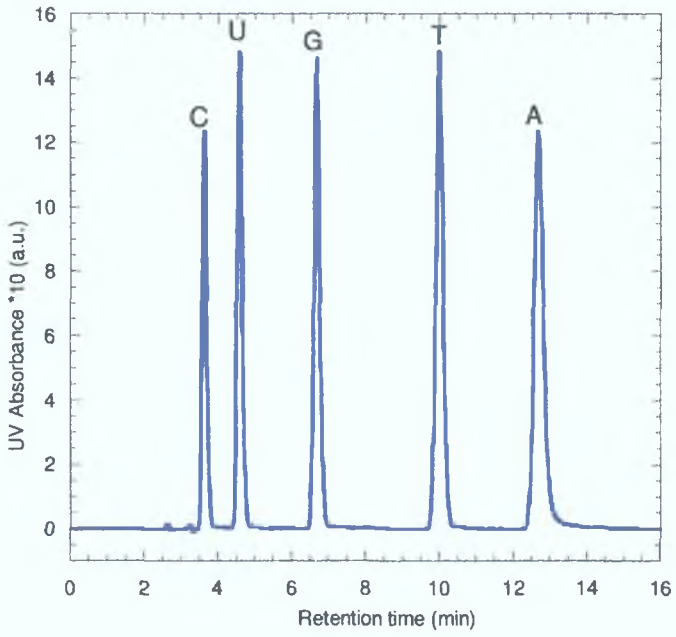

Fig. 2.5: HPLC separation of DNA bases and internal standard U separation with UV detection at 254 nm using a Restek Ultra C-28 fully endcapped column with mobile phase of 50 mM ammonium acetate with 50 mM acetic acid in 5% methanol and a flowrate of 1 ml/min.

2.3.5 Optimisation of Electrochemical Detection

Electrochemical (EC) detectors only detect species that are electrochemically active. This detection method operates by oxidising or reducing electroactive analytes and measuring the current produced. The amount of current produced is a quantitative indicator of the concentration of that species present in the solution. The species being analysed in this thesis is 8-oxoG. It has a lower oxidising potential than any of the unmodified bases C, G, T and A. In order to optimise the EC detector for the detection of 8-oxoG, the voltammetric behaviour of this analyte must first be examined. The current generated by 8-oxoG oxidation was measured as a function of applied potential over the range +350 mV to +650 mV vs. Ag/AgCl. The data was plotted as a hydrodynamic voltammogram (HDV), shown in Fig. 2.6. At 450 mV 8-

oxoG began to be oxidised. The oxidation current increased steadily until +525 mV, where the curve levelled off. At +550 mV, 8-oxoG was almost completely oxidised. This potential was much lower than the oxidation potential of G (850 mV vs. Ag/AgCl). It should also be significantly lower than the oxidation potentials of all 8-oxoG oxidation products that could potentially interfere with the analysis of 8-oxoG itself. The potential chosen for the EC detector was therefore +550 mV vs. Ag/AgCl.

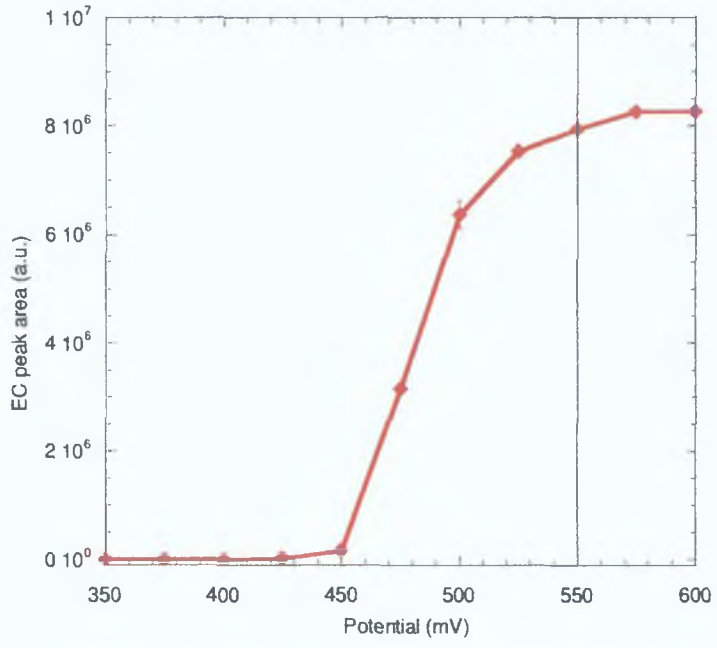

Fig. 2.6: Hydrodynamic voltammogram of 8-oxoG oxidation at a glassy carbon electrode from +350 mV to +600 mV vs. Ag/AgCl.

Fig. 2.7 shows the chromatogram generated by the EC detector at a potential of +550 mV vs. Ag/AgCl and a sensitivity of 5 nA. The large solvent front at 3 min is typical for EC detection. 8-oxoG elutes at approx. 7 min and is clearly resolved from the solvent front. As can be seen from Fig. 2.5, however, G is still eluting at 7 min retention time. The two peaks of G and 8-oxoG therefore coelute. Control studies, however, showed no current generated at +550 mV for G, therefore this technique is suitable for the quantitative detection of 8-oxoG in the presence of G. The small peak at approx. 11 min may correspond to a T oxidation product, which is

also electrochemically active. It is frequently reported in the literature as a second oxidation product of DNA oxidation detectable by electrochemical means.[34] As it is not of interest in this study, may not be fully released from the DNA backbone during the acid hydrolysis, and may be unstable in acid hydrolysis it was not quantified at this point.

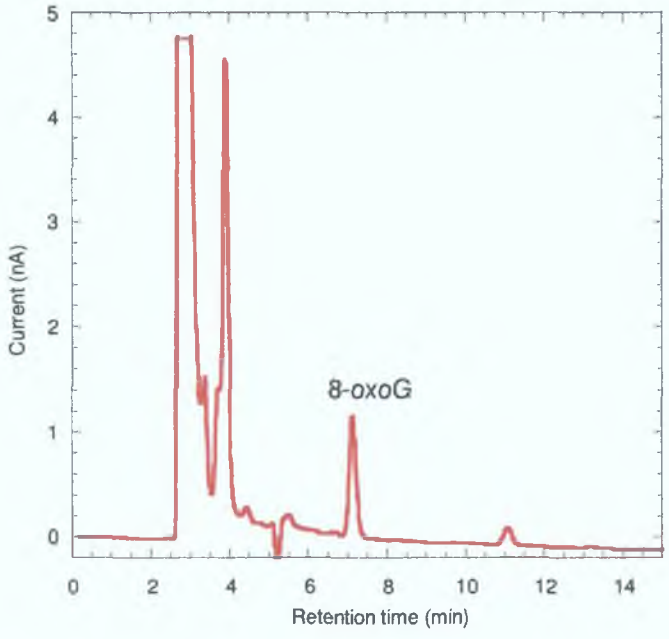

Fig. 2.7: HPLC separation with EC detection of 8-oxoG at a potential of +550 mV vs. Ag/AgCl using a Restek Ultra C-28 fully endcapped column with mobile phase of 50 mM ammonium acetate with 50 mM acetic acid in 5% methanol and a flowrate of 1 ml/min. Sensitivity 5 nA.

2.3.6 UV and EC detector Calibration

The UV detector was calibrated over a range of 0.1 to 1 mM G. 0.5 mM U was added as an internal standard. The calibration curve for G was plotted, as shown in Fig. 2.8. With a correlation coefficient (R^2) of 0.99, the calibration plot was clearly linear from 0.1 to 1 mM concentrations of G. (Error bars are included, but are smaller than the diameter of data points themselves.) The EC detector was

calibrated in an analogous manner over a range of 1 to 5 μM 8-oxoG. The resulting calibration curve is plotted in Fig. 2.9. The R^2 value, at 0.98, was lower than the preferred value of 0.99. However, the plot is linear, and as the limit of detection of the EC detector is being approached, it was deemed acceptable.

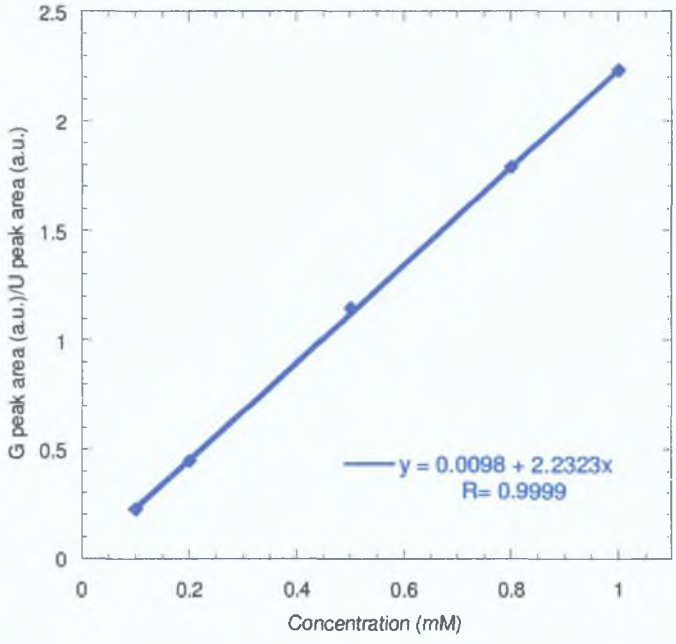

Fig. 2.8*: Calibration curve for G from 0.1 to 1 mM, with internal standard U, 254 nm, Restek Ultra C-28 fully endcapped column with mobile phase of 50 mM ammonium acetate/50 mM acetic acid in 5% methanol and flowrate of 1 ml/min.*

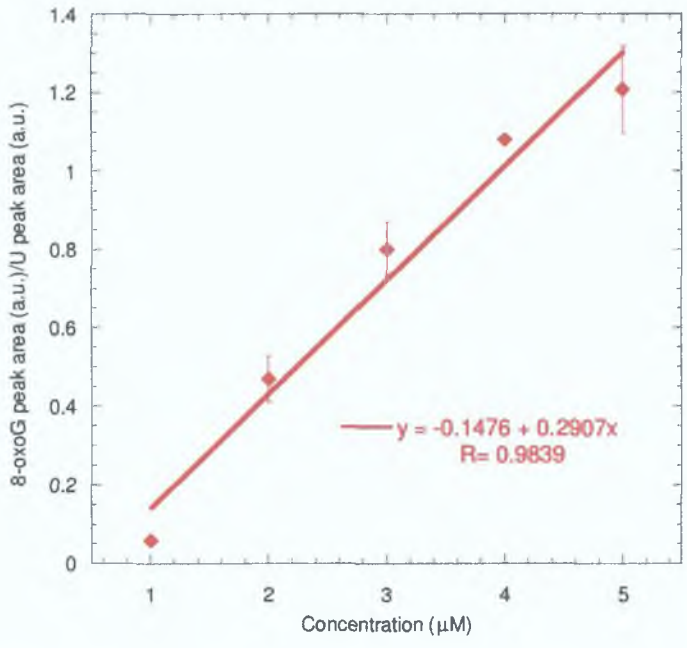

Fig. 2.9: Calibration curve for 8-oxoG from 1 to 5 μM, with internal standard U using a Restek Ultra C-18 fully endcapped column with mobile phase of 50 mM ammonium acetate with 50 mM acetic acid in 5% methanol and a flowrate of 1 ml/min. Sensitivity 5 nA.

2.3.7 HPLC Method for analysis of DNA bases

The optimised method is as follows: A mobile phase of 50 mM ammonium acetate with 50 mM acetic acid in 5% methanol at a flow rate of 1 ml/min was used to separate analytes using a completely endcapped Restek column, Ultra C-18, with a 1 cm online guard column. Unmodified bases were detected using UV detection at 254 nm. For UV detection of 8-oxoG, the detector was set to 280 nm, while for the detection of potential further oxidation products of 8-oxoG oxidation it was set to 214 nm. 8-oxoG was detected using EC detection with a cell potential of +550 mV *vs.* Ag/AgCl and a sensitivity of 5 nA. U was added as an internal standard for quantitative analysis, with 0.5 mM being added to each sample.

2.4 Results

2.4.1 Rate of 8-oxoG formation and oxidation in Guanine

The iron-mediated Fenton reaction was used to oxidise G to 8-oxoG in order to observe the rate of 8-oxoG formation and G degradation. Free base G (0.8 mM) was incubated with 150 μM iron(II)sulphate and 50 mM H_2O_2 at 37 °C, as described in Section 2.2. Samples were taken at five min intervals from 0 to 120 min and analysed using HPLC-UV-EC. The concentration of 8-oxoG within the G samples was monitored with increasing incubation time is illustrated in Fig. 2.10.

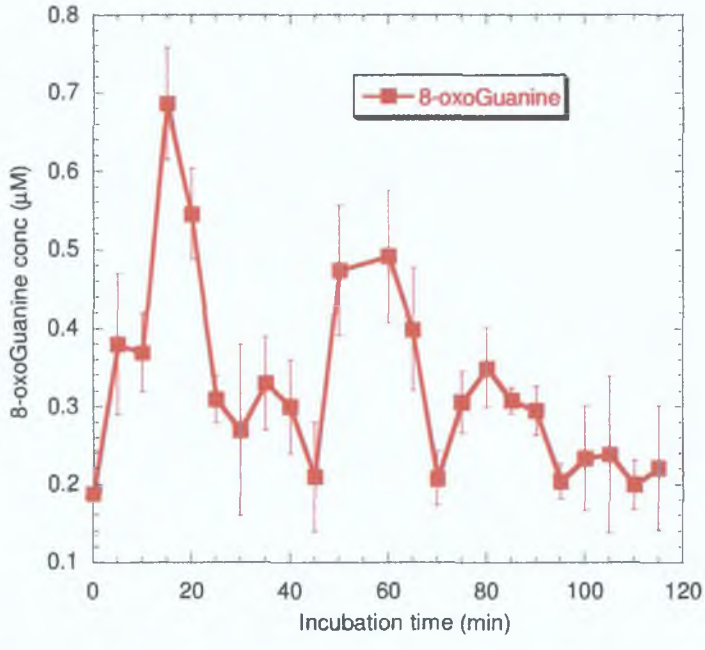

Fig. 2.10: Concentration of 8-oxoG in free G from 0 – 120 min incubation with 150 μM iron(II)sulphate and 50 mM H_2O_2 at 37 °C, EC detection at a potential of +550 mV vs. Ag/AgCl, sensitivity 5 nA, mobile phase of 50 mM ammonium acetate with 50 mM acetic acid in 5% methanol and a flowrate of 1 ml/min.

There was an immediate generation of 8-oxoG, which doubled in concentration (0.19 μM to 0.38 μM) within the first five min of incubation. An even sharper increase in concentration was observed from ten to fifteen min, where a maximum concentration of 8-oxoG (0.68 μM) was reached after 15 min incubation with Fenton reagents. For the next 35 min the overall trend was for a decrease in concentration, although this decrease was not linear. A surge in concentration again occurred from 50 to 55 min, but on this occasion the maximum concentration reached was only about 70% of the previous maximum at 15 min. After 60 min incubation, the concentration decreased once more. The concentration of 8-oxoG, as plotted in Fig. 2.10, does not increase linearly with increasing incubation time. Instead it oscillated with respect to time, with an overall trend towards a decrease in concentration after a concentration maximum at approx. 15 min incubation. In order to observe these oscillations more closely, the time period from 0 to 20 min, where the maximum concentration of 8-oxoG occurred, was studied in more detail, with samples taken at 1 min intervals, shown in Fig. 2.11.

There was a residual level of 8-oxoG in the sample was taken when Fenton reagents were added and aliquots were taken immediately, so that 8-oxoG was found to be generated immediately on addition of the Fenton reagents. Control samples of free G did not contain a detectable amount of 8-oxoG. 8-oxoG was generated for 4 min, whereafter the concentration dropped sharply until about 9 min incubation. After 9 min incubation, the concentration again increased. This increase continued up to 15 min incubation. After 15 min the concentration of 8-oxoG again decreased, and continued to decrease for the next three min incubation. After 18 min it once again began to be generated. This oscillating pattern of 8-oxoG formation followed by a drop in concentration was repeated continually, but overall the concentration decreased after 15 min.

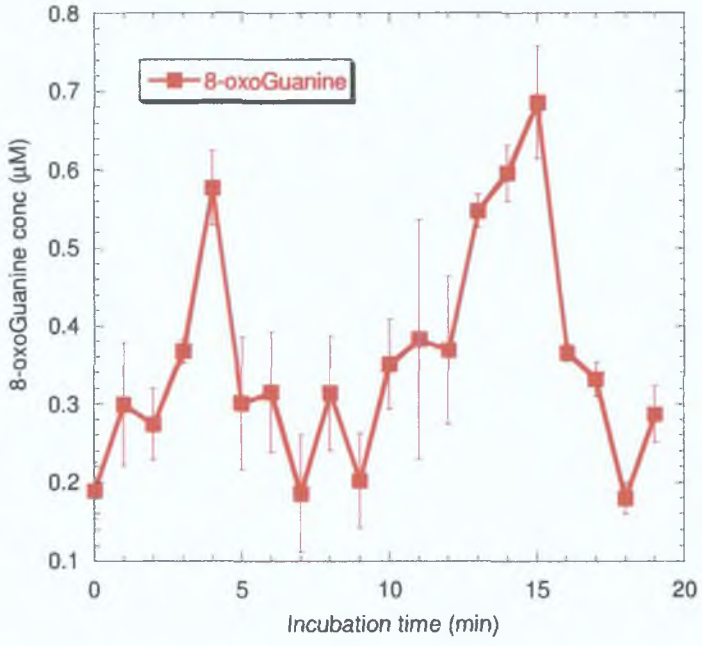

Fig. 2.11: Concentration of 8-oxoG in free G, from 0 – 20 min incubation with 150 µM iron(II)sulphate and 50 mM H_2O_2 at 37 °C, EC detection at a potential of +550 mV vs. Ag/AgCl, sensitivity 5 nA, mobile phase of 50 mM ammonium acetate with 50 mM acetic acid in 5% methanol and a flowrate of 1 ml/min. (n=6)

The concentrations of both G (blue) and 8-oxoG (red) in free G from 0 to 20 min are plotted in Fig. 2.12. The concentration of G decreased immediately on incubation with the Fenton reagents; however, as with 8-oxoG, this decrease was not linear. Subtle oscillations with significantly smaller amplitudes than their 8-oxoG counterparts can be seen as the incubation time was increased. The concentration of free G decreased from 0 to 4 min incubation with Fenton reagents. After 4 min incubation the concentration of G returned to its initial concentration; thereafter the overall pattern was towards its decrease, presumably by oxidation to 8-oxoG. At this point it was noted that G, on incubation with the Fenton reagents iron(II)sulphate and H_2O_2, was observed to decrease; though not linear, this decrease continued with incubation time. After 15 min the concentration of 8-oxoG was also seen to decrease. This meant that, after 15 min incubation, the concentrations both of G and

8-oxoG decreased, so both species were being consumed, presumably oxidised, by the Fenton reagents.

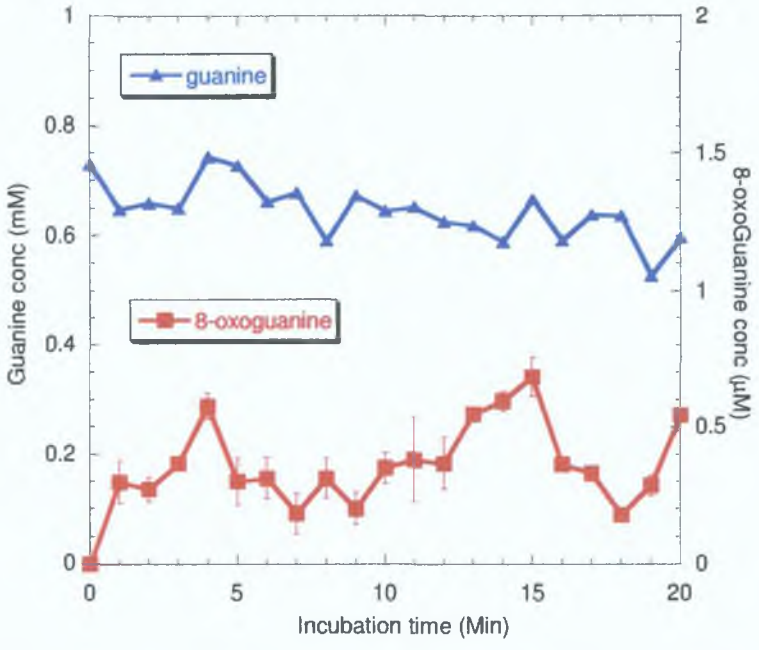

Fig. 2.12: Concentration of G and 8-oxoG in free G, from 0 – 20 min incubation with 150 μM iron(II)sulphate and 50 mM H_2O_2 at 37 °C, UV detection at 254 nm, EC detection at a potential of 550 mV vs. Ag/AgCl, sensitivity 5 nA, mobile phase of 50 mM ammonium acetate with 50 mM acetic acid in 5% methanol and a flowrate of 1 ml/min. (n=6)

To examine whether the oscillations in 8-oxoG concentration were dependent on the concentration of G in the reaction, two free G solutions, one 800 μM as usual, and one 8 μM, were incubated simultaneously with the Fenton reagents. Samples were taken at five min intervals from 0 to 60 min. The concentration of 8-oxoG in both samples was measured and plotted in Fig. 2.13. (For comparison, values for 8 μM free G are multiplied by 100 so that the effective initial concentration of both data sets is the same, *i.e.,* 800 μM.)

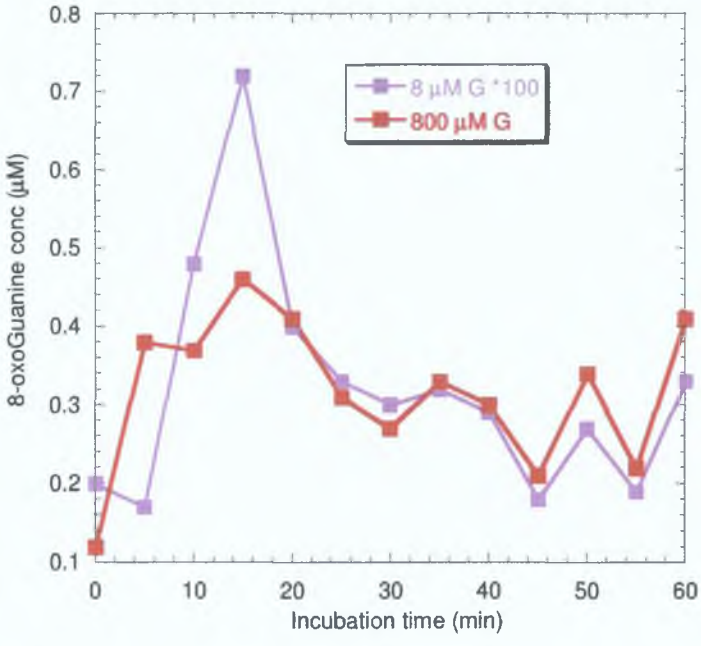

*Fig. 2.13: Concentration of 8-oxoG in 800 µM free G (red) and, in 8 µM free G (purple)*100 from 0 – 60 min incubation with 150 µM iron(II)sulphate and 50 mM H_2O_2 at 37 °C, EC detection at a potential of +550 mV vs. Ag/AgCl, sensitivity 5 nA, mobile phase of 50 mM ammonium acetate with 50 mM acetic acid in 5% methanol and a flowrate of 1 ml/min. (n=6)*

With the exception of the concentration of 8-oxoG at 15 min, there is a striking correlation between the oscillations observed at the two concentrations of free G. Given the reproducible nature of the oscillations in 8-oxoG concentration between the two free G concentrations, it would appear as though the *pattern of oscillations* in 8-oxoG concentration might be independent of G concentration for the concentration range 8 µM to 800 µM.

2.4.2 Rate of 8-oxoG formation in PolyGuanylic Acid

Incubation of free G with Fenton reagents generated 8-oxoG, where its concentration was observed to oscillate with increasing incubation time. *In vivo* G

does not exist as a free base, but is normally covalently bound to the DNA backbone. To investigate what, if any, effect the polymer backbone would have on the oscillations of 8-oxoG concentration, PolyGuanylic acid (PolyG) was incubated with the Fenton reagents iron(II)sulphate and H_2O_2.

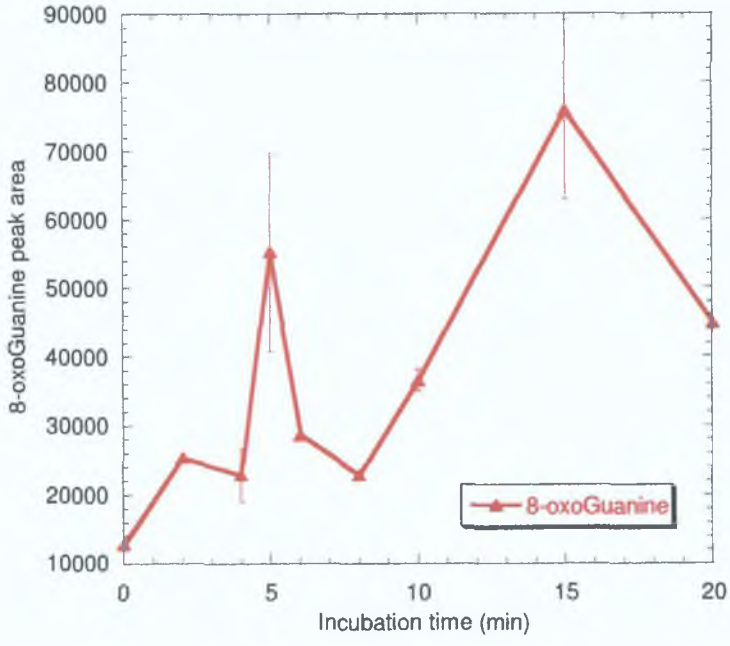

Fig. 2.14: Concentration of 8-oxoG in PolyG, from 0 – 20 min incubation with 150 μM iron(II)sulphate and 50 mM H_2O_2 at 37 °C, EC detection at a potential of +550 mV vs. Ag/AgCl, sensitivity 5 nA, mobile phase of 50 mM ammonium acetate with 50 mM acetic acid in 5% methanol and a flowrate of 1 ml/min. (peak area plotted as integrated peak area, not normalised with internal standard) (n=6)

Samples were taken after 0, 2, 4, 5, 6, 8, 10, 15 and 20 min incubations, and the changes in 8-oxoG concentration with increasing incubation time were plotted in Fig. 2.14. The resulting plot looks similar to that of Fig. 2.13, which shows the concentration of 8-oxoG in free G over the same time frame. Again the concentration of 8-oxoG increased up to 5 min incubation, only to drop sharply before increasing again to a maximum concentration at approx. 15 min incubation. The polymer backbone appears to have no effect on the oscillatory nature of 8-oxoG

concentration with increasing incubation time with the Fenton reagents, or indeed to affect the frequency of the oscillations.

2.4.3 Rate of 8-oxoG formation and oxidation in double stranded DNA

8-oxoG was shown to be generated by the iron-mediated Fenton oxidation of free G (Section 2.2.1) and of PolyG (Section 2.2.2). Oxidation of both free G and PolyG resulted in similar oscillating patterns of 8-oxoG concentration over the examined incubation time of 20 min. This demonstrated that the polymer backbone of PolyG did not influence the mechanism of oxidation of G to 8-oxoG. The next step in this analysis was the Fenton oxidation of G within the DNA double helix. Double stranded (ds) DNA was incubated with the Fenton reagents. 8-oxoG was formed immediately. As with free G and PolyG, its concentration was found to oscillate. This is shown in Fig. 2.15.

The concentration of G was also monitored. It was observed to decrease immediately. From 0 – 2 min there was a sharp decrease in its concentration, indicating its immediate consumption. The rate of G decrease slowed significantly after this point, though as with free G (Fig. 2.12), the overall trend was for its decrease over time. Again, as for free G, this decrease was not a linear one. Instead, the concentration was found to oscillate with increasing incubation time. Corresponding to the initial decrease in G concentration, there was an immediate increase in 8-oxoG concentration on incubation with the Fenton reagents. This is illustrated in more detail in Fig. 2.16.

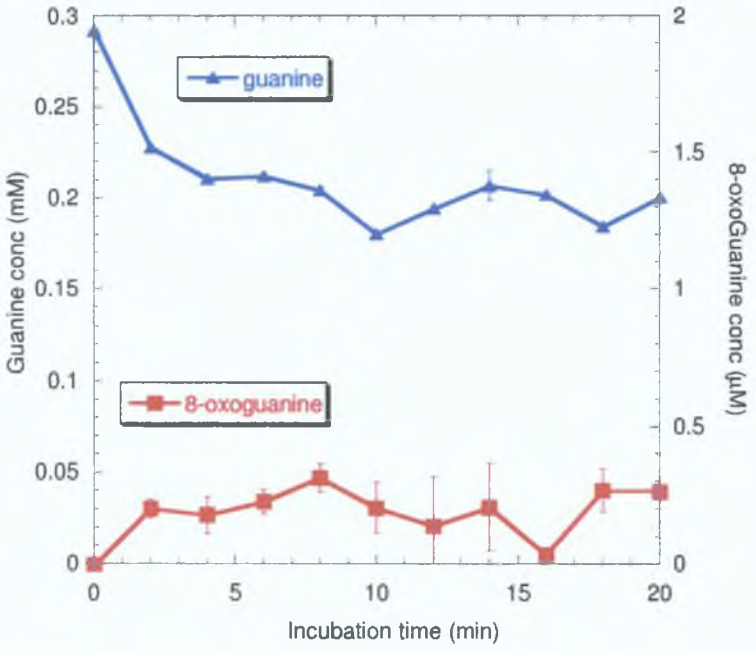

Fig. 2.15: Concentration of G and 8-oxoG in ds DNA from 0 – 20 min incubation with 150 μM iron(II)sulphate and 50 mM H_2O_2 at 37 °C. (n=4)

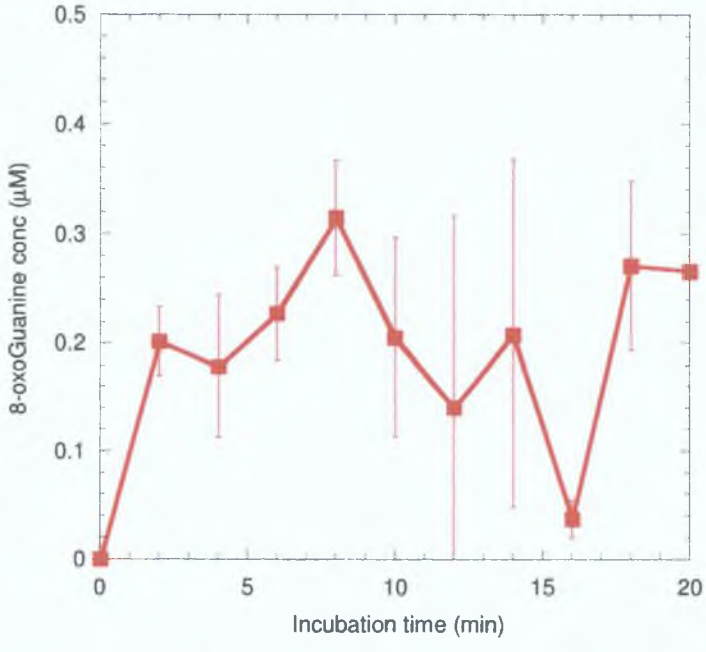

Fig. 2.16: Concentration of 8-oxoG in ds DNA from 0 – 20 min incubation with 150 μM iron(II)sulphate and 50 mM H_2O_2 at 37 °C. (n=4)

The same oscillatory pattern was observed for 8-oxoG concentrations in DNA as had been observed for free G (Fig. 2.11). From 0 to 2 min incubation there was a steady increase in 8-oxoG concentration. After a slight dip in concentration by 4 min, the concentration was observed to increase until 8 min incubation. This first concentration maximum occurred slightly later than with free G, which was expected, due primarily to the shielding effect of the DNA double helical structure. Again, as with free G, the concentration dropped sharply after this maximum, only to increase and reach a second concentration maximum at 18 min. This is also slightly later than the free G maximum, which was observed at 15 min. This pattern differs from the free G pattern in that the second concentration maximum of 8-oxoG is slightly less than the initial maximum; for free G the second maximum was significantly greater than the first. After 18 min, the overall level of 8-oxoG decreased, indicating that 8-oxoG was consumed in the continuing presence of the hydroxyl radical.

2.4.4 Rate of 8-oxoG oxidation

Having a lower oxidation potential than G, 8-oxoG is readily oxidisable. Given the trend of decreasing 8-oxoG concentration after approx. 15 min incubation with the Fenton reagents in the previous results, it would appear that is it readily oxidisable by the Fenton reagents. In order to investigate whether 8-oxoG was readily oxidised in the presence of the Fenton reagents, 8-oxoG std was incubated with 150 μM iron(II)sulphate and 50 mM H_2O_2. 8-oxoG should be easily oxidised, if it were consumed in an oscillatory fashion, however, this could be one of the factors that caused the oscillations in 8-oxoG concentration and the trend towards an overall decrease in concentration after its initial formation, *i.e.,* that as it was formed and its concentration increased, it was further oxidised by the same reagents that were involved in its generation. As can be seen from Fig. 2.17, it was immediately oxidised, with 95% consumption after just 5 min incubation.

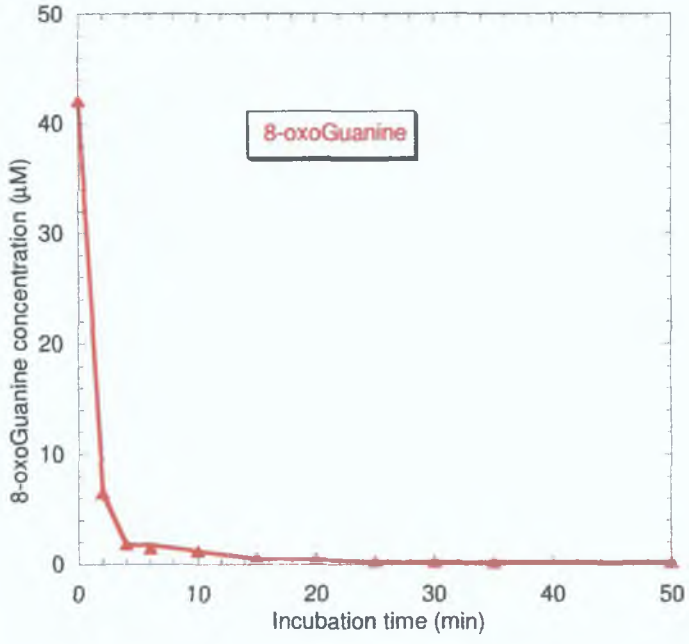

Fig. 2.17: Concentration of 8-oxoG from 0 – 90 min incubation with 150 µM iron(II)sulphate and 50 mM H_2O_2 at 37 °C, EC detection at a potential of +550 mV vs. Ag/AgCl, sensitivity 5 nA, mobile phase of 50 mM ammonium acetate with 50 mM acetic acid in 5% methanol and a flowrate of 1 ml/min. (n=6)

The oscillatory pattern repeatedly observed for G, PolyG and DNA oxidation was not observed here whatsoever. Neither, however, was all the 8-oxoG consumed as the incubation period increased. After 50 min incubation there was still a significant concentration of 8-oxoG (0.28 µM). Given the rapid decrease of 8-oxoG initially, it was expected that 8-oxoG would have been completely oxidised by this stage. While it was possible that all the Fenton reagents were consumed, this was unlikely given the excess of the H_2O_2 (50 mM) during the reaction, and the relatively low rate of reaction (76 $M^{-1}s^{-1}$). Nonetheless, based on the initial levels of 8-oxoG oxidation, and the initial levels of 8-oxoG formation observed previously in this study (from free G in Fig. 2.11), it was concluded that the rate of 8-oxoG oxidation is far greater than that of G oxidation.

2.4.5 Rate of 8-oxoG formation and oxidation induced by H_2O_2

H_2O_2 spontaneously degrades in solution. The Fenton reaction is simply the iron-catalysed decomposition of H_2O_2. It may be possible that the spontaneous degradation of H_2O_2, *i.e.*, breakdown of H_2O_2 other than by the Fenton reaction, may account for the patterns of 8-oxoG concentration oscillations observed. In order to investigate whether these reactions were the cause for the oscillations observed, control incubations were carried out. These incubations were analogous to those previously described, except that only 50 mM H_2O_2 was added, and the 150 µM iron(II)sulphate was omitted. These incubations were carried out for both free G and DNA solutions. The results for free G incubations are illustrated in Fig. 2.18.

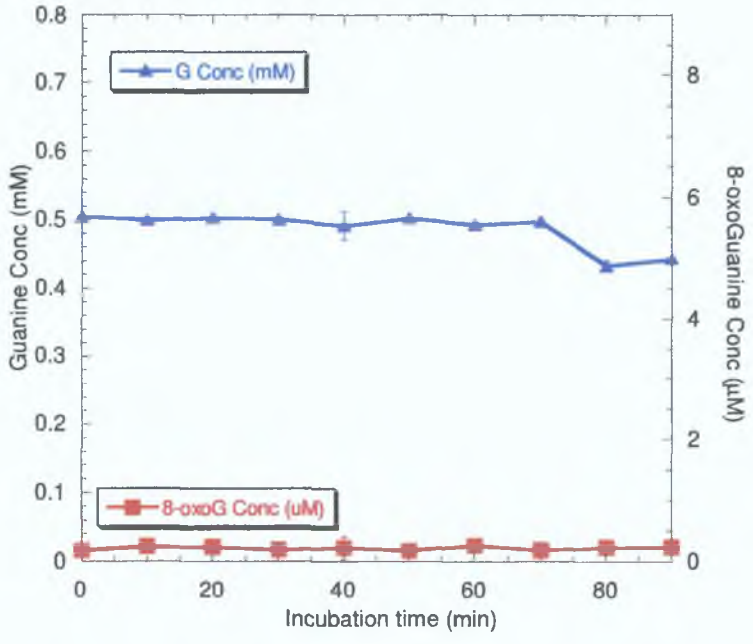

Fig. 2.18: Concentration of G and 8-oxoG from 0 – 90 min incubation of G with H_2O_2 only at 37 °C, UV detection at 254 nm, EC detection at a potential of +550 mV vs. Ag/AgCl, sensitivity 5 nA, mobile phase of 50 mM ammonium acetate with 50 mM acetic acid in 5% methanol and a flowrate of 1 ml/min. (n=6)

As can be seen from Fig. 2.18, a residual concentration of 8-oxoG was generated by this reaction. However, there was no increase in the concentration of 8-oxoG present as the incubation time with H_2O_2 increased and the concentration of 8-oxoG did not oscillate with increasing incubation time. Neither was there any consumption of free G as the incubation time increased, nor any oscillations in its concentration. Therefore it can be concluded that it is not the products of spontaneous degradation of H_2O_2 with G base which leads to the oscillatory pattern observed when G was incubated with the Fenton reagents H_2O_2 and iron(II)sulphate.

This control incubation was then repeated, this time using DNA, to eliminate G oxidation by the products of spontaneous degradation of H_2O_2 as a possible cause of the oscillatory pattern of 8-oxoG concentration during incubation with the Fenton reagents. The results are illustrated in Fig. 2.19.

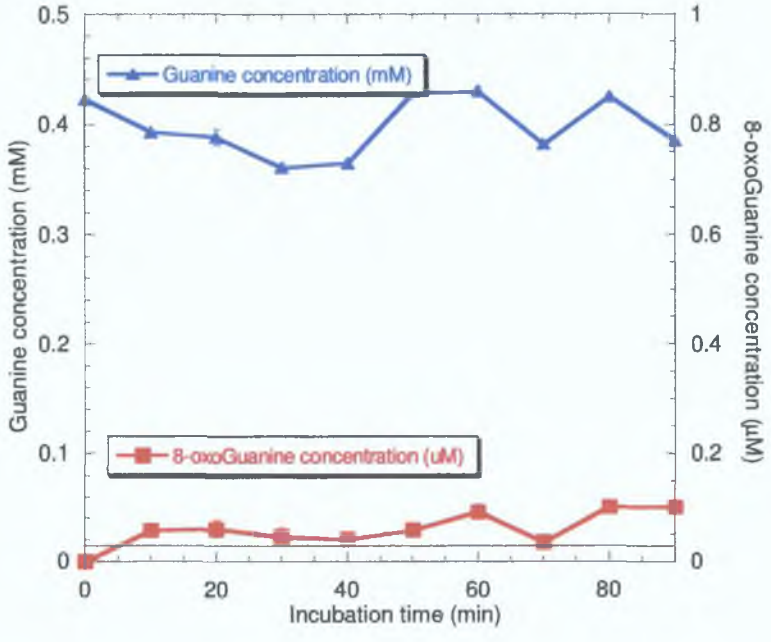

Fig. 2.19: Concentration of G and 8-oxoG from 0 – 90 min incubation of ds DNA with H_2O_2 only at 37 °C, UV detection at 254 nm, EC detection at a potential of +550 mV vs. Ag/AgCl, sensitivity 5 nA, mobile phase of 50 mM ammonium acetate with 50 mM acetic acid in 5% methanol and a flowrate of 1 ml/min. (n=4)

As shown in Fig. 2.19, 8-oxoG is generated to a small extent in this reaction. The highest concentration reached is only 0.1 μM, which is significantly less than that generated by the Fenton reaction (as shown in Fig. 2.15). In fact, most of the 8-oxoG concentrations are close to the detection limit (shown as the solid black line at 0.03 μM), with an average concentration of 0.0625 ± 0.025 μM. The amount of 8-oxoG found in untreated DNA was 0.06 ± 0.02 μM, the same as that generated by this reaction. It can be concluded therefore, that the incubation of ds DNA with H_2O_2 alone did not contribute either to the generation of 8-oxoG or to its oscillation in concentration as observed for the Fenton mediated oxidation of G within ds DNA. G concentration was also observed to oscillate slightly in Fig. 2.18. This oscillation was probably caused by the slight amount of G oxidation that was expected from the spontaneous degradation of H_2O_2. The level of G oxidation was significantly less than that observed for the Fenton-mediated oxidation of G, as shown in Fig. 2.15. The oxidation of G on the incubation of ds DNA with H_2O_2 alone did not significantly contribute to the oxidation of G.

2.4.6 Mass Spectroscopic analysis of 8-oxoG oxidation in DNA

The results of the investigation indicate that although 8-oxoG is generated initially, as the reaction continues its concentration oscillates with an overall trend towards a decrease. It is highly probable therefore that 8-oxoG is readily consumed by further oxidation. In order to investigate possible oxidation products of 8-oxoG oxidation, HPLC-MSMS was used to probe for new species. Unlike either UV or EC detection, mass spectrometry (MS) allows structural information about a species to be obtained, enabling identification without the need for commercial standards. Use of MSMS facilitates even more in depth structural analysis, as species of interest can be further fragmented. Fig. 2.20 shows the extracted ion chromatograms for *m/z* 152 ($[G + H]^+$), *m/z* 168 ($[8\text{-oxoG} + H]^+$), and *m/z* 158 ($[Gh + H]^+$) for the HPLC separation of salmon testes (st) DNA hydrolsyates incubated with the Fenton reagents for 60 min.

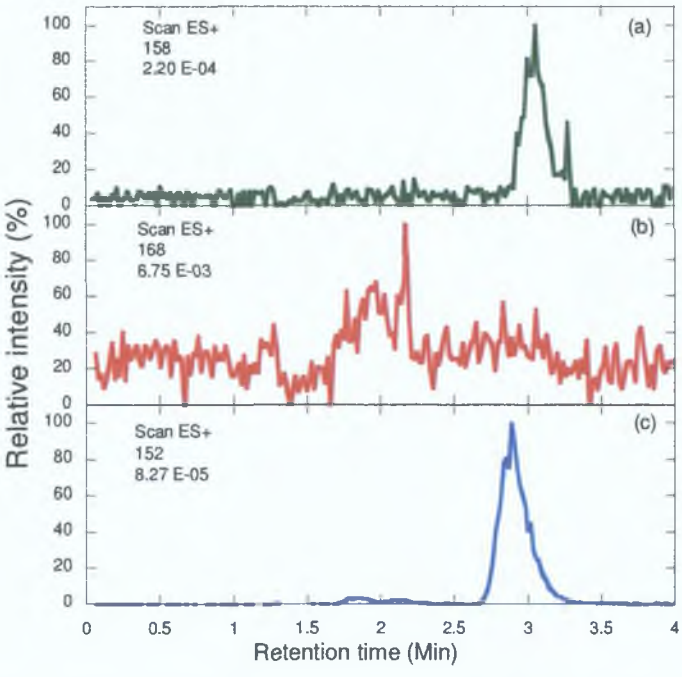

Fig. 2.20: Extracted ion chromatograms (a) m/z 158 ($[Gh + H]^+$), (b) m/z 168 ($[8\text{-}oxoG + H]^+$), and (c) m/z 152 ($[G + H]^+$) for DNA incubated for 60 min with 150 μM iron(II)sulphate and 50 mM H_2O_2 at 37 °C, flow rate of 0.3 ml/min, mobile phase of 17 mM ammonium acetate with 20 mM acetic acid in 5% methanol. Full scan spectra were taken at a cone voltage of 15 V using positive electrospray ionisation (ESI).

Due to different operating conditions used in HPLC-MS/MS, *i.e.*, column length and flow rate, the retention times of the DNA bases differed from those of the HPLC-UV-EC. For DNA oxidised for 60 min with Fenton reagents, at a retention time of approx. 2.9 min, a peak *m/z* 152, which would correspond to protonated G ions was observed to elute. To investigate for 8-oxoG oxidised products, extracted ion chromatograms (EIC) for potential products of 8-oxoG oxidation were extracted from the Total Ion Chromatogram (TIC). Potential products considered were Gh (MW 157)[35] Spiroimidinohydantoin (Sp)[36] and Imidazolone (Iz)[37] which, according to literature were the most likely products of one electron oxidations, such as that of the Fenton reaction. Ion chromatograms for *m/z* 184, corresponding to $[Sp + H]^+$ ions, *m/z* 158 corresponding to $[Gh + H]^+$ ions and *m/z* 113 corresponding to [Iz +

$H]^+$ were extracted from the TIC recorded. From these EICs, a peak corresponding to an elution of ions at *m/z* 158 was detected, suggesting the presence of guanidinohydantoin (Gh). The $[Gh + H]^+$ ions eluted with $[G + H]^+$ ions, and had a relative intensity of just 2.5% of the protonated G ions. No evidence of Sp or Iz ions was detected. Based on this data, it was concluded that Gh was possibly a product of DNA oxidation by the Fenton reaction.

EICs were also extracted at a *m/z* of 168, the mass to charge ratio corresponding to protonated 8-oxoG, *i.e.*, $[8\text{-oxoG} + H]^+$. No peak for this product was observed under any ionisation conditions, despite the EC chromatogram indicating its presence (see Fig. 2.15). Although the ionisation parameters were optimised with 8-oxoG standard, no 8-oxoG could be detected under any ionisation conditions. The absence of 8-oxoG therefore did not indicate the absence of this species; it merely demonstrated the ease at which it was further oxidised, even when using 'soft' ionisation techniques. Often, however, when a species itself is unstable during the electrospray ionisation process, its potassium (+39) and sodium (+23) adducts are significantly more stable and can be found in the resulting mass spectra. Fig. 2.21 shows the mass spectrum at 2.9 min of the TIC from the HPLC-MS. In addition to the ions of *m/z* 152, and *m/z* 158, there are also two ions of *m/z* 174 and *m/z* 190. These correspond to the ions $[G + Na]^+$ (*m/z* 174) and $[8\text{-oxoG} + Na]^+$ (*m/z* 190). It is also possible that the ion of *m/z* 190 could correspond to the $[G + K]^+$ ion, which would have the same mass as $[8\text{-oxoG} + Na]^+$. To exclude this possibility, the mass spectrum of free G was analysed. The ion of *m/z* 190 was not present in the sample of free G only. However, the ion of *m/z* 190 was present when 8-oxoG was present; this confirms the peak of *m/z* 190 to be that of $[8\text{-oxoG} + Na]^+$. This was the sole peak which confirmed the presence of 8-oxoG.

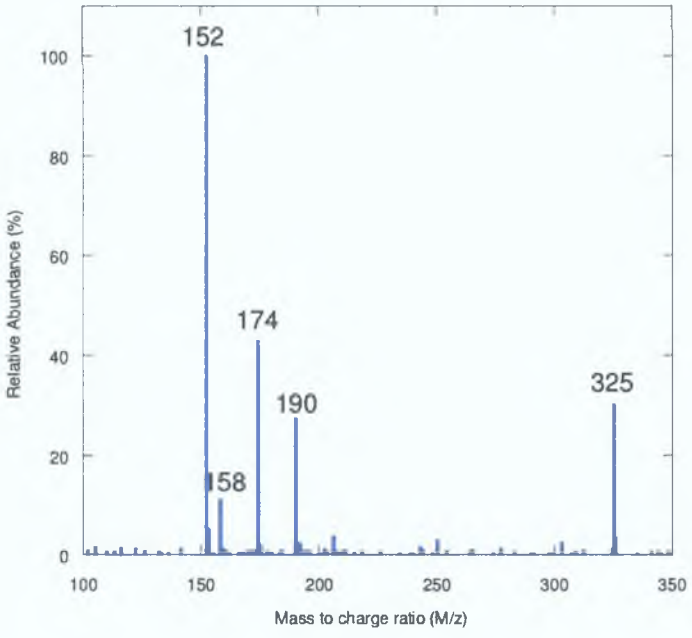

Fig. 2.21: Mass spectrum of the ion fraction eluting at 3.0 min of acid hydrolysed DNA incubated with iron(II)sulphate and H_2O_2 for 60 min at 37 °C, flow rate of 0.3 ml/min, mobile phase of 17 mM ammonium acetate with 20 mM acetic acid in 5% methanol. Full scan spectra were taken at a cone voltage of 15 V using positive electrospray ionisation (ESI).

2.5 Discussion

In this study G was oxidised by •OH (generated by the Fenton reaction, as described in Reaction 2.1), as shown in Scheme 2.2. The first step involves the addition of the •OH radical at the C8 position. This radical then undergoes a further loss of an electron and a proton, to form 8-oxo-7,8-dihydroGuanine.

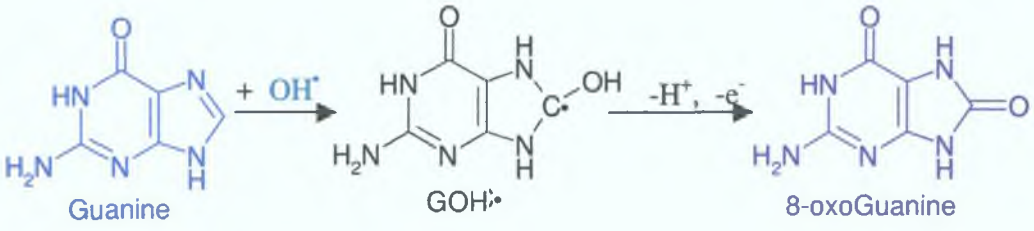

Scheme 2.2: Proposed scheme for guanine oxidation to 8-oxo-7,8-dihydroGuanine, with guanine depicted in blue, and 8-oxo-7,8-dihydroGuanine depicted in red. [38]

In order to measure the rate at which G was oxidised by •OH, and also the rate at which 8-oxoG was generated, free G was incubated with Fenton reagents, and samples taken at regular time intervals. An increase in 8-oxoG concentration and a corresponding decrease in G concentration would have been expected due to the oxidation of G and generation of 8-oxoG. As illustrated in Fig. 2.10, however, neither behaviour was observed. Although 8-oxoG was immediately generated, and its concentration increased from 0 to 15 min incubation with the Fenton reagents, this increase was not linear. From 0 to 5 min incubation, there was a significant increase in the concentration of 8-oxoG with increasing oxidation, with its concentration increasing from 0.2 μM to almost 0.4 μM. However, from 5 to 10 min incubation there was actually a slight decrease in concentration. From 10 to 15 min the 8-oxoG concentration increased at a higher rate than from 0 to 5 min, reaching almost 0.7 μM. From 15 to 45 min incubation, however, the concentration of 8-oxoG dropped dramatically, almost back to its level prior to incubation with the Fenton reagents. As this point the cycle began again, with the concentration of 8-oxoG increasing from 45 to 60 min incubation, only to fall sharply once more, so that after 70 min incubation, 8-oxoG concentration returned to its level at 45 min. The pattern

emerging was not towards a steady state; instead oscillations in 8-oxoG concentration that repeated with increasing incubation time were observed. Although until 15 min incubation, the overall trend was towards an increase in concentration; as the reaction progressed, 8-oxoG was consumed in free G, presumably by further oxidation, and so an overall decrease in concentration was observed.

As with 8-oxoG, the concentration of G also oscillated as incubation time increased, as shown in Fig. 2.12. It is possible that these oscillations could be ascribed to the regeneration of G during its oxidation, which is a minor pathway for G(-H)•. •OH can add to G at the C4, C5 and C8 positions. Approx. 25% of •OH adds to C5, which results in the formation of 8-oxoG. However, the adducts formed at C4 and C5 decay back to form the original base, in a type of "auto-repair" mechanism.[39] However, the amplitudes of G oscillations were considerably lower than those of 8-oxoG. In the case of G concentration, it was considered that the regeneration of the parent base G via the "auto-repair" mechanism outlined above would not be sufficient to result in significant regeneration of G. Instead the minor oscillations that were observed are far more likely to have been caused by experimental error during sampling, so that overall the concentration of G was just observed to decrease with increasing incubation time. As the Fenton reaction with free G progressed, both G and 8-oxoG were consumed. In the absence of one of the Fenton reagents, the concentration of free G remained constant, *i.e.,* G was not consumed, as illustrated in Fig. 2.18. It can therefore be concluded that the •OH, and not one of the starting Fenton reagents, reacted with G. 8-oxoG has an oxidation potential approx. 0.3 V lower than G,[40] and is also readily oxidised by •OH, as shown in Fig. 2.19. It can be concluded therefore that the overall decreases in G and 8-oxoG concentrations with increasing incubation time was caused by their oxidation by •OH.

This availability of two species, having different oxidation potentials, to be oxidised by •OH might be a possible reason for the oscillations in 8-oxoG observed. Fig. 2.12 plots the concentration of free G and 8-oxoG in a sample of free G as the incubation time with •OH increased. 8-oxoG was observed to be generated

immediately on incubation of G with •OH-generating agents. From 0 to 4 min, there was an excess of G over 8-oxoG in the sample, so that G, and not 8-oxoG, was preferentially oxidised by •OH. By 4 min, there was a substantially higher concentration of 8-oxoG available for further oxidation, and the level of G had also decreased somewhat. At this point, the rate of 8-oxoG oxidation was faster than the rate of 8-oxoG formation, and so there was an overall decrease in concentration until 10 min. As 8-oxoG was consumed, there was a decrease in the level of 8-oxoG available for •OH attack, and so •OH once again preferentially reacted with G (so that the rate of oxidation of 8-oxoG was dependant on its concentration). This caused a decrease in the rate of oxidation of 8-oxoG, as its concentration decreased with its oxidation. This in turn allowed for an increase in the rate of 8-oxoG formation as •OH increasingly reacted with G and not 8-oxoG, which had the effect of further increasing the concentration of 8-oxoG, from 10 to 15 min. This reached a maximum concentration of approx. 0.68 μM at 15 min. At this point the concentration of 8-oxoG was sufficiently high for the rate of 8-oxoG oxidation to exceed the rate of G oxidation, and so, after 15 min incubation the concentration of 8-oxoG again decreased, just as after 4 min, as 8-oxoG was oxidised further. With increasing incubation time, this oscillating pattern of 8-oxoG formation/oxidation continued. After 15 min incubation, however, the overall trend was for a decrease in the rate of 8-oxoG concentration. The consumption of G as the reaction progressed lead to a decrease in the rate of 8-oxoG formation over time. The 8-oxoG concentration decreased whenever the rate of its formation exceeded the rate of its consumption. As the rate of formation decreased, an ever lower rate of consumption (oxidation) exceeded it with every wave oscillation. Therefore, over time, the level of 8-oxoG in the sample was seen to decrease.

The oscillations were more than likely governed by the relative concentrations of both G and 8-oxoG and their relative rates of oxidation. This is illustrated in Fig. 2.14, which graphs the oscillations in 8-oxoG concentration for two G samples, one with a concentration of 8 μM, and one with a concentration of 800 μM. Although one sample was 100-fold more concentrated, both generated

proportionally the same concentration of 8-oxoG relative to their G concentration. Moreover, the oscillations in 8-oxoG concentration with increasing incubation time were almost identical within experimental error (apart from the samples at 15 min incubation), demonstrating that the oscillation mechanism is also independent of the initial concentration of G over the concentration range 8 μM to 800 μM. In this concentration range therefore, the pattern of 8-oxoG concentration oscillations are independent of initial G concentration. Moreover, it is highly probable that even at 8 μM, G is in excess, and the reaction between G and •OH is a pseudo-first-order reaction.

The trend of the Fenton-mediated oxidation of G was for an overall decrease in both the concentration of G and 8-oxoG. Fig. 2.22 shows the ratio [8-oxoG]/{[8-oxoG]+[G]}. After an initial peak at 5 min, peaks repeated with a frequency of approx. 15 min. If 8-oxoG were the only product, the denominator of the ratio (*i.e.*, the total concentration of G and 8-oxoG) would remain constant, and overall this ratio would increase, regardless of the oscillations. However, from 20 - 100 min, the overall trend underlying the concentration oscillations was a decrease with time, suggesting that 8-oxoG is just an intermediate in an overall reaction, or at any rate, not the only product formed during G oxidation by •OH.

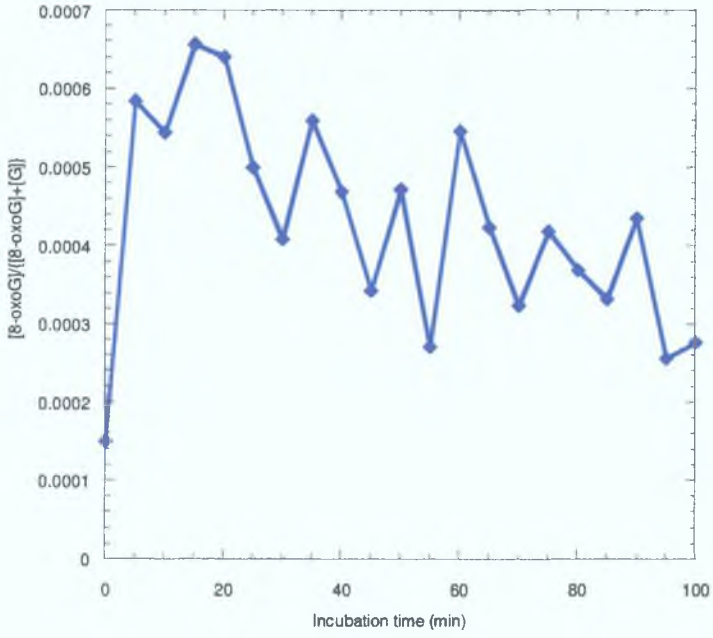

Fig. 2.22: Ratio of [8-oxo-7,8-dihydroGuanine]/{[8-oxo-7,8-dihydroGuanine]+[guanine]} for 800 μM G incubated with 150 μM iron(II)sulphate and 50 mM H_2O_2 at 37 °C.

G in DNA was expected to react in a similar manner on exposure to •OH (generated by the Fenton reaction) as free G, as the •OH has been shown to attack G bases (as well as the other DNA bases and the backbone).[19]

Fig. 2.16 graphs the concentration of 8-oxoG in a DNA sample which has been oxidised by Fenton reagents. The concentration profile of 8-oxoG was seen to oscillate in an analogous manner to that observed for free G (Fig. 2.10), with an overall trend for repeating oscillations of 8-oxoG concentration over time. After the maximum 8-oxoG concentration of approx. 0.3 μM at 8 min, there was an overall decrease in its concentration over time. As the oscillations repeated the maximum 8-oxoG concentration continually decreased. No steady state level of 8-oxoG concentration was achieved over the time period examined. The concentrations of 8-oxoG for the first and second maxima differed for both G and DNA. In the case of free G, the second concentration maximum was greater than the first; this was not

the case for DNA, where both concentration maxima were approx. equal, within experimental error. The maximum concentrations of 8-oxoG in DNA (Fig. 2.16) occurred around 3 min later than for free G, at approx. 8 and 18 min. This delay was expected, because of the shielding effect of the phosphodiester sugar backbone of DNA. The double helix of DNA is like a winding staircase with the bases protected between the two polymer backbones. •OH attacks all biomolecules, and so the initial •OH generated may not attack the bases directly, but instead abstract hydrogens from the sugars of DNA, which are on the outer layer of the double helix. This accounts for the slightly slower rate of 8-oxoG formation. (About 20% of •OH attack the 2'-deoxyribose sugars of the DNA backbone, extracting hydrogen from the carbon atoms, with extraction at the C4 position probably the most important process.[39]) Fig. 2.13 illustrates the oscillations observed when PolyG (G covalently attached to a polymer backbone, but not protected within a double helical structure) was oxidised by Fenton reagents. 8-oxoG concentration maxima occurred at 4 and 15 min, just as with free G, demonstrating that the polymer backbone of itself did not cause a delay in the maxima observed. The polymer backbone only restricted the oxidation of bases within the double helix. In this case, as observed by Lloyd *et al.*,[41] •OH also reacts with the DNA backbone by breaking one or both of the strands (by abstracting hydrogens from the sugar backbone) in addition to adding to the DNA bases themselves.

As with free G, there was also a decrease in the ratio [8-oxoG]/{[8-oxoG]+[G]} over time for DNA, as shown in Fig. 2.23. This again indicates that 8-oxoG was not the only product of •OH-mediated G damage (this time within DNA), or that it is merely an intermediate in this oxidation pathway.

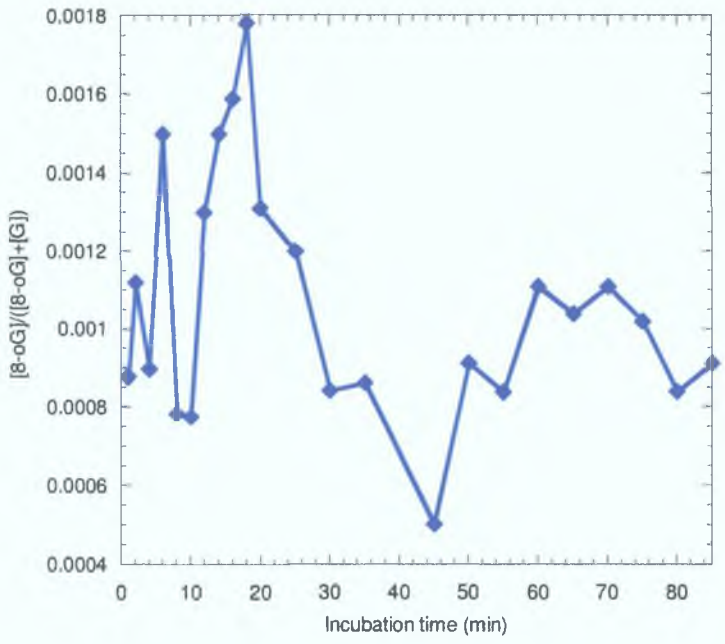

Fig. 2.23: Ratio of [8-oxo-7,8-dihydroGuanine]/{[8-oxo-7,8-dihydroGuanine]+[guanine]} for DNA incubated with 150 μM iron(II)sulphate and 50 mM H_2O_2 at 37 °C.

The results clearly indicate the formation of further oxidation products. However, apart from 8-oxoG, no other direct oxidation products of G itself (*e.g.* FapyG, Imidazolone) were considered during this analysis. Instead the study focussed on the concentration of 8-oxoG, due to its importance as a biomarker as outlined in Chapter 1. The results of this study, however, imply the formation of other products besides those of 8-oxoG and G. Figs 2.22 and 2.23 demonstrate that there was a decrease in the ratio [8-oxoG]/{[8-oxoG]+[G]} as the incubation time with the Fenton reagents increased, which is consistent with the oxidation of 8-oxoG.

HPLC-MS was used to analyse DNA samples which had been incubated with the Fenton reagents for 60 min, to investigate what, if any, other oxidised products of G oxidation were generated. 60 min incubation time was chosen as by this time, at least two complete oscillations should have occurred, so that 8-oxoG

oxidation products should be present in solution. A number of compounds emerged from the literature as potential final oxidation products. In double stranded DNA, Guanidinohydantoin (Gh) was observed as the main product by a number of authors[38,42] and was found to be generated via a 5-OH intermediate of 8-oxoG. The product 2,5-diaminoimidazolone (Iz) also emerged as possible oxidation products of Gh oxidation.[37]

For the initial MS analysis, the oxidation products of Gh oxidation were not considered. This oxidation, according to literature, is far slower, with the half life of Gh reported to be approximately 10 hr.[35] As the incubation period was only 60 min, Gh oxidation was deemed highly unlikely to have taken place. Even taking long range charge transfer into account, the continuing presence of 8-oxoG in solution, which has a lower oxidation potential than Gh, would not have favoured its oxidation.

For MS analysis, samples were firstly ionised, using positive electrospray ionisation. The operating conditions were optimised using G and 8-oxoG standards. With the 8-oxoG standard however, the protonated ion (*m/z* 168) was not be detected. The sodium adduct ion was detected at *m/z* 190, with control experiments implying that that it was $[8\text{-oxoG} + Na]^+$ and not the $[G + K]^+$ ion. (which would have had the same mass). As Gh was more stable than 8-oxoG, at the very least the sodium adduct ion, if not the protonated ion, would be detected. However, an indepth optimisation of the MS ionisation was not carried out at this stage. This may have lead to the detection of *m/z* 168, but as UV and EC detection already confirmed the presence of this product, it was deemed unnecessary at this point.

The protonated form of Gh was expected to have a mass to charge ratio (*m/z*) 158. The extracted ion chromatograms plotted in Fig. 2.9 showed peaks at *m/z* 152 $[G + H^+]$ at a retention time of 2.9 min and *m/z* 158 $[Gh + H^+]$ at 3.1 min. This confirmed the presence of G and also suggested the presence of Gh in the DNA sample. The peak area of protonated Gh ions corresponded to just 2.5% of the

relative intensity of protonated G ions, and co-eluted with the G ions. Without a available standard with which to calibrate the instrument, however, it could not be assumed that the relationship between the relative intensities of both species was proportional to their relative concentrations. In this instance therefore, although HPLC-MS?MS is capable of quantitative measurement, it could not be used in that capacity for the purpose of determining the concentration of Gh in the DNA samples analysed.

As discussed, the absence of a peak of *m/z* 168 did not correspond to a lack of 8-oxoG in the sample. The mass spectrum obtained from the TIC between 2.9-3.1 min (where both G and Gh eluted) illustrated in Fig. 2.21, showed peaks at *m/z* 152, and *m/z* 158, and also peaks at *m/z* 174 and *m/z* 190. The latter two peaks corresponded to the ions $[G + Na]^+$ (*m/z* 174) and $[8\text{-oxoG} + Na]^+$ (*m/z* 190), confirming the presence of 8-oxoG. From this HPLC-MS analysis, the species Gh was suggested as a possible oxidation product of 8-oxoG oxidation.

2.6 Conclusions

The rate of 8-oxoG formation and oxidation, both in free G and in ds DNA, was investigated in this study. During *in vitro* analysis, 8-oxoG was shown to be generated immediately on incubation with reagents iron(II)sulphate and H_2O_2; reagents which produce •OH via the Fenton reaction. The concentration of 8-oxoG was observed to oscillate repeatedly with increasing incubation time, though with an overall trend towards a decrease. G was shown to be oxidised immediately, with a sharp initial drop in concentration recorded on incubation with the Fenton reagents. Its concentration also oscillated over the incubation time studied. As with 8-oxoG, its concentration also tended towards a decrease.

For free G, a maximum concentration of 0.68 μM was observed after 15 min incubation with the Fenton reagents. Thereafter, for 8-oxoG, the repeating oscillations, which occurred with a frequency of approx. 15 min, resulted in an overall decrease in 8-oxoG concentration, with each maximum smaller than its predecessor. For ds DNA a maximum concentration of 0.3 μM was observed at 8 min. In the case of free G, the second concentration maximum was greater than the first; this was not the case of DNA. The difference in concentration between the two maxima in DNA is sufficiently small, however, as to be within experimental error. Oscillations in the ratio [8-oxoG]/{[8-oxoG]+[G]} were superimposed on a general decreasing trend as the incubation time with the Fenton reagents increased, consistent with the oxidation of 8-oxoG. Overall, both the concentrations of G and 8-oxoG were observed to decrease as the oxidation reaction progressed. The decrease in concentrations of both G and 8-oxoG were not linear, but oscillated with increasing incubation time with the Fenton reagents. Of the two species, the 8-oxoG oscillations were more pronounced in amplitude. Furthermore, underlying these oscillations was a trend of initial 8-oxoG oxidation (no 8-oxoG initially in free G) followed by its further oxidation.

To investigate the 8-oxoG oscillations more fully, a number of parameters were then explored. Interactions with the products of possible spontaneous decomposition of H_2O_2 were eliminated as possible causes of 8-oxoG oxidation during this reaction. The role of the polymer backbone of DNA was also analysed, and it was concluded that it protected the DNA within the double helical structure. The oscillations in 8-oxoG concentration were found to be independent of the initial concentration of G over a concentration range 8 μM to 800 μM. It is highly probable that even at 8 μM, G is in excess, and the reaction between G and •OH is a pseudo-first-order reaction.

These results are consistent with a competitive consecutive process in which G is oxidised to 8-oxoG, which is itself further oxidised, possibly to Gh. A simple competitive reaction is outlined in Section 2.4; it is unfortunately unlikely to lead to oscillating concentrations of 8-oxoG.[43] Oscillating reactions studied in detail typically have very complex pathways, *e.g.* the chlorite-iodide reaction has 13 elementary steps[44] and the reaction of NADH with O_2 catalysed by peroxidases has 37 elementary steps.[45] The reaction outlined does however highlight the inherent instability of 8-oxoG in the continuing presence of the oxidising reagents such as •OH.

On the basis of this investigation, and the ease of oxidation of 8-oxoG, 8-oxoG may not be a viable biomarker for DNA damage. Its concentration depends not only on the amount of oxidative damage caused to DNA, but also to the length of time it was exposed to the damaging reagent, which also potentially has the ability to oxidise 8-oxoG. The products of 8-oxoG oxidation, such as Gh, should be investigated in more detail, as they may emerge as more suitable biomarkers of oxidative DNA damage. Unless the reaction is highly site-specific, however, it should be remembered that in all likelihood, further oxidation of 8-oxoG in DNA is extremely unlikely.

2.7 References

1. Ames, B. N.; Endogenous oxidative DNA damage, aging and cancer, *Free Radical Research Communications* **1989**, *7*, 121-128.

2. Beckman, K. B.; Ames, B. N.; Oxidative decay of DNA, *Journal of Biological Chemistry* **1997**, *272*, 19633-19636.

3. Kasai, H.; Crain, P. F.; Kuchino, Y.; Nishimura, S.; Ootsuyama, A.; Tanooka, H.; Formation of 8-hydroxyguanine moiety in cellular DNA by agents producing oxygen radicals and evidence for its repair, *Carcinogenesis* **1986**, *7*, 1849-1851.

4. Doddridge, Z. A.; Cullis, P. M.; Jones, G. D. D.; Malone, M. E.; 7,8-Dihydro-8-oxo-2'-deosyguanosine residues in DNA are radiation damage "hot" spots in the direct radiation damage pathway, *Journal of the American Chemical Society* **1998**, *120*, 10998-10999.

5. Melvin, T.; Cunniffe, S. M. T.; O'Neill, P.; Parker, A. W.; Roldan-Arjona, T.; Guanine is the target for direct ionization damage in DNA, as detected using excision enzymes., *Nucleic Acids Research* **1998**, *26*, 4935-4942.

6. Paillous, N.; Vicendo, P.; Mechanisms of photosensitized DNA cleavage, *Journal of Photochemistry and Photobiology B: Biology* **1993**, *20*, 203-209.

7. Aust, A. E.; Everleigh, J. F.; Mechanisms of DNA oxidation, *Experimental Biology and Medicine* **1999**, *222*, 246-252.

8. Koshinen, M.; Vodickova, L.; Vodicka, P.; Warner, S. C.; Hemminki, K.; Kinetics of formation of specific styrene oxide adducts in double stranded DNA, *Chemico-Biological Interactions* **2001**, *138*, 111-124.

9. Miura, T.; Muraoka, S.; Fujimoto, Y.; Zhao, K.; DNA damage induced by catechol derivatives, *Chemico-Biological Interactions* **2000**, *126*, 125-136.

10. Halliwell, B.; Oxygen and nitrogen are pro-carcinogens. Damage to DNA by reactive oxygen, chlorine and nitrogen species: measurement, mechanism and the effects of nutrition., *Mutation Research/Genetic Toxicology and Environmental Mutagenesis* **1999**, *424*, 37-52.

11. Halliwell, B.; Gutteridge, J. M. C.; Oxygen toxicity, oxygen radicals, transition metals and disease, *Biochemical Journal* **1984**, *219*, 1-14.

12. Dreher, D.; Junod, A. F.; Review: Role of oxygen free radicals in cancer development, *European Journal of Cancer* **1996**, *32A*, 30-38.

13. Walling, C.; Fenton's reagent revisited, *Accounts of Chemical Research* **1975**, *8*, 135-131.

14. Wink, D. A.; Nims, R. W.; Saavedra, J. E.; William E. Utermahlen, J.; Ford, P. C.; The Fenton oxidation mechanism: reactivities of biologically relevant substrates with two oxidizing intermediates differ from those predicted for the hydroxyl radical, *Proceedings of the Natural Academy of Sciences USA* **1994**, *91*, 6604-6608.

15. Meneghini, R.; Iron homeostasis, oxidative stress and DNA damage, *Free Radical Biology and Medicine* **1997**, *23*, 783-792.

16. Kruszewski, M.; Labile iron pool: the main determinant of cellular response to oxidative stress, *Mutation Research/Fundamentals and Molecular Mechanisms of Mutagenesis* **2003**, *531*, 81-92.

17. Turi, J. L.; Yang, F.; Garick, M. D.; Piantadose, C. A.; Ghio, A. J.; The iron cycle and oxidative stress in the lung, *Free Radical Biology and Medicine* **2004**, *36*, 850-857.

18. Pryor, W. A.; Why is the hydroxyl radical the only radical that commonly adds to DNA? Hypothesis: it has a rare combination of high electrophilicity, high thermochemical reactivity, and a mode of production that can occur near DNA., *Free Radical Biology and Medicine* **1988**, *4*, 219-223.

19. Cadet, J.; Delatour, T.; Douki, T.; Gasparutto, D.; Pouget, J.-P.; Ravanat, J.-L.; Sauvaigo, S.; Hydroxyl Radicals and DNA base damage, *Mutation Research/Fundamentals and Molecular Mechanisms of Mutagenesis* **1999**, *424*, 9-21.

20. Steenken, S.; Jovanovic, S. V.; How easily oxidisable is DNA? One-electron transfer reduction potentials of adenosine and guanosine radicals in aqueous solution Steen Steenken, Slobadan V. Jovanovic, *Journal of the American Chemical Society* **1997**, *119*, 617-618.

21. Floyd, R. A.; The role of 8-hydroxyguanine in carcinogenesis, *Carcinogenesis* **1990**, *11*, 1447-1450.

22. Kasai, H.; Analysis of a form of oxidative DNA damage, 8-hydroxy-2'-deoxyguanosine, as a marker of cellular oxidative stress during carcinogenesis, *Mutation Research/Reviews in Mutation Research* **1997**, *387*, 147-163.

23. Halliwell, B.; Effect of diet on cancer development: is oxidative DNA damage a biomarker?, *Free Radical Biology and Medicine* **2002**, *32*, 968-974.

24. Prat, F.; Houk, K. N.; Foote, C. S.; Effect of guanine stacking on the oxidation of 8-oxoguanine in B-DNA, *Journal of the American Chemical Society* **1998**, *120*, 845-846.

25. Lloyd, D. R.; Philips, D. H.; Carmicheal, P. L.; Generation of putative intrastrand cross-links and strand breaks in DNA by transistion metal ion-mediated oxygen radical attack, *Chemical Research in Toxicology* **1997**, *10*, 393-400.

26. Helbock, H. J.; Beckman, K. B.; Shigenaga, M. K.; Walter, P. B.; Woodall, A. A.; Yeo, H. C.; Ames, B. N.; DNA oxidation matters: the HPLC-electrochemical detection assay of 8-oxo-deoxyguanosine and 8-oxo-guanine, *Proceedings of the Natural Academy of Sciences USA* **1998**, *95*, 288-293.

27. Floyd, R. A.; West, M. S.; Eneff, K. L.; Schneider, J. E.; Wong, P. K.; Tingey, D. T.; Hogsett, W. E.; Conditions influencing yield and analysis of 8-hydroxy-2'-deoxyguanosine in oxidatively damaged DNA, *Analytical Biochemistry* **1990**, *188*, 155-158.

28. Ravanat, J.-L.; Gremaud, E.; Markovic, J.; Turesky, R. J.; Detection of 8-oxoguanine in cellular DNA using 2,6-Diamino-8-oxopurine as an internal standard for high-performance liquid chromotography with electrochemical detection, *Analytical Biochemistry* **1998**, *260*, 30-37.

29. Carmichael, P. L.; Hewer, A.; Osborne, M. R.; Strain, A. J.; Philips, D. H.; Detection of bulky DNA lesions in the liver of patients with Wilson's disease and primary haemochromatosis, *Mutation Research/Fundamentals and Molecular Mechanisms of Mutagenesis* **1995**, *326*, 235-243.

30. Ravanat, J.-L.; Turesky, R. J.; Gremaud, E.; Trudel, L. J.; Stadler, R. H.; Determination of 8-oxoguanine in DNA by gas chromatography-mass spectrometry and HPLC-electrochemical detection: overestimation of the background level of the oxidized base by the gas-chromatography-mass spectrometry assay, *Chemical Research in Toxicology* **1995**, *8*, 1039-1045.

31. Vasquez, H.; Seifert, W.; Strobel, H.; High performance liquid chromatographic method with electrochemical detection for the analysis of O^6-methylguanine, *Journal of Chromatography B* **2001**, *759*, 185-190.

32. Zhou, L. Oxidative voltammetric electrochemical analysis of chemically induced DNA damage, University of Connecticut, 2002.

33. Harris, D. C. *Quantitative Chemical Analysis*, 5th ed.; W.H. Freeman and Company: New York.

34. Frelon, S.; Douki, T.; Favier, A.; Cadet, J.; Hydroxyl radical is not the main reactive species involved in the degredation of DNA bases by copper in the presence of hydrogen peroxide, *Chemical Research in Toxicology* **2003**, *16*, 191-197.

35. Luo, W.; Muller, J. G.; Rachlin, E. M.; Burrows, C. J.; Characterisation of hydantoin products from one-electron oxidation of 8-oxo-7,8-dihydroguanosine in a nucleoside model, *Chemical Research in Toxicology* **2001**, *14*, 927-938.

36. Sugden, K. D.; Campo, C. K.; Martin, B. D.; Direct oxidation of guanine and 7,8-dihydro-8-oxoguanine in DNA by a high-valent chromium complex: a possible mechanism for chromate genotoxicity, *Chemical Research in Toxicology* **2001**, *14*, 1315-1322.

37. Kino, K.; Sugiyama, H.; Possible cause of GC CG transversion mutation by guanine oxidation product, imidazolone, *Chemistry and Biology* **2001**, *8*, 369-378.

38. Goyal, R. N.; Jain, N.; Garg, D. K.; Electrochemical and enzymic oxidation of guanosine and 8-hydroxyguanosine and the effects of oxidation products in mice, *Bioelectrochemistry and Bioenergetics* **1997**, *43*, 105-114.

39. Breen, A. P.; Murphy, J. A.; Reactions of oxyl radicals with DNA, *Free Radical Biology and Medicine* **1995**, *18*, 1033-1077.

40. Duarte, V.; Muller, J. G.; Burrows, C. J.; Insertion of dGMP and dAMP during in vitro DNA synthesis opposite an oxidised form 7,8- dihydro-8-oxoguanine, *Nucleic Acids Research* **1999**, *27*, 496-502.

41. Lloyd, D. R.; Carmichael, P. L.; Phillips, D. H.; Comparison of the formation of 8-hydroxy-2'-deoxyguanosine and single- and double-strand breaks in DNA mediated by Fenton reactions, *Chemical Research in Toxicology* **1998**, *11*, 420-427.

42. Hickerson, R. P.; Prat, F.; Muller, J. G.; Foote, C. S.; Burrows, C. J.; Sequence and stacking dependence of 8-oxoguanine oxidation: comparison of one-electron versus singlet oxygen mechanism, *Journal of the American Chemical Society* **1999**, *121*, 9423-9428.

43. Zuman, P.; Patel, R. Techniques in organic reaction kinetics; Wiley: New York, 1984; pp 66-100.

44. Epstein, I. R.; Kustin, K.; A mechanism for dynamical behaviour in the oscillatory chlorite-iodide reaction, *Journal of Physical Chemistry* **1985**, *89*, 2275-2282.

45. Scheeline, A.; Olson, D. L.; Williksen, E. P.; Horras, G. A.; The peroxidase-oxidase oscillator and its constituent chemistries, *Chemistry Reviews* **1997**, *97*, 739-756.

Chapter Three

Investigation of Copper as a Catalyst in Fenton Reaction-Mediated Oxidative DNA Damage

3.1 Introduction

In Chapter 2, G was oxidised by •OH generated by the iron catalysed Fenton reaction. Iron, however, is not the only transition metal available which is believed to generate oxidative DNA damage via the Fenton reaction.[1] A series of publications by Lloyd *et al.*[2-4] examined in detail the Fenton reaction-mediated damage to DNA, investigating the transition metals copper(II), cobalt(II), nickel(II), chromium(VI), chromium(III), iron(II), vanadium(III), cadmium(II) and zinc(II) as possible catalysts, with the number of DNA lesions recorded shown in Table 3.1.[4]

Table 3.1: comparison of oxidative lesions and strand breaks generated by the Fenton reaction.[4]

transition metal ion	oxidative lesions per 10^5 nucleosides	strand breaks
copper(II)	85.6	+++
chromium(VI)	25.1	+
cobalt(II)	47.5	-
iron(II)	21.7	++
nickel(II)	26.2	-
vanadium(III)	17.1	++
cadmium(II)	-	+
chromium(III)	n/a	+++
zinc(II)	-	-

Zinc(II), chromium(III) and cadmium(II) did not generate oxidative DNA lesions, while chromium(VI), cobalt(II) and nickel(II) generated levels of DNA lesions which either reached a steady state or continued to increase with increasing concentrations of metal. In the case of copper(II), iron(II) and vanadium(III), however, the trend with increasing metal concentration from 25 to 1000 μM was quite different. The levels of oxidative DNA damage were observed to fluctuate with increasing metal concentration, with maximum oxidative DNA damage observed at approx. 200 μM, but no damage recorded at maximum metal concentration (1 mM).

* +, minimal strand breaks; ++, moderate strand breaks; +++, extensive strand breaks; -, no strand breaks

These oscillations in DNA damage were not explored during the course of the investigations into the effects of transition metal on oxidative DNA damage. In light of the oscillations in oxidative DNA damage measured for iron(II)-mediated Fenton reaction in Chapter 2, however, one possible explanation could be that similar oscillations in copper(II) and vanadium(III) mediated damage could be the cause of the fluctuating levels of DNA damage recorded.

Along with iron, copper is one of the most important transition metals *in vivo*, and is a constituent of a number of important enzymes.[5] The adult human body contains approx. 80 μg of copper. The main source of copper is dietary, where it is absorbed probably as complexes or small peptides. Copper complexes enter the blood, where most of it binds tightly to serum albumin in equilibrium with a small pool of copper complexes. The total blood concentration of copper is about 16 μM.[6] In the liver, copper is incorporated into a glycoprotein ceruloplasmin (CP), and then released into circulation. Unlike iron in transferrin, CP does not exchange copper or bind extra copper readily. Cells must take up and degrade CP to obtain copper. Along with iron, copper can also become available *in vivo* for Fenton reactions to occur, as it is present in blood plasma as metalloproteins and as a number of transport and storage complexes. Copper also exists, however, in the cell nucleus where it may be involved in the condensation of DNA-histone fibres into higher order chromatin structures.[7,8] There is therefore a possibility that endogenous DNA-associated copper may be able to promote oxidative DNA damage to DNA. Copper can associate with DNA either by intercalation or by complexation to purine bases, especially to the N7 of G.[9]

The aim of this research was to determine whether the oscillations in 8-oxoG concentration observed in Chapter 3 were unique to iron, or whether they also occurred for other transition metals. Copper was chosen as an alternative catalyst to iron for the Fenton reaction mediated oxidation of DNA, as it was also an essential *trace* metal element *in vivo*, and had previously mediated oxidative DNA damage, as discussed above.

This work describes the copper-catalysed oxidation of G, 8-oxoG, PolyG and ds DNA. Free G and 8-oxoG were incubated with $CuSO_4$ and H_2O_2 for a range of incubation times, according to the protocol outlined in Chapter 2. The concentrations of both G and 8-oxoG were measured simultaneously, using HPLC separation with UV detection to monitor G and U, and using EC detection to monitor the concentration of 8-oxoG. PolyG and ds DNA were hydrolysed in 88% formic acid to release the unmodified DNA bases and 8-oxoG, which were then also analysed by HPLC-UV-EC.

In the case of free G, an oscillatory pattern of 8-oxoG concentration with increasing incubation with Fenton reagents was detected, and the concentration of G was observed to decrease. Similarly, 8-oxoG concentration oscillations were observed for PolyG incubations. For DNA incubations with the copper Fenton reagents, 8-oxoG was observed, again in an oscillatory pattern. The oscillations had a greater amplitude and narrower periodicity than those observed for analogous iron Fenton reactions, discussed in Chapter 2. The oxidation state of the copper ions involved in the oxidation of DNA was investigated. Finally the nature of the ROS generated when DNA was incubated with Cu(II) and H_2O_2, including the possibility that •OH was not involved, was discussed.

3.2 Materials and Methods

3.2.1 Materials

3.2.1.1 Chemicals

All chemicals were obtained as described in Chapter 2 in Section 2.2.1.1.

3.2.1.2 Buffers

The mobile phase for gradient HPLC-EC was prepared as described in Chapter 2 in Section 2.2.1.2.

3.2.2 Apparatus

3.1.1.1 HPLC Instrumentation

The HPLC system consisted of a Varian ProStar 230 solvent delivery module, with a Varian ProStar 310 UV-VIS detector. The system was operated using Varian ProStar 6.0 chromatography software. UV chromatograms were recorded using this software, while EC chromatograms were generated using a Shimadzu 3.1 Integrator. All other parameters were as described in Chapter 2 in Section 2.2.2.1.

3.2.3 Methods

3.2.3.1 Oxidation of Guanine

A stock solution of 10mM Guanine was prepared daily in 0.1 M NaOH, pH 11. 800 µl 10 mM 8-oxoG was incubated with 200 µl 1.5 mM copper(II) sulphate and 200 µl 0.5 M H_2O_2 at 37 °C with constant stirring. Duplicate 100 µl aliquots were taken after various incubation times. 50 µl 10 mM Uracil (prepared daily in 0.1

M NaOH) was added as an internal standard and the reaction was quenched with 1 ml 200 proof cold ethanol. The solution was dried immediately under a stream of nitrogen gas. The dried hydrolysates were refridgerated at 4 °C until further use. Immediately prior to analysis by HPLC, they were redissolved in 100 µl 10 mM NaOH and 900 µl 50 mM ammonium acetate buffer, pH 5.5, and filtered through a 25 mm Pall Acrodisc GF syringe filter with 0.45 µm pore size prior to injection. The final concentration of G was 0.8 mM.

3.2.3.2 Oxidation of 8-oxo-7,8-dihydroGuanine

A stock solution of 2.4 mM 8-oxo-7,8-dihydroGuanine (8-oxoG) was prepared in 0.1 M NaOH, pH 11. It was divided into 1 ml aliquots and frozen until required. Aliquots were defrosted immediately prior to use, to prevent decomposition of 8-oxoG. 800 µl 2.4 mM 8-oxoG was incubated with 200 µl 1.5 mM copper(II) sulphate and 200 µl 0.5 M H_2O_2 at 37 °C with constant stirring. Final concentrations in the reaction flask were 2 mM 8-oxoG, 150 µM copper(II)sulphate and 50 mM H_2O_2. Duplicate 100 µl aliquots were taken after various incubation times. 50 µl 10 mM Uracil was added as an internal standard and the reaction was quenched with 1 ml 200 proof cold ethanol. The solvent was evaporated to dryness under a stream of nitrogen gas. The dried hydrolysates were refridgerated at 4 °C until further use. Immediately prior to analysis by HPLC, they were redissolved in 1 ml 10 mM NaOH and filtered through a 25 mm Pall Acrodisc GF syringe filter with 0.45 µm pore size prior to injection. The final concentration of 8-oxoG was 200 µM.

3.2.3.3 Oxidation of PolyGuanylic Acid

A stock solution of 0.20 mg/ml PolyGuanylic acid (PolyG) was prepared in 50 mM ammonium acetate buffer, pH 5.5. 800 µl 0.20 mg/ml PolyG was incubated with 200 µl 1.5 mM copper(II) sulphate and 200 µl 0.5 M H_2O_2 at 37 °C with constant stirring. Duplicate 100 µl aliquots were taken after various incubation times. 50 µl 10 mM Uracil was added as an internal standard and the reaction was

quenched with 1 ml 200 proof cold ethanol. The solvent was evaporated to dryness under a stream of nitrogen gas.

3.2.3.4 Oxidation of DNA

A stock solution of 2.0 mg/ml DNA was prepared in 50 mM ammonium acetate buffer, pH 5.5. It was stored at 4 °C overnight prior to use to allow the DNA dissolve completely. 800 µl 0.20 mg/ml DNA was incubated with 200 µl 1.5 mM copper(II)sulphate and 200 µl 0.5 M H_2O_2 at 37 °C with constant stirring. Duplicate 100 µl aliquots were taken after various incubation times. 50 µl 10 mM U (prepared daily in 0.1 M NaOH) was added as an internal standard and the reaction was quenched with 1 ml 200 proof cold ethanol. The solvent was evaporated to dryness under a stream of nitrogen gas.

3.2.3.5 PolyG and DNA Hydrolysis

Both PolyG and DNA were hydrolysed prior to HPLC analysis. The oxidised PolyG or DNA sample was hydrolysed by adding 600 µl 88% (v/v) formic acid in evacuated and sealed Pierce hydrolysis tubes and heating at 140 °C for 30 min in a vacuum. The solvent was evaporated to dryness under a stream of nitrogen gas. The dried hydrosylates were refrigerated at 4 °C until further use. Prior to analysis they were redissolved in 1 ml 50 mM ammonium acetate buffer, pH 5.5, and filtered through a 25 mm Pall Acrodisc GF syringe filters with 0.45 µm pore size prior to injection. The final concentration of DNA was 160 µg/ml.

3.3 Results

3.3.1 Rate of 8-oxoG formation and oxidation in free G

The concentration of G and 8-oxoG from 0 to 90 min in free G incubated with 150 μM copper(II)sulphate and 50 mM H_2O_2 at 37 °C was measured using HPLC-UV-EC. The amount of 8-oxoG generated and G consumed was measured at five min intervals. The unmodified base G and internal standard U were monitored using UV detection, while 8-oxoG was simultaneously measured with EC detection, as described in Section 3.2. An immediate generation of 8-oxoG, and a corresponding decrease in free G concentration was expected, as had occurred for the analogous iron incubations in Chapter 2.

The results are illustrated in Fig. 3.1. The concentration of free G was observed to decrease, although not in a linear manner. However, as previously observed, when iron was utilised as the catalyst for the Fenton reaction (Chapter 2), these very minor oscillations were deemed to have occurred due to experimental error, and were not generated by regeneration of G base. The limit of detection (LOD) of the electrochemical detector was 0.05 μM, and only on 5 occasions did the levels of 8-oxoG produced exceed this level. The maximum 8-oxoG concentration, reached at 5 min., was approx. 0.54 μM. For the analogous iron-catalysed oxidation of free G (Fig. 2.4), the maximum 8-oxoG concentration, which was reached at 4 min., was approx. 0.57 μM. In terms of the maximum concentrations therefore, the two transition metal systems were comparable. However, the minimum concentrations observed varied drastically between both systems. The minimum 8-oxoG concentration recorded for iron did not fall below 0.2 μM at any measured incubation time, whereas for the copper system being analysed here, the minimum concentrations were undetectable and therefore less than 0.05 μM. During the iron analysis, the oscillations in concentration were observed to gradually increase and decrease with increasing incubation time. This was again observed for the copper

analysis, however, in this case, the minimum 8-oxoG concentrations fell below the LOD of the EC detector.

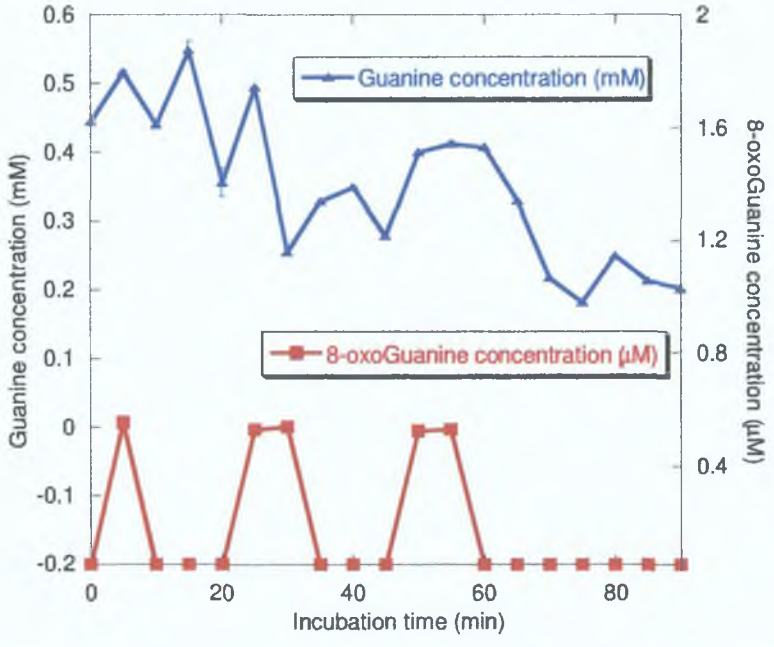

Fig. 3.1: Concentration of G (blue) and 8-oxoG (red) from 0 – 90 min incubation of free G with 150 µM copper(II)sulphate and 50 mM H_2O_2 at 37 °C, UV detection at 254 nm, EC detection at a potential of +550 mV vs. Ag/AgCl, sensitivity 5 nA, mobile phase of 50 mM ammonium acetate with 50 mM acetic acid in 5% methanol and a flowrate of 1 ml/min. (n=6)

3.3.2 Rate of 8-oxoG formation in PolyGuanylic Acid

Chapter 2 demonstrated that the polymer backbone of PolyG did not affect the iron catalysed Fenton reaction. However, given the different behaviour observed for the copper catalysed Fenton reaction of G in Section 3.2.1, it was necessary to investigate the effect of the polymer backbone once more. PolyG was incubated with copper(II)sulphate and H_2O_2. Samples were taken every 5 min from 0 to 60 min, and the results are illustrated in Fig. 3.2.

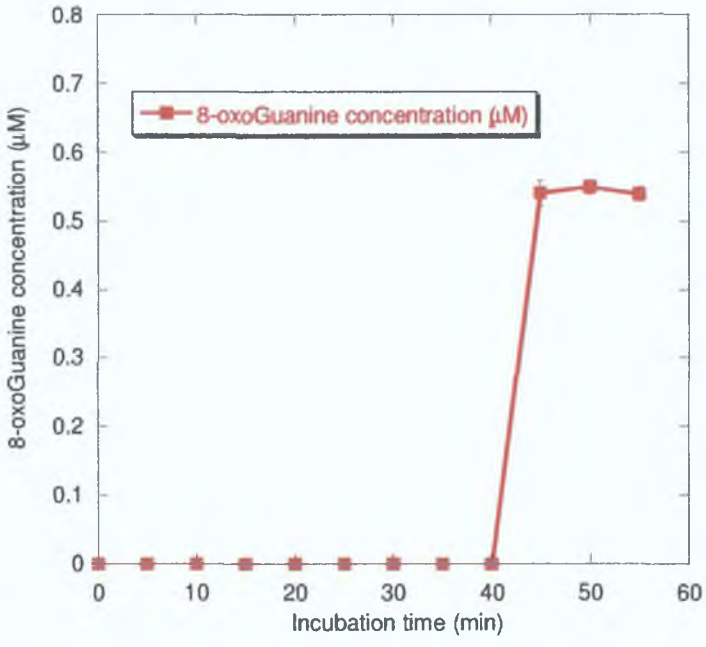

Fig. 3.2: Concentration of 8-oxoG (red) in PolyG from 0 – 60 min incubation with 150 μM copper(II)sulphate and 50 mM H_2O_2 at 37 °C, UV detection at 254 nm, EC detection at a potential of +550 mV vs. Ag/AgCl, sensitivity 5 nA, mobile phase of 50 mM ammonium acetate with 50 mM acetic acid in 5% methanol and a flowrate of 1 ml/min. (n=4)

It can be seen from Fig. 3.2 that only very low levels of 8-oxoG were generated during oxidative attack on PolyG. Only after 45 min incubation with Fenton reagents did the level of 8-oxoG produced exceed 0.05 μM, which was the smallest amount which could be measured using the HPLC-EC system. After 45 min incubation the concentration of 8-oxoG was comparable to that recorded for free G in Fig. 3.1, but did not exceed 0.55 μM at any stage during the copper-mediated oxidative attack on PolyG.

3.3.3 Rate of 8-oxoG formation and oxidation in double stranded DNA

8-oxoG was generated in oscillating concentrations during the copper-mediated oxidation of free G (Section 3.2.1) or PolyG (Section 3.2.2), but the minimum concentrations during oscillations were below the LOD of the detector. The next advancement in this analysis was the oxidation of G within DNA. Similar results, *i.e.*, the formation of 8-oxoG at intermittent incubation times, but without any apparent overall pattern, were expected. 0.16 mg/ml ds DNA was incubated with 150 µM copper(II)sulphate and 50 mM H_2O_2 at 37 °C with constant stirring. Samples were taken at five min intervals from 0 to 50 min. The concentration of 8-oxoG detected during this analysis is illustrated in Fig. 3.3.

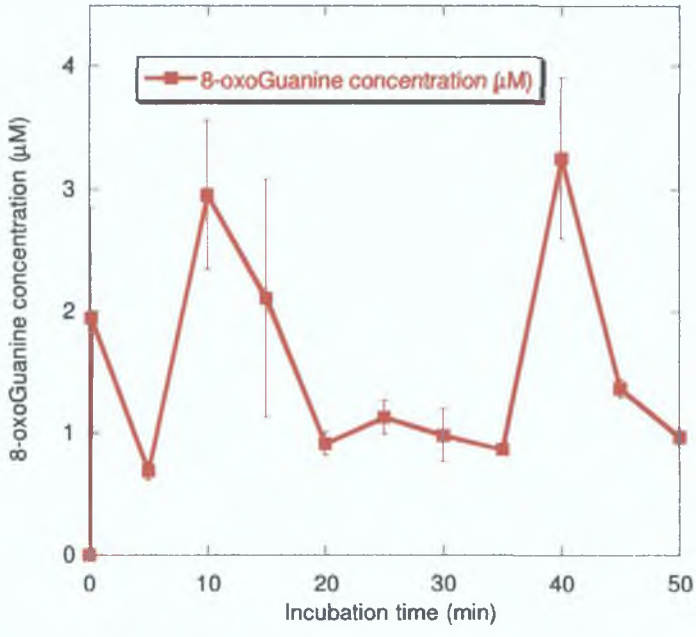

Fig. 3.3: Concentration of 8-oxoG in ct DNA from 0 – 50 min incubation with 150 µM copper(II)sulphate and 50 mM H_2O_2 at 37 °C, EC detection at a potential of +550 mV vs. Ag/AgCl, sensitivity 5 nA, mobile phase of 50 mM ammonium acetate with 50 mM acetic acid in 5% methanol and a flowrate of 1 ml/min. (n=4)

In this case, 8-oxoG was generated immediately. The concentration was seen to drop at 5 min, only to have increased to ~3 μM at 10 min. This concentration is approx. 6-fold higher than the concentration recorded for the analogous iron-mediated oxidation (Fig. 2.7). From this point until about 30 min, sampling every 5 min, the overall trend was for a decrease in concentration, although this decrease was not linear. The concentration of 8-oxoG was seen to increase again with a second maximum of equal intensity at 40 min, whereafter the concentration was again seen to decrease. From 0 to 50 min therefore, there was a very significant generation of 8-oxoG, with the concentration appearing to oscillate as the incubation time increased. This was in contrast to the results previously observed for copper-mediated oxidative attack on free G and PolyG, were significantly lower levels of 8-oxoG were detected under equivalent sampling conditions. In order to ascertain whether this oscillatory pattern continued with increasing incubation time, this study was extended to a time period of 3 hours. Fig. 3.4 plots the concentration of 8-oxoG over this extended time frame.

Oscillations were seen to continue with further maxima at ~68, 88, 125 and 150 min. This oscillating pattern of an increase in 8-oxoG concentration followed by a decrease in 8-oxoG concentration was repeated. Overall, the trend observed was a decrease in the amplitude of these oscillations, where at 150 min, the height of the oscillation is only about one third the height observed initially. At 25 min, 110 min and 170 min, secondary oscillations were observed, up to ten-fold lower than the primary oscillations.

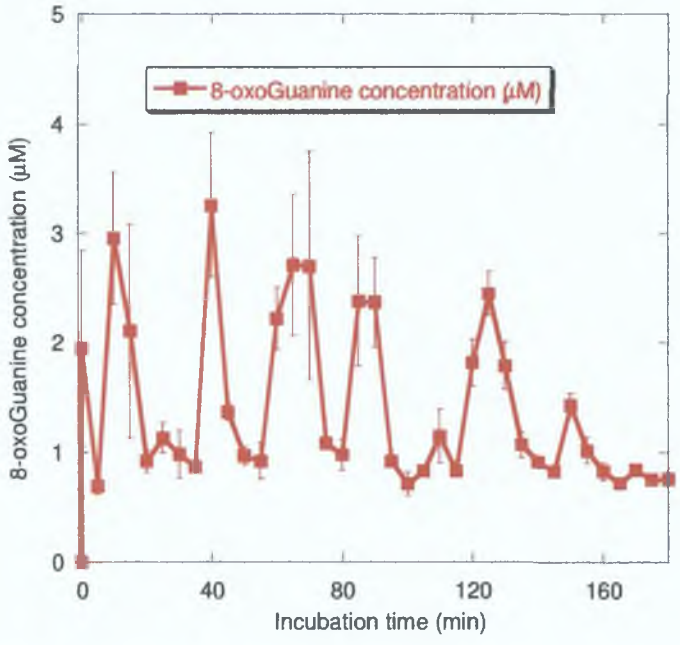

Fig. 3.4: Concentration of 8-oxoG (red) in ct DNA from 0 – 180 min incubation with 150 μM copper(II)sulphate and 50 mM H_2O_2 at 37 °C, EC detection at a potential of +550 mV vs. Ag/AgCl, sensitivity 5 nA, mobile phase of 50 mM ammonium acetate with 50 mM acetic acid in 5% methanol and a flowrate of 1 ml/min. (n=4)

The 5 min sampling frequency was previously found to be adequate for the analysis of 8-oxoG generated during the iron-generated oxidation of G, with multiple data points recorded for each oscillation, so that the sampling frequency was more than twice the period of the oscillations. This sampling frequency was, however, inadequate for a complete picture of all oscillations that were occurring during analysis of the analogous copper-generated oxidation of G. It was therefore decided to increase the sampling frequency to 1 min intervals. Fig. 3.5 shows the 8-oxoG concentration in ct DNA incubated with $CuSO_4$ and H_2O_2 from 20 to 60 min. This timeframe was chosen as both a secondary oscillation at 25 min, and a primary oscillation at 40 min were observed to occur when a sampling frequency of 5 min was used.

However, when a sampling frequency of 1 min was used, 3 primary oscillation maxima were recorded at 30, 35 and 40 min. The width of these oscillations was far narrower than was expected based on the previous experiments, with a complete oscillation taking under 5 min to occur. The maximum concentrations were even greater than those recorded for 5 min sampling intervals, reaching over 4 μM at 35 min.

A broad trend can be observed for these oscillations. A secondary maximum of approx. 0.84 μM occurred at 25 min. The next (primary) maximum at 30 min was of much higher concentration, at 3.35 μM, with the following maximum at 35 min even greater, with a concentration of 4.29 μM. This was the greatest 8-oxoG concentration observed over this timeframe. Concentration maxima of subsequent oscillations decreased sequentially. At 40 min incubation the maximum concentration was 3.19 μM, and at 45 min the maximum had decreased significantly, to 1.42 μM. There was an overall trend towards increasing 8-oxoG concentration with successive maxima until 35 min incubation; beyond this time, the overall trend was towards a decreasing 8-oxoG concentration.

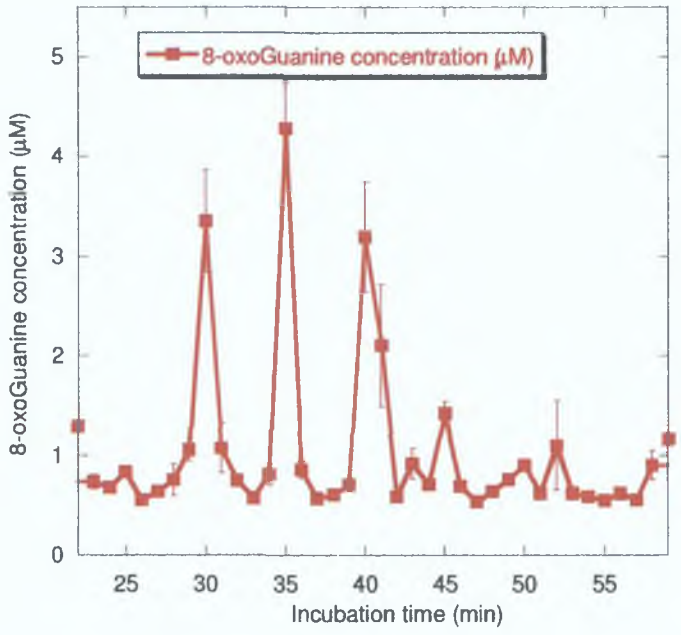

Fig. 3.5: Concentration of 8-oxoG in ct DNA from 0 – 60 min incubation with 150 µM copper(II)sulphate and 50 mM H_2O_2 at 37 °C, EC detection at a potential of +550 mV vs. Ag/AgCl, sensitivity 5 nA, mobile phase of 50 mM ammonium acetate with 50 mM acetic acid in 5% methanol and a flowrate of 1 ml/min. (n=4)

The data in Fig. 3.4 shows a secondary oscillation at approx. 25 min and an oscillation maximum of over 3 µM at 40 min. In contrast, the data in Fig. 3.5 plotted 3 oscillation maxima greater than 3 µM at 30, 35 and 40 min. Even taking the sampling frequency into account, this difference in 8-oxoG concentrations would appear to question the reproducibility of the copper-mediated oxidation of DNA in this investigation. In Fig. 3.6, however, the data from Fig. 3.4, with a 5 min sampling frequency (blue trace), and the data from Fig. 3.5, with a 1 min sampling frequency (red trace) are overlaid, showing this not to be the case.

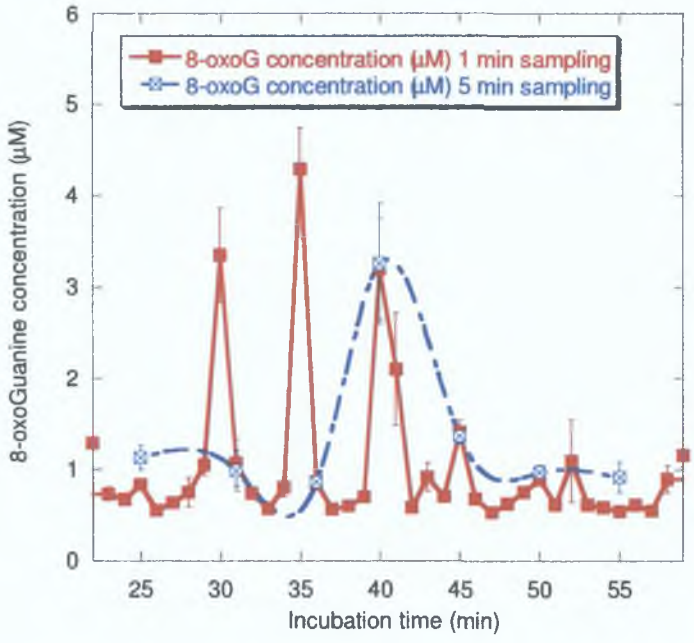

Fig. 3.6: Concentration of 8-oxoG in ct DNA from 0 – 60 min incubation with 150 μM copper(II)sulphate and 50 mM H_2O_2 at 37 °C, EC detection at a potential of +550 mV vs. Ag/AgCl, sensitivity 5 nA, mobile phase of 50 mM ammonium acetate with 50 mM acetic acid in 5% methanol and a flowrate of 1 ml/min. (n=4)

Different stocks of all solutions, including that of ct DNA were used to collect the data plotted in Figs 3.4 and 3.5. Based on Fig. 3.6, however, there was a high level of reproducibility evident, even though different sampling frequencies were used for both experiments. Of the 7 data points which overlapped, there was only a significant deviation, *i.e.,* greater than 5% RSD, between just 2 data points (25 and 55 min).

It was clear from Fig. 3.6 that the 5 min sampling time is inadequate, as it only records one of three oscillation maxima that were observed during the one min oscillations. For accurate data collection, the sampling frequency should be at least twice the period of the oscillations. The sampling frequency of 1 min, however, appeared to be sufficient, as oscillations took at least 2 min to complete.

3.3.4 Rate of 8-oxoG oxidation

In the previous section, 8-oxoG was observed to be generated in concentrations of up to 4 μM when DNA was oxidised by the copper-mediated Fenton reaction. On each occasion where 8-oxoG was generated, however, it was rapidly consumed, with complete consumption within two min. It would therefore appear that 8-oxoG is readily oxidised by copper-mediated oxidation. In order to investigate if that were the case, 10 μM 8-oxoG standard was incubated with the Fenton reagents, with samples taken at 1 min intervals from 0 to 20 min. The results are illustrated in Fig. 3.7.

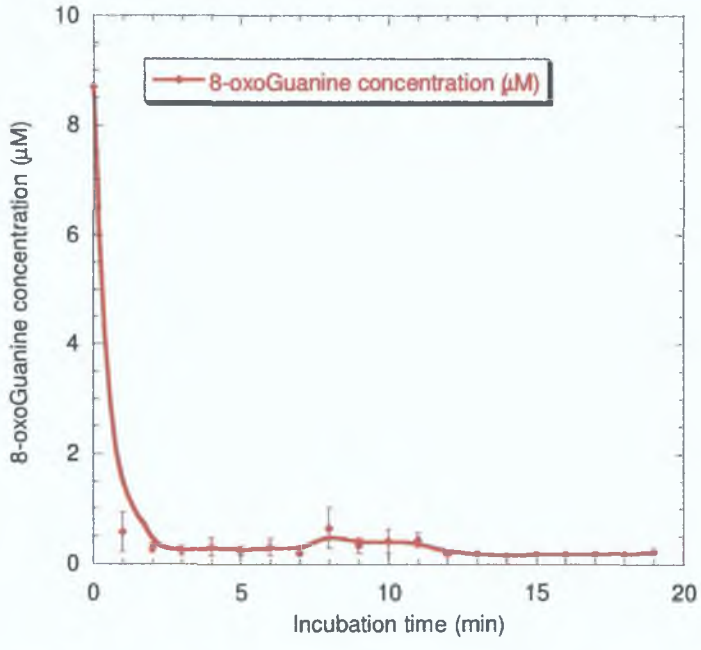

Fig. 3.7: Concentration of 8-oxoG in 8-oxoG standard from 0 –20 min incubation with 150 μM copper(II)sulphate and 50 mM H_2O_2 at 37 °C, EC detection at a potential of +550 mV vs. Ag/AgCl, sensitivity 5 nA, mobile phase of 50 mM ammonium acetate with 50 mM acetic acid in 5% methanol and a flowrate of 1 ml/min. (n=6)

95% of the free 8-oxoG was oxidised within 2 min of oxidative attack. The 8-oxoG was not entirely consumed, however. The 8-oxoG concentration did reach a steady state concentration at 12 min incubation, suggesting that the Fenton reagents could have been completely consumed and that this was may have been the reason for the continuing presence of 8-oxoG in the sample. The excess of H_2O_2 used during the reaction should mean that this was not likely to occur, however. From 2 min incubation with the copper-generating oxidants until steady state at 12 min incubation, the level of 8-oxoG was observed to decrease.

3.3.5 Investigation of copper oxidation state during the Fenton reaction

During the Fenton mediated 8-oxoG oxidation, iron is oxidised from Fe(II) to Fe(III) (Reaction 2.1). If copper reacts in an analogous manner to iron, it too should be oxidised. Only metal catalysts in their lower oxidation state were previously observed to behave as a Fenton reagent.[10] In the case of copper, this would imply that Cu(I), and not Cu(II), is the initial oxidation state of copper during the Fenton reaction, where it generates •OH as shown in Reaction 3.1, as generation of the higher oxidised form of copper, Cu(III) is extremely rare.

$$H_2O_2 + Cu(I) \xrightarrow{k_1} Cu(II) + HO^- + HO\cdot \qquad \text{(Reaction 3.1)}$$

For the Fenton reaction to occur therefore, the copper ion must first be reduced to Cu(I). Coordination of Cu(II) to a G-C base pair in DNA has been shown to result in the oxidation of G with concomitant reduction of Cu(II) to Cu(I), which could explain the ease of reduction of Cu(II).[11] The Cu(I) is then oxidised to Cu(II) as it catalyses the decomposition of H_2O_2. If this is the case, then similar patterns of 8-oxoG oxidation should be generated for both Cu(I) and Cu(II) starting complexes. To investigate this, ct DNA was oxidised in two parallel incubations. In the first reaction, ct DNA was incubated with copper(I)chloride (Cu(I) ion) and H_2O_2, while

in the second reaction ct DNA was incubated with copper(II)chloride (Cu(II) ion) and H_2O_2.

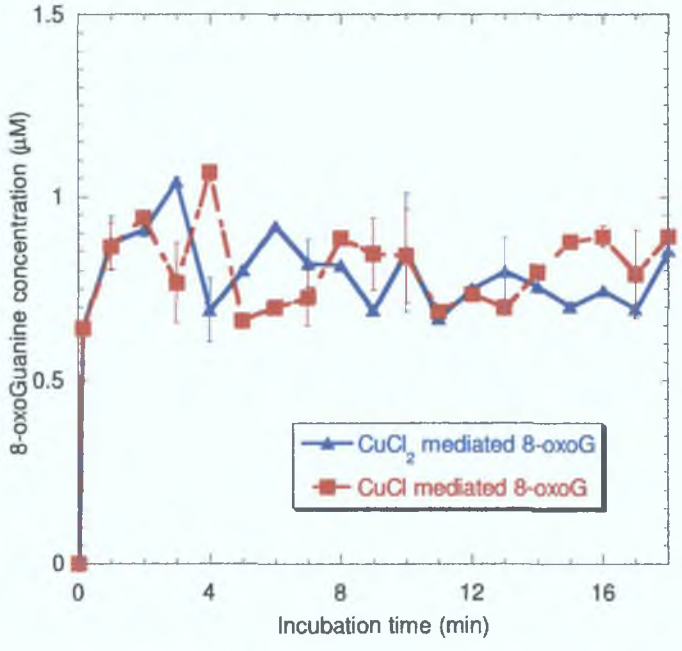

Fig. 3.8: Concentration of 8-oxoG in ct DNA from 0 –20 min incubation with 150 μM copper(II)chloride and 50 mM H_2O_2 (blue trace) and with 150 μM copper(I)chloride and 50 mM H_2O_2 (red trace) at 37 °C, EC detection at a potential of +550 mV vs. Ag/AgCl, sensitivity 5 nA, mobile phase of 50 mM ammonium acetate with 50 mM acetic acid in 5% methanol and a flowrate of 1 ml/min. (n=6)

Fig. 3.8 plots the levels of 8-oxoG generated when the metal catalyst copper is added to the Fenton reaction as Cu(I) (red) and as Cu(II) (blue). Both were observed to generate 8-oxoG immediately on incubation with DNA. At 0 min and 1 min incubations the concentrations were almost identical, increasing from 0.64 μM to 0.87 μM for Cu(II) and from 0.64 μM to 0.86 μM for Cu(I). There appeared to be no delay in the Fenton-mediated oxidation of 8-oxoG when the copper catalyst was added as Cu(II) instead of Cu(I). This would imply that Cu(II) was immediately oxidised to Cu(I), with possible reasons for this ease of oxidation outlined in Section 3.4. As the incubation time increased, the pattern of 8-oxoG oscillations differed slightly between the two analyses. The magnitude of 8-oxoG generated for both

systems was comparable, however, so it could be concluded that the same level of 8-oxoG was generated for both Cu(I) and Cu(II).

Both oxidation states of copper yielded different coloured compounds, with Cu(I) green in solution and Cu(II) blue in solution. These coloured solutions were used for a simple colorimetric analysis of the oxidation states of copper that were generated during the Fenton reaction oxidation of DNA. Solutions were prepared of copper(I)chloride, copper(II)chloride, H_2O_2 and 8-oxoG. Copper(I)chloride was green with a fine precipitate, while copper(II)chloride was pale blue with no precipitate observed. H_2O_2 and 8-oxoG were colourless solutions.

The effect of adding H_2O_2 to both copper solutions is shown in Fig. 3.9 (a) and (b). Its addition to copper(II)chloride (a) did not change the colour of the solution; therefore it was assumed that neither did it change the oxidation state of the copper ions. Addition of H_2O_2 to copper(I)chloride (b), however, caused the solution to change from green to yellow, indicating the formation of copper(I)hydroxide.[12] Significant effervescence was observed in both cases.

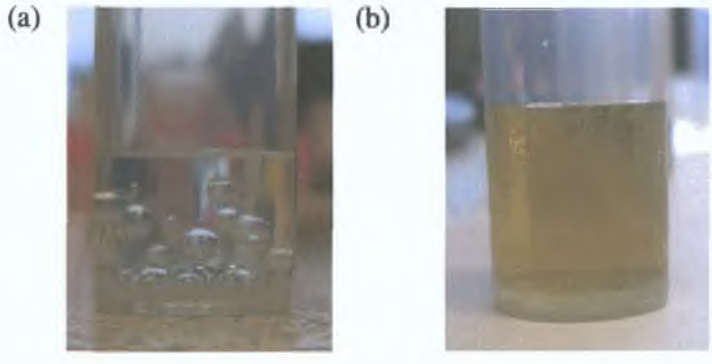

Fig. 3.9: Images of the addition of H_2O_2 to solutions of (a) copper(II)chloride and (b) copper(I)chloride.

8-oxoG was then added to both solutions (without H_2O_2), which resulted in changes in colour for only the copper(I) solution, as shown in Fig. 3.10. Addition of 8-oxoG to copper(II)chloride (a) resulted in an immediate colour change from pale blue to deep turquoise green with accompanying precipitate. This colour change corresponded with the reduction of copper from Cu(II) to Cu(I). When 8-oxoG was added to copper(I)chloride (b), the solution remained green, indicating the continuing presence of Cu(I).

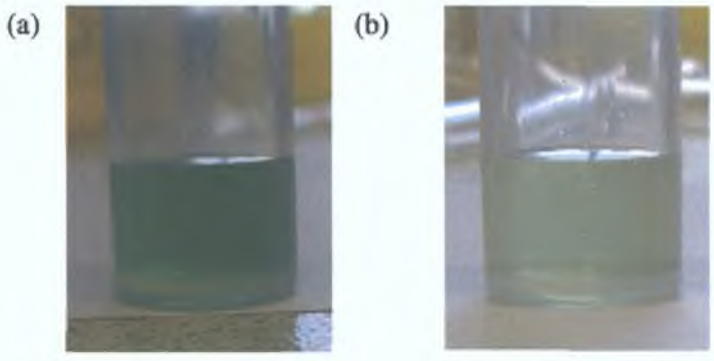

Fig. 3.10: Images of the addition of 8-oxoG to solutions of (a) copper(II)chloride and (b) copper(I)chloride.

Finally, both H_2O_2 and 8-oxoG were added to both solutions, which resulted in changes in colour for both solutions, as shown in Fig. 3.11. For copper(II)chloride (a), an immediate colour change resulted, with the solution turning a dark yellow, with instant effervescence and generation of a substantial amount of precipitate. For copper(I)chloride (b), the solution again turned a dark yellow. In further agreement with copper(II)chloride, instant effervescence and generation of precipitate were also observed. There was significantly less precipitate generated for the copper(I)chloride reaction with H_2O_2 and 8-oxoG than for the analogous copper(II)chloride reaction. This analysis illustrated that the presence of the organic substrate 8-oxoG appeared to cause the reduction of copper ions from Cu(II) to Cu(I), as evidenced by the immediate colour change to green, indicative of Cu(II). There was no reduction of the copper ions by H_2O_2. Both Cu(I) and Cu(II) mediated oxidation of 8-oxoG yielded substantial amounts of effervescence and precipitate.

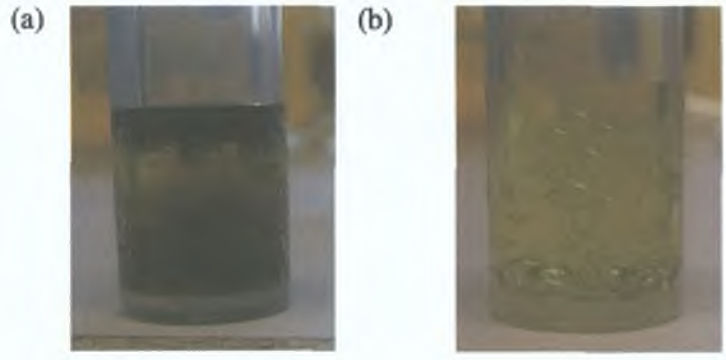

Fig. 3.11: Images of the addition of H_2O_2 and 8-oxoG to solutions of (a) copper(II)chloride and (b) copper(I)chloride.

3.4 Discussion

When Guanine was incubated with iron(II)sulphate and H_2O_2, there was immediate formation of 8-oxoG. As incubation time increased, the concentration of 8-oxoG was observed to oscillate. 8-oxoG has an oxidation potential approx. 0.3 V lower than G,[13] and is readily oxidised by •OH. It was therefore assumed that 8-oxoG generated by the oxidation of G could also be readily oxidised further when incubated with Fenton reagents, and that this contributed significantly to the oscillatory pattern whereby 8-oxoG was continually generated and consumed. Copper was expected to act in an analogous manner to iron (as Cu(I) reaction with H_2O_2 has been reported to be significantly faster than Fe(II)),[14] and so catalyse the formation of •OH and hence the generation of 8-oxoG. It was therefore expected that the incubation of G *standard* with copper(II)sulphate and H_2O_2 would result in similar oscillatory patterns of 8-oxoG concentration, assuming that Cu(II) could be readily reduced to Cu(I) to facilitate the initiation of the reaction.

Fig. 3.1 shows the concentration of G and 8-oxoG in free G. The expected pattern of 8-oxoG formation and oscillation was detected, however, the minimum concentrations of 8-oxoG were below the LOD of the detector, and so for the minimum concentrations during the oscillations, no 8-oxoG was detected. There are two possible causes for this lack of 8-oxoG. The first is that no oxidative damage occurred, or that significantly lower levels of 8-oxoG concentration were generated for the copper system than for the iron system. 8-oxoG is generated by the oxidation of free G. Therefore, the concentration of free G at a given time should indicate its level of oxidation to 8-oxoG. In Fig. 3.1, the concentration of free G dropped drastically with increasing copper-catalysed oxidation. After 20 min incubation, the concentration of free G was 0.35 mM (from an initial concentration of 0.8 mM). For the analogous iron incubation (Fig. 2.4), the free G concentration at 20 min was significantly higher, at 0.59 mM. An increased amount of free G was oxidised using the copper system; therefore an increased concentration of 8-oxoG would have been expected. With the high levels of free G oxidation (with respect to iron-catalysed

oxidations), the possibility that lower levels of 8-oxoG were generated was deemed highly unlikely to occur. In fact, significantly greater concentrations of 8-oxoG would have been expected from the copper incubations.

The second alternative is that any 8-oxoG generated was immediately consumed before it could be detected. If 8-oxoG was easily consumed before any chance of detection, however, it seems unlikely that it would have emerged as a leading potential biomarker. The mechanism of formation of •OH when Cu(II) is incubated with H_2O_2 could determine the plausibility of the rapid oxidation of 8-oxoG as a potential cause for the absence of significant levels of 8-oxoG. For the copper-mediated oxidation of free G, two main possibilities for the generation of •OH emerged. The first possibility was that the copper ions complexed to the N7 of G.[15] If this were the case, the •OH would have been generated in very close proximity to G, and therefore be likely to oxidise G to 8-oxoG. In this situation, the generation of further •OH would have been expected to occur as soon as the copper ion reduced back to Cu(I) and could react with another H_2O_2 molecule. Further oxidation of 8-oxoG would therefore have been expected to take place very rapidly. In this instance, it would be expected that 8-oxoG would be rapidly further oxidised, and so have a very short lifetime in solution. In this way it was possible that 8-oxoG generated was immediately consumed before it could be detected. The second possibility was that •OH was generated from copper ions in solution, which were not complexed to any free G. Such formation of •OH might not have necessarily caused either the formation or the oxidation of 8-oxoG; however, consumption of G was observed, suggesting G oxidation had occurred. As the reaction was constantly stirred, 8-oxoG generated by this method would not be automatically subjected to further oxidation upon copper reduction. No MS analysis was carried out to try to detect 8-oxoG oxidation products.

The oscillations in 8-oxoG concentration observed in Fig. 3.1 were quite different to those observed for the analogous iron-mediated oxidation. The oscillating pattern for iron-mediated 8-oxoG generation and oxidation observed in

Chapter 2 plotted not only the maximum and minimum levels of 8-oxoG concentration, but also intermediate levels of 8-oxoG as the concentration increased towards the maximum or decreased towards the minimum levels. Even if the minimum 8-oxoG concentrations were below the LOD of the EC detector, intermediate concentrations of 8-oxoG were expected to be observed approaching the 8-oxoG that was detected. This did not occur, however, suggesting that the period of the oscillations, in addition to the amplitude of the oscillations, was different from the iron-mediated generation of 8-oxoG concentration oscillations.

To determine whether a polymer backbone would have any effect on the copper-catalysed oxidation of G, PolyG oxidation was analysed. The polymer backbone could have a number of consequences on the oxidation of G. Firstly the G would no longer be free in solution, but covalently attached to the polymer backbone. This would concentrate G in one particular area, and so in this area of the reaction vessel there should be an increase in the rate of reaction between G and the Fenton reagents, with a corresponding increase in both G and 8-oxoG oxidation. Secondly the backbone itself could react with •OH. •OH reacts with all biomolecules, and in the case of DNA about 20% of the radical reacts with the polymer backbone while the remainder attacks the DNA bases.[16] In this instance the presence of the polymer backbone would serve to decrease the rate of reaction between G and the Fenton reagents. There was no 8-oxoG detected upon incubation of PolyG with copper(II)sulphate and H_2O_2, as illustrated in Fig. 3.2. Only after 45 min was a significant amount of 8-oxoG detected, which did not increase with increasing incubation time. From 0 to 40 min incubation with the copper-mediated Fenton reaction, no 8-oxoG was detected. Again the two main possibilities to explain this lack of 8-oxoG would be that either no 8-oxoG was generated, or that any generated was immediately consumed. In the case of free G, the formation of 8-oxoG via copper ions complexed to the N7 of G could cause the formation and further oxidation of 8-oxoG in rapid succession. When G with complexed copper was covalently bound to the polymer backbone, however, •OH generated from this copper now not only had the potential to damage the G to which it was complexed,

but also adjacent G along the backbone. •OH generated by this mechanism therefore had greater oxidising power for PolyG than for free G. This is potentially a reason why no 8-oxoG was detected for the first 40 min of incubation, as a greater amount of 8-oxoG generated was immediately further oxidised, and so did not remain in solution long enough to be detected.

The investigations with both free G and PolyG yielded maximum 8-oxoG concentrations of less than 0.6 μM in both cases. This magnitude of 8-oxoG concentration is comparable to that generated for iron-mediated Fenton oxidation. The oscillations in 8-oxoG concentration observed for iron(II) were not detected in this study, however.

Based on the results for free G and PolyG, ct DNA incubations with copper(II)sulphate and H_2O_2 were not expected to generate any 8-oxoG. As illustrated in Fig. 3.3, however, this was clearly not the case. 8-oxoG was immediately detectable, and in significantly higher concentrations than in previous studies with iron. Up to 3 μM 8-oxoG was measured, which represents about a 6-fold increase on the maximum concentrations observed with iron. The 8-oxoG oscillatory pattern was comparable, however, to the iron study, in that the oscillations were dependant on incubation time. 8-oxoG was generated immediately and appeared to be consumed until about 5 min, where after the concentration increased to ~ 3 μM at 10 min. From 10 to 20 min this concentration again decreased, only to increase again to ~ 1 μM at 25 min. The concentration then decreased at 30 min, only for a second major generation of 8-oxoG of ~ 3 μM, which reached a maximum concentration at 40 min incubation. Thereafter, the concentration of 8-oxoG was again observed to decrease. When the incubation time was increased until 180 min, as plotted in Fig. 3.4, the oscillations continued. This time, however, each of the successive maxima after 40 min incubation was significantly lower in concentration. The maxima at 120, 150 and 170 min appeared to show a reaction that is approaching equilibrium. The reaction appeared to be approaching a steady state concentration of 8-oxoG of approximately 0.7 μM.

A 5 min sampling frequency was adequate for the analysis of iron-catalysed oxidation, as evidenced by the significant number of data points per period, shown in Chapter 2. Due to the absence of intermediate levels of 8-oxoG during the oscillations observed in Fig. 3.4, however, it was possible that a complete illustration of the concentration oscillations that are occurring in this reaction was not elucidated using a 5 min sampling frequency. In order to obtain a complete picture of 8-oxoG concentration oscillations, it was felt that a 1 min sampling frequency was necessary to study the oscillatory pattern. The results of this study were illustrated in Fig. 3.5. Three primary oscillations were recorded at 30, 35 and 40 min. Only one of these was detected using a 5 min sampling frequency. The characteristic intermediate levels of 8-oxoG concentration between successive maxima were detected during this analysis, however, and it was found to take two min for a complete oscillation to occur. Sampling at 1 min intervals was therefore acceptable for accurate data collection.

Fig. 3.8 plots the levels of 8-oxoG generated when copper was added to the reaction as Cu(I) (copper(I)chloride) and as Cu(II) (copper(II)chloride). The increase in concentration from 0 to 1 min incubation with both catalysts was almost identical. This suggested that initially the rate of 8-oxoG formation for both systems was the same. As the concentrations of both DNA and H_2O_2 were equal (aliquots of the same solution), the copper moiety in both systems must have behaved in an analogous manner. A quantum chemical study of the interactions between Cu(II) and DNA in the literature provided an insight into the nature of the complex formed.[11] It was found that coordination of Cu(II) to a GC base pair within the DNA double helix could induce an oxidation of GC with concurrent reduction of the copper ion to Cu(I). The ability of Cu(II) to oxidise the GC base pair depends inversely on the number of water molecules directly interacting with it. Therefore the local environment of Cu(II) would determine its oxidising power. It was illustrated in Fig. 3.10 that the addition of 8-oxoG, which would also have an N7 available for complexation with copper ions, to copper(II)chloride immediately resulted in the reduction of Cu(II) to Cu(I). This reduction, in the absence of any obvious reducing

agents, suggests that the reduction of Cu(II) via its coordination of the N7 of 8-oxoG is a viable mechanism for the generation of Cu(I) used in the copper-mediated Fenton oxidation of DNA. [11] This reduction of Cu(II) to Cu(I) also causes the oxidation of the base to which it is complexed, namely G. The one electron oxidation of G leads to the cation radical $G^{+}\bullet$. This is readily hydrated to form G8OH•. This radical can be further oxidised to form 8-oxoG, or can be reduced to form FapyG. In the copper-mediated reaction used in this study therefore, it is probable that the oxidation is not generated by either the ROS •OH or $^{1}O_2$, but instead is initiated by the one electron oxidation of G. One electron oxidation can be distinguished from both the ROS generated by analysing the final products generated. $^{1}O_2$ forms 8-oxoG, but not FapyG, from G and does not oxidise any other DNA bases. •OH damages all four DNA bases, causing over 60 products. One electron oxidation forms both 8-oxoG and FapyG. Therefore the analysis of FapyG and of Thymine adducts can be used for identify the oxidation mechanism involved.

The nature of the oxidising mechanism generated by Cu(II) and H_2O_2 has previously investigated by a number of groups. DNA damage induced by Cu(II) and H_2O_2 was studied by Yamomoto and Kawanishi, to identify the nature of the oxidising species involved. They concluded that Cu(II) bound to DNA but that Cu(I) participated in the DNA damage, based on the inhibition of damage by the Cu(I) scavenger bathocuproine.[17] Scavanging reactions indicated that •OH was not the primary oxidative species. An oxidising species similar to •OH, *e.g.* a bound •OH, such as a copper-hydroperoxo complex was suspected to be involved, as all four DNA bases were damaged to some extent. Singlet oxygen ($^{1}O_2$) was considered as the possible oxidant due to the $^{1}O_2$-like pattern of damaged DNA bases which was detected. It was ruled out as the primary reactive species, however, because no enhancement in DNA damage was detected when the reaction was carried out in D_2O, where the lifetime of $^{1}O_2$ would be increased approx. 30-fold.[18] This implied that an oxidant similar to $^{1}O_2$, such as a bound $^{1}O_2$, again a copper-peroxide complex, could cause the damage recorded. The following reaction mechanism

(Scheme 3.1) was proposed, where the interconversion of Cu(I) and Cu(II) was important for DNA damage to occur:

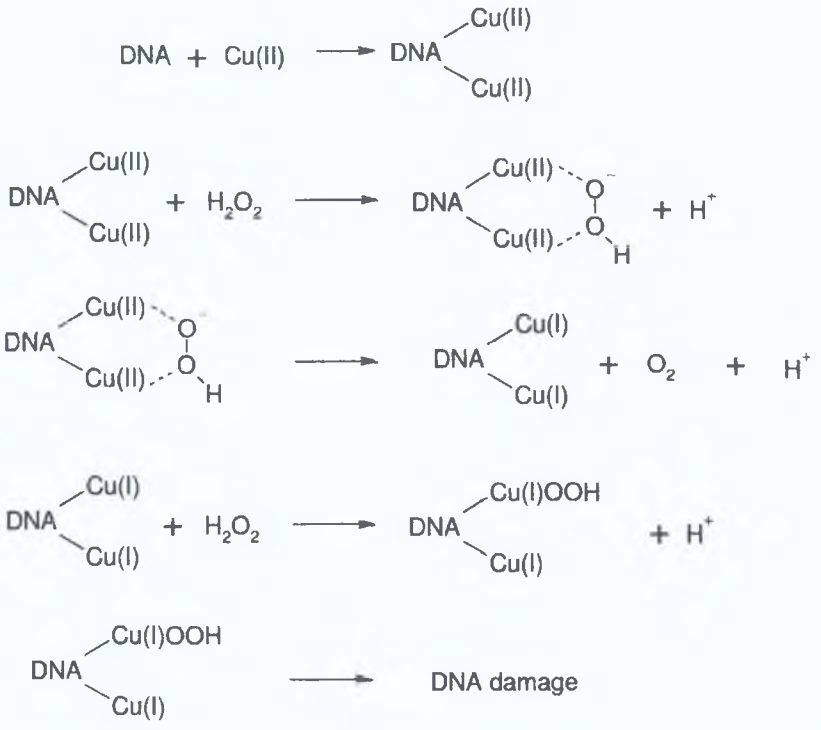

Scheme 3.1: Proposed mechanism for DNA damage induced by Cu(II) and H_2O_2.[17]

A subsequent study confirmed that copper-induced DNA damage was site specific, occurring only at sites where copper ions were bound to the DNA backbone.[19] It was found that the Cu(II) was quickly reduced to Cu(I), which then bound to DNA with high affinity. H_2O_2 then entered the DNA-Cu(I) coordination complex oxidising Cu(I) and modifying bases. The rate of DNA base damage was far slower than the rate of DNA- Cu(I) oxidation however, suggesting the formation of an intermediate oxidising species, *e.g.* Cu(III) or a copper-oxo complex, which reacted slowly with DNA bases. The ease at which Cu(II) could be converted into Cu(I) was illustrated in an EPR spectrometry study.[20] The spectra generated by Cu(II) incubated with H_2O_2 was found to be analogous to that generated by Cu(I) incubated with H_2O_2, leading to the conclusion by the author that in all probability the Cu(II) had been reduced to Cu(I) almost instantly upon incubation.

The nature of the copper-hydroperoxo intermediate was investigated in the analysis of oxidative DNA damage by catechol in the presence of copper(I).[21] The nature of the intermediate is illustrated in the scheme shown in Reaction 3.2:

$$H_2O_2 + DNA - Cu(I) \rightarrow DNA - Cu(I)OOH + H^+ \rightarrow HO^\bullet + DNA - Cu(II)OH$$

(Reaction 3.2)

By comparing the damage patterns caused by catechol in the presence of copper to those caused by free •OH, free $^1O_2$ and hydroxyl radical produced from the decomposition of DNA-copper-peroxide intermediates, the authors concluded that this intermediate was the cause of the damage found in their investigation. Suspected •OH generated by the degradation of the copper-hydroperoxo intermediate was not detected by scavenging reagents; instead it was proposed that this •OH was not released into the bulk medium but reacted immediately with DNA.

Further analysis of the degradation of DNA bases by copper in the presence of H_2O_2 again lead to the conclusion that the ROS species involved was not •OH.[9] The DNA base damage generated from γ-irradiation (known to form •OH) was compared to that of Cu(I)/H_2O_2 induced oxidative damage. (In this way, the problem with ROS scavenging experiments, namely the possibility that the ROS generated by DNA-Cu complexes reacting directly with H_2O_2 reacts with DNA before it can be scavenged, was overcome.) A number of differences between the two systems were observed. The level of G adducts accounted for 51% of oxidised bases in γ-irradiated DNA, but this rose to 82% for the Cu(I) system. In addition, a 7-fold increase in DNA damage was recorded when the Cu(I) reaction was carried out in D_2O. As $^1O_2$ oxidises predominantly G, and its lifetime is enhanced in D_2O, it was proposed that it was predominantly responsible for the oxidative damage detected, being generated *in situ* via a DNA-copper-hydroperoxo complex. The presence of T and A adducts however, suggested that •OH was possibly a minor pathway for oxidative DNA damage induced by Cu(I)/H_2O_2. The compound methional scavenges not only •OH,

but also weaker oxidants of similar activity. It partially inhibited DNA damage for a number of Cu(I)-hydroperoxo complexes, where •OH scavengers had no effect, also indicating the presence of a weaker •OH-like oxidant.[7,22]

Recently, a reaction mechanism for the oxidation caused by the Cu(I)/H_2O_2 system was proposed in the literature.[23] This was elucidated in part by monitoring the concentration of H_2O_2 as the reaction progressed by titration with $KMnO_4$. For a low concentration of copper, the following mechanism, Reactions 3.3-3.7, was proposed:

$$Cu(II) + H_2O_2 \rightarrow Cu(I)OOH^+ + H^+ \qquad \text{(Reaction 3.3)}$$

$$Cu(I)OOH^+ \xrightarrow{slow} Cu(I) + O_2^- + H^+ \qquad \text{(Reaction 3.4)}$$

$$Cu(I) + H_2O_2 \rightarrow Cu(I) + OH^- + HO^\bullet \qquad \text{(Reaction 3.5)}$$

$$HO^\bullet + H_2O_2 \rightarrow H_2O + O_2^- + H^+ \qquad \text{(Reaction 3.6)}$$

$$O_2^- + H_2O_2 \rightarrow O_2 + OH^- + HO^\bullet \qquad \text{(Reaction 3.7)}$$

The copper-hydroperoxo complex Cu^+•OOH was generated in Reaction 3.3, which subsequently decomposed as shown in Reaction 3.4, leading to the reactions in Reactions 3.5 and 3.8. The rate determining step was the decomposition of Cu(I)•OOH, in Reaction 3.3. If there is an increased concentration of copper however the rate determining step was no longer the unimolecular decay of the copper-hydroperoxo complex, but instead its bimolecular decomposition, shown in Reaction 3.8.

$$2Cu(I)OOH^+ \xrightarrow{slow} 2Cu(I) + H_2O_2 + O_2 \qquad \text{(Reaction 3.8)}$$

If the concentration of copper was sufficiently high (120 μM), the superoxide species, instead of reacting with H_2O_2 as shown in Reaction 3.7, could react with Cu(II), as shown in Reaction 3.9.

$$O_2^- + Cu(II) \rightarrow O_2 + Cu(I) \qquad \text{(Reaction 3.9)}$$

In this way the Cu(II) could be regenerated completing the catalytic cycle. In this proposal however, Cu(I) reacted with H_2O_2 via the Fenton reaction to yield •OH, in Reaction 3.5. This was in contradiction to all the investigations discussed previously, where it was shown by a multitude of experiments that the reaction of Cu(I) with H_2O_2 yielded a copper-hydroperoxo complex. The exact fate of this complex is uncertain, but it either reacts or its degradation products react as a 'bound' $^1O_2$-like species, which also exhibits partial 'bound' •OH-like behaviour. It is generally accepted, based on the extensive investigations outlined in this section, that Cu(I) oxidation does not proceed via the formation of •OH. The mechanism outlined in Reactions 3.3 to 3.9 is therefore unlikely to represent the pathway by which Cu(I) results in oxidative stress to DNA. Instead, $^1O_2$ or a $^1O_2$-like species is more likely to be generated during Cu(I) oxidation.

In $^1O_2$ oxidation in DNA (not in the free nucleoside), G is the main target for attack, where it preferentially undergoes cycloaddition, generating 8-oxoG as the main adduct, with the mechanism in Scheme 3.2 proposed:[24]

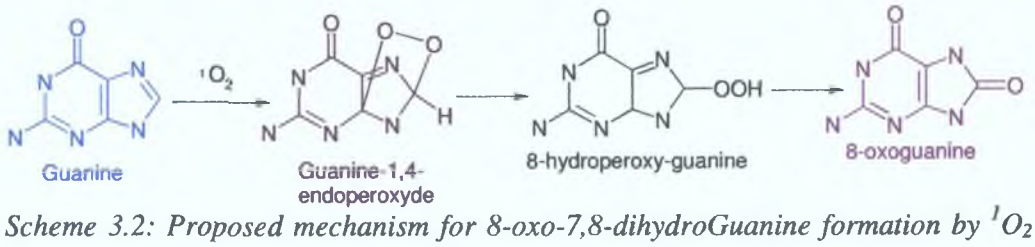

Scheme 3.2: Proposed mechanism for 8-oxo-7,8-dihydroGuanine formation by $^1O_2$ attack.[24]

As with 8-oxoG generated by •OH, 8-oxoG generated by $^1O_2$ is not the final species of the oxidation. It is thought to undergo further reaction with $^1O_2$ to generate oxaluric acid via an oxidised guanidinohydantoin intermediate, as shown in Scheme 3.3.[25] It was proposed that $^1O_2$ oxidation of 8-oxoG occurred via cycloaddition to form 5-hydroperoxy-8-oxoG which decomposed to give guanidinohydantoin. This was oxidised to parabanic acid, and on further oxidation

yielded oxaluric acid, the final product of the $^1O_2$ oxidation. Elsewhere cyanuric acid was proposed as the final product of $^1O_2$ oxidation of 8-oxoG.[26]

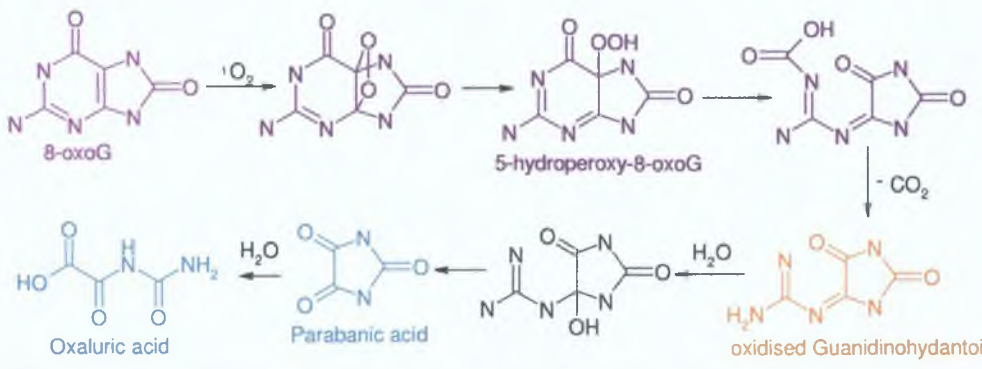

Scheme 3.3: Proposed mechanism for oxaluric formation from 8-oxo-7,8-dihydroGuanine by $^1O_2$ attack, 8-oxo-7,8-dihydroGuanine depicted in red, intermediate complexes depicted in orange and final oxidation products depicted in green.[25]

Further oxidation products of 8-oxoG oxidation by •OH are still a matter of debate, with a number of species and potential mechanisms proposed. At pH 7.0 it was proposed that guanidinohydantoin (Gh) was the product formed, via a 5-OH intermediate.[27] It was subsequently demonstrated that Gh itself was further oxidised, and so was not the final product of G oxidation.[28] Scheme 3.4 summarises the variety of oxidation products proposed for the 8-oxoG oxidation by •OH and $^1O_2$.

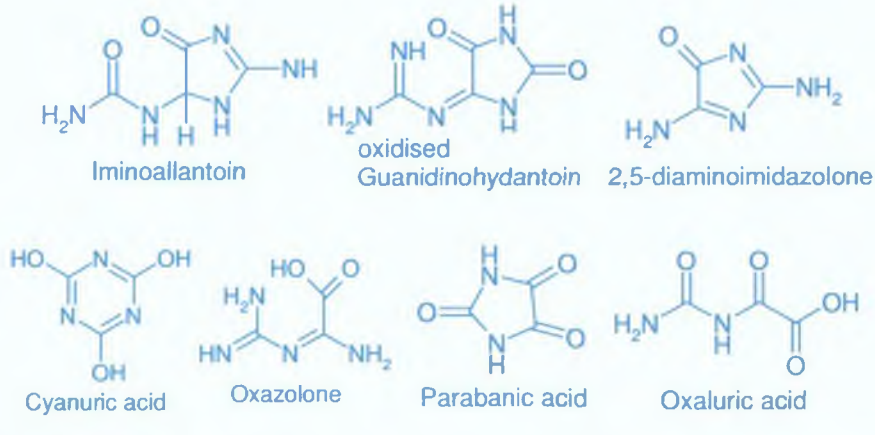

Scheme 3.4: Proposed oxidation products of •OH and $^1O_2$ oxidation, depicted in blue.

It is, however, probable that, as previously discussed, neither ROS are involved, and that one electron oxidation of G, yielding $G^{+}\bullet$, takes place when Cu(II) is reduced to Cu(I). As discussed previously, this is a probable route to generate Cu(I); therefore it is highly likely that $G^{+}\bullet$ is also generated during this spontaneous reaction, and that copper causes DNA damage via one electron oxidation.

All three mechanisms of DNA damage (one electron oxidation, $^{1}O_2$ and •OH) have in common that they generate 8-oxoG and then further oxidise it via the formation of a Gh or oxGh intermediate. In the case of •OH, 8-oxoG is only one of about 60 oxidative adducts formed, but in the case of $^{1}O_2$, 8-oxoG is the main adduct generated in DNA and in the case of one electron oxidation, 8-oxoG and FapyG are the main adducts generated. All three systems could have caused the 8-oxoG concentration patterns observed in this chapter during the investigation into copper-catalysed oxidation of free G, PolyG and DNA, but the most likely mechanism is that of one electron oxidation, because of the ability of Cu(II) to complex with G and generate $G^{+}\bullet$.

3.5 Conclusions

In this study, the rate of 8-oxoG formation and oxidation by the copper-catalysed Fenton reaction was investigated in free G, PolyG and ds DNA. For free G incubations, 8-oxoG was only generated intermittently, at a concentration of approx. 0.55 μM. The oscillations in concentration observed for the iron catalysed oxidation of free G in Chapter 2 were again detected, but with lower minimum concentrations than previously observed. Free G was shown to be oxidised immediately, with a drop in concentration recorded on incubation with the Fenton reagents, and an overall decrease in concentration with increasing incubation time, which was interpreted as a linear decrease within experimental error.

PolyG was also subjected to copper-mediated oxidative stress. For the first 40 min of incubation, no 8-oxoG was detected. After this incubation time, what appeared to be a steady state concentration of 8-oxoG was detected, again at a concentration of 0.55 μM. For both free G and PolyG, a sampling frequency of 5 min was used. This was subsequently shown to lead to incomplete oscillation patterns, but could not explain the lack of 8-oxoG detected in both systems.

The incubation of ds DNA with the copper Fenton reagents leads to significantly different results to those recorded for free G and PolyG. A comparable incubation to the earlier analyses, with 5 min sampling intervals, lead to the detection of 8-oxoG which oscillated with increasing incubation time. For subsequent analysis with a 1 min sampling frequency, concentration maxima were detected at concentrations greater than 3 μM, with a maximum concentration of 3.2 μM observed.

The oxidation state of copper which was involved in the oxidation of DNA was studied briefly. In the first study, parallel DNA incubations were carried out, one with copper(I)chloride (Cu(I)), and one with copper(II)chloride (Cu(II)). The concentration of 8-oxoG generated by both systems was then measured. It was found

that the initial rate of 8-oxoG formation in both cases was identical. Further colorimetric analysis of the two solutions, based on the green colour of Cu(I) and the blue colour of Cu(II) also leads to the conclusion that Cu(II) was readily reduced to Cu(I) to participate in the generation of ROS for the oxidation of DNA. This was supported by literature analysis, which concluded that Cu(II) formed a complex with G, such that it was instantly reduced with concurrant oxidation of G. Based on this data, and the results observed in this thesis, G oxidation in this case therefore appears to be initiated by one electron oxidation and not by addition of •OH.

The exact nature of the ROS generated by Cu(II) and H_2O_2 was discussed in detail based on published literature, with a copper-hydroperoxo complex, Cu(I)OOH, emerging as the probable complex resulting from the interaction. Where Cu(II) and H_2O_2 were incubated with DNA, the copper ion first bound to the DNA, probably to the N7 of G, and then reacted with H_2O_2 to yield the Cu(I)OOH complex. Simply the coordination of Cu(II) and GC base pair was shown to be capable of reducing the copper ion to Cu(I), so that it was available for reaction with the H_2O_2. Therefore, Cu(II) initiated the formation of 8-oxoG by one electron oxidation, and not via the production of either ROS. The final species of 8-oxoG oxidation were also discussed.

On the basis of this investigation, and the different patterns of 8-oxoG oxidation that emerged between this work and that in Chapter 2, the copper and iron catalysed oxidation of DNA does not appear to proceed via the same mechanism. Copper(II) and H_2O_2 do not seem to react via the Fenton reaction, nor to generate •OH. Instead one electron oxidation probably occurs, the oxidising properties of which are more similar to $^1O_2$ oxidation than •OH oxidation.

3.6 References

1. Halliwell, B.; Gutteridge, J. M. C. *Free Radicals in Biology and Medicine*, 2nd ed.; Clarendon Press, 1989.

2. Lloyd, D. R.; Carmichael, P. L.; Phillips, D. H.; Comparison of the formation of 8-hydroxy-2'-deoxyguanosine and single- and double-strand breaks in DNA mediated by Fenton reactions, *Chemical Research in Toxicology* **1998**, *11*, 420-427.

3. Lloyd, D. R.; Phillips, D. H.; Oxidative DNA damage mediated by copper (II), iron (II) and nickel (II) Fenton reactions: evidence for site-specific mechanisms in the formation of double strand breaks, 8-hydroxydeoxyguanosine and putative intrastrand cross-links, *Mutation Research/Fundamentals and Molecular Mechanisms of Mutagenesis* **1999**, *424*, 23-36.

4. Lloyd, D. R.; Philips, D. H.; Carmicheal, P. L.; Generation of putative intrastrand cross-links and strand breaks in DNA by transistion metal ion-mediated oxygen radical attack, *Chemical Research in Toxicology* **1997**, *10*, 393-400.

5. Kawanishi, S.; Hiraku, Y.; Murata, M.; Oikawa, S.; The role of metals in site-specific DNA damage with reference to carcinogenesis, *Free Radical Biology and Medicine* **2002**, *32*, 822-832.

6. Li, Y.; Trush, M. A.; DNA damage resulting from the oxidation of hydroquinone by copper: role for a Cu(II)/Cu(I) redox cycle and reactive oxygen generation, *Carcinogenesis* **1993**, *14*, 1303-1311.

7. Sakano, K.; Oikawa, S.; Hiraku, Y.; Kawanishi, S.; Mechanism of metal-mediated DNA damage induced by a metabolite of carcinogenic acetamide, *Chemico-Biological Interactions* **2004**, *149*, 51-59.

8. Burkitt, M. J.; Copper-DNA adducts, *Methods in Enzymology* **1994**, *234*, 66-79.

9. Frelon, S.; Douki, T.; Favier, A.; Cadet, J.; Hydroxyl radical is not the main reactive species involved in the degredation of DNA bases by copper in the presence of hydrogen peroxide, *Chemical Research in Toxicology* **2003**, *16*, 191-197.

10. Goldstein, S.; Meyerstein, D.; Czapski, G.; The Fenton reagents, *Free Radical Biology and Medicine* **1993**, *15*, 435-445.

11. Noguera, M.; Bertran, J.; Sodupe, M.; A quantum chemical study of Cu2+ interacting with guanine-cytosine base pair. Electrostatic and oxidative effects on intermolecular proton-transfer processes, *Journal of Physical Chemistry A* **2004**, *108*, 333-341.

12. Ali, F. E.; Barnham, K. J.; Barrow, C. J.; Separovic, F.; Metal catalyzed oxidation of tyrosine residues by different oxidation systems of copper/hydrogen peroxide, *Journal of Inorganic Biochemistry* **2004**, *98*, 173-184.

13. Duarte, V.; Muller, J. G.; Burrows, C. J.; Insertion of dGMP and dAMP during in vitro DNA synthesis opposite an oxidised form 7,8- dihydro-8-oxoguanine, *Nucleic Acids Research* **1999**, *27*, 496-502.

14. Packer, L.; Oxygen Radicals in Biological Systems, *Methods in Enzymology* **1984**, *Vol. 105*, 7.

15. Burda, J. V.; Sponer, J.; Hobza, P.; Ab initio study of the interaction of guanine and adenine with various momo- and bivalent metal cations (Li^+, Na^+, K^+, Rb^+, Cs^+, Cu^+, Ag^+, Au^+, Mg^{2+}, Ca^{2+}, Sr^{2+}, Ba^{2+}, Zn^{2+}, Cd^{2+}, and Hg^{2+}), *Journal of Physical Chemistry* **1996**, *100*, 7250-7255.

16. Breen, A. P.; Murphy, J. A.; Reactions of oxyl radicals with DNA, *Free Radical Biology and Medicine* **1995**, *18*, 1033-1077.

17. Yamamoto, K.; Kawanishi, S.; Hydroxyl free radical is not the main active species in site-specific DNA damage induced by copper (II) ion and hydrogen peroxide, *Journal of Biological Chemistry* **1989**, *264*, 15435-15440.

18. Khan, A. U.; Direct spectral evidence of the generation of singlet molecular oxygen ($^1\Delta_g$) in the reaction of potassium superoxide with water, *Journal of the American Chemical Society* **1981**, *103*, 6516-6517.

19. Drouin, R.; Rodriguez, H.; Gao, S.-W.; Gebreyes, Z.; O'Connor, T. R.; Holmquist, G. P.; Akman, S. A.; Cupric ion/ascorbate/hydrogen peroxide-induced DNA damage: DNA-bound copper ion primarily induces base modifications, *Free Radical Biology and Medicine* **1996**, *21*, 261-273.

20. Mello-Fihlo, A. C.; Meneghini, R.; Iron is the intracellular metal involved in the production of DNA damage by oxygen radicals, *Mutation Research/Fundamentals and Molecular Mechanisms of Mutagenesis* **1991**, *251*, 109-113.

21. Schweigert, N.; Acero, J. L.; Gunten, U. v.; Canonica, S.; Zehnder, A. J. B.; Eggen, R. I. L.; DND degredation by the mixture of copper and catechol is caused by DNA-copper-hydroperoxo complexes, probably DNA-Cu(I)OOH, *Environmental and Molecular Mutagenesis* **2000**, *36*, 5-12.

22. Ogawa, K.; Hiraku, Y.; Oikawa, S.; Murata, M.; Sugimura, Y.; Kawamura, J.; Kawanishi, S.; Molecular mechanisms of DNA damage induced by procarbazine in the presence of Cu(II), *Mutation Research/Genetic Toxicology and Environmental Mutagenesis* **2003**, *539*, 145-155.

23. Perez-Benito, J. F.; Reaction pathways in the decomposition of hydrogen peroxide catalyzed by copper (II), *Journal of Inorganic Biochemistry* **2004**, *98*, 430-438.

24. Paillous, N.; Vicendo, P.; Mechanisms of photosensitized DNA cleavage, *Journal of Photochemistry and Photobiology B: Biology* **1993**, *20*, 203-209.

25. Duarte, V.; Gasparutto, D.; Yamaguchi, L. F.; Ravanat, J.-L.; Martinez, G. R.; Medeiros, M. H. G.; Mascio, P. D.; Cadet, J.; Oxaluric acid as the major product of singlet oxygen-mediated oxidation of 8-oxo-7,8-dihydroguanine in DNA, *Journal of the American Chemical Society* **2000**, *122*, 12622-12628.

26. Raoul, S.; Cadet, J.; Photosensitized reaction of 8-oxo-7,8-dihydro-2'-deoxyguanosine: Identification of 1-(2-deoxy-β-D-*erythro*-pentofuranosyl)cyanuric acid as the major singlet oxygen oxidation product, *Journal of the American Chemical Society* **1996**, *118*, 1892-1898.

27. Goyal, R. N.; Jain, N.; Garg, D. K.; Electrochemical and enzymic oxidation of guanosine and 8-hydroxyguanosine and the effects of oxidation products in mice, *Bioelectrochemistry and Bioenergetics* **1997**, *43*, 105-114.

28. Luo, W.; Muller, J. G.; Rachlin, E. M.; Burrows, C. J.; Characterisation of hydantoin products from one-electron oxidation of 8-oxo-7,8-dihydroguanosine in a nucleoside model, *Chemical Research in Toxicology* **2001**, *14*, 927-938.

Chapter Four

Identification of the Products of Iron- and Copper-mediated 8-oxo-7,8-dihydroGuanine Oxidation

4.1 Introduction

In Chapters 2 and 3, free G, PolyG and ds DNA were oxidised by iron- and copper-mediated Fenton reagents respectively. 8-oxoG was generated in all cases, as the primary oxidation product of G oxidation. As the incubation time with the oxidants increased, however, the concentration of 8-oxoG tended towards a decrease in concentration with increasing oxidation. This implies that 8-oxoG is not the final product of guanine oxidation, but is probably readily further oxidised. It has a lower oxidation potential than any of the unmodified DNA bases, including Guanine itself,[1] and has been identified as a "hotspot" for further oxidation.[2] (This is important when considering oxidants only capable of oxidising to a certain extent, but does not apply to strong oxidants such as •OH, which are capable of oxidising all DNA bases.) 8-oxoG may not induce all G→T transversions, and is not responsible for G→C.[3] This also indicates that other species, as well as 8-oxoG, are generated during G oxidation.

The exact nature of the final product of 8-oxoG oxidation is a matter of debate and seems to be dependent on the nature (*e.g.* nucleoside, singe-stranded oligomer, double-stranded oligonucleotide) and environmental conditions (pH, temperature) of the substrate, as well as the nature of the oxidising species. Cr(V)-Salen complex oxidation of 8-oxo-7,8-dihydro-2'-deoxyguanosine (8-OHdG) lead to the formation of two products, Guanidinohydantoin (Gh) and Spiroiminodihydantoin (Sp).[4] When 8-OHdG was incorporated within a ds oligonucleotide, only Sp was generated. An in depth analysis of the factors affecting Gh and Sp formation was studied using $NaIrCl_6$, a one electron oxidant that was selective towards 8-OHdG.[5] Oxidising 8-OHdG at pH 4 lead to 100% Gh. Increasing the pH to 7, however, lead to an overwhelming generation (90%) of Sp, at the expense of Gh. ss and ds oligonucleotides containing 8-OHdG were also oxidised at this pH. This resulted in 55% Gh and 40% Sp in ss oligonucleotides, but 95% Gh in ds oligonucleotides. Temperature also affected the final oxidation products. At 22 °C, the products of

8-OHdG oxidation in ss oligonucleotides were 55% Gh and 45% Sp. At 4 °C the Gh yield increased to 95% at the expense of Sp, while at 50 °C, the Sp yield increased to 95% at the expense of Gh. Whether Gh or Sp was formed depended on pH, temperature and the nature of 8-oxoG. All three oxidation products were proposed to be formed via a 5-OH-8-OHdG intermediate, as shown in Scheme 4.1.

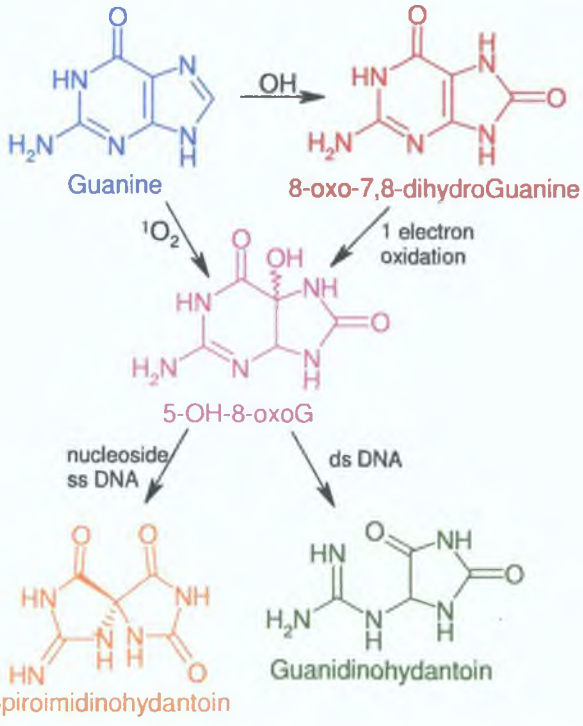

Scheme 4.1: Formation of Sp and Gh via 5-OH-8oxoG, guanine depicted in blue, 8-oxo-7,8-dihydroGuanine depicted in red, and intermediate complexes depicted in orange and green.[5]

pH 5.8 was assigned as the pKa of 5-OH-8-OHdG, the common intermediate of Gh and Sp, during peroxynitrite oxidation of 8-OHdG.[6] It was proposed that below pH 5.8, 5-OH-8-OHdG was protonated and electrophilic attack by H_2O was favoured, leading to formation of Gh. Above pH 5.8, 5-OH-8-OHdG was deprotonated, which favoured the formation of Sp. The protonation state of 5-OH-8-OHdG dictated the nature of the final oxidation product of 8-OHdG oxidation.

Guanosine (dG) oxidation by $^1O_2$ (generated by Type II photooxidation) yielded 95% Sp.[7] Oxidation of 8-OHdG, however, did not lead to Sp, but to 50% cyanuric acid and 35% imidazolone (Iz), which degraded to oxazolone (Oz), with less than 10% Sp detected.[8] O_2 oxidation of ss oligonucleotides also generated Iz.[9] The yield of Iz was 5 – 10% of dG decomposition, which corresponded to approx. 50% of 8-OHdG generated. Chemical induction of $^1O_2$ by $DHPNO_2$ resulted in oxaluric acid (Oxa), via the decomposition of oxidised guanidinohydantoin (oxGh), as shown in Scheme 4.2.[10] (Parabanic acid (Pa) is unstable and spontaneously breaks down to Oxa.)[11] Recently, low temperature (-78 °C) photooxidation was shown to yield 5-OH-8-OHdG, which rearranged to Sp on warming to room temperature.[12] •OH oxidation of dG and DNA under reducing conditions resulted in the formation of Oz,[13] however, for •OH oxidation induced by Fe(II) ions, further oxidation of 8-oxoG was expected to be prevented.[14] γ-irradiation of solid state DNA, also known to generate •OH, resulted in the formation of Pa and Oxa.[15]

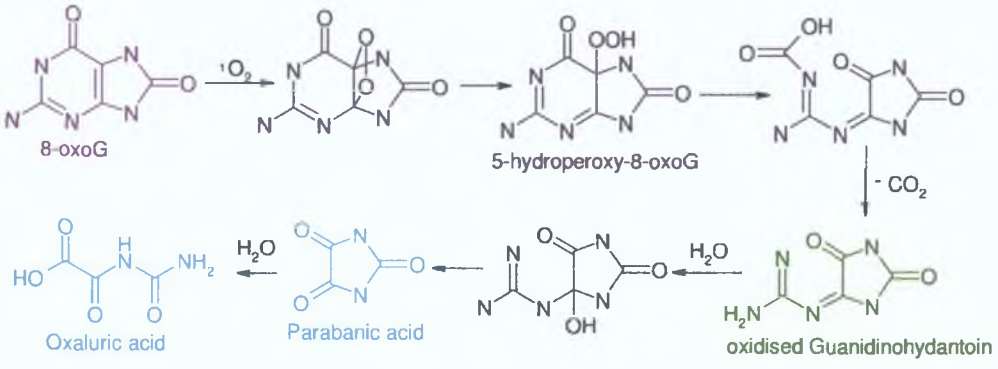

Scheme 4.2: Formation of Oxa via oxGh degradation, 8-oxo-7,8-dihydroGuanine depicted in red, intermediates depicted in green and final oxidation products depicted in blue.[10]

oxGh and Iz were also generated from G oxidation without the formation of 8-oxoG, by 2 electron oxidation with $MnTMPyP/KHSO_4$.[16] It should be remembered therefore that the formation of these products does not automatically imply the formation of 8-oxoG. However, most of the studies outlined above begin with the oxidation of 8-OHdG, and not dG, proving that 8-OHdG oxidation can produce the products outlined.

8-oxoG was shown to bind in Hoogsten mode to A, and so cause G•T→T•A transversion mutations, shown in Scheme 4.3.[9] Iz could bind to G (also in Hoogsten mode), causing G•T→C•G transversions.

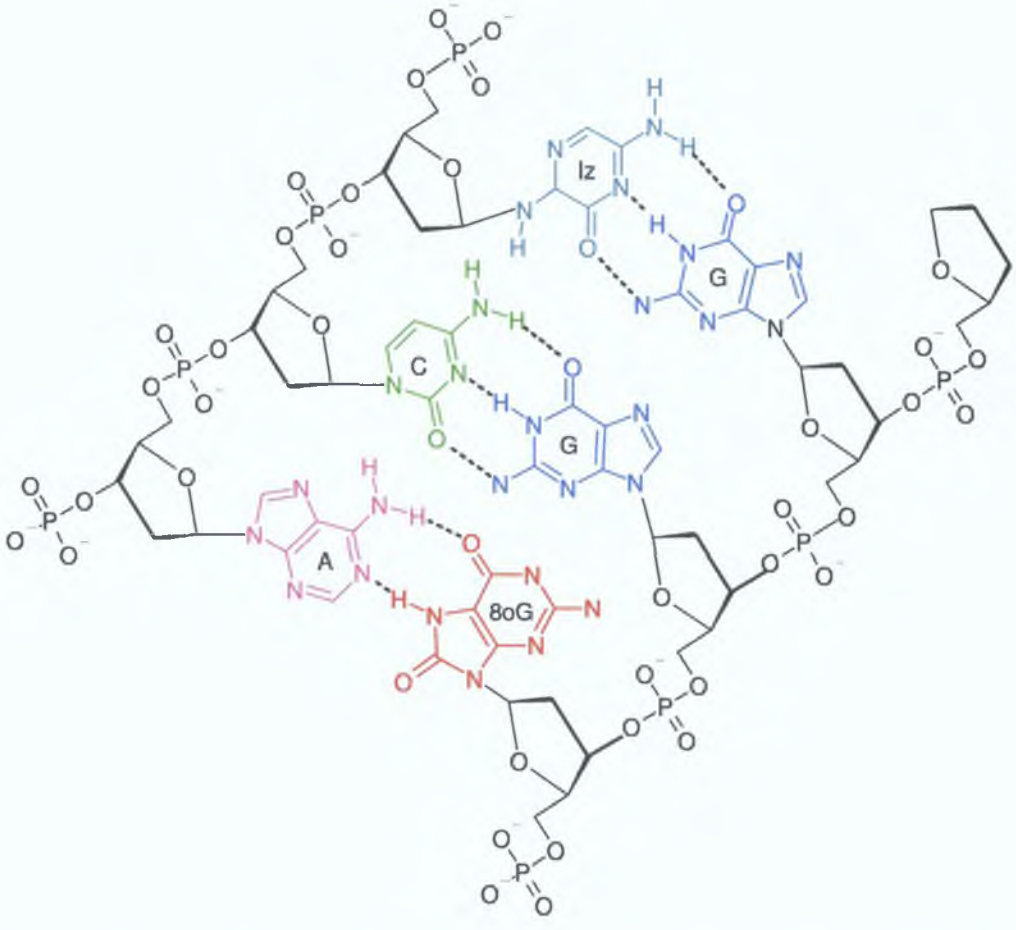

Scheme 4.3: Binding of 8-oxoG (8oG in scheme for clarity) and Iz within ds DNA[9]

Iz slowly isomerises to form Oz, which gave rise to predominantly G→T transversions, and to a much lesser extent G→C transversions, and also blocks DNA synthesis.[17] Sp resulted in a 2:1 preference for insertion of A instead of G opposite it, which resulted in G→T and G→C transversions. Gh caused G→C transversions. With mutation frequencies of approx. 100%, both Sp and Gh demonstrated a more dramatic effect than 8-oxoG, which had a mutation frequency of ~ 3%. Sp was

shown to be a much stronger block to DNA synthesis than Gh.[18] Oxa lead to G→C and G→T transversions, and was also a block during DNA synthesis.[3] The products generated when 8-oxoG is subjected to oxidation all incorporated the wrong base opposite them with a higher frequency than 8-oxoG itself. Further oxidation may therefore serve to increase the mutagenicity (during replication) of DNA which has undergone oxidative stress and so final products of oxidative attack on DNA need to be fully elucidated.

The aim of this study was to investigate what, if any, oxidation products are generated from the iron(II)- and copper(II)-mediated Fenton attack on 8-oxoG. 8-oxoG was incubated with iron(II) and H_2O_2, copper(II) and H_2O_2, or water (control samples). It was then separated from its oxidation products using HPLC and analysed using UV and MS detection. For both the iron- and copper-mediated Fenton oxidation of 8-oxoG, oxidised Guanidinohydantoin (oxGh) was detected as the primary oxidation product. It was generated immediately, and did not degrade significantly, even after 96 hr incubation with Fenton reagents. Oxaluric acid (Oxa) was detected after this time as a final oxidation product of oxGh oxidation. It was shown that oxGh was not generated from 8-oxoG degradation in the absence of Fenton reagents. A mechanism was proposed for the oxidation of 8-oxoG via a 5-OH-8-oxoG intermediate to oxGh.

4.2 Materials and Methods

4.2.1 Materials

4.2.1.1 Chemicals

Parabanic acid (P209) and cyanuric acid (185809) were purchased from Sigma Aldrich. 30% (v/v) hydrogen peroxide (H_2O_2) solution was purchased from Merck. Oxaluric acid was synthesized by hydrolyzing parabanic acid. All other chemicals were obtained as described in Chapter 2 in Section 2.2.1.1.

4.2.1.2 Buffers

The mobile phase for gradient HPLC-EC was prepared as described in Chapter 2 in Section 2.2.1.2.

For MS analysis, LC-MS Chromasolv water and methanol were used. For HPLC-MSMS, Eluent A consisted of 10 mM ammonium acetate buffer, pH 5.5, and Eluent B 50/50 methanol/water. All mobile phases were vacuum filtered using 47 mm Pall Nylaflo nylon membranes with 0.45 μm pore size and stirred overnight prior to use.

4.2.2 Apparatus

4.2.2.1 HPLC Instrumentation

All HPLC-EC separations were performed on a Varian ProStar 230 solvent delivery module, with a Varian ProStar 310 UV-VIS detector as described in Chapter 3 in Section 3.1.1.1.

4.2.2.2 Mass Spectrometry

For Mass Spectrometry, a Bruker Daltonics Esquire 3000 LC-MS (ion trap) was used with a Supelco Supelcosil LC-18 reversed phase column (2.1 mm id x 250 mm, particle size 5 μm). Eluent A consisted of 10 mM ammonium acetate buffer, pH 5.5; Eluent B 50/50 methanol/water. A flow rate of 0.2 ml/min was used with a linear gradient elution of 0 - 10% B from 0-22 min, 10 - 0% B from 22 - 25 min. Full scan spectra were taken at a cone voltage of 15 V using both positive and negative electrospray ionisation (ESI). ESI conditions were optimised using accompanying software.

4.2.3 Methods

4.2.3.1 Oxidation of 8-oxo-7,8-dihydroGuanine

8-oxo-7,8-dihydroGuanine (8-oxoG) was oxidised by iron(II)sulphate as described in Chapter 2 in Section 2.2.3.2, and was oxidised by copper(II)sulphate as described in Chapter 3 in Section 3.2.3.1.

4.3 Results

4.3.1 Iron-catalysed 8-oxo-7,8-dihydroGuanine oxidation

8-oxoG was incubated with iron(II)sulphate and H_2O_2 as described in Chapter 2, and samples were taken every 30 s from 0 to 5 min. Fig. 4.1 illustrates the HPLC separation with UV detection at 280 nm of 8-oxoG incubated for 0 min and for 5 min with the iron Fenton reagents.

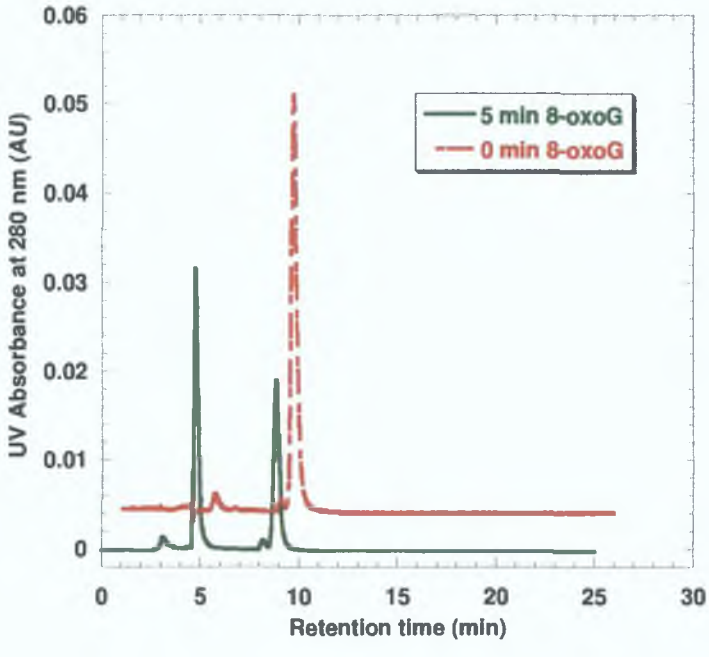

Fig. 4.1: HPLC separation with UV detection at 280 nm of 2.4 mM 8-oxoG incubated for 0 min (red) and 5 min (green), showing Product 1 eluting at 4.6 min, and 8-oxoG eluting at 8.2 min. (MS mobile phase as described in Chapter 2: Eluent A 10 mM ammonium acetate buffer, pH 5.5, Eluent B 50/50 methanol/water).

There was a dramatic decrease in the concentration of 8-oxoG, accompanied by a new peak at 4.6 min (Product 1). As shown in Fig. 4.2, Product 1 was immediately generated upon incubation with iron(II) and H_2O_2.

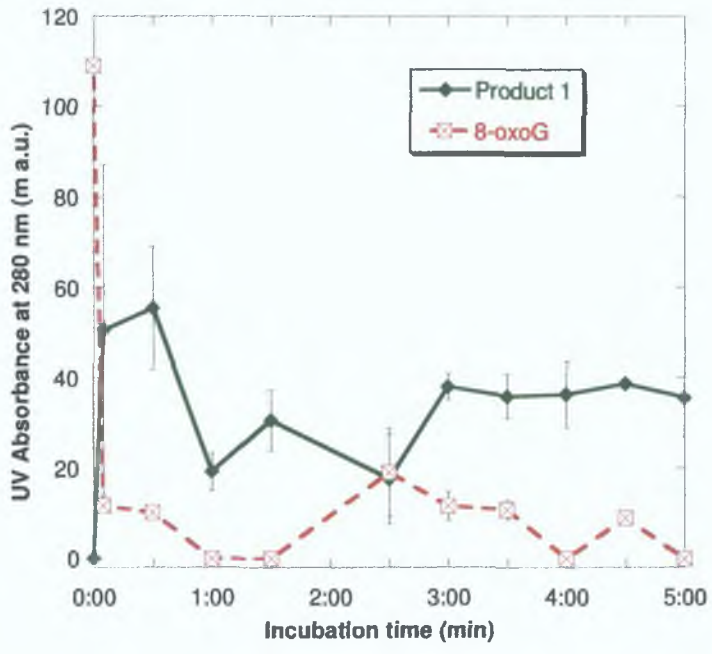

Fig. 4.2: Concentration of Product 1 (green) and 8-oxoG (red) for 0 – 5 min incubation of 8-oxoG with iron(II)sulphate and H_2O_2. (n=6)

The concentration of 8-oxoG was observed to oscillate as the incubation time with the Fenton reagents increased, as previously found in Chapter 2. Although the concentration of Product 1 did not increase linearly with incubation time, overall there was an increase in its concentration. The oscillations observed for 8-oxoG concentration were not observed for Product 1 concentration. There did not appear to be a direct relationship between 8-oxoG and Product 1 concentrations, but the general trend was towards an increase in Product 1 concentration and a decrease in 8-oxoG concentration. As shown in Fig. 4.3, Product 1 continued to be generated as the incubation time with iron(II)sulphate and H_2O_2 increased up to 12 hr. After 2 hr, 8-oxoG was no longer detected. From 8 to 12 hr, the level of Product 1 appeared to be decreasing slightly, at a steady rate. After 96 hr incubation with the Fenton reagents, Product 1 could still be detected using UV detection.

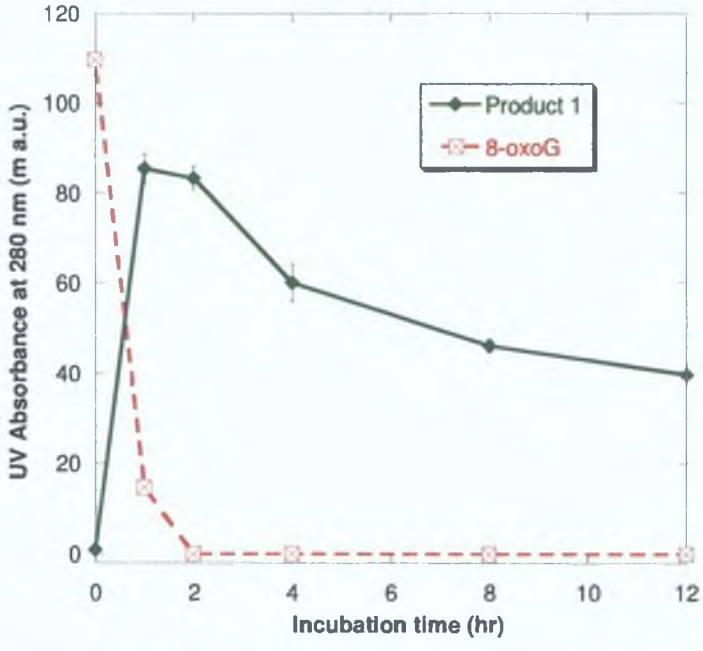

Fig. 4.3: Concentration of Product 1 (green) and 8-oxoG (red) for 0 – 12 hr incubation of 8-oxoG with iron(II)sulphate and H_2O_2. (n=6)

4.3.2 Copper-catalysed 8-oxo-7,8-dihydroGuanine oxidation

8-oxoG was incubated with copper(II)sulphate and H_2O_2, and again samples were taken every 30 s from 0 to 5 min. As with the iron-mediated oxidation (Fig. 4.1), Product 1 was immediately generated. The results are illustrated in Fig. 4.4. The same magnitude of Product 1 was generated for both copper(II)- and iron(II)-mediated oxidation of 8-oxoG. Again, the concentration of 8-oxoG was observed to oscillate with increasing incubation with the Fenton reagents. However, the overall trend towards decreasing concentration of Product 1 and decreasing concentration of 8-oxoG was detected.

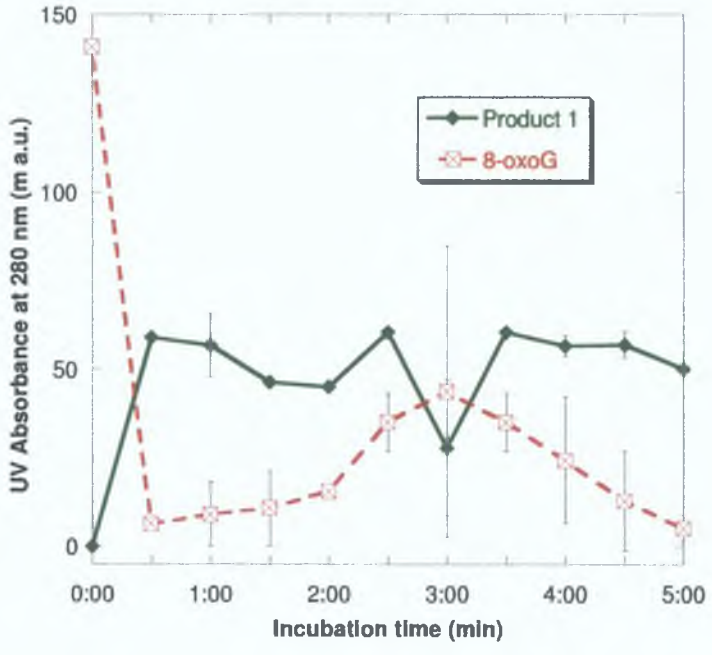

Fig. 4.4: Concentration of Product 1 (green) and 8-oxoG (red) for 0 – 5 min incubation of 8-oxoG with copper(II)sulphate and H_2O_2. (n=6)

As with the iron analysis, 8-oxoG was then incubated with copper(II)sulphate and H_2O_2 for incubation periods of up to 12 hr (data not shown), to investigate whether Product 1 was the final product of 8-oxoG oxidation, or would itself be further oxidised. Product 1 continued to be generated as the incubation time with copper(II)sulphate and H_2O_2 increased up to 12 hr. From 8 to 12 hr, the level of Product 1 decreased slightly over this timeframe. As was observed for the shorter incubation period, the same magnitude of Product 1 was observed for both iron(II)- and copper(II)-mediated reactions, with no 8-oxoG detected as the incubation time increased. From 8 to 12 hr, the level of Product 1 appeared to be decreasing slightly, at a regular rate.

4.3.3 8-oxoG oxidation without Fenton reagents

To exclude the possibility that Product 1 was not generated by the Fenton-catalysed oxidation of 8-oxoG, 8-oxoG was incubated with deionised water for 96 hr, under analogous conditions to the Fenton incubations. No Product 1 was observed, even after 96 hr incubation. This product is solely generated by the Fenton reaction. The concentration of 8-oxoG decreased slightly with increasing incubation time, but the magnitude of the degradation was significantly less than 8-oxoG oxidation by Fenton reagents, and was attributed to the inherent instability of 8-oxoG.

4.3.4 Mass Spectrometric Analysis of Product 1

To identify the nature of Product 1, it was analysed using HPLC-ESI ion trap MS. Table 4.1 outlines the suspected final oxidation products of 8-oxoG oxidation, based on literature publications outlined in Section 4.1. 8-oxoG oxidation might result firstly in the formation of 5-OH-8oxoG, as this had been observed as a precursor to Gh and Sp. Along with oxGh, these have been detected as the precursors to Pa and Oxa, Cy, Iz and Oz. Therefore, initially 5-OH-8oxoG, Gh, oxGh and Sp were the only products expected.

Table 4.1: suspected final oxidation products of 8-oxoG oxidation

Oxidised Product	Molecular Weight
5-OH-8-oxoG	183
guanidinohydantoin (Gh)	157
oxidised guanidinohydantoin (oxGh)	155
spiroimidinohydantoin (Sp)	183
parabanic acid (Pa)	114
oxaluric acid (Oxa)	132
cyanuric acid (Cy)	129
imidazolone (Iz)	112
oxazolone (Oz)	130

Using 8-oxoG standard, electrospray ionisation (ESI) parameters (positive mode) were optimised using the accompanying software. The nebuliser pressure was set to 50 psi, the drying gas 8.00 l min^{-1}, and the drying temperature to 350 °C. (Full acquisition parameters listed in Appendix 1) 8-oxoG samples from 0 – 5 min iron- and copper-mediated 8-oxoG oxidation were analysed using HPLC-MS. Ion chromatograms (EIC) were extracted from the Total Ion Chromatograms (TIC) of both sample data sets. The ions in both sets were the same, *i.e.*, ions of *m/z* (mass to charge ratio) 128, 129, 156, and 168 were detected in both samples. Fig. 4.5 plots the TIC and the EIC of ions with *m/z* 128, 129, 156, and 168 for 8-oxoG incubated for 90 s with copper(II)sulphate and H_2O_2.

The ion of *m/z* 168 corresponded to the $[8\text{-oxoG} + H]^+$ ion, the protonated ion of undamaged 8-oxoG. The ion of *m/z* 156 eluted at 5.6 min, which corresponded to the retention time of Product 1. In order to obtain structural information about this ion, MS/MS, which would give the fragmentation pattern of this ion, was carried out. ESI-MS/MS of the ion *m/z* 156.1 resulted in fragments of 139.1, 113.1 and 114.1, as illustrated in Fig. 4.6.

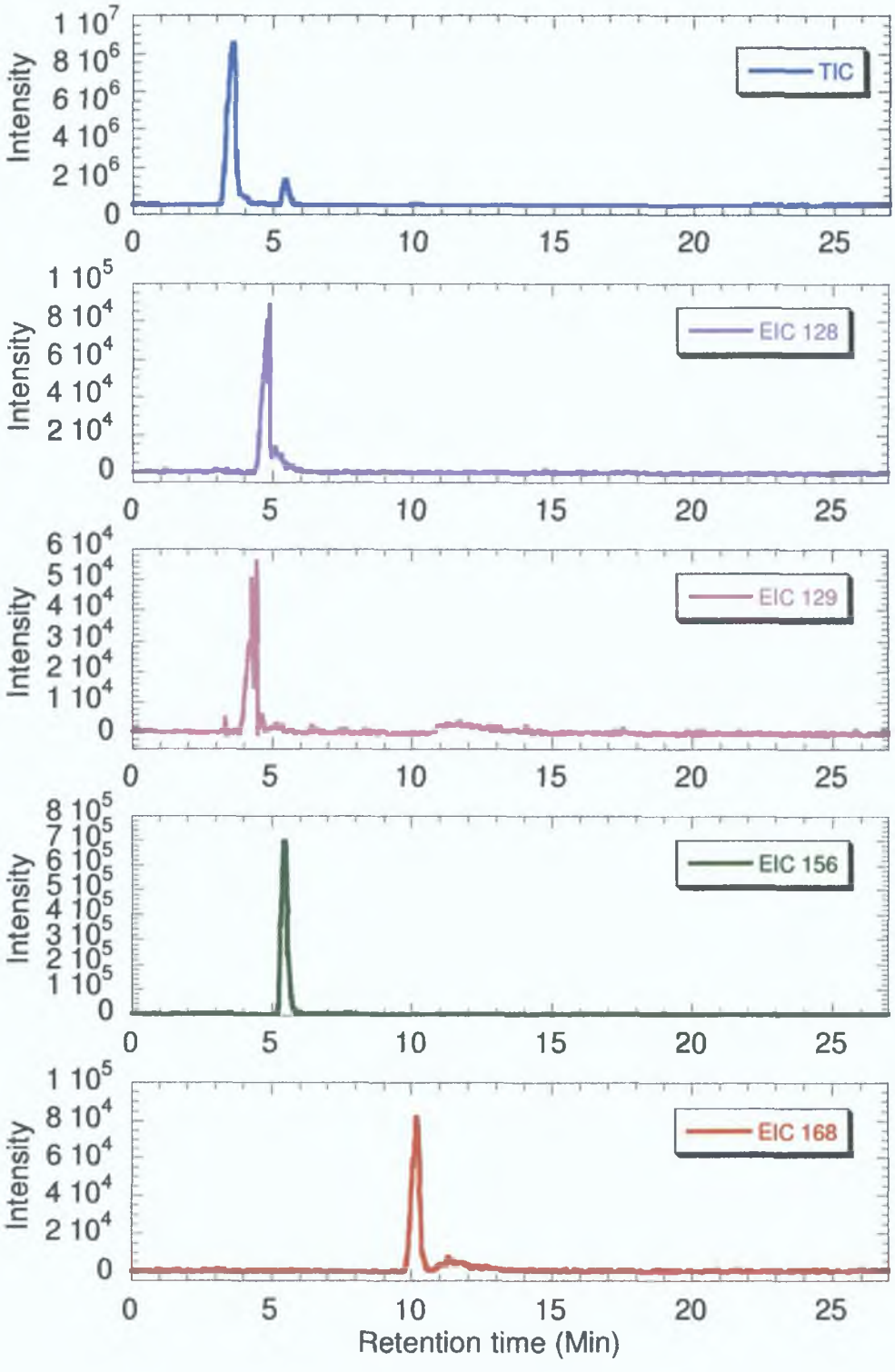

Fig. 4.5: TIC, EICs for 8-oxoG incubated for 90 s with copper(II)suphate and H_2O_2.

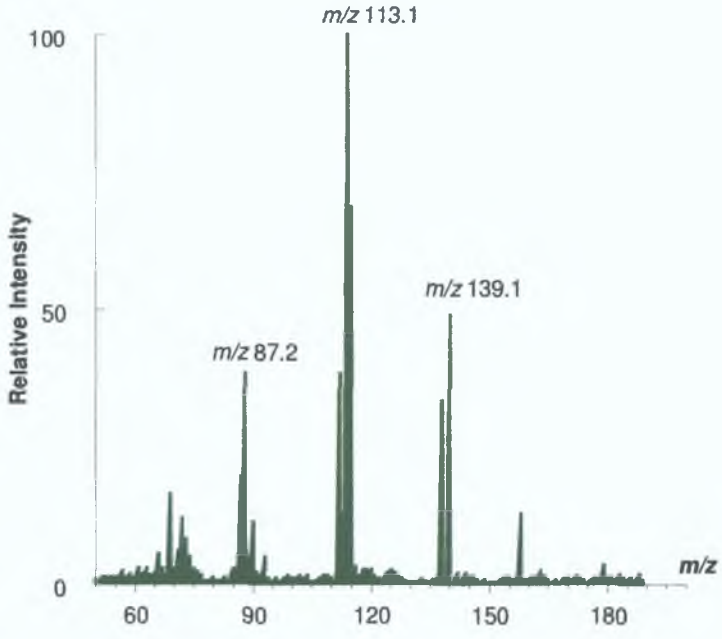

Fig. 4.6: ESI-MSMS of ion m/z 156.1 (Product 1, which elutes at 5.6 min) showing fragments 139.1, 113.1 and 87.2 (present in background eluent).

Product 1 was found to have a *m/z* of 156, which was proposed to be the protonated ion, so that Product 1 had a molecular weight of 155.1. Product 1 was therefore proposed to be oxidised Guanidinohydantoin, oxGh, and the ion of *m/z* 156 corresponded to the $[oxGh + H]^+$ ion. oxGh has a molecular weight of 155.1, as shown in Scheme 4.4. The fragment ion of *m/z* 139.1 represents the loss of NH_3 from oxGh. The fragment ion of *m/z* 113.1 represents a compound of mass 112.1. A possible structure of this compound is proposed in Scheme 4.4.

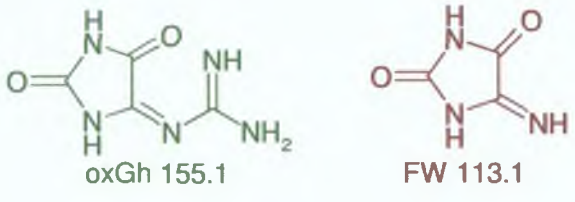

Scheme 4.4: Proposed structures of compound 155.1 and of fragment compounds 112.1 and 113.1.

Due to the overwhelming evidence of Sp formation as the main product of 8-OHdG oxidation, (with Gh being formed preferentially in oligodeoxynucleotides[4]), Sp was expected to be generated in this study. It was not detected, however, and it so was concluded that Sp was not formed, or at the very least, was not a significant product of oxidation, during 8-oxoG oxidation by either iron or copper and H_2O_2.

4.3.5 Mass Spectrometric Analysis of Product 2, Product 3.

As illustrated in Fig. 4.5, two ions of *m/z* 128.1 and 129.1 were also detected in significant quantities during MS analysis of 8-oxoG, which was incubated both with copper- and iron-mediated Fenton reagents. These ions did not correspond to any of the expected oxidation products listed in Table 4.1. As illustrated in Fig. 4.7, the levels of these products, which also had a UV absorbance at 280 nm, did not increase with increasing incubation time. Moreover, they also appeared at the same magnitude in the control samples. Therefore they were deemed not to be products of Fenton oxidation, and were possibly impurities in the 8-oxoG standard, which was not further purified prior to use. The ions of *m/z* 128.1 and 129.1 corresponded to the protonated ions of Product 2 and Product 3, which therefore probably had molecular weights of 127.1 and 128.1 respectively.

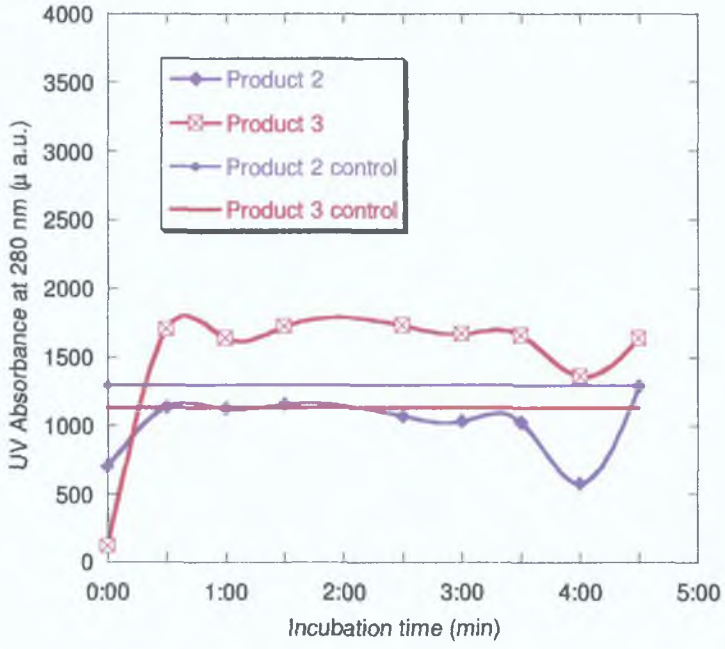

Fig. 4.7: Concentration of Product 2 (purple) and Product 3 (pink) for 0 – 5 min incubation of 8-oxoG with copper(II)sulphate and H_2O_2. (n=6)

4.3.6 Further oxidative species

oxGh was observed during this analysis to be the product of 8-oxoG oxidation by iron- and copper-mediated Fenton oxidants. It was found by Cadet *et al.*, however, to further degrade to Pa and finally Oxa during $^1O_2$ oxidation.[10] Hydration of oxGh formed by the one electron oxidation of Gh also lead to the formation of Pa,[19] raising the possibility that oxGh may be another intermediate in the overall oxidation mechanism of 8-oxoG. Therefore, although it appeared not to be decreasing in concentration with increasing incubation time, which would be expected if it were an intermediate species, incubated samples were analysed for the presence of further oxidative species, which have been outlined in Table 4.1 and are shown in Scheme 4.6.

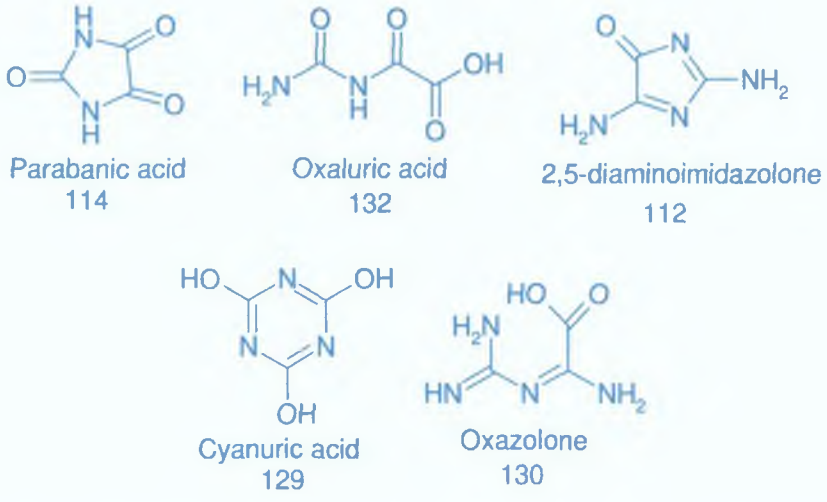

Scheme 4.6: Oxidation products of oxGh (final oxidation products of 8-oxoG oxidation) depicted in blue.

HPLC mobile phase pH and ESI (negative mode) was optimised using Pa, Cy and Oxa standards and each of the incubated samples were analysed for the presence of any of the above species. Only for samples incubated for 96 hr with Fenton reagents were any of the above compounds detected. EIC for the deprotonated Oxa ion at *m/z* 131, plotted in Fig. 4.8, shows a peak of approx 4% of the overall intensity of the TIC at 3.3 minutes (eluting with the solvent front) for 8-oxoG incubated for 96 hr with iron(II)sulphate and H_2O_2. This peak was not present in the control sample; it did, however, appear in samples incubated with copper(II)sulphate and H_2O_2, although ion intensities observed were about one third lower than for corresponding iron incubations. The MS of this peak, plotted in Fig. 4.9 shows the $[Oxa- H]^-$ ion at *m/z* 131. EICs for the deprotonated Cy ion at *m/z* 128 were inconclusive; apparent Cy ion peaks were not reproducible. It was therefore concluded that Oxa was probably generated after 96 hr incubation of 8-oxoG with both iron and copper Fenton reagents. That oxGh should be quantitatively oxidised to Pa and subsequently to Oxa, is in agreement with an overall decrease in its concentration with increasing incubation time with the Fenton reagents. It is possible that at pH 11, the products were formed, but were instantly degraded, so that they were only detected in trace amounts after 96 hr incubation.

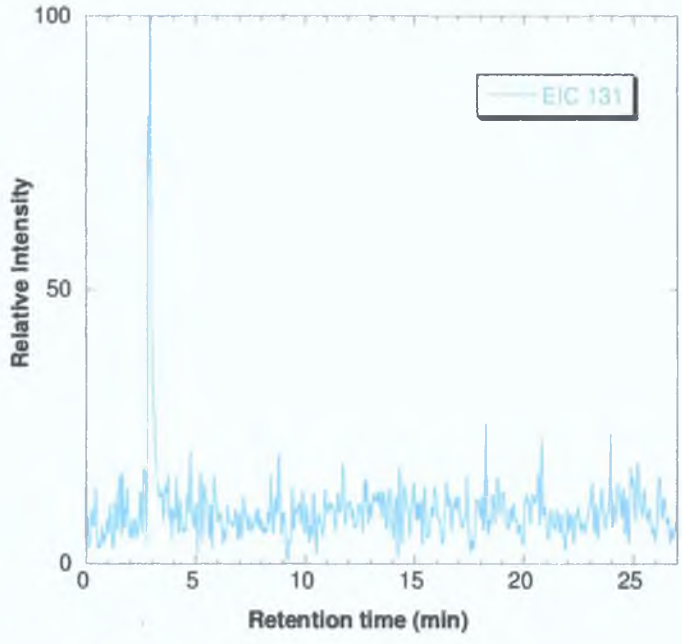

Fig. 4.8: EIC for suspected deprotonated Oxa ion at m/z 131 for 8-oxoG incubated for 96 hr with iron(II)sulphate and H_2O_2.

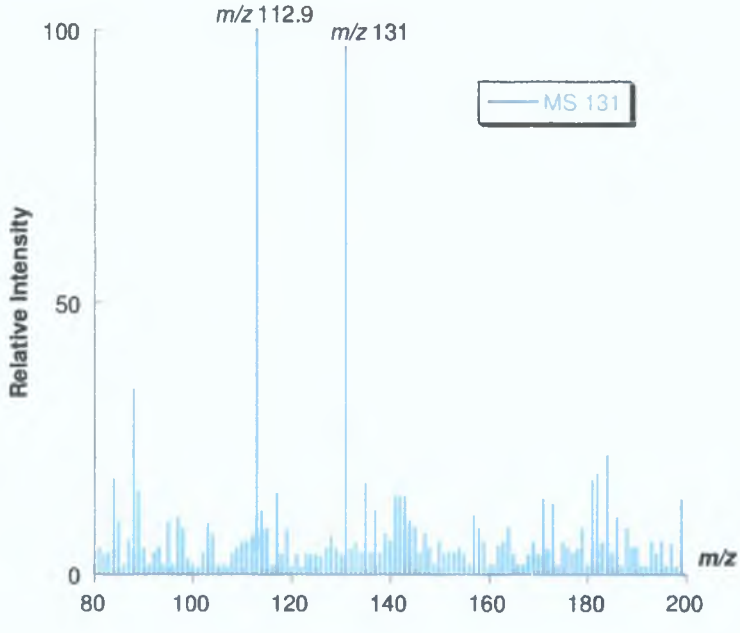

Fig. 4.9: MS of suspected deprotonated Oxa ion at m/z 131 for 8-oxoG incubated for 96 hr with iron(II)sulphate and H_2O_2.

4.3.7 8-oxo-7,8-dihydroGuanine degradation product

In control samples, where 8-oxoG was incubated with deionised water, the concentration of 8-oxoG was observed to decrease as incubation time increased, presumably by the degradation of 8-oxoG to another species. There was no corresponding increase, however, in the concentration of oxGh; this was not the product of 8-oxoG degradation in the absence of Fenton oxidants. After 96 hr incubation in water, a new peak was found, which eluted before 8-oxoG, as shown in Fig. 4.10. MS analysis of this peak revealed an ion of *m/z* 167. ESI-MSMS of this ion did not yield any fragmentation patterns, as shown in Fig. 4.11. This product was one unit more than 8-oxoG itself, plotted in Fig. 4.12. No structure was elucidated for this compound during this investigation.

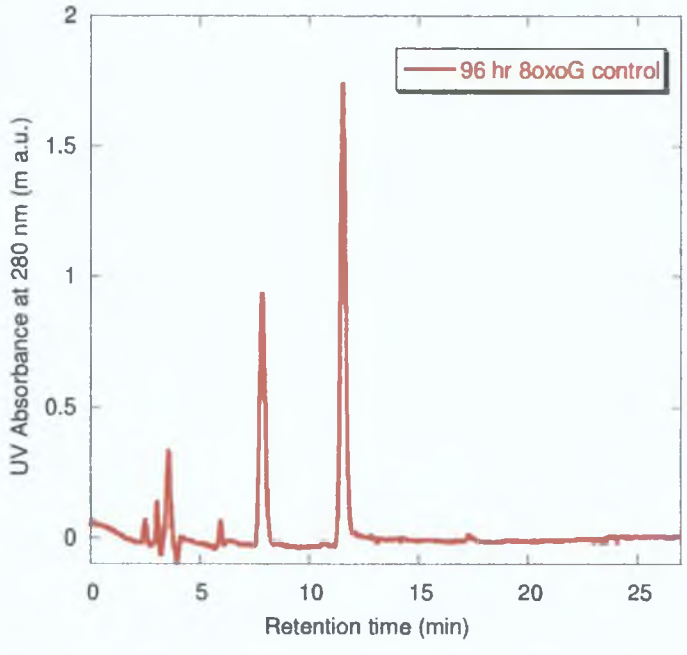

Fig. 4.10: HPLC separation of 8-oxoG incubated for 96 hr with water (control) with UV detection at 280 nm showing a new peak eluting at 8.1 min.

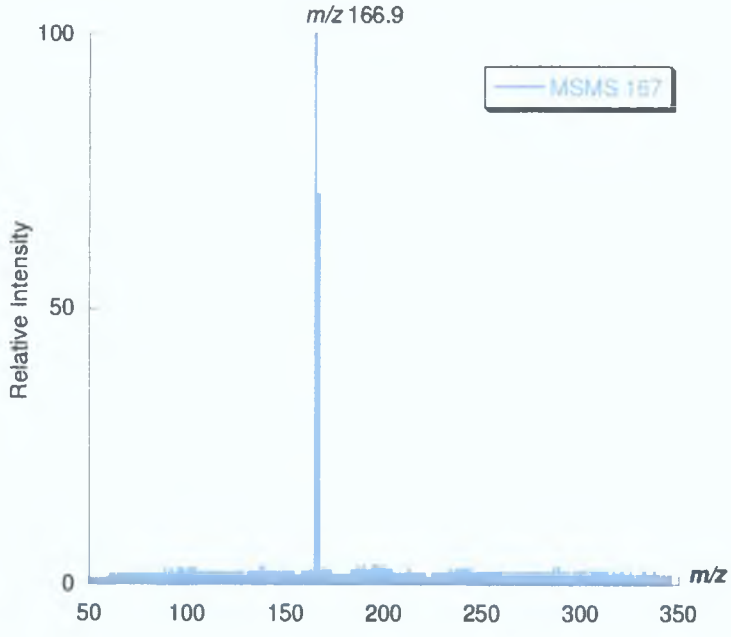

Fig. 4.11: ESI-MSMS of ion m/z 166.9, the ion generated upon 8-oxoG degradation.

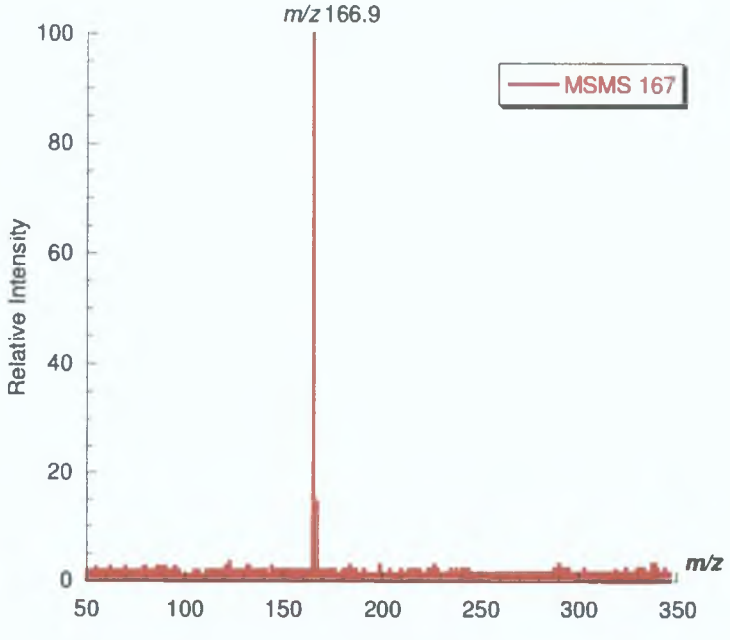

Fig. 4.12: ESI-MSMS of ion m/z 166.9, the deprotonated 8-oxoG ion [8-oxoG - H]⁻.

4.4 Discussion

A new species, Product 1, which eluted at 5.6 min, as illustrated in Fig. 4.1, was generated immediately on incubation of 8-oxoG with iron(II)sulphate and H_2O_2, shown in Fig. 4.2. Product 1 was identified as oxidised guanidinohydantoin, oxGh. The concentration of 8-oxoG oscillated with increasing incubation, as had previously been observed in Chapter 2. The concentration of oxGh generated was also observed to fluctuate to a minor extent with increasing incubation time. This fluctuation was significantly less than the 8-oxoG concentration oscillation, however. Overall it was observed that the concentration of 8-oxoG decreased and the concentration of oxGh increased inititally, but then slowly decreased with increasing incubation with the iron(II) Fenton reagents. This is expected, as oxGh is unstable and is further oxidised to both parabanic acid (Pa) and oxaluric acid (Oxa). A quantitative decrease in oxGh concentration with a concurrant increase in Pa concentration was expected. The absence of Pa may have been due to the alkaline pH (pH 11) that was used for this analysis, so that its absence should not imply that it was not generated. As illustrated in Fig. 4.3, from 8 to 12 hr incubation with the Fenton reagents, the concentration of oxGh tended towards a steady but slow decrease in concentration. After 2 hr incubation, no 8-oxoG was detected in any sample.

The nature of the oxidant generated by copper(II)-mediated Fenton reaction was expected to behave as a one electron oxidant, as discussed in Chapter 3. This was in contrast to the •OH generated from the iron(II)-mediated Fenton reaction discussed in Chapter 2. Due to the differing nature of the oxidising species therefore, different oxidation products of 8-oxoG were expected. However, the oxidised species generated by oxidation of 8-oxoG by copper(II)sulphate and H_2O_2 was also identified as oxGh, the same species observed for the iron(II) system. Furthermore, the magnitude of oxGh generated using copper(II) as a catalyst was the same as that generated using iron(II). The overall trend was for oxGh increase and 8-oxoG

decrease during increasing incubation with Fenton reagents. Increasing the incubation time to 12 hr, again a steady state oxGh concentration was observed.

Both iron- and copper-mediated oxidation of 8-oxoG lead to the immediate formation of oxGh, which did not degrade significantly, even after 96 hr incubation with the Fenton reagents. One electron oxidation previously only yielded oxGh on further oxidation of Gh; Gh was initially formed and only degraded to oxGh over a time frame of several hr, Gh having a half life of 23 hr at room temperature at pH 10.[19] In the Fenton oxidation of 8-oxoG in this research, no Gh was found, even at the initial stages of incubation, *i.e.,* from just 30 s incubation. Instead oxGh was generated immediately, without any Gh first being formed. This implied that the formation of oxGh did not proceed via further oxidation of Gh, and therefore that one electron oxidation of Gh did not occur during the Fenton reaction. $^1O_2$-mediated oxidation of 8-oxoG in single stranded DNA had previously been observed to generate oxGh via the unstable 5-OOH-8oxoG intermediate, as illustrated in Scheme 4.2.[10] In that mechanism, oxGh was the first stable intermediate of 8-oxoG oxidation, therefore its immediate detection would be likely. $^1O_2$-mediated oxidation of 8-oxoG could therefore yield significant oxGh as the primary product of 8-oxoG oxidation, as was observed for both iron and copper catalyzed oxidation in Fig. 4.2 and 4.4 respectively. During both iron and copper Fenton oxidation only oxGh, but not 5-OOH-8oxoG, was observed. 5-OOH-8oxoG was shown to be an unstable intermediate, however, that was readily further oxidised. Lack of detection of this species did therefore not exclude $^1O_2$-mediated oxidation as a possible mechanism for the generation of oxGh. The only ROS known to generate oxGh directly is $^1O_2$; this implied that $^1O_2$, or a $^1O_2$-like species, was involved in the oxidation of 8-oxoG in both iron(II)- and copper(II)-mediated Fenton reagent oxidation of 8-oxoG.

Although the concentration of oxGh did not decrease significantly with increasing incubation time, based on previous studies outlined in Section 4.1, further oxidation of oxGh was expected to occur. When DNA was subjected to $^1O_2$-mediated oxidation, the oxidation of 8-oxoG was observed to occur via oxGh

intermediate, finally yielding Pa and Oxa.[10] •OH oxidation of dG and DNA resulted in the formation of Oz.[13] γ-irradiation of solid state DNA, also known to generate •OH, resulted in the formation of Pa and Oxa.[15] One electron oxidation of 8-oxoG and 8-oxoG oligonucleotides was found to result in Sp or Gh, which was shown to be further oxidised to Pa.[19] Samples incubated for 48 and 96 hr with Fenton reagents were therefore analysed for the presence of these species. As shown in Fig. 4.7, Oxa was detected after 96 hr incubation of 8-oxoG with iron-mediated Fenton reagents. It was also detected in the copper-mediated Fenton reaction, but at lower concentrations. Detection of Oxa as a final oxidation product of 8-oxoG oxidation therefore implied that •OH or a •OH like species, or $^1O_2$, or a $^1O_2$-like species, was involved in the oxidation of 8-oxoG.

When 8-oxo-7,8-dihydro-2'-deoxyguanosine (8-OHdG) was subjected to iron- and copper- catalysed oxidation, however, the oxidation product was not oxGh, but Sp.[20]This may have been due to the reduced pH (pH 7) at which the reaction occurred. This was in line with previous studies, where its oxidation by one electron oxidants,[5] Cr(V),[4] $^1O_2$[12,21] and peroxynitrites[6,22] all resulted in Sp formation. The 8-oxoG oxidation product of these oxidants, however, was found to be Gh when an oligonucleotide substrate was oxidised. Recently, a possible reason for the differences in oxidation product during peroxynitrite oxidation of 8-OHdG was proposed.[22] It was observed during this oxidation that at low pH, the formation of Gh predominated, but at higher pH, Sp yield increased at the expense of Gh. 5-OH-8-OHdG, the common intermediate of Gh and Sp, was found to have a pK_a of 5.8. It was proposed that below pH 5.8, 5-OH-8-OHdG was protonated at N7. This caused the amide group to undergo hydrolysis, followed by decarboxylation, leading to formation of Gh. Above pH 5.8, 5-OH-8-OHdG was deprotonated, so that electrophilic attack by H_2O was not favoured, and 5-OH-8-OHdG rearranged to form Sp. The protonation state of 5-OH-8-OHdG dictated the nature of the final oxidation product of 8-OHdG oxidation. This is not the intermediate proposed for the formation of oxGh, however. Instead 5-OOH-8-OHdG was proposed as the reactive intermediate. It is possible, however, that both Sp and oxGh are formed via

this intermediate, and that the pH of this intermediate determines whether oxGh or Sp is formed.

The exact nature of the ROS involved in the oxidation of DNA and DNA bases by metal-mediated Fenton reactions has been the subject of much debate and research. As previously discussed in Chapter 2, iron(II) and H_2O_2 are reported to generate •OH via the Fenton reaction according to Reaction 4.1.[23]

$$H_2O_2 + Fe(II) \xrightarrow{k_1} Fe(III) + HO^- + HO\cdot \quad k_1 = 76\ lmol^{-1}s^{-1} \quad \text{(Reaction 4.1)}$$

A recent study by Wink *et al.*, however, questioned this generation of •OH.[24] They found that the reaction of iron(II) and H_2O_2 lead to two intermediates; neither being •OH. Instead they proposed that the first intermediate (X) was probably a peroxo complex, *e.g.* Fe(II)(OOH), and the second intermediate (Y) an iron(IV) oxo complex, *e.g.* FeO^{2+}. Scheme 4.8 outlines the mechanism proposed:

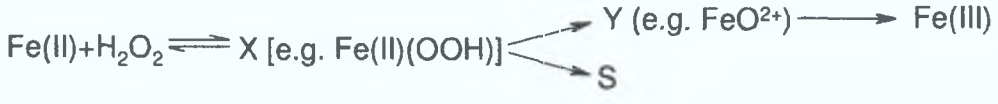

Scheme 4.8: Proposed mechanism for reaction of iron(II) and H_2O_2[24]

A subsequent publication examined the feasibility of the Fenton reaction on thermodynamic grounds.[25] It was found that the familiar outer sphere mechanism used to represent the Fenton reaction (Reaction 4.1) to be thermodynamically extremely unfavourable and therefore unlikely to occur. Far more likely was an inner sphere mechanism where a ferrous peroxide complex was generated. However, this could still result in the formation of •OH. The DNA damage induced by Cu(II) and H_2O_2 has also been investigated.[26] It was concluded that Cu(II) was the species which bound to DNA but that Cu(I) participated in the DNA damage. Scavanging reactions indicated that •OH was not the primary oxidative species, but a "bound •OH", such as a copper-peroxide complex may be involved. In a similar manner $^1O_2$ was ruled out as a primary reactive species, but a "bound $^1O_2$", again a copper-peroxide complex, could cause the damage recorded. A publication by Frelon *et al.*[27]

analysed the degradation of DNA bases by copper in the presence of H_2O_2 and again concluded that the ROS species involved was not •OH. Instead the authors concluded that $^1O_2$ was instead predominantly responsible for the oxidative damage that occurred, with $^1O_2$ being generated *in situ* via a DNA-copper-hydroperoxo complex. A recent investigation demonstrated how the Cu(II)/H_2O_2 system generated a very effective oxidation.[28] It concluded that the Cu(II)/H_2O_2 system was unlikely to proceed via the Fenton mechanism, but the copper-hydroperoxo complex Cu(I)•OOH, and proposed a reaction scheme for this oxidation.[29] From Chapter 3 in this thesis, one electron oxidation was proposed for the Cu(II) oxidation of G to yield the cation radical G^{+}•, which subsequently formed 8-oxoG.

The results of 8-oxoG oxidation carried out during this investigation indicated that both copper and iron generate the same 8-oxoG oxidation product (oxGh), and quantitative analysis showed that a similar magnitude of OxGh is generated by both metal systems. This investigation analysed the oxidation of 8-oxoG, and therefore excluded any influences of binding of the metal to the DNA chain, and intermediates that might be generated as a consequence of this binding. It had previously been proposed that the iron-mediated Fenton reaction generated •OH, but that the copper-mediated Fenton reaction proceeded via one electron oxidation. Whereas one electron oxidaiton primarily oxidises G, •OH generates over 60 oxidation products, oxidising all 4 DNA bases. This analysis was confined to the oxidation of 8-oxoG, and so the other DNA bases A, T and C were not considered. Potential damage to those bases was therefore not analysed. If damage had occurred to those bases, it would have indicated that •OH was also generated by the copper-mediated Fenton reaction, whereas absence of damage, specifically at the 5'-G of a GG doublet would have implied that one electron oxidation was involved. The role of $^1O_2$ in copper-mediated Fenton oxidation has also been proposed. In order to investigate this, the product generated from G8OH• reduction, *i.e.,* FapyG, should be analysed. This is formed during one electron oxidation, but not during $^1O_2$ mediated oxidation, so that its presence would indicate that one electron oxidation was involved.

4.5 Conclusions

The products of 8-oxoG oxidation were investigated in this study. During analysis, a new product, oxidised guanidinohydantoin (oxGh), was shown to be generated immediately on incubation with reagents iron(II)sulphate and H_2O_2 and with reagents copper(II)sulphate and H_2O_2. The concentration of 8-oxoG was observed to oscillate with increasing incubation time, with an overall trend towards its decrease. The concentration of oxGh was also observed to oscillate slightly with increasing incubation time, but these oscillations were significantly less than those observed for 8-oxoG, and could be within experimental error. The overall trend was towards its slow but steady decrease. For both metal systems, the overall trend with increasing incubation time was towards an increase of oxGh with a corresponding decrease in 8-oxoG, with a similar magnitude of oxGh generated by both systems.

Mass spectrometry was used to identify the product of 8-oxoG oxidation as oxGh. Analysis of the fragmentation pattern of oxGh confirmed the identity of this 8-oxoG oxidation product. Mass spectrometry operated in negative mode was utilised to investigate whether any products of oxGh oxidation were present. These were expected due to the unstable nature of oxGh. Oxaluric acid was detected after 96 hr incubation of 8-oxoG with both iron- and copper-mediated Fenton reagents. 8-oxoG incubated without Fenton reagents for 96 hr was found to result in the formation of a product of molecular weight one a.m.u. greater than 8-oxoG. It was not identified, and fragmentation patterns did not give any insight into possible structures.

4.6 References

1. Prat, F.; Houk, K. N.; Foote, C. S.; Effect of guanine stacking on the oxidation of 8-oxoguanine in B-DNA, *Journal of the American Chemical Society* **1998**, *120*, 845-846.

2. Doddridge, Z. A.; Cullis, P. M.; Jones, G. D. D.; Malone, M. E.; 7,8-Dihydro-8-oxo-2'-deosyguanosine residues in DNA are radiation damage "hot" spots in the direct radiation damage pathway, *Journal of the American Chemical Society* **1998**, *120*, 10998-10999.

3. Duarte, V.; Gasparutto, D.; Jacquinod, M.; Ravanat, J.-L.; Cadet, J.; Repair and mutagenic potential of oxaluric acid, a major product of singlet oxygen-mediated oxidation of 8-oxo-7,8-dihydroguanine, *Chemical Research in Toxicology* **2001**, *14*, 46-53.

4. Sugden, K. D.; Campo, C. K.; Martin, B. D.; Direct oxidation of guanine and 7,8-dihydro-8-oxoguanine in DNA by a high-valent chromium complex: a possible mechanism for chromate genotoxicity, *Chemical Research in Toxicology* **2001**, *14*, 1315-1322.

5. Burrows, C. J.; Muller, J. G.; Kornyushyna, O.; Luo, W.; Duarte, V.; Leipold, M. D.; David, S. S.; Structure and potential mutagenicity of new hydantoin products from guansoine and 8-oxo-7,8-dihydroguanine oxidation by transition metals, *Environmental Health Perspectives* **2002**, *110*, 713-717.

6. Niles, J. C.; Wishnok, J. S.; Tannenbaum, S. R.; Spiroimidinohydantoin and guanidinohydantoin are the dominant products of 8-oxoguanosine oxidation at low fluxes of peroxynitrite: mechanistic studies with ^{18}O., *Chemical Research in Toxicology* **2004**, *17*, 1510-1519.

7. Ravanat, J.-L.; Cadet, J.; Reaction of singlet oxygen with 2'-deoxyguanosine and DNA. Isolation and characterisation of the main oxidation products., *Chemical Research in Toxicology* **1995**, *8*, 379-388.

8. Raoul, S.; Cadet, J.; Photosensitized reaction of 8-oxo-7,8-dihydro-2'-deoxyguanosine: Identification of 1-(2-deoxy-β-D-*erythro*-pentofuranosyl)cyanuric acid as the major singlet oxygen oxidation product, *Journal of the American Chemical Society* **1996**, *118*, 1892-1898.

9. Kino, K.; Sugiyama, H.; Possible cause of GC CG transversion mutation by guanine oxidation product, imidazolone, *Chemistry and Biology* **2001**, *8*, 369-378.

10. Duarte, V.; Gasparutto, D.; Yamaguchi, L. F.; Ravanat, J.-L.; Martinez, G. R.; Medeiros, M. H. G.; Mascio, P. D.; Cadet, J.; Oxaluric acid as the major product of

singlet oxygen-mediated oxidation of 8-oxo-7,8-dihydroguanine in DNA, *Journal of the American Chemical Society* **2000**, *122*, 12622-12628.

11. Sumrada, R.; Cooper, T. G.; Oxaluric acid: a non-metabolizable inducer of the allantoin degradative enzymes in *Saccharomyces cerevisiae*, *Journal of Bacteriology* **1974**, *117*, 1240-1247.

12. McCallum, J. E. B.; Kuniyoshi, C. Y.; Foote, C. S.; Characterisation of 5-hydroxy-8-oxo-7,8-dihydroguanosine in the photosensitized oxidation of 8-oxo-7,8-dihydroguanosine and its arrangement to spiroimidinohydantoin, *Journal of the American Chemical Society* **2004**, *126*, 12677-12682.

13. Cadet, J.; Berger, M.; Buchko, G. W.; Joshi, P. C.; Raoul, S.; Ravanat, J.-L.; 2,2-diamino-4-[(3,5-di-O-acetyl-2-deoxy-ß-D-erythro- pentofuranosyl)amino]-5-(2H)-oxazolone: a novel and predominant radical oxidation product of 3',5'-di-O-acetyl-2'-deoxyguanosine, *Journal of the American Chemical Society* **1994**, *116*, 7403-7404.

14. Cadet, J.; Douki, T.; Gasparutto, D.; Ravanat, J.-L.; Review: Oxidative damage to DNA: formation, measurement and biochemical features, *Mutation Research/Fundamentals and Molecular Mechanisms of Mutagenesis* **2003**, *531*, 5-23.

15. Cai, Z.; Seville, M. D.; Electron and hole transfer from DNA base radicals to oxidised products of guanine in DNA, *Radiation Research* **2003**, *159*, 411-419.

16. Chworos, A.; Seguy, C.; Pratviel, G.; Meunier, B.; Characterization of the Dehydro-Guanidinohydantoin Oxidation Product of Guanine in a Dinucleotide, *Chemical Research in Toxicology* **2002**, *15*, 1643-1651.

17. Duarte, V.; Gasparutto, D.; Jacquinod, M.; Cadet, J.; *In vitro* synthesis opposite oxazolone and repair of this DNA damage using modified oligonucleotides, *Nucleic Acids Research* **2000**, *28*, 1555-1563.

18. Henderson, P. T.; Delaney, J. C.; Muller, J. G.; Neeley, W. L.; Tannenbaum, S. R.; Burrows, C. J.; Essigmann, J. M.; The hydantoin lesions formed from oxidation of 7,8-dihydro-8-oxoguanine are potent sources of replication errors in vivo, *Biochemistry* **2003**, *42*, 9257-9262.

19. Luo, W.; Muller, J. G.; Rachlin, E. M.; Burrows, C. J.; Characterisation of hydantoin products from one-electron oxidation of 8-oxo-7,8-dihydroguanosine in a nucleoside model, *Chemical Research in Toxicology* **2001**, *14*, 927-938.

20. White, B.; Tarun, M. C.; Gathergood, N.; Rusling, J. F.; Smyth, M. R.; Oxidized Guanidinohydantoin and Spiroiminodihydantoin are major products of iron- and copper-mediated 8-oxoguanine and 8-oxodeoxyguanosine oxidation, *manuscript submitted* **2005**.

21. Martinez, G. R.; Loureiro, A. P. M.; Marques, S. A.; Miyamoto, S.; Yamaguchi, L. F.; Onuki, J.; Almeida, E. A.; Garcia, C. C. M.; Barbosa, L. F.; Medeiros, M. H. G.; Di Mascio, P.; Oxidative and alkylating agents in DNA, *Mutation Research/Reviews in Mutation* **2003**, *544*, 115-127.

22. Niles, J. C.; Wishnok, J. S.; Tannenbaum, S. R.; Spiroiminodihydantoin Is the Major Product of the 8-Oxo-7,8-dihydroguanosine Reaction with Peroxynitrite in the Presence of Thiols and Guanosine Photooxidation by Methylene Blue, *Organic Letters* **2001**, *3*, 963-966.

23. Walling, C.; Fenton's reagent revisited, *Accounts of Chemical Research* **1975**, *8*, 135-131.

24. Wink, D. A.; Nims, R. W.; Saavedra, J. E.; William E. Utermahlen, J.; Ford, P. C.; The Fenton oxidation mechanism: reactivities of biologically relevant substrates with two oxidizing intermediates differ from those predicted for the hydroxyl radical, *Proceedings of the Natural Academy of Sciences USA* **1994**, *91*, 6604-6608.

25. Winterbourne, C. C.; Toxicity of iron and hydrogen peroxide: the Fenton reaction, *Toxicology Letters* **1995**, *82/83*, 969-974.

26. Yamamoto, K.; Kawanishi, S.; Hydroxyl free radical is not the main active species in site-specific DNA damage induced by copper (II) ion and hydrogen peroxide, *Journal of Biological Chemistry* **1989**, *264*, 15435-15440.

27. Frelon, S.; Douki, T.; Favier, A.; Cadet, J.; Hydroxyl radical is not the main reactive species involved in the degredation of DNA bases by copper in the presence of hydrogen peroxide, *Chemical Research in Toxicology* **2003**, *16*, 191-197.

28. Ali, F. E.; Barnham, K. J.; Barrow, C. J.; Separovic, F.; Metal catalyzed oxidation of tyrosine residues by different oxidation systems of copper/hydrogen peroxide, *Journal of Inorganic Biochemistry* **2004**, *98*, 173-184.

29. Perez-Benito, J. F.; Reaction pathways in the decomposition of hydrogen peroxide catalyzed by copper (II), *Journal of Inorganic Biochemistry* **2004**, *98*, 430-438.

Chapter Five

Development of a Kinetic Model describing 8-oxo-7,8-dihydroGuanine Oscillations

5.1 Introduction

In Chapters 2, 3 and 4, the concentration of 8-oxoG was observed to oscillate repeatedly on incubation with both the iron and copper Fenton reagents. The aim of this chapter is to elucidate a mechanism to explain the oscillations observed.

In 1973, Briggs and Rauscher reported an oscillating 'iodine-clock' reaction, suitable for undergraduate investigation.[1] Using potassium iodate, hydrogen peroxide, perchloric acid, malonic acid, manganese(II) sulphate and starch, they observed striking cyclic colour changes from colourless to gold to blue. This reaction, subsequently named the Briggs-Rauscher (BR) reaction, is the oxidation of malonic acid by hydrogen peroxide and iodate, catalysed by the manganese(II) ion.[2]

In 1982, De Kepper and Epstein proposed a mechanism to explain the oscillations observed,[3] based on ten elementary steps, as follows, where MA and IMA represent malonic acid and iodomalonic acids, respectively.

$$2H^+ + I^- + IO_3^- = HOI + HIO_2 \qquad \text{(Reaction 5.1)}$$

$$H^+ + HIO_2 + I^- = 2HOI \qquad \text{(Reaction 5.2)}$$

$$HOI + I^- + H^+ = I_2 + H_2O \qquad \text{(Reaction 5.3)}$$

$$HIO_2 + IO_3^- + H^+ = 2IO_2 + H_2O \qquad \text{(Reaction 5.4)}$$

$$2HIO_2 = HOI + IO_3^- + H^+ \qquad \text{(Reaction 5.5)}$$

$$IO_2 + Mn(II) + H_2O = HIO_2 + Mn(III)OH^{2+} \qquad \text{(Reaction 5.6)}$$

$$H_2O_2 + Mn(III)OH^{2+} = HO_2 + Mn(II) + H_2O \qquad \text{(Reaction 5.7)}$$

$$2HO_2 = H_2O_2 + O_2 \qquad \text{(Reaction 5.8)}$$

$$I_2 + MA = IMA + I^- + H^+ \qquad \text{(Reaction 5.9)}$$

$$HOI + H_2O_2 = I^- + O_2 + H^+ + H_2O \qquad \text{(Reaction 5.10)}$$

Reactions 5.1 to 5.3 result in the consumption of iodide, I^-, and the generation of iodine, I_2. HIO_2 (highlighted in yellow) is formed in Reaction 5.1, and is then consumed in Reaction 5.2 and Reaction 5.4 and decomposed in Reaction 5.5. The autocatalytic production (*i.e.,* the formation of a product that is a reactant in previous steps) of HIO_2 is achieved in Reaction 5.6, while Reaction 5.7 regenerates Mn(II). Reactions 5.9 and 5.10 regenerate I^- through the consumption of I_2. This completes the cycle, allowing the mechanism to begin again. During the course of this mechanism, two steady states exist, high iodide concentration, [I^-], and low iodide concentration, [I^-]. Switching between these steady states depends on whether or not [I^-] is high enough so that HIO_2 reacts preferentially via the non radical Reaction 5.2, rather than the radical Reaction 5.4. (Reaction 5.4 leads to the autocatalysis of HIO_2 via the formation of IO_2.) Switching between Reaction 5.2 and 5.4 takes places at a critical [I^-], namely 3.7 x $10^7[IO_3^-]$. The BR reaction, as described by this mechanism, therefore has two steady states (bistability), and an autocatalytic step, where a key intermediate (HIO_2) is consumed and regenerated. The reaction is also far from equilibrium and it is described by nonlinear equations (*i.e.,* its reactions are higher than first order [4]). The mechanism proposed therefore fulfils the four parameters required for oscillations to occur.[5]

The most thoroughly studied chemical oscillator is the Belousov-Zhabotinskii (BZ) reaction,[6] of which the BR reaction is a hybrid. Both reactions involve the oxidation of malonic acid (MA), the BR reaction by hydrogen peroxide and iodate catalysed by the manganese(II) ion, and the BZ reaction by hydrogen peroxide and bromate, catalysed by the cerium(III) ion. The oscillations in bromide concentration, [Br^-], and cerium(III) concentration, [Ce(III)] are shown in Fig. 5.1.[6] Initially Br^- reacts with BrO_3^-, $HBrO_2$ and malonic acid and so there is a decrease in [Br^-] (region A-B in Fig. 5.1). Once [Br^-] has fallen sufficiently, BrO_3^- can also react with Ce(III) and $HBrO_2$ (region B-C). [Br^-] drops even more rapidly in this region, as it can also react with HOBr and $HBrO_2$, which are formed from the reaction of BrO_3^- with Ce(III). There then follows an induction period, where [HOBr] and

[Ce(IV)] remain high and [Br^-] remains low (region C-D). Bromomalonic acid (BrMA) is produced during this time according to Reaction 5.11.

$$HOBr + MA \rightarrow BrMA + H_2O \qquad \text{(Reaction 5.11)}$$

BrMA reacts with Ce(IV) and HOBr to regenerate both Br^- and Ce(III). This continues until a critical point, D, in Fig. 5.1, where BrO_3^- no longer reacts with Ce(III), but instead reacts with Br^-. There is a rapid increase in [Br^-] (region D-E), as BrO_3^- is not reacting with Ce(III) to produce HOBr and $HBrO_2$ which consume Br^-. Also in this region [Ce(IV)]/[Ce(III)] falls, as Ce(III) is not reacting with BrO_3^-. But [Br^-] is being consumed by BrO_3^- at a faster rate than it is being generated by BrMA (region E-F). At point F, [Br^-] has dropped sufficiently that BrO_3^- again reacts with Ce(III) (region F-G), beginning the cycle again.

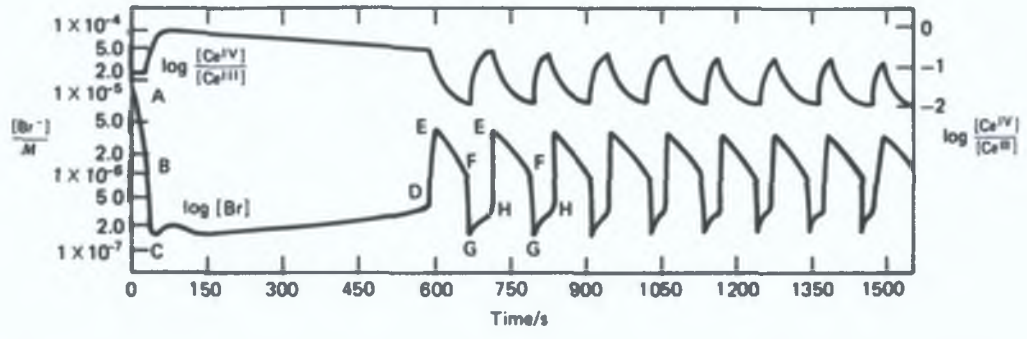

Fig. 5.1: Potentiometric traces of a bromide-sensitive electrode (lower curve) and of a tungsten electrode (upper curve) that responded to cerium(IV). The 0.8 M sulphuric acid solution contained malonic acid, potassium bromate, BrO_3^-, with a small amount of bromide, Br^-, and cerium(III) catalyst. [Reproduced from Moore and Pearson,[6] which is adapted from Field, Kőrős and Noyes.[7]]

In this reaction, the two bistable states are high [Br^-] and low [Br^-], and the autocatalytic step is the regeneration of $HBrO_2$. This is analogous to the BR reaction, where the bistable states are high [I^-] and low [I^-], and the autocatalytic step is the regeneration of HIO_2. A ten step elementary reaction mechanism, elucidated by

Field, Kőrős and Noyes,[7] used this to create a simplified model for the complex processes that occur during the reaction, called the Oregonator model, to highlight the two steady states and autocatalysis that occur during the mechanism. The Oregonator model is described in Reactions 5.12 – 5.16.

Process A:	$A + Y \rightarrow X + P$	(Reaction 5.12)
	$X + Y \rightarrow 2P$	(Reaction 5.13)
Process B:	$A + X \rightarrow 2X + Z$	(Reaction 5.14)
	$2X \rightarrow A + P$	(Reaction 5.15)
Process C:	$Z \rightarrow fY$	(Reaction 5.16)

where A = BrO_3^-, concentration assumed constant, P = HOBr, X = $HBrO_2$, Y = Br^-, Z = 2Ce(IV) and [H^+] and [Ce(III)] are assumed constant. Process A and Process B are two competing reactions. Switching between them occurs because they are coupled to Process C. Process A consists of a series of nonradical reactions, while process P is a series of radical reactions, and includes the autocatalytic regeneration of X. Consumption of Y in Process A leads to Process B. After a delay while Z and P accumulate, Process C poisons Process B by the production of Y from the products of Process B. Through Process C, Ce(IV) is reduced to Ce(III), completing the cycle and allowing for the next oscillation. Use of the Oregonator model therefore allows for the mechanistic processes of an extremely complex reaction to be exposed.

Models such as the Oregonator have advanced the understanding of oscillatory mechanisms and have served as a basis for the development of similar models to elucidate the underlying mechanisms for other oscillatory reactions. One such model which has been developed is the Urbanalator, created by considering only the steps which were observed experimentally during the course of the oscillations.[8] It was developed to explain the Peroxidase-Oxidase (PO) oscillator, the only single enzyme system to exhibit oscillations *in vitro* in homogenous stirred solutions.[9] The Urbanalator model is shown in Scheme 5.1, where species depicted

in red are present initially, and blue numbers represent the apparent sequence of events which combine to create an oscillatory cycle, as assigned in the Urbanalator model. As the PO oscillator only involves a single enzyme, it has become an important minimal case for the study of complex behaviour in biochemical systems.

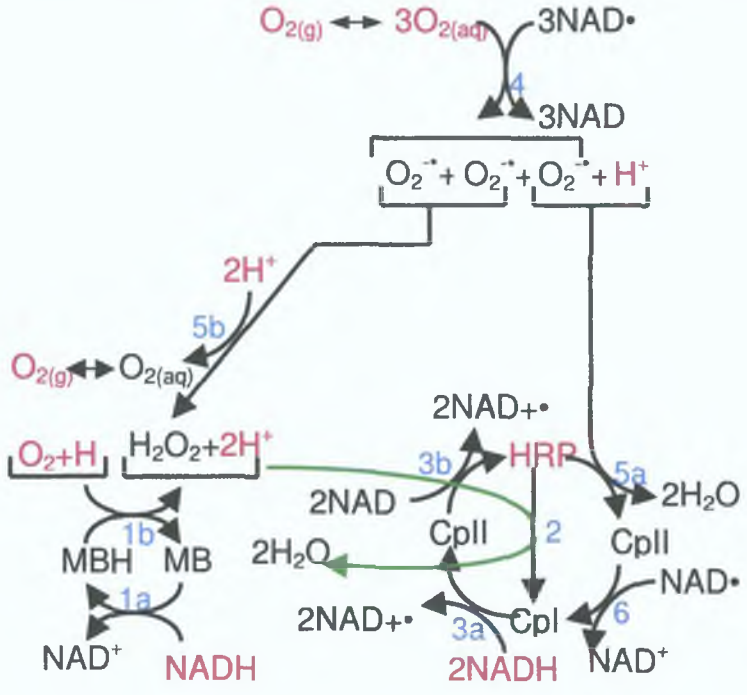

Scheme 5.1: The Urbanalator model of the Peroxidase-Oxidase reaction. (Reproduced from Olson et al.[10]) Species depicted in red are present initially, while blue numbers 1-6 represent the apparent sequence of events which combine to create an oscillatory cycle, as assigned in the Urbanalator model. (Arrow depicted in green for clarity.) MB = methyl blue; all other abbreviations explained in text.

Peroxidases are a class of enzymes that use hydrogen peroxide to oxidise a variety of organic compounds. Some peroxidases can catalyse oxidation using molecular oxygen in place of hydrogen peroxide. This type of reaction is called a Peroxidase-Oxidase reaction.[11] The PO reaction is the oxidation of organic electron donors by molecular oxygen, catalysed by Horseradish peroxidase (HRP). When the oxidation of nicotinamide adenine dinucleotide (NADH) by molecular oxygen in a flow system was carried out, the concentration of both reactants, as well as enzyme

intermediates, have been observed to oscillate.[9,12] The overall reaction mechanism is shown in Reaction 5.18.

$$2NADH + O_2 + 2H^+ \xrightarrow{HRP} 2NAD^+ + 2H_2O \qquad \text{(Reaction 5.18)}$$

The main redox states of HRP are controlled by the ferric heme group at the centre of the enzyme. In its native form the iron is found as iron(III). The removal of 2 e^- yields CompoundI (CpI), a free radical compound containing iron(IV). The reduction by a single e^- produces CompoundII (CpII), which still contains iron(IV). Binding of a molecule of oxygen as an axial ligand of iron(III) yields CompoundIII (CpIII). At the heart of the oscillations, therefore, are the higher oxidation states of iron, with 2 intermediate states being involved in the catalytic cycle.

As with the BR and BZ oscillation reactions, the PO reaction involves switching between two processes, two stable steady states (bistability), namely the reaction of NAD• with molecular oxygen and the reaction of NAD• with CpIII. As illustrated in Scheme 5.1, NAD• reacts with O_2 (Reaction 4). HRP in its native form is oxidised to CpIII by its reaction with $O_2^{-\bullet}$, (Reaction 5a) until the native HRP is depleted. Disproportion of $O_2^{-\bullet}$ to form hydrogen peroxide (Reaction 5b) then becomes rate limiting and NAD• begins to react with CpIII (Reaction 6). This is an autocatalytic reaction, replenishing NAD•. This also begins a cycle whereby HRP is also regenerated in its native form,[13] thus completing the oscillatory cycle.

The three examples of oscillatory reactions outlined above, namely the Briggs-Rauscher, the Belousov-Zhabotinsky and the Peroxidase-Oxidase reactions, represent three of the most thoroughly studied oscillation reactions in the literature. The oscillations in each case are based on the existence of two competing processes, both of which are capable of generating steady states (bistability). Switching between these processes depends on whether a key intermediate, which is consumed in one process and autocatalyically regenerated in the other, reacts with one of two reagents, whose concentrations vary as the cycle progresses. These systems are far

from equilibrium, and as equilibrium is approached the oscillations dampen until they disappear completely. The reactions in each process are described by equations which are nonlinear, *i.e.*, second order or higher. These are the underlying conditions which generate the oscillations observed in the above reactions.

For the oscillations observed in Chapters 2 and 3 to occur, the four conditions required for oscillations, namely nonlinear reaction equations, systems far from equilibrium, bistability and autocatalysis, must be fulfilled. It is assumed that the reactions are nonlinear, and that the system is far from equilibrium. The goal of this chapter is therefore to identify the two competing processes which lead to bistability, and to identify the key intermediate, which is autocatalytically regenerated by one of the processes.

The development of a model describing the oscillations observed began with a theoretical analysis of the reactions that occur during the iron-mediated Fenton reaction as reported in the literature. The classic iron-mediated Fenton reaction, which generates •OH, has been investigated in detail, and the rate constants for a number of key processes that occur during this reaction have been determined. Neither the copper-mediated Fenton reaction nor the iron-mediated Fenton reaction, which is assumed to generate a metal peroxide complex, have been investigated in this detail in the literature. For this reason, only the classic iron-mediated Fenton reaction is considered in the development of the kinetic model outlined in this chapter. The reaction rates reported in the literature were used to identify two competing processes for the generation and consumption of 8-oxoG, which was identified as the key intermediate involved. The parameters which lead to switching between both processes were also identified. Eight key reactions were presented as the basis for which the oscillations could occur. Finally, two possible biological roles for 8-oxoG oscillations are proposed. The first suggests oscillations are a method for protecting DNA against oxidative attack, while the second proposal suggests oscillations allow the ROS to exist in high enough concentrations for them to act as information messengers.

5.2 Development of a Kinetic Model

5.2.1 Reactions in the iron-mediated Fenton oxidation

Table 5.1: Reactions in the iron-mediated Fenton oxidation of organic substrate RH.

no.	Reaction	Rate constant ($M^{-1}s^{-1}$)	Ref.
5.19	$H_2O_2 + Fe(II) \xrightarrow{k_{19}} Fe(III) + HO^- + HO\cdot$	$k_{19} = 76$	14
5.20	$H_2O_2 + Fe(III) \xrightarrow{k_{20}} Fe(II) + H^+ + HOO\cdot$	$k_{20} = 0.002\text{-}0.01$	15
5.21	$Fe(II) + HO\cdot \xrightarrow{k_{21}} Fe(III) + HO^-$	$k_{21} = 3 \times 10^8$	14
5.22	$HO\cdot + RH \xrightarrow{k_{22}} H_2O + R\cdot$	$k_{22} = 10^7 - 10^9$	14
5.23	$R\cdot + Fe(III) \xrightarrow{k_{23}} Fe(II) + \text{Product.}$	rate N/A	14
5.24	$2R\cdot \xrightarrow{k_{24}} (Dimer)\,\text{Product.}$	rate N/A	14
5.25	$R\cdot + Fe(II) \xrightarrow{k_{25}} Fe(III) + \text{Product.}$	rate N/A	14

Table 5.1 summarises the main reactions of the iron-mediated Fenton reaction, reported in the literature. Reaction 5.19 is the classic Fenton reaction, where oxidation of Fe(II) results in the formation of Fe(III) and •OH. The corresponding reaction with Fe(III) (Reaction 5.20) occurs 4-5 orders of magnitude more slowly. •OH, once formed, reacts with Fe(II) (Reaction 5.21), or if one is present, with an organic substrate, denoted RH (Reaction 5.22). •OH can add across a double bond at $10^9 - 10^{10}$ $M^{-1}s^{-1}$,[14] so that this reaction occurs at a rate 3 – 30 times faster than the corresponding reaction with Fe(II). Once R• has been generated, it can react with a number of species, including Fe(III) (Reaction 5.23), Fe(II) (Reaction 5.25) and with another R• (Reaction 5.24). Reaction 5.23 is a primary mechanism by which Fe(II) is regenerated in order to further participate in the iron-mediated Fenton reaction.[16]

5.2.2 G(-H)• and •OH-mediated formation and oxidation of 8-oxoG

•OH reacts with G by adding across the C4-C5 double bond, or at the C8 position. Approximately 60% of •OH adds to C4, 15% to C5 and the remaining 25% to C8,[17] generating G4OH•, G5OH• and G8OH•, respectively, shown in Reaction 5.26.[17]

$$G + HO\cdot \xrightarrow{k_{26}} G4OH\cdot + G5OH\cdot + G8OH\cdot \qquad k_{26} = 9.2 \times 10^{9}\ M^{-1}s^{-1}$$

(Reaction 5.26)

For the purposes of clarity, as they behave in a similar manner,[18] G4OH• and G5OH• will only be referred to as G4OH• from this point. (This is in keeping with previous studies by Cadet *et al.*,[19] where the only radicals considered as Products of Reaction 5.26 were G4OH• and G8OH•.) G8OH• is redox ambivalent, and can be either oxidised to from 8-oxoG or reduced to form formamidopyrimidine, FapyG.[17] In an oxidising environment, G8OH• is predominantly oxidised to form 8-oxoG. This is the first process by which 8-oxoG is generated.

G4OH• is readily dehydrated to form the neutral G radical, G(-H)•.[18] This is the same radical formed from the deprotonation of the G cation radical, $G^{+\bullet}$. (This deprotonation occurs spontaneously at neutral pH, as $G^{+\bullet}$ is a weak acid, with a pKa of 3.9.[20]) G(-H)• is readily reduced, regenerating the parent base G, as illustrated in Reactions 5.27,[21] 5.28 and 5.29.

$$G(-H)\cdot + G8OH\cdot \xrightarrow{k_{27}} G + 8oxoG$$

(Reaction 5.27)

$$G(-H)\cdot + 8oxoG \xrightarrow{k_{28}} G + 8oxoG^{+}\cdot \qquad k_{28} = 4.6 \times 10^{8}\ M^{-1}s^{-1}$$

(Reaction 5.28)

$$G(-H)\cdot + Fe(II) \xrightarrow{k_{29}} G + Fe(III)$$

(Reaction 5.29)

k_{27} is assumed to be greater than k_{28} as G8OH• has a lower oxidation potential than 8-oxoG.[22] Reaction 5.27 is the second process by which 8-oxoG is generated. G(-H)• can also be further oxidised, however, and in the absence of reducing species, is readily further oxidised in the presence of oxygen to imidazolone (Iz).[19]

Although a primary product of G oxidation, 8-oxoG readily undergoes further oxidation in a similar manner to its parent base, G. G oxidation by •OH has been shown to occur at a rate of 9.2×10^9 $M^{-1}s^{-1}$,[17] and 8-oxoG oxidation by an analogous manner is expected to occur at an even faster rate, as 8-oxoG is easier to oxidise than its parent base G. When subjected to one-electron oxidation, the decomposition of 8-oxoG (15% per min) has been determined to be about 4 times faster than the decomposition of G (4% per min).[20] 8-oxoG oxidation by •OH is the first process by which 8-oxoG is consumed. As G oxidation by •OH is expected to occur at a slower rate than 8-oxoG oxidation by •OH, the net result of these two reactions is expected to result in the complete further oxidation of 8-oxoG.

As seen from Reaction 5.28, 8-oxoG is also consumed by the reduction of G(-H)•. This is the second process by which 8-oxoG is consumed. As G8OH• is slightly more easily oxidised than 8-oxoG, the net reaction of Reactions 5.27 and 5.28 should be the formation of 8-oxoG as the reaction progresses.

Based on the previous investigations of the Fenton reaction and of G oxidation outlined above, it is proposed that the oscillations in 8-oxoG may be generated by the simplified reaction mechanism outlined in Table 5.2.

Table 5.2: Simplified reaction mechanism generating 8-oxo-7,8-dihydroGuanine oscillations during iron-mediated Fenton oxidation of Guanine.

no.	Reaction	Rate constant ($M^{-1}s^{-1}$)	Ref.
5.19	$H_2O_2 + Fe(II) \xrightarrow{k_{19}} Fe(III) + HO^- + HO\cdot$	$k_{19} = 76$	14
5.26	$G + HO\cdot \xrightarrow{k_{26}} G4OH\cdot + G5OH\cdot + G8OH\cdot$	$k_{26} = 9.2 \times 10^9$	17
5.30	$G8OH\cdot - H^+ \xrightarrow{k_{30}} 8oxoG$	rate N/A	
5.31	$8oxoG + HO\cdot \xrightarrow{k_{31}} 5-OH-8oxoG$	$k_{31} > k_{26}$	20
5.32	$G4OH\cdot - H_2O \xrightarrow{k_{32}} G(-H)\cdot$	$k_{32} = 6 \times 10^3$	19
5.27	$G(-H)\cdot + G8OH\cdot \xrightarrow{k_{27}} G + 8oxoG$	$k_{27} > k_{28}$	23
5.28	$G(-H)\cdot + 8oxoG \xrightarrow{k_{28}} G + 8oxoG^+\cdot$	$k_{28} = 4.6 \times 10^8$	21
5.23	$8oxoG^+\cdot + Fe(III) \xrightarrow{k_{23}} Fe(II) + 8oxoG_{ox}$.	rate N/A	16

The two main processes involved in the proposed mechanism outlined in Table 5.2 are the •OH formation and further oxidation of 8-oxoG and the G(-H)• formation and oxidation of 8-oxoG. •OH is a stronger oxidant than G(-H)•. This is reflected in the reaction rates, with the reaction rate of OH• with G (10^9 $M^{-1}s^{-1}$) one order of magnitude higher than the reaction rate of G(-H)• with 8-oxoG (10^8 $M^{-1}s^{-1}$). The rate of formation of •OH, however, at 76 $M^{-1}s^{-1}$, is 9 orders of magnitude slower than the rate of its consumption. [•OH] is therefore expected to decrease rapidly via Reactions 5.26 and 5.31. It is proposed that in the absence of •OH, 8-oxoG formation and oxidation by G(-H)• becomes the dominant process. This process results in the net formation of 8-oxoG, but also produces an oxidised 8-oxoG product, 8-oxoG$^{+\bullet}$. This radical reacts with Fe(III) to regenerate Fe(II). Fe(II) then reacts via the Fenton reaction to regenerate •OH, and so •OH again becomes the dominant process.

Elucidation of these two competitive process forms the basis of the proposed mechanism for the oscillations in 8-oxoG concentration as the reaction continues. The two bistable states proposed are the 8-oxoG formation and further oxidation by

•OH, and the 8-oxoG formation and oxidation by G(-H)•, which are dominant for high [•OH] and low [•OH] respectively. When [•OH] is high, the predominant reaction is 8oxG oxidation by •OH. When [•OH] diminishes, the system switches to G(-H)• reactions, which regenerates the key intermediate 8-oxoG, but also generates Fe(II) allowing the Fenton reaction to be renewed, regenerating •OH and switching back to first process. The autocatalytic step proposed is the regeneration of 8-oxoG. These reactions result in the eight key steps proposed in the simplified mechanism for the oscillations in 8-oxoG concentration, which is outlined in Table 5.2.

Table 5.2 is not an exhaustive list of all the reactions that can occur between the numerous intermediates and reactive species that are generated during the course of the reaction. The reactions contained in this table, however, are the key reactions that may generate the oscillations in 8-oxoG concentration observed in Chapters 2 and 3.

5.3 Biological Implications for 8-oxoG Oscillations

A number of oscillating reactions have been reported in cellular biology, from ovarian systems with period lengths of 28 days to neuronal systems with period lengths of 0.01 – 10 s.[24] The number of oscillating biochemical processes reported in cells has continued to increase as the measurement of metabolites becomes increasingly possible.[25] While the purpose of metabolic oscillations is not completely understood, they may serve to increase the thermodynamic efficiency of the metabolism or to protect proteins from otherwise harmful substances that are produced during cell metabolism and cell signalling.[25]

The oscillations in 8-oxoG concentration might also serve a protective function, protecting DNA from sustained oxidative damage. According to Reactions 5.27 and 5.28, 8-oxoG is further oxidised via the regeneration of the G base. Therefore, further 8-oxoG oxidation serves to protect DNA from further oxidation, and traces of 8-oxoG effectively prevent further oxidative damage from occurring, as suggested in Scheme 5.2. As shown, multiple oxidative attacks result only in the oxidation of one G base.

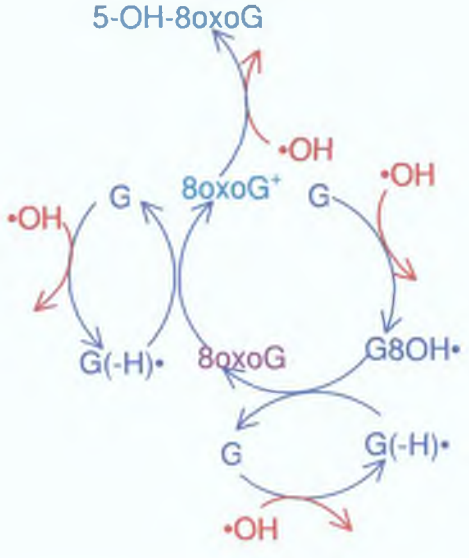

Scheme 5.2: Proposed recycling of G and G(-H)• during 8-oxoG formation and further oxidation.

It has also been proposed that oscillation mechanisms can be used for the transfer of information during cellular function. ROS such as •OH have recently been implicated as cellular messengers, and it has been suggested that they are necessary for the transfer of information during normal cellular metabolism.[25] Oscillation reactions allow the ROS to exist at lower concentrations than are required for the information to be transferred. The oscillatory reaction allows the concentration of the ROS to be increased to the necessary levels for the time period required for information exchange to occur, but this high level of ROS is only present for a transient time period. Moreover, the oscillation reactions consume the ROS, so that they cannot react with other species and so the expected oxidative DNA damage does not occur.

The presence of oscillatory reactions may therefore serve two functions, both protecting cellular material such as DNA from oxidative damage by the ROS, and also allowing the ROS to participate in information exchange necessary for normal cellular function.

5.4 References

1. Briggs, T. S.; Rauscher, W. C.; An oscillating iodine clock, *Journal of Chemical Education* **1973**, *50*, 496.

2. Fujieda, S.; Ogata, H.; Calorimetry and potentiometry of chemical oscillations in Briggs-Rauscher reactions with simultaneous measurements of the produced oxygen volume, *Talanta* **1996**, *43*, 1989-1995.

3. De Kepper, P.; Epstein, I. R.; A mechanistic study of oscillations and bistability in the Briggs-Rauscher reaction, *Journal of the American Chemical Society* **1982**, *104*, 49-55.

4. Scott, S. K. *Oscillations, waves, and chaos in chemical kinetics*; Oxford University Press: New York, 1994; Vol. 18.

5. Ferino, I.; Rombi, E.; Oscillating reactions, *Catalysis Today* **1999**, *52*, 291-305.

6. Moore, J. W.; Pearson, R. G. *Kinetics and Mechanism*, 3rd ed.; Wiley: New York, 1981.

7. Field, R. J.; Koros, E.; Noyes, R. M.; Oscillations in chemical systems. II. Thorough analysis of temporal oscillation in the bormate-cerium-malonic acid system, *Journal of the American Chemical Society* **1972**, *94*, 8649-8664.

8. Larter, R.; Hemkin, S.; Further refinements of the peroxidase-oxidase oscillator mechanism: mixed-mode oscillations and chaos, *Journal of Physical Chemistry* **1996**, *100*, 18924-18930.

9. Scheeline, A.; Olson, D. L.; Williksen, E. P.; Horras, G. A.; The peroxidase-oxidase oscillator and its constituent chemistries, *Chemistry Reviews* **1997**, *97*, 739-756.

10. Olson, D. L.; Williksen, E. P.; Scheeline, A.; An experimentally based model of the peroxidase-NADH biochemical oscillator: an enzyme-mediated chemical switch, *Journal of the American Chemical Society* **1995**, *117*, 2-15.

11. Olson, D. L.; Scheeline, A.; Theoretical investigation of the peroxidase-oxidase chemical oscillator for quantitative enzyme analysis, *Analytica Chimica Acta* **1990**, *255*, 381-390.

12. Kirkor, E. S.; Scheeline, A.; Hauser, M. J. B.; Principal component analysis of dynamical features in the peroxidase-oxidase reaction, *Analytical Chemistry* **2000**, *72*, 1381-1388.

13. Bensen, D. S.; Scheeline, A.; Reduction of dimension of a chemically realistic model for the proixidase-oxidase oscillator, *Journal of Physical Chemistry B* **1996**, *100*, 18911-18915.

14. Walling, C.; Fenton's reagent revisited, *Accounts of Chemical Research* **1975**, *8*, 135-131.

15. Malik, P. K.; Oxidation of Safranine T in Aqueous Solution Using Fenton's Reagent: Involvement of an Fe(III) Chelate in the Catalytic Hydrogen Peroxide Oxidation of Safranine T, *Journal of Physical Chemistry A* **2004**, *108*, 2675-2681.

16. Koppenol, W. H.; The Haber-Weiss cycle - 70 years later, *Redox Report* **2001**, *6*, 229-234.

17. Steenken, S.; Purine bases, nucleosides, and nucleotides: aqueous solution chemistry and transformation reactions of their radical cations and e- and OH adducts, *Chemistry Reviews* **1989**, *89*, 503-520.

18. Breen, A. P.; Murphy, J. A.; Reactions of oxyl radicals with DNA, *Free Radical Biology and Medicine* **1995**, *18*, 1033-1077.

19. Cadet, J.; Douki, T.; Gasparutto, D.; Ravanat, J.-L.; Review: Oxidative damage to DNA: formation, measurement and biochemical features, *Mutation Research/Fundamentals and Molecular Mechanisms of Mutagenesis* **2003**, *531*, 5-23.

20. Ravanat, J.-L.; Saint-Pierre, C.; Cadet, J.; One-electron oxidation of the guanine moiety of 2'-deoxyguanosine: influence of 8-oxo-7,8-dihydro-2'-deoxyguanosine, *Journal of the American Chemical Society* **2003**, *125*, 2030-2031.

21. Steenken, S.; Jovanovic, S. V.; Bietti, M.; Bernhard, K.; The trap depth (in DNA) of 8-oxo-7,8-dihydro-2'-deoxyguanosine as derived from electron-transfer equilibria in aqueous solution, *Journal of the American Chemical Society* **2000**, *122*, 2373-2374.

22. Shukla, L. I.; Adhikary, A.; Pazdro, R.; Becker, D.; Sevilla, M. D.; Formation of 8-oxo-7,8-dihydroguanine-radicals in γ-irradiated DNA by multiple one-electron oxidations, *Nucleic Acids Research* **2004**, *32*, 6565-6574.

23. Douki, T.; Spinelli, S.; Ravanat, J.-L.; Cadet, J.; Hydroxyl radical-indcued degrataion of 2'-deoxyguanosine under reducing conditions, *Journal of the Chemistry Society, Perkin Transactions* **2002**, 2, 1875-1880.

24. Hess, B.; Periodic patterns in biology, *Naturwissenschaften* **2000**, *87*, 199-211.

25. Hauser, M. J. B.; Kummer, U.; Larsen, A. Z.; Olsen, L. F.; Oscillatory dynamics protect enzymes and possibly cells against toxic substances, *Journal of the Chemistry Society, Faraday Discussions* **2001**, *120*, 215-227.

Chapter Six

Conclusions and Future Developments

6.1 Future developments in the investigation of Fenton reaction oxidation (Chapter 2, 3 & 4)

In Chapters 2 and 3, the Fenton reaction was shown to generate significant oxidative DNA damage, generating 8-oxo-7,8-dihydroGuanine (8-oxoG) as a primary oxidation product. In Chapter 4, oxidised Guanidinohydantoin (oxGh) was identified as the main product of 8-oxoG oxidation. However, the exact nature of the reactive oxygen species (ROS) which induced this damage has not yet been fully elucidated. As discussed in the above chapters, iron(II) was believed to generate the hydroxyl radical (•OH),[1-3] while copper(II) was believed to generate singlet oxygen ($^1O_2$).[4-6] These ROS have previously been shown to generate different DNA oxidation products. As shown in Chapter 4, however, both iron(II) and copper(II) generated oxGh, and in similar magnitudes, when they were used to catalyse the Fenton reaction mediated oxidation of 8-oxoG. This implies that a similar ROS was generated for both oxidation mechanisms.

Further study of the metal catalysed Fenton reaction should therefore include investigation of the ROS generated by both iron(II)- and copper(II)-mediated 8-oxoG oxidation. Identification of the ROS involved is important for a number of reasons. Individual ROS have been studied extensively in detail, and the ensuing damage caused has also been investigated in detail. Identification of the exact nature of the ROS involved should therefore increase the understanding of the consequences of the Fenton reactant-mediated oxidation to DNA. The results in Chapter 4 (Section 4.3) suggest that a similar ROS, if not the same ROS, is involved in both the iron- and copper-mediated Fenton reaction. Identification of the exact nature of the ROS will increase the understanding of the ROS involved in these reactions. This should in turn elucidate the effect of the nature of the transition metal on the final oxidative DNA damage that is generated. Moreover, identification of the ROS involved in the metal-mediated Fenton reaction should aid in the understanding of the underlying mechanism that causes oxidative DNA damage.

Two main methods are envisaged for the identification of these ROS. The first involves the direct detection of the ROS generated, whereas for the second method, DNA damage known to be generated solely by that particular ROS is detected. $^1O_2$ can be identified by its phosphorescence emission at $\lambda = 1270$ *nm*, following laser excitation. The emitted light is collected by a germanium photodiode array. Certain scavengers can also be employed to aid the identification of the ROS, *e.g.,* sodium azide and 1,4-diazabicyclo [2.2.2] octane (DABCO)[7] scavenge $^1O_2$; dimethyl sulfoxide (DMSO), ethanol and formate[8] scavenge •OH; while methional not only scavenges •OH, but also weaker ROS with a similar reactivity. Inhibition of DNA damage as a result of these scavengers can be used to identify the nature of the ROS involved. However, possible inhibition via chelation with the transition metal may interfere with this analysis.[9] Moreover, if the transition metal is complexed to the DNA, it is also possible that the highly reactive ROS will react with the DNA before the reaction can be inhibited by the scavenger, so that lack of inhibition of reaction would not necessarily imply that the ROS was not present. Electron Paramagnetic Resonance (also known as Electron Spin Resonance, EPR) could also be used to differentiate between the ROS generated during the Fenton reaction, as it is highly sensitive for the detection of free radicals. The lifetimes of the ROS themselves are too short to be observed directly, but they can react with spin traps, producing more stable adduct radicals that can be observed. Unfortunately many spin traps, *e.g.* 5,5-dimethyl-1-pyrroline N-oxide (DMPO) cannot differentiate between •OH and $^1O_2$, as the same adduct is formed for both ROS. Less common spin traps can be more selective and therefore more suitable, however. 2,2,6,6-tetramethyl-4-piperidone (TMPD) reacts with $^1O_2$ to form 2,2,6,6,-tetramethyl-4-piperidone-N-oxyl (TAN). Although other ROS also react with TMPD, they do not result in the formation of TAN, and so this method is specific for $^1O_2$ detection.

The second method for the identification of the ROS involved in oxidative DNA damage involves the analysis of the oxidation products generated. γ-irradiation of water is known to generate •OH, and the oxidative damage to DNA generated has been investigated in detail, with all four DNA bases subject to further oxidation.[10] In

contrast, $^1O_2$ reacts exclusively with guanine base (G), and this is the only base that it subject to oxidation.[11] Measuring the formation of thymine oxidation products could therefore provide insight into whether •OH or $^1O_2$ was the primary ROS involved. The guanine oxidation product FapyG is another oxidative product formed by •OH but not by $^1O_2$.[12] However, monitoring of its production is not suitable for ROS determination, as it could still be formed by the Fenton reaction, even if $^1O_2$ is the primary ROS, due to the reducing metal species present in solution.[13] The lifetime of $^1O_2$ is extended up to 30-fold in D_2O (58 μs in D_2O as opposed to 2 μs in H_2O),[14] and so carrying out the experiments in D_2O solutions will therefore increase the lifetime of $^1O_2$ in solution. If $^1O_2$ is the ROS involved therefore, there will be a significant enhancement in the level of oxidative DNA damage that is generated, which would also imply that $^1O_2$ is the ROS generated.

The electrochemical (EC) detection of 8-oxoG in Chapters 2, 3 and 4 was hindered slightly by the detection of concentrations which approached the limit of detection (LOD) of the detector. This was partly responsible for the significant deviations that occurred between duplicate samples (as evidenced by error bars of up to 30%). Future development of the analysis employed throughout this thesis should therefore include increasing the sensitivity of the EC detector (lowering the LOD). The use of polymer modified electrodes should allow for a significant increase in sensitivity. This has been investigated in depth for the voltammetric analysis of oxidative DNA damage, as discussed in Chapter 1. Modification of the working electrode with an osmium polymer has been shown to selectively catalyse the oxidation of 8-oxoG, and so increase the current generated by its detection.[15] The incorporation of this polymer onto the working electrode of the EC detector would permit an increase in the signal generated by 8-oxoG, enhancing the sensitivity of the detector and allowing for a more accurate monitoring of 8-oxoG concentration.

These error bars could also have been generated by the inefficient quenching of the reaction by ethanol, which is a •OH scavenger. As discussed in Chapter 5, the oscillations may be due to two competing reactions, one of which involves the

reaction of two Guanine intermediates. Ethanol would not be expected to quench this reaction. The time lag between repeat HPLC analysis might have been sufficient to lead to artifactual 8-oxoG oxidation between successive analyses, which could have lead to the error bars observed. Duplicate samples were not taken instantaneously, due to constraints on the analytical method, instead they were taken in quick succession, resulting in a difference of 2 – 4 s between duplicate samples. This could also have been a source of the deviations observed. One possible method to reduce errors generated in this way would be to sample singly at 15 s intervals, which would be possible using the current analytical methodology. This would also be very beneficial in analysing the periods of the oscillations in 8-oxoG concentration, as the number of sample points per period would be increased considerably.

Further development should also include the enzymatic hydrolysis of DNA. Acid hydrolysis has solely been used in this thesis to release the DNA bases prior to analysis. While it has been established that this does not lead to degradation of 8-oxoG,[16] its effects on the products of 8-oxoG oxidation have yet to be investigated. It is possible therefore, that the use of acid hydrolysis may degrade 8-oxoG oxidation products, or may artifactually generate oxidation products. In order to investigate whether the use of this technique leads to any of these effects, enzymatic hydrolysis should also be used during the analysis, even though this leads to the release of DNA nucleosides and not DNA bases, as in the case of acid hydrolysis.

Chapter 4 investigated the products of 8-oxoG oxidation mediated by the Fenton reaction, and found that oxidised Guanidinohydantoin (oxGh) was the main product of 8-oxoG base oxidation. It cannot be assumed, however, that oxGh is also the main product of oxidation of the 8-oxoG nucleoside, or of 8-oxoG within the DNA double helix. It has previously been shown that Spiroiminodihydantoin was the primary product of Guanosine (guanine nucleoside), but for analogous conditions, Guanidinohydantoin was the primary product for Guanosine oxidation within DNA.[17] Investigations into the oxidation of 8-oxoG should be broadened to

include the analysis of oxidation products generated from 8-oxoG in G and within DNA, just as was undertaken for Chapters 2 and 3.

It was also illustrated in Chapter 4 that Oxaluric acid (Oxa) is a potential final product of 8-oxoG oxidation, *i.e.*, that oxGh is itself also an intermediate complex and is slowly oxidised to Oxa. In order to examine the nature of the final product of oxidative attack on 8-oxoG, and therefore of oxidative attack on G and on DNA itself, the substrates 8-oxoG, G and DNA should be incubated with the Fenton reagents for extended periods of time (up to 96 hr), to investigate the nature of the final products of oxidative attack.

A more biologically relevant model, where DNA will continue to be incubated with hydrogen peroxide and various transition metals, should be considered for the future development of work carried out to date. This should consist of a number of steps. Cellular DNA should be subjected to Fenton reaction mediated oxidation, with the DNA isolated and analysed after oxidation had occurred. Prosthetic groups from proteins, such as heme centres from cytochrome C, should be used to provide the transition metal ion for the Fenton reaction. The use of representative prosthetic groups should subsequently be replaced in the model by the use of metal prosthetic groups from the misfolded proteins implicated in neurodegeneration, which should in turn be replaced by the misfolded proteins themselves. This will result in the characterisation of oxidative stress levels and type of ROS generated by the misfolded proteins.

6.2 Chapter 5

In Chapter 5, 8 keys reactions were proposed, which may lead to the oscillations in 8-oxoG concentration observed in the preceding chapters. The validity of these reactions, and the extent to which they explain the 8-oxoG oscillations, has not been investigated, however. The immediate future work in this study should involve simulating the concentrations of the reactants, intermediates and products generated by the reactions proposed, as the reaction continues. A specialised computer simulation program, KinFitSim 2.0 (Iryna Svir, Kharkov National University of Radioelectronics, Kharkov, Ukraine) has been purchased for this purpose. To date, the only intermediate that has been quantitatively monitored over the course of the reaction is 8-oxoG, and the only reactant which has been monitored is the parent base, G. The reaction should therefore also be repeated experimentally, and the concentration of the start compounds, H_2O_2 and Fe(II), of the intermediates Fe(III), G(-H)· and 5-OH-8oxoG, and of end products 8-oxoG_{ox} and O_2 gas evolved. The concentration of these species observed experimentally should be compared to the concentrations observed from the simulation.

In Chapter 5, only the key reactions that may contribute to the 8-oxoG concentration oscillations were proposed. Oscillation reactions studies in the literature, however, have shown a significantly higher number of elementary reactions than key reactions, due to the complexity of the processes involved. A number of side reactions may also contribute to the patterns of concentration observed, including the oxidation of Fe(II) by G(-H)·, consuming the metal before it can react with H_2O_2. Inclusion of these secondary reactions in the kinetic model should increase the accuracy of this model.

Finally, the reaction time should be extended beyond the three hours analysed to date. Oscillatory reactions normally do not continue indefinitely, but slowly come to a steady state. The composition of the steady state, and the time taken to achieve this state, should be investigated.

6.3 Summary and General Outlook

The aim of the research undertaken for this thesis has been the analysis of 8-oxoG formation and further oxidation, to provide further insight into the mechanisms by which oxidative DNA damage occurs. The results obtained complement a growing body of research which highlights the constraints of 8-oxoG as a potential biomarker for oxidative DNA damage. The oscillatory nature of 8-oxoG and G concentration with continuing oxidative stress underscores the complex mechanism by which oxidative DNA damage occurs. One of the primary reasons for these oscillations is the regeneration of the parent complex when oxidation occurs at the C4 or C5 position of the compound. This regeneration means that any oxidation at C4 or C5, which represents approx. 75% of G oxidation, has no long term effect. The identification of oxGh as a primary oxidation product of 8-oxoG oxidation is also significant. Although it has previously been identified as a product of G oxidation,[18,19] its detection in this research represents the first time that it has been identified as an oxidation product from Fenton mediated oxidation. This research has also drawn attention to the similarities between the transition metals iron and copper, as catalysts for the Fenton reactant mediated oxidation of DNA, suggesting that they could both generate the same reactive oxygen species. The exact nature of these species has not been elucidated to date.

On completion of this work proposed in this Chapter, significant advancements could be foreseen for the understanding of the role of 8-oxoG and 8-oxoG oxidation, and of the Fenton reaction, in oxidative DNA damage. Further understanding of the role of 8-oxoG, and of the products of 8-oxoG oxidation, may be used to investigate whether oxidative DNA damage is instrumental in initiating disease, or is merely a biproduct of the onset of disease. If it is shown to initiate disease, its identification may serve as the basis for the early detection of such diseases, which would have a very significant impact on the development of medicinal devices for disease diagnosis. If oxidative DNA damage is determined not to initiate disease, but is merely a biproduct, the stage in the disease progression in

which the level of oxidative DNA damage increases significantly may also have an important medicinal impact. In this case, oxidative DNA damage detection may serve as an early detection method for the onset of disease, and may therefore also be central to the development of techniques for early disease diagnosis.

A greater understanding of the role of transition metal mediated Fenton oxidation of DNA will also have considerable impact. A number of transition metals, including iron, copper, nickel and zinc, are essential *in vivo*. One of the primary potential methods by which they are suspected of generating oxidative DNA damage is the Fenton reaction. Elucidation of the mechanism by which this oxidative DNA damage occurs, especially if it emerges that the transition metals all behave in a similar manner, has the potential to lead to methods to detect, repair and inhibit such damage.

Oxidative DNA damage has been implicated in heart disease, cancer and ageing. The elucidation of the mechanisms by which this damage occurs will play a significant part in the clarification of the role played by this damage in disease initiation and propagation. This in turn will have a considerable impact on the manner in which these diseases are diagnosed and treated, and may ultimately aid in the cure and prevention of these diseases.

6.4 References

1. Halliwell, B.; Gutteridge, J. M. C. *Free Radicals in Biology and Medicine*, 2nd ed.; Clarendon Press, 1989.

2. Walling, C.; Fenton's reagent revisited, *Accounts of Chemical Research* **1975**, *8*, 135-131.

3. Halliwell, B.; Gutteridge, J. M. C.; Oxygen toxicity, oxygen radicals, transition metals and disease, *Biochemical Journal* **1984**, *219*, 1-14.

4. Yamamoto, K.; Kawanishi, S.; Hydroxyl free radical is not the main active species in site-specific DNA damage induced by copper (II) ion and hydrogen peroxide, *Journal of Biological Chemistry* **1989**, *264*, 15435-15440.

5. Frelon, S.; Douki, T.; Favier, A.; Cadet, J.; Hydroxyl radical is not the main reactive species involved in the degredation of DNA bases by copper in the presence of hydrogen peroxide, *Chemical Research in Toxicology* **2003**, *16*, 191-197.

6. Drouin, R.; Rodriguez, H.; Gao, S.-W.; Gebreyes, Z.; O'Connor, T. R.; Holmquist, G. P.; Akman, S. A.; Cupric ion/ascorbate/hydrogen peroxide-induced DNA damage: DNA-bound copper ion primarily induces base modifications, *Free Radical Biology and Medicine* **1996**, *21*, 261-273.

7. An, Y.-A.; Chen, C.-H. B.; Anderson, J. L.; Sigman, D. S.; Foote, C. S.; Rubin, Y.; Sequence-specific modification of guanosine in DNA by a C60-linked deoxyolignucleotides: evidence for a non-singlet oxygen mechanism, *Tetrahedron* **1996**, *52*, 5179-5189.

8. Zhu, B.-Z.; Zhao, H.-T.; Kalyanarman, B.; Frei, B.; Metal-independant production of hydroxyl radicals by halogenated quinones and hydrogen peroxide: an ESR spin trapping study, *Free Radical Biology and Medicine* **2002**, *32*, 465-473.

9. Ando, T.; Yoshikawa, T.; Tanigawa, T.; Kohno, M.; Norimasa, Y.; Kondo, M.; Quantification of singlet oxygen from hematoporphyrin derivative by electron spin resonance, *Life Sciences* **1997**, *61*, 1953-1959.

10. Frelon, S.; Douki, T.; Ravanat, J.-L.; Pouget, J.-P.; Tornabene, C.; Cadet, J.; High-performance liquid chromatography-tandem mass spectrometry measurement of radiation-induced base damage to isolated and cellular DNA, *Chemical Research in Toxicology* **2000**, *13*, 1002-1010.

11. Paillous, N.; Vicendo, P.; Mechanisms of photosensitized DNA cleavage, *Journal of Photochemistry and Photobiology B: Biology* **1993**, *20*, 203-209.

12. Cadet, J.; Douki, T.; Modification of DNA bases by photosensitized one-electron oxidation, *International Journal of Radiation Biology* **1999**, *75*, 571-581.

13. Frelon, S.; Douki, T.; Favier, A.; Cadet, J.; Comparative study of base damage induced by gamma radiation and Fenton reaction in isolated DNA, *Journal of the Chemistry Society, Perkin Transactions* **2002**, *1*, 2866-2870.

14. Kwong, D. W. J.; Chan, O. Y.; Wong, R. N. S.; Musser, S. M.; Vaca, L.; Chan, S. I.; DNA-photocleavage activities of vanadium(V)-peroxo complexes, *Inorganic Chemistry* **1997**, *36*, 1276-1277.

15. Dennany, L.; Forster, R. J.; White, B.; Smyth, M. R.; Rusling, J. F.; Direct Electrochemiluminescence detection of oxidized DNA in ultrathin films containing $[Os(bpy)_2(PVP)_{10}]^{2+}$, *Journal of the American Chemical Society* **2004**, *126*, 8835-8841.

16. Ravanat, J.-L.; Turesky, R. J.; Gremaud, E.; Trudel, L. J.; Stadler, R. H.; Determination of 8-oxo-7,8-dihydroGuanine in DNA by gas chromatography-mass spectrometry and HPLC-electrochemical detection: overestimation of the background level of the oxidized base by the gas-chromatography-mass spectrometry assay, *Chemical Research in Toxicology* **1995**, *8*, 1039-1045.

17. Burrows, C. J.; Muller, J. G.; Kornyushyna, O.; Luo, W.; Duarte, V.; Leipold, M. D.; David, S. S.; Structure and potential mutagenicity of new hydantoin products from guansoine and 8-oxo-7,8-dihydroguanine oxidation by transition metals, *Environmental Health Perspectives* **2002**, *110*, 713-717.

18. Chworos, A.; Seguy, C.; Pratviel, G.; Meunier, B.; Characterization of the Dehydro-Guanidinohydantoin Oxidation Product of Guanine in a Dinucleotide, *Chemical Research in Toxicology* **2002**, *15*, 1643-1651.

19. Duarte, V.; Gasparutto, D.; Yamaguchi, L. F.; Ravanat, J.-L.; Martinez, G. R.; Medeiros, M. H. G.; Mascio, P. D.; Cadet, J.; Oxaluric acid as the major product of singlet oxygen-mediated oxidation of 8-oxo-7,8-dihydroguanine in DNA, *Journal of the American Chemical Society* **2000**, *122*, 12622-12628.

Chapter Seven

Appendices

7.1 Appendix 1a – MS Parameters for positive ESI

Mode	
Mass Range mode	Std/Normal
Ion Polarity	Positive
Ion Source Type	ESI
Current Alternating Ion Pol	N/A
Alternating Ion Polarity	N/A
Detector & Block Vages	
Multiplier Vage	1750 V
Dynode Vage	7.0 kV
Scan Delay	500 µs
Skimmer 1 Block	0.0 V
Skimmer 2 Block	300.0 V
Tune Source	
Trap Drive	30.8
Skim 1	15.0 V
Skim 2	6.4 V
Octopole RF Amplitude	105.9 Vpp
Octopole Delta	2.40 V
Lens 1	-3.8 V
Lens 2	-47.2 V
Octopole	2.57 V
Capillary Exit	82.9 V
Cap Exit Offset	67.9 V
HV End Plate Offset	-638 V
Current End Plate	1108.97 nA
HV Capillary	4000 V
Current Capillary	98.882 nA
Dry Temp (measured)	354 °C
Dry Gas (measured)	8.01 l/min
Nebulizer (measured)	50.56 psi
Trap	
Scan Begin	50.00 m/z
Scan End	400.00 m/z
Averages	20 Spectra
Charge Control	On
ICC Target	50000
ICC Actual	59913
Accumulation time	100000 µs
Max. Accu time	100000 µs

MS/MS Manual Mode	
Fast Calc	On
ISTD	Off
MS/MS Automatic	
Auto MS/MS	Off
Rolling Averaging	
Rolling	Off
Compressed Spectra	
Compressed Spectra	Off

7.2 Appendix 1b –MS Parameters for negative ESI

Mode	
Mass Range mode	Std/Normal
Ion Polarity	Negative
Ion Source Type	ESI
Current Alternating Ion Pol	N/A
Alternating Ion Polarity	N/A
Detector & Block Vages	
Multiplier Vage	1750 V
Dynode Vage	7.0 kV
Scan Delay	500 µs
Skimmer 1 Block	0.0 V
Skimmer 2 Block	-300.0 V
Tune Source	
Trap Drive	33.5
Skim 1	-15.0 V
Skim 2	-6.0 V
Octopole RF Amplitude	105.9 Vpp
Octopole Delta	-2.40 V
Lens 1	5.0 V
Lens 2	60.0 V
Octopole	-2.23 V
Capillary Exit	-82.9 V
Cap Exit Offset	-67.9 V
HV End Plate Offset	-638 V
Current End Plate	1452.47 nA
HV Capillary	4000 V
Current Capillary	89.366 nA
Dry Temp (measured)	355 °C
Dry Gas (measured)	8.01 l/min
Nebulizer (measured)	50.56 psi
Trap	
Scan Begin	50.00 m/z
Scan End	400.00 m/z
Averages	20 Spectra
Charge Control	On
ICC Target	50000
ICC Actual	6885
Accumulation time	100000 µs
Max. Accu time	100000 µs

MS/MS Manual Mode	
Fast Calc	On
ISTD	Off
MS/MS Automatic	
Auto MS/MS	Off
Rolling Averaging	
Rolling	Off
Compressed Spectra	
Compressed Spectra	Off

7.3 Publications

- *Oscillating formation of 8-oxoguanine during DNA oxidation;* Blanaid White, Malcolm R. Smyth, James D. Stuart, James F. Rusling (2003). *J. Am. Chem. Soc.;* (Communication) **125**(22); 6604-6605

- *Direct electrochemiluminescence detection of oxidized DNA in ultrathin films containing* $[Os(bpy)_2(PVP)_{10}]^{2+}$; Lynn Dennany, Robert J. Forster, Blanaid White, Malcolm R. Smyth, James F. Rusling (2004). *J. Am. Chem. Soc.;* (Article); **126**(28); 8835-8841.

- *Oxidized guanidinodihydantoin* (Gh^{ox}) *and spiroiminodihydantoin (Sp) are major products of iron- and copper-mediated 8-oxoguanine and 8-oxodeoxyguanosine oxidation*; Blánaid White, Maricar C. Tarun, Nicholas Gathergood, James F. Rusling, Malcolm R. Smyth (2005) *manuscript submitted,*

7.4 Oral Presentations

- **School of Chemical Sciences Research Day**
  Dublin City University, Glasnevin, Dublin 9, Ireland, 26 March 2003
  "8-oxoguanine formation and oxidation during hydroxyl radical attack"
  Blánaid White, James F. Rusling, Malcolm R. Smyth

- **Analytical Research Forum incorporating Research and Development Topics**
  Sunderland University, United Kingdom, 21-23 July 2003
  "DNA damage – 8-oxoguanine formation and oxidation during hydroxyl radical attack"
  Blánaid White, James F. Rusling, Malcolm R. Smyth

- **Postgraduate Research Topics in Electroanalytical Chemistry**
  Birkbeck, University of London, United Kingdom, 1 December 2004
  "Electroanalytical detection of oxidative DNA damage"
  Blánaid White, James F. Rusling, Malcolm R. Smyth

7.5 Poster Presentations

- **2nd Annual Conference on Analytical Sciences in Ireland**
  Institute of Technology, Tallaght, Dublin 24, Ireland, 4-5 April 2002
  "Development of a method for early detection of oxidative DNA damage"
  Blánaid White, James F. Rusling, Malcolm R. Smyth

- **55th Irish Universities Chemistry Research Colloquium**
  Trinity College Dublin, Ireland, 14-16 May 2003
  "Oscillating formation of 8-oxoguanine during Fenton-mediated DNA oxidation"
  Blánaid White, James F. Rusling, Malcolm R. Smyth

- **ESEAC 2004. 10th International Conference on Electroanalysis**
  National University of Ireland, Galway, Ireland, 6-10 June 2004
  "Electrochemical detection of copper-induced oxidative DNA damage"
  Blánaid White, James F. Rusling, Malcolm R. Smyth